

MACHINABILITY OF NICKEL BASED SUPERALLOYS WITH CARBIDE AND CERAMIC TOOLS IN MILLING

Sumit Kanti Sikdar

A Thesis

in

The Department

of

Mechanical and Industrial Engineering

Presented in Partial Fulfillment of the Requirements

for the Degree of Doctor of Philosophy

at

Concordia University

Montreal, Quebec, Canada

August, 2007

© Sumit Kanti Sikdar, 2007



Library and
Archives Canada

Bibliothèque et
Archives Canada

Published Heritage
Branch

Direction du
Patrimoine de l'édition

395 Wellington Street
Ottawa ON K1A 0N4
Canada

395, rue Wellington
Ottawa ON K1A 0N4
Canada

Your file *Votre référence*
ISBN: 978-0-494-31152-3
Our file *Notre référence*
ISBN: 978-0-494-31152-3

NOTICE:

The author has granted a non-exclusive license allowing Library and Archives Canada to reproduce, publish, archive, preserve, conserve, communicate to the public by telecommunication or on the Internet, loan, distribute and sell theses worldwide, for commercial or non-commercial purposes, in microform, paper, electronic and/or any other formats.

The author retains copyright ownership and moral rights in this thesis. Neither the thesis nor substantial extracts from it may be printed or otherwise reproduced without the author's permission.

AVIS:

L'auteur a accordé une licence non exclusive permettant à la Bibliothèque et Archives Canada de reproduire, publier, archiver, sauvegarder, conserver, transmettre au public par télécommunication ou par l'Internet, prêter, distribuer et vendre des thèses partout dans le monde, à des fins commerciales ou autres, sur support microforme, papier, électronique et/ou autres formats.

L'auteur conserve la propriété du droit d'auteur et des droits moraux qui protègent cette thèse. Ni la thèse ni des extraits substantiels de celle-ci ne doivent être imprimés ou autrement reproduits sans son autorisation.

In compliance with the Canadian Privacy Act some supporting forms may have been removed from this thesis.

Conformément à la loi canadienne sur la protection de la vie privée, quelques formulaires secondaires ont été enlevés de cette thèse.

While these forms may be included in the document page count, their removal does not represent any loss of content from the thesis.

Bien que ces formulaires aient inclus dans la pagination, il n'y aura aucun contenu manquant.


Canada

ABSTRACT

Machinability of Nickel Based Superalloys with Carbide and Ceramic Tools in Milling

Sumit Kanti Sikdar

Concordia University, 2007

Nickel based superalloys are used in the aerospace industry for manufacturing gas turbines because of their ability to withstand large loads at high temperatures. But this property, however, makes it one of the most difficult materials to machine necessitating frequent tool replacement due to wear and hence reduced productivity. Also, as the tool wears, the quality of the machined surface deteriorates correspondingly or may even become damaged. This thesis presents a study of how nickel-based superalloys respond to machining during a milling operation. Special consideration in this study has been given to experimental testing, accuracy and precision. Tool wear and surface roughness were investigated for Titanium Aluminum Nitride (TiAlN) coated and uncoated carbide tools under wet (coolant) and dry cutting conditions. Cutting tests were performed on a CNC milling machine to obtain tool wear and surface roughness. Average flank wear and maximum flank wear were determined by using a tool-wear measuring microscope. Surface roughness parameters were measured using a portable stylus type surface roughness tester (Mitutoyo). Based on tool wear, coated carbide tools performed better than uncoated tools and coolant further reduced tool wear and surface roughness during the cutting operation. Tool life equations were established from experimental results in order to determine tool life under wet (coolant) and dry cutting conditions. On the other hand, wear and surface roughness were also investigated for ceramic tools under different cutting conditions. Tests using ceramic tools (Whisker reinforced and Kyon 2100) were

carried out under dry conditions and they performed well at high cutting speeds though the machined surface was found to deteriorate when the feed rate was high. The adhesion of workpiece material was confirmed through energy dispersive X-ray (EDX) analysis. Stability lobes were established in order to identify stable cutting conditions for nickel based superalloys. Wear mechanisms were determined under stable and unstable (chatter) conditions.

ACKNOWLEDGEMENTS

I would like to express the sincerest gratitude and appreciation to my supervisors, Dr. M. Chen and Dr. S. Engin for their valuable time, supervisions, suggestions and encouragement throughout this thesis work. I feel extremely fortunate to have had the opportunity of working with them and benefiting from their experience and insight. The financial and technical support of the Pratt & Whitney, Canada is also acknowledged and appreciated. I would like to thank the technical staff in the Mechanical and Industrial Engineering Department, Brian Cooper, William Chicoine, Alex Macpherson and Juan Alfara.

I would like to thank Dr. Florence Paray and Helen Campbell for their help while working at McGill University Material Science Laboratory.

I would like to thank Melissa Cote, Ecole Polytechnique Manufacturing Laboratory.

I would like to thank my committee members for the time they spent on me and the insight they provided me.

Finally special thanks to my parents and to my wife Subarna Paul for their moral support and constant encouragement.

TABLE OF CONTENTS

LIST OF FIGURES	x
LIST OF TABLES	xxii
NOMENCLATURE	xxiii
CHAPTER 1: INTRODUCTION	
1.1 Nickel based superalloys	2
1.2 High speed machining	3
1.3 Problem definition	5
1.4 Research objectives	9
1.5 Research approach	10
1.6 Contributions of thesis	10
1.7 List of publications	12
1.8 Outline of thesis	13
CHAPTER 2: LITERATURE REVIEW	
2.1 Wear and machined surface quality	16
2.2 Wet (coolant) and dry machining	24
2.3 High speed machining operation	28
2.5 Wear mechanisms under stable and unstable (chatter vibration)	33
CHAPTER 3: EQUIPMENT AND INSTRUMENTATION	
3.1 Equipment for machining experiments	42
3.1.1 CNC milling machine	43
3.1.2 Surface roughness machine	45

3.1.3 Microscope	45
3.2 Cutting tool materials	48
3.2.1 Carbide tools	48
3.2.2 Ceramic tools	49
CHAPTER 4: WEAR AND SURFACE QUALITY FOR CARBIDE TOOLS	
4.1 Carbide tools for machining operation	52
4.1.1 Selection of cutting conditions	54
4.2 Tool wear criteria	55
4.3 Experimental work	57
4.4 Experimental results	60
4.4.1 Tool wear for uncoated and coated carbides	60
4.4.2 Effect of cutting speed on tool wear	70
4.4.3 Effect of coolant on tool wear	73
4.4.4 Wear mechanisms for carbides	88
4.4.5 Surface roughness parameters	93
4.4.6 Surface roughness in wet and dry conditions	94
4.5 Discussion	102
CHAPTER 5: HIGH SPEED MACHINING: WEAR AND SURFACE ROUGHNESS FOR CERAMIC TOOLS	
5.1 High speed machining operation	107
5.2 Ceramic tools for nickel based superalloys machining	107
5.3 Selection of cutting conditions for ceramic tools	109
5.4 Experiments with ceramic tools in high speed machining	109

5.5 Experimental results	111
5.5.1 Tool wear for ceramic tools	111
5.5.2 Effect of cutting speed on cutting length (tool life)	125
5.6 Wear mechanisms examination using microscope (SMM)	130
5.6.1 Micro analysis of wear mechanisms for ceramic tools	131
5.7 X-ray examination for wear surface using EDX spectroscopy	142
5.7.1 Microstructure and energy dispersive X-ray (EDX) for ceramic tools	143
5.8 Surface roughness in machining operation	150
5.8.1 Roughness parameters	150
5.8.2 Results of surface roughness under different cutting conditions	151
5.8.3 Micro analysis of machined surface	155
5.9 Discussion	161

CHAPTER 6: WEAR MECHANISMS UNDER STABLE AND UNSTABLE (CHATTER) CONDITIONS

6.1 Wear mechanisms	167
6.2 Determination of cutting force coefficients from cutting forces	168
6.2.1 Experimental procedures for cutting force test	171
6.2.2 Cutting force coefficients	175
6.3 Determination of machine tool dynamics (vibration)	177
6.3.1 Establishment of stability lobes for nickel based superalloys	182
6.3.2 Determination of the effect of dynamic behaviour of the system on stability	186

6.4 Microphone sound spectrum and wear mechanisms	188
6.4.1 Analysis of microphone sound spectrum	188
6.4.2 Determination of wear mechanisms	191
6.5 Discussion	208
CHAPTER 7: MILLING PROCESS	
7.1 Effect of cutting parameters on milling process	212
7.2 Analytical prediction of uncut chip thickness	216
7.3 Discussion	219
CHAPTER 8: SUMMARY, CONCLUSIONS AND SUGGESTED FUTURE WORK	
8.1 Summary	220
8.2 Conclusions	222
8.3 Suggested future work	224
REFERENCES	225

LIST OF FIGURES

CHAPTER 3

Figure 3.1: CNC milling machine	43
Figure 3.2: Coolant supplied through nozzles in CNC milling machine	44
Figure 3.3: Surface roughness machine	45
Figure 3.4: Microscope for tool wear measurement	46
Figure 3.5: Scanning metallographic microscope for wear mechanisms examination	47
Figure 3.6: Carbide inserts (APKT and APCT)	49
Figure 3.7: Carbide insert (HM90APKT)	49
Figure 3.8: Tool holder for Whisker reinforced ceramic	50
Figure 3.9: Tool holder for Kyon 2100	50

CHAPTER 4

Figure 4.1: Different forms of tool wear on cutting tool	56
Figure 4.2: Flank wear vs. Cutting time (APKT, uncoated insert $v = 50$ m/min, $f = 0.025$ mm/tooth, wet (coolant) cutting)	61
Figure 4.3: Flank wear vs. Cutting time (APKT, uncoated insert $v = 50$ m/min, $f = 0.025$ mm/tooth, dry cutting)	61
Figure 4.4: Flank wear vs. Cutting time (APKT, uncoated insert $v = 70$ m/min, $f = 0.025$ mm/tooth, wet cutting)	62
Figure 4.5: Flank wear vs. Cutting time (APKT, uncoated insert $v = 70$ m/min, $f = 0.025$ mm/tooth, dry cutting)	62
Figure 4.6: Flank wear vs. Cutting time (APCT, uncoated insert $v = 50$ m/min, $f = 0.025$ mm/tooth, wet cutting)	63
Figure 4.7: Flank wear vs. Cutting time (APCT, uncoated insert $v = 50$ m/min, $f = 0.025$ mm/tooth, dry cutting)	63

Figure 4.8: Flank wear vs. Cutting time (APCT, uncoated insert $v = 70$ m/min, $f = 0.025$ mm/tooth, wet cutting)	64
Figure 4.9: Flank wear vs. Cutting time (APCT, uncoated insert $v = 70$ m/min, $f = 0.025$ mm/tooth, dry cutting)	64
Figure 4.10: Flank wear vs. Cutting time (HM90APKT, coated insert $v = 70$ m/min, $f = 0.025$ mm/tooth, wet cutting)	65
Figure 4.11: Flank wear vs. Cutting time (HM90APKT, coated insert $v = 70$ m/min, $f = 0.025$ mm/tooth, dry cutting)	66
Figure 4.12: Flank wear vs. Cutting time (HM90APKT, coated insert $v = 90$ m/min, $f = 0.025$ mm/tooth, wet cutting)	66
Figure 4.13: Flank wear vs. Cutting time (HM90APKT, coated insert $v = 90$ m/min, $f = 0.025$ mm/tooth, dry cutting)	67
Figure 4.14: Flank wear vs. Cutting time (APKTIC928, coated insert $v = 70$ m/min, $f = 0.025$ mm/tooth, wet cutting)	67
Figure 4.15: Flank wear vs. Cutting time (APKTIC928, coated insert $v = 70$ m/min, $f = 0.025$ mm/tooth, dry cutting)	68
Figure 4.16: Flank wear vs. Cutting time (APKTIC928, coated insert $v = 90$ m/min, $f = 0.025$ mm/tooth, wet cutting)	68
Figure 4.17: Flank wear vs. Cutting time (APKTIC928, coated insert $v = 90$ m/min, $f = 0.025$ mm/tooth, dry cutting)	69
Figure 4.18: Maximum flank wear vs. cutting time (APKT, uncoated insert, $f = 0.025$ mm/tooth, wet (coolant) cutting)	70
Figure 4.19: Maximum flank wear vs. cutting time (APCT, uncoated insert, $f = 0.025$ mm/tooth, wet (coolant) cutting)	71
Figure 4.20: Maximum flank wear vs. cutting time (HM90APKT, coated insert, $f = 0.025$ mm/tooth, wet (coolant) cutting)	72
Figure 4.21: Maximum flank wear vs. cutting time (APKTIC928, coated insert, $f = 0.025$ mm/tooth, wet (coolant) cutting)	73
Figure 4.22: Maximum flank wear vs. cutting time (APKT, uncoated insert, $v = 40$ m/min, $f = 0.025$ mm/tooth)	74

Figure 4.23: Maximum flank wear vs. cutting time (APKT, uncoated insert, $v= 60$ m/min, $f= 0.025$ mm/tooth)	75
Figure 4.24: Maximum flank wear vs. cutting time (APCT, uncoated insert, $v= 40$ m/min, $f= 0.025$ mm/tooth)	75
Figure 4.25: Maximum flank wear vs. cutting time (APCT, uncoated insert, $v= 60$ m/min, $f= 0.025$ mm/tooth)	76
Figure 4.26: Maximum flank wear vs. cutting time (HM90APKT, coated insert, $v= 80$ m/min, $f= 0.025$ mm/tooth)	76
Figure 4.27: Maximum flank wear vs. cutting time (HM90APKT, coated insert, $v= 100$ m/min, $f= 0.025$ mm/tooth)	77
Figure 4.28: Maximum flank wear vs. cutting time (APKTIC928, coated insert, $v= 80$ m/min, $f= 0.025$ mm/tooth)	77
Figure 4.29: Maximum flank wear vs. cutting time (APKTIC928, coated insert, $v= 100$ m/min, $f= 0.025$ mm/tooth)	78
Figure 4.30: Tool life vs. cutting speed (APKT, uncoated insert, $f= 0.025$ mm/tooth)	79
Figure 4.31: Tool life vs. cutting speed (APCT, uncoated insert, $f= 0.025$ mm/tooth)	79
Figure 4.32: Tool life vs. cutting speed (HM90APKT, coated insert, $f= 0.025$ mm/tooth)	80
Figure 4.33: Tool life vs. cutting speed (APKTIC928, coated insert, $f= 0.025$ mm/tooth)	81
Figure 4.34: Tool life, APKTIC928 coated insert, $f= 0.025$ mm/tooth	83
Figure 4.35: SMM micrograph of wear surface (APKT, uncoated carbide insert, cutting speed= 70 m/min, feed= 0.025 mm/tooth, wet cutting)	88
Figure 4.36: SMM micrograph of wear surface (APCT, uncoated carbide insert, cutting speed= 70 m/min, feed= 0.025 mm/tooth, wet cutting)	89
Figure 4.37: SMM micrograph of wear surface (APKTIC928, coated carbide insert, cutting speed= 70 m/min, feed= 0.025 mm/tooth, wet cutting)	90
Figure 4.38: SMM micrograph of wear surface (HM90APKT, coated carbide insert, cutting speed= 70 m/min, feed= 0.025 mm/tooth, wet cutting)	91

Figure 4.39: SMM micrograph of wear surface (APKTIC928, coated carbide insert, cutting speed= 110 m/min, feed= 0.025mm/tooth, dry cutting)	92
Figure 4.39: Surface roughness (R_a)	93
Figure 4.41: Peak to valley roughness height (R_t)	94
Figure 4.42: Surface roughness (R_a) for wet and dry conditions (HM90APKT, coated insert, $v = 70$ m/min)	95
Figure 4.43: Surface roughness (R_a) for wet and dry conditions (HM90APKT, coated insert, $v = 90$ m/min)	95
Figure 4.44: Surface roughness (R_a) for wet and dry conditions (APKTIC928, coated insert, $v = 70$ m/min)	96
Figure 4.45: Surface roughness (R_a) for wet and dry conditions (APKTIC928, coated insert, $v = 90$ m/min)	96
Figure 4.46: Surface roughness (R_a) for wet and dry conditions (APKT, uncoated insert, $v = 40$ m/min)	97
Figure 4.47: Surface roughness (R_a) for wet and dry conditions (APKT, uncoated insert, $v = 70$ m/min)	97
Figure 4.48: Surface roughness (R_a) for wet and dry conditions (APCT, uncoated insert, $v = 40$ m/min)	98
Figure 4.49: Microscopic examination of machined surface for wet condition (HM90APKT, coated insert, $R_a = 0.31 \mu\text{m}$, $R_t = 1.2 \mu\text{m}$, $v = 70$ m/min, $f = 0.025$ mm/tooth)	99
Figure 4.50: Microscopic examination of machined surface for dry condition (HM90APKT, coated insert, $R_a = 0.78 \mu\text{m}$, $R_t = 2.6 \mu\text{m}$, $v = 70$ m/min, $f = 0.035$ mm/tooth)	99
Figure 4.51: Surface roughness (R_a) for wet and dry conditions (APCT, uncoated insert, $v = 70$ m/min)	100
Figure 4.52: Surface roughness (R_t) for wet and dry conditions (HM90APKT, coated insert, $v = 70$ m/min)	100
Figure 4.53: Surface roughness (R_t) for wet and dry conditions (APKT, uncoated insert, $v = 70$ m/min)	101

CHAPTER 5

Figure 5.1: Flank wear vs. Cutting length (Whisker reinforced ceramic tool, $v = 250$ m/min, $f = 0.03$ mm/tooth, dry cutting)	111
Figure 5.2: Flank wear vs. Cutting length (Whisker reinforced ceramic tool, $v = 350$ m/min, $f = 0.03$ mm/tooth, dry cutting)	112
Figure 5.3: Flank wear vs. Cutting length (Whisker reinforced ceramic tool, $v = 450$ m/min, $f = 0.03$ mm/tooth, dry cutting)	112
Figure 5.4: Flank wear vs. Cutting length (Whisker reinforced ceramic tool, $v = 550$ m/min, $f = 0.03$ mm/tooth, dry cutting)	113
Figure 5.5: Flank wear vs. Cutting length (Whisker reinforced ceramic tool, $v = 650$ m/min, $f = 0.03$ mm/tooth, dry cutting)	113
Figure 5.6: Flank wear vs. Cutting length (Whisker reinforced ceramic tool, $v = 750$ m/min, $f = 0.03$ mm/tooth, dry cutting)	114
Figure 5.7: Flank wear vs. Cutting length (Whisker reinforced ceramic tool, $v = 850$ m/min, $f = 0.03$ mm/tooth, dry cutting)	114
Figure 5.8: Flank wear vs. Cutting length (Whisker reinforced ceramic tool, $v = 950$ m/min, $f = 0.03$ mm/tooth, dry cutting)	115
Figure 5.9: Flank wear vs. Cutting length (Whisker reinforced ceramic tool, $v = 1050$ m/min, $f = 0.03$ mm/tooth, dry cutting)	116
Figure 5.10: Flank wear vs. Cutting length (Whisker reinforced ceramic tool, $v = 1150$ m/min, $f = 0.03$ mm/tooth, dry cutting)	116
Figure 5.11: Flank wear vs. Cutting length (Whisker reinforced ceramic tool, $v = 1250$ m/min, $f = 0.03$ mm/tooth, dry cutting)	117
Figure 5.12: Flank wear vs. Cutting length (Whisker reinforced ceramic tool, $v = 1350$ m/min, $f = 0.03$ mm/tooth, dry cutting)	117
Figure 5.13: Flank wear vs. Cutting length (Whisker reinforced ceramic tool, $v = 1450$ m/min, $f = 0.03$ mm/tooth, dry cutting)	118
Figure 5.14: Flank wear vs. Cutting length (Kyon 2100 ceramic tool, $v = 250$ m/min, $f = 0.03$ mm/tooth, dry cutting)	119

Figure 5.15: Maximum flank wear vs. Cutting length ($v = 450$ m/min, $f = 0.04$ mm/tooth, dry cutting)	120
Figure 5.161: Maximum flank wear vs. Cutting length ($v = 550$ m/min, $f = 0.04$ mm/tooth, dry cutting)	121
Figure 5.17: Maximum flank wear vs. Cutting length ($v = 650$ m/min, $f = 0.04$ mm/tooth, dry cutting)	121
Figure 5.18: Maximum flank wear vs. Cutting length ($v = 750$ m/min, $f = 0.04$ mm/tooth, dry cutting)	122
Figure 5.19: Maximum flank wear vs. Cutting length ($v = 850$ m/min, $f = 0.04$ mm/tooth, dry cutting)	122
Figure 5.20: Maximum flank wear vs. Cutting length ($v = 950$ m/min, $f = 0.04$ mm/tooth, dry cutting)	123
Figure 5.21: Maximum flank wear vs. Cutting length ($v = 1050$ m/min, $f = 0.04$ mm/tooth, dry cutting)	123
Figure 5.22: Maximum flank wear vs. Cutting length ($v = 1150$ m/min, $f = 0.04$ mm/tooth, dry cutting)	124
Figure 5.23: Cutting length vs. cutting speed (Whisker reinforced ceramic tool, $f = 0.03$ mm/tooth, dry cutting)	126
Figure 5.24: Cutting length vs. cutting speed (Whisker reinforced ceramic tool, $f = 0.07$ mm/tooth, dry cutting)	127
Figure 5.25: Cutting length vs. cutting speed (Kyon 2100 ceramic tool, $f = 0.03$ mm/tooth, dry cutting)	128
Figure 5.26: Cutting length vs. cutting speed (Kyon 2100 ceramic tool, $f = 0.11$ mm/tooth, dry cutting)	129
Figure 5.27: SMM micrograph of wear surface (Whisker ceramic tool, cutting speed = 250 m/min, feed= 0.03 mm/tooth)	131
Figure 5.28: SMM micrograph of wear surface (Whisker ceramic tool, cutting speed = 350 m/min, feed= 0.03 mm/tooth)	132
Figure 5.29: SMM micrograph of wear surface (Whisker ceramic tool, cutting speed = 450 m/min, feed= 0.03 mm/tooth)	132

Figure 5.30: SMM micrograph of wear surface (Whisker ceramic tool, cutting speed = 550 m/min, feed= 0.03 mm/tooth)	133
Figure 5.31: SMM micrograph of wear surface (Whisker ceramic tool, cutting speed = 650 m/min, feed= 0.03 mm/tooth)	133
Figure 5.32: SMM micrograph of wear surface (Whisker ceramic tool, cutting speed = 750 m/min, feed= 0.03 mm/tooth)	134
Figure 5.33: SMM micrograph of wear surface (Whisker ceramic tool, cutting speed = 850 m/min, feed= 0.03 mm/tooth)	134
Figure 5.34: SMM micrograph of wear surface (Kyon 2100 ceramic tool, cutting speed = 250 m/min, feed= 0.03 mm/tooth)	135
Figure 5.35: SMM micrograph of wear surface (Kyon 2100 ceramic tool, cutting speed = 850 m/min, feed= 0.03 mm/tooth)	135
Figure 5.36: SMM micrograph of wear surface (Whisker ceramic tool, cutting speed = 950 m/min, feed = 0.12 mm/tooth)	136
Figure 5.37: SMM micrograph of wear surface (Whisker ceramic tool, cutting speed = 1050 m/min, feed = 0.12 mm/tooth)	137
Figure 5.38: SMM micrograph of wear surface (Whisker ceramic tool, cutting speed = 1150 m/min, feed = 0.12 mm/tooth)	137
Figure 5.39: SMM micrograph of wear surface (Whisker ceramic tool, cutting speed = 1250 m/min, feed = 0.12 mm/tooth)	138
Figure 5.40: SMM micrograph of wear surface (Whisker ceramic tool, cutting speed = 1350 m/min, feed = 0.12 mm/tooth)	138
Figure 5.41: SMM micrograph of wear surface (Whisker ceramic tool, cutting speed = 1450 m/min, feed = 0.12 mm/tooth)	139
Figure 5.42: SMM micrograph of wear surface (Kyon 2100 ceramic tool, cutting speed = 1050 m/min, feed = 0.12 mm/tooth)	140
Figure 5.43: SMM micrograph of wear surface (Kyon 2100 ceramic tool, cutting speed = 1150 m/min, feed = 0.12 mm/tooth)	140
Figure 5.44: SMM micrograph of wear surface (Kyon 2100 ceramic tool, cutting speed = 1250 m/min, feed = 0.12 mm/tooth)	141

Figure 5.45: X-ray examination instrument (SEM with EDX)	142
Figure 5.46: Microstructure of wear surface (Whisker ceramic tool, cutting speed = 850 m/min, feed = 0.03 mm/tooth)	143
Figure 5.47: Energy dispersive X-ray (EDX) analysis of wear surface (Whisker ceramic tool, cutting speed = 850 m/min, feed = 0.03 mm/tooth)	144
Figure 5.48: Microstructure of wear surface (Whisker ceramic tool, cutting speed = 950 m/min, feed = 0.03 mm/tooth)	144
Figure 5.49: Energy dispersive X-ray analysis (EDX) of wear surface (Whisker ceramic tool, cutting speed = 950 m/min, feed = 0.03 mm/tooth)	145
Figure 5.50: Microstructure of wear surface (Whisker ceramic tool, cutting speed = 1250 m/min, feed = 0.12 mm/tooth)	145
Figure 5.51: Energy dispersive X-ray (EDX) analysis of wear surface (Whisker ceramic tool, cutting speed = 1250 m/min, feed = 0.12 mm/tooth)	146
Figure 5.52: Microstructure of wear surface (Kyon 2100 ceramic tool, cutting speed = 850 m/min, feed = 0.03 mm/tooth)	147
Figure 5.53: Energy dispersive X-ray (EDX) analysis of wear surface (Kyon 2100 ceramic tool, cutting speed = 850 m/min, feed = 0.03 mm/tooth)	147
Figure 5.54: Microstructure of wear surface (Kyon 2100 ceramic tool, cutting speed = 1250 m/min, feed = 0.12 mm/tooth)	148
Figure 5.55: Energy dispersive X-ray (EDX) analysis of wear surface (Kyon 2100 ceramic tool, cutting speed = 1250 m/min, feed = 0.12 mm/tooth)	149
Figure 5.56: Surface roughness (R_a) for Whisker ceramic tool for different cutting speeds	151
Figure 5.57: Surface roughness (R_t) for Whisker ceramic tool for different cutting speeds	152
Figure 5.58: Surface roughness (R_a) for Kyon 2100 ceramic tool for different cutting speeds	153
Figure 5.59: Surface roughness (R_t) for Kyon 2100 ceramic tool for different cutting speeds	154
Figure 5.60: Microscopic examination of machined surface (Whisker ceramic tool, $R_a = 0.96 \mu\text{m}$, $R_t = 3.22 \mu\text{m}$, cutting speed = 250 m/min, feed = 0.11 mm/tooth)	155

Figure 5.61: Microscopic examination of machined surface (Whisker ceramic tool, $R_a = 0.41 \mu\text{m}$, $R_t = 1.2 \mu\text{m}$, cutting speed = 850m/min, feed = 0.03 mm/tooth)	156
Figure 5.62: Microscopic examination of machined surface (Whisker ceramic tool, $R_a = 0.46 \mu\text{m}$, $R_t = 1.6 \mu\text{m}$, cutting speed = 850m/min, feed = 0.04mm/tooth)	157
Figure 5.63: Microscopic examination of machined surface (Whisker ceramic tool, $R_a = 0.52 \mu\text{m}$, $R_t = 1.9 \mu\text{m}$, cutting speed = 1250 m/min, feed = 0.08mm/tooth)	158
Figure 5.64: Microscopic examination of machined surface (Kyon 2100 ceramic tool, $R_a = 1.0 \mu\text{m}$, $R_t = 3.7 \mu\text{m}$, cutting speed = 250 m/min, feed = 0.12 mm/tooth)	158
Figure 5.65: Microscopic examination of machined surface (Kyon 2100 ceramic tool, $R_a = 0.5 \mu\text{m}$, $R_t = 1.8 \mu\text{m}$, cutting speed = 850 m/min, feed = 0.05 mm/tooth)	159
Figure 5.66: Microscopic examination of machined surface (Kyon 2100 ceramic tool, $R_a = 0.62 \mu\text{m}$, $R_t = 2.3 \mu\text{m}$, cutting speed = 850 m/min, feed = 0.07 mm/tooth)	160

CHAPTER 6

Figure 6.1: CNC milling machine	172
Figure 6.2: Dynamometer and Workpiece	172
Figure 6.3: Charge amplifier and Computer-data acquisition system for cutting force measurement	173
Figure 6 4: Microphone with data acquisition system	174
Figure 6.5: Average cutting force vs. Feed (cutting speed =70 m/min (1170 rpm), depth of cut=0.5 mm, full immersion)	175
Figure 6.6: Attachment of accelerometer on the cutting tool	177
Figure 6.7: Hammer with Data acquisition system	178
Figure 6.8: Magnitude of transfer function in X direction	179
Figure 6.9: Magnitude of transfer function in Y direction	180
Figure 6.10: Stability lobes for half immersion down milling	183
Figure 6.11: Vibration test for greater overhanged tool length	186

Figure 6.12: Stability lobes for the change of dynamic behaviour, half immersion down milling	187
Figure 6.13: Microphone sound spectrum (Cutting speed =1170 rpm, depth of cut = 1.2 mm)	188
Figure 6.14: Microphone sound spectrum (Cutting speed =1505 rpm, depth of cut = 1.4 mm)	189
Figure 6.15: Microphone sound spectrum (Cutting speed =1505 rpm, depth of cut = 3.3 mm, unstable cut)	190
Figure 6.16: Tool wear measuring microscope	191
Figure 6.17: SMM microscope for wear mechanisms	192
Figure 6.18: Stability lobes for half immersion down milling	192
Figure 6.19: Flank wear vs. Cutting time, cutting speed = 50 m/min (836rpm), depth of cut = 1 mm, feed= 0.025 mm/tooth, stable cut	194
Figure 6.20: Wear surface, Cutting speed= 50 m/min (836 rpm), depth of cut = 1 mm , feed = 0.025 mm/tooth, stable cut	194
Figure 6.21: Maximum flank wear vs. Cutting time, cutting speed = 50 m/min (836rpm,) stable depth of cut = 1 mm, unstable depth of cut =2.2 mm feed= 0.025 mm/tooth	195
Figure 6.22: Wear surface, cutting speed= 50 m/min (836 rpm), depth of cut = 2.2 mm, feed = 0.025 mm/tooth, unstable(chatter)	195
Figure 6.23: SMM micrograph of wear surface, cutting speed= 50 m/min (836 rpm), depth of cut = 2.2 mm, feed = 0.025 mm/tooth, unstable(chatter)	196
Figure 6.24: Wear surface, cutting speed= 50 m/min (836 rpm), depth of cut = 2.5 mm, feed = 0.025 mm/tooth, unstable(chatter)	196
Figure 6.25: SMM micrograph of wear surface, cutting speed= 50 m/min (836 rpm), depth of cut = 2.5 mm, feed = 0.025 mm/tooth, unstable(chatter)	197
Figure 6.26: Flank wear vs. Cutting time, cutting speed = 70 m/min (1170 rpm,) depth of cut = 0.7 mm, feed= 0.025 mm/tooth, stable cut	198
Figure 6.27: Wear surface, cutting speed= 70 m/min (1170 rpm), depth of cut = 0.7 mm , feed = 0.025 mm/tooth, stable cut	198

Figure 6.28: Maximum flank wear vs. Cutting time, cutting speed = 70 m/min (1170 rpm,) stable depth of cut = 0.7 mm, unstable depth of cut =2.2 mm, feed= 0.025 mm/tooth	199
Figure 6.29: Wear surface, cutting speed= 70 m/min (1170 rpm), depth of cut = 2.2 mm, feed = 0.025 mm/tooth, unstable(chatter)	199
Figure 6.30: Flank wear vs. Cutting time, cutting speed = 70 m/min (1170 rpm,) depth of cut = 1.2 mm, feed= 0.025 mm/tooth, stable cut	200
Figure 6.31: Wear surface, cutting speed= 70 m/min (1170 rpm), depth of cut = 1.2 mm , feed = 0.025 mm/tooth, stable cut	200
Figure 6.32: Maximum flank wear vs. Cutting time, cutting speed = 70 m/min (1170 rpm,) stable depth of cut = 1.2 mm, unstable depth of cut =2.5 mm, feed= 0.025 mm/tooth	201
Figure 6.33: Wear surface, cutting speed= 70 m/min (1170 rpm), depth of cut = 2.5 mm, feed = 0.025 mm/tooth, unstable(chatter)	201
Figure 6.34: SMM micrograph of wear surface, cutting speed= 70 m/min (1170 rpm), depth of cut = 2.5 mm, feed = 0.025 mm/tooth, unstable(chatter)	202
Figure 6.35: Wear surface, cutting speed= 70 m/min (1170 rpm), depth of cut = 2.8 mm, feed = 0.05 mm/tooth, unstable(chatter)	202
Figure 6.36: SMM micrograph of wear surface, cutting speed= 70 m/min (1170 rpm), depth of cut = 2.8 mm, feed = 0.05 mm/tooth, unstable(chatter)	203
Figure 6.37: Flank wear vs. Cutting time, cutting speed = 90 m/min (1505 rpm,) depth of cut = 1.4 mm, feed= 0.025 mm/tooth, stable cut	204
Figure 6.38: Wear surface, cutting speed= 90 m/min (1505 rpm), depth of cut = 1.4 mm , feed = 0.025 mm/tooth, stable cut	204
Figure 6.39: Maximum flank wear vs. Cutting time, cutting speed = 90 m/min (1505 rpm,) stable depth of cut = 1.4 mm, unstable depth of cut =3.3 mm, feed= 0.025 mm/tooth	205
Figure 6.40: Wear surface, cutting speed= 90 m/min (1505 rpm), depth of cut = 3.3 mm, feed = 0.025 mm/tooth, unstable(chatter)	205
Figure 6.41: SMM micrograph of wear surface, cutting speed= 90 m/min (1505 rpm), depth of cut = 3.3 mm, feed = 0.025 mm/tooth, unstable(chatter)	206
Figure 6.42: Flank wear vs. Cutting time, cutting speed = 90 m/min (1505 rpm,) depth of cut = 1.6 mm, feed= 0.025 mm/tooth, stable cut	206

Figure 6.43: Wear surface, cutting speed= 90 m/min (1505 rpm),
depth of cut = 1.6 mm , feed = 0.025 mm/tooth, stable cut 207

Figure 6.44: Flank wear vs. Cutting time, cutting speed = 90 m/min (1505 rpm,) depth of
cut = 1.8 mm, feed= 0.025 mm/tooth, stable cut 207

Figure 6.45: Wear, cutting speed= 90 m/min (1505 rpm),
depth of cut = 1.8 mm , feed = 0.05 mm/tooth, stable cut 208

CHAPTER 7

Figure 7.1: Up milling 213

Figure 7.2: Down milling 214

Figure 7.3: Resultant cutting speed (R) vs. Contact angle (θ)
(cutting speed = 1500 m/min, feed = 2 mm/tooth) 215

Figure 7.4: Chip thickness in milling operation 217

LIST OF TABLES

CHAPTER 4

Table 4.1: Test matrix for uncoated carbide (APKTIC28)	58
Table 4.2: Test matrix for uncoated carbide (APCTIC28)	59
Table 4.3: Test matrix for coated carbide (APKTIC928)	59
Table 4.4: Test matrix for coated carbide (HM90APKT)	60
Table 4.5: Different values of " n " and " C "	85
Table 4.6: Tool life for coated carbide tools	85
Table 4.7: Tool life for coated carbide tools	86
Table 4.8: Tool life for coated carbide tools	86
Table 4.9: Tool life for uncoated carbide tools	87
Table 4.10: Tool life for uncoated carbide tools	87
Table 4.11: Tool life for uncoated carbide tools	87

CHAPTER 5

Table 5.1 Test matrix for Whisker reinforced and Kyon 2100 ceramic tool	110
---	-----

CHAPTER 6

Table 6.1: Identified modal parameters in X direction	180
Table 6.2: Identified modal parameters in Y direction	181

NOMENCLATURE

C	constant
f	feed (mm/tooth)
F_a	axial cutting force (N)
F_t	tangential cutting force (N)
F_r	radial cutting force (N)
K_{tc}	cutting coefficient for tangential component
K_{te}	edge cutting coefficient for tangential component
K_{ac}	cutting coefficient for axial component
K_{ae}	edge cutting coefficient for axial component
K_{rc}	cutting coefficient for radial component
K_{re}	edge cutting coefficient for radial component
R_a	average surface roughness
R_t	surface roughness height
T	tool life
t_c	chip thickness (mm)
V	cutting speed (m/min)
$V_{B\max}$	maximum flank wear
V_B	average flank wear
n	spindle speed (rpm)
w	width of cutter (mm)
N	number of tooth
ω_n	natural frequency (Hz)
ζ	damping ratio

CHAPTER 1

Introduction

Analyzing and understanding cutting process mechanisms is a key issue in developing an economical and safe high speed machining process. Beyond the adoption of this new machining technology, the construction of machine tools and their peripheral equipment must also be considered. Industrial practitioners will only be willing to accept high speed machining technology when comprehensive solutions exist. Thus results for a large variety of work piece materials and common production methods are essential to prove the superiority of innovative machining technology. On the other hand, in recent years there has been growing interest in cutting materials used mostly for machining operation, particularly carbide and ceramic of which the latter figures prominently in this ever-growing group of materials. Nickel based superalloys play an extremely important

role in gas turbine engines, especially in turbine-disks, because it provides the necessary strength at their operating temperature.

1.1 Nickel-based superalloys

Nickel based superalloys are well known as the typical difficult-to-cut material and, indeed, machining industries are presently confronted with materials that are more difficult and challenging to machine than anything else that previously existed. Included in this category are high nickel alloys, also known as “superalloys”. The constant drive for higher productivity through increased metal removal rates and decreased overheads is yet another challenge for the machining industries. Nickel-based super-alloys are especially popular in the manufacture of strong, high temperature resistance components for aerospace applications. The processing methods and tooling involved in the manufacture of nickel alloy components are costly items. Nickel based superalloys contain at least 50% nickel, whereas in nickel iron alloy, nickel is the major solute component. In addition, elements such as silicon, phosphorous, sulphur, oxygen and nitrogen must be controlled through appropriate melting processes. Other additives are chromium, aluminium, zirconium, magnesium, carbon, molybdenum, niobium and tungsten. Inconel 718 is one of the nickel based super-alloys widely used in the aerospace industry because of its strength, high temperature tolerance and its resistance to corrosion. The microstructure of Inconel 718 comprises an austenite face centered cubic (FCC) matrix phase with other secondary faces. The microstructure of large grains containing Ni_3Nb (orthorhombic) precipitated phase and a heavy concentration of carbides at the grain boundaries. The difficulty of dislocation motion through the microstructure is responsible for high tensile and yield strength of Inconel

718. The structure breaks down only when held at temperatures higher than its ageing temperature for extended periods. The main problems encountered when machining Inconel 718 are shorter tool life, work piece surface damage and subsurface metallurgical damage due to work hardening. In general, material removal rates are low irrespective of the cutting process. A recent development of cutting tool materials may provide the solution to higher metal removal rates, as well as the possible elimination of some costly processes necessary to machine nickel based super-alloys.

1.2 High speed machining (HSM)

High speed machining is widely used in the manufacturing industry and the current demands to remove a great amount of material while still restoring surface accuracy poses a great challenge. High speed machining could be defined as a manufacturing process that operates at cutting speeds higher than those normally used. This actually represents an increase of five to ten times that of conventional cutting but the real range of cutting speed is dependent upon the material properties and actual cutting condition. The criteria that defines high speed milling in the manufacturing industry is the combination of cutting speeds and feed rates. The principal purpose of using high speed machining is to obtain higher productivity rates by utilizing machine tools more efficiently, reducing machining time and lowering labor costs while still maintaining product quality. Other notable results are:

- Obtaining specific dimensional requirements without using two or three different machining procedures.

- Reducing unwanted thermal effects in the work piece microstructure by eliminating the heat from chips, thus lowering thermally induced deformations or structural changes in the work piece material.

On the other hand, the cutting forces in high speed milling are lower than in conventional milling thereby enhancing tool life, obtaining greater accuracy of finite parts and reducing machining errors. At the same time, lower cutting forces permit high speed machining of thin walled parts, leading to superior material usage and improving the structure especially where weight is an issue for example in the aerospace industry. Another significant aspect of high speed machining is the fact that dry cutting is now preferred in many applications, especially when machining with ceramic tools. This leads to the elimination of some problems such as disposal of used coolant which causes health and environmental hazards concerns. In high speed machining, machine tools should be designed in such a way that they satisfy high speed machining technology. This includes the base passing through the main spindle, guide ways, feeding drives, chip removal, cooling system and providing security and safety features. Bases should be designed such as to ensure a better dynamic performance of the whole system. Several kinds of main spindles have been introduced such as active magnetic bearings and air operated bearings both of which have better performance characteristics in order to comply with the requirements of high-speed machining. Due to the high feed rates needed in high speed machining, only anti-friction guide ways such as roller or ball bearing slidings are allowed in the design. As for the feed drives, conventional power screws have now been replaced with ball screw drives and new drives such as linear motors, characterized by their high rigidity, zero backlash and very high response and

accuracy, are now being adopted in industrial CNC machines. Finally, security and safety features need to be stricter in order to prevent accidents and protect the worker. For example the machine should be completely encapsulated to prevent cooling liquid from spilling outside the machine. It is clearly seen from literature that high speed milling is a new technology but for which more research is required. Moreover, advances in this area have generally resulted from changes in practice, particularly the introduction of new work piece material.

1.3 Problem definition

The study of metal cutting process is important for the development of advanced machine tools. Metal cutting is a complex process since it involves friction, plastic flow and fracture of materials under conditions more extreme than those normally found in materials subjected to testing or in other production processes. The cutting operations are used to remove material from the work piece of which the most common are milling, turning and grinding. However, all metal cutting operations share the same principles of mechanics but their geometry and kinematics may differ from each other. In a turning operation, the tool travels parallel to the axis of a rotating work piece. The tool feed rate is usually very much slower than the work piece surface speed. On the other hand the milling operation is a metal removal process using a tool with one or more teeth rotating about a fixed axis, each tooth removing material from a work piece fed past the tool. The milling process is a more complex operation owing to its intermittent nature and thus many factors affect the tool wear in this operation. In milling, the cutting forces periodically changes as the chip thickness varies. The tooth periodically enters and exits from the work piece; hence it experiences stress and temperature cycling during the

cutting process. As the tool enters the work piece, it gets heated. The tool starts cooling when it exits from the work piece. Many manufacturing processes involve some aspects of metal cutting operations. The most crucial and determining in factor to successful maximization of the manufacturing process in any typical metal cutting process is tool wear. Tool state alone, however, is not solely responsible for defining the limits of the cutting process. Other penalties can be incurred if attention is paid exclusively to the condition of the tool. Machine and tool parameters such as the cutting conditions, tool material and work piece material are known to affect the tool life. Tool life represents the useful life of a tool, expressed in time from the start of a cut to some end point defined by failure criteria. Tool life and surface roughness are often taken as a yardstick for comparing the behaviour of the tool and work piece materials. The term “machinability” refers to the ease with which a given material can be machined. The criteria of machinability are tool life or tool wear, tooth marks or roughness, cutting forces, cutting temperatures, cooling effect and cutting conditions (speed, feed and depth of cut). The difficulty in predicting tool life arises from the fact that tool wear is a very complex phenomenon and depends on many factors including the properties of the materials involved, the physical and chemical properties of the surfaces, temperature and cutting speed. In a complex machining process such as milling, an operation which involves several geometric cutter parameters and operating variables such as feed, speed and depth of cut, the study of tool wear becomes more difficult. It is very difficult to select cutting parameters (cutting speed, feed and depth of cut) without knowing tool life and wear mechanisms. It is also well known that the prediction of the tool life in the milling process is made difficult due to the complicated tool failure mechanisms. During cutting,

high temperatures develop, therefore coolant should be used to transfer heat from the cutting zone. Most published research works on development machining process have been concentrated mainly on the turning process, whilst the milling process has received little attention due to the complexity of this process. Analytical works based on published papers in the milling process is very limited. From the literature survey, it is found that the analytical model is based on a velocity diagram proposed by Astakhov *et al* [1997] in a turning process, where chip thickness was assumed to be constant. But in the milling process, chip thickness is not constant and it changes with respect to the contact angle with the work piece. So it is important to know the behaviour of chip formation in a milling process. Alauddin *et al* [1998] conducted a few experiments based on up-milling and down-milling but those experiments were conducted at very low cutting speeds (20 m/min). It is found that until now, no significant research work had been done to compare these processes based on change of geometrical parameters due to the complexity of the milling operation and experimental set-up. Quality of finish of a machined surface is affected by tooth marks which follow the undulation of the revolution marks. The presence of either type of mark alters the geometric conditions of the surface and, consequently, the quality of the finish. Therefore the height of the tooth marks should be reduced in order to improve the quality of the work piece. It is also important to predict cutting force co-efficients because they can be determined from tool geometries which allow us to predict cutting forces for a variety of cutting conditions. Therefore, the study of tool life, uncut chip thickness, tooth marks, wear mechanisms, cooling effect, chatter vibration and machining strategy (up or down-milling) are very important in the milling process. Nickel based super-alloys are known as one of the most difficult to machine in

order to satisfy cutter life and surface quality requirement. Nickel based superalloys contain additions of chromium, aluminium, titanium, cobalt, molybdenum and other elements in varying quantities to give higher performance. With a material of such composition, the problem of tool wear and surface quality of the work piece during machining are more prominent if proper cutting tool is not selected. Their outstanding high temperature strength and extreme toughness create difficulties during machining due to their work hardening tendency which results in very high cutting forces and significant BUE (built-up-edge) formation during machining. Therefore, most of major parameters including tool materials, tool geometry, machining method (up or down milling), chip formation, machined tooth marks, cutting speed, feed, depth of cut and cutting environment (dry/coolant) should be studied during nickel material machining. Cutting nickel material is difficult due its low thermal conductivity and the high chemical affinity to all known cutting tool materials. The machining of nickel material thus presents a challenge to produce new cutting tools that can be used to cut this material. On the other hand, higher tool wear, low permissible cutting speeds and poor quality of machined surface present new challenges for manufacturing industry. Cutting tools are subject to higher stress and higher temperature by modern machining technologies, such as dry, high speed or high performance machining. Therefore, the special cutting tools (ceramic tools and TiAlN coated and uncoated carbide tools) were used to machine the nickel materials. SiC Whisker reinforced and Kyon2100 ceramic tools are a recent innovation that has come into prominence for potential structural applications because of the significant improvements in the properties of these tool materials. The incorporation of SiC whiskers into alumina ceramics results in an increasing strength, fracture toughness,

thermal conductivity, and high temperature creep resistance. Also, TiAlN coated carbide tool showed advantages at high process temperatures and forms a thin passive layer at the tool surface, which prevents a rapidly progressing diffusion or oxidation wear.

1.4 Research objectives

One of the most common and extensively used processes in the manufacturing industry is the milling process. Recently, high speed milling is being introduced as a tool for better performance, surface finish and tool life with low cost. Usually the surface produced by conventional machining gives higher roughness values than those produced by high speed machining. There is little experimental data available in the open literature regarding the use of TiAlN coated carbide, whisker-reinforced and kyon 2100 ceramic tools for milling of Inconel 718. Our literature review also showed that few research works had been published for high speed milling of Inconel 718 with ceramic tools. Therefore, the objectives of this thesis are as follows:

1. Establishment of tool life equations for different carbide tools from experimental data. Tool wear, wear mechanism and surface roughness analysis using carbide tools under wet (coolant) and dry conditions.
2. Determination of the effect of cutting parameters on tool wear, tool life and surface quality for ceramic tools in high speed machining operation.
3. Analysis of wear mechanisms for ceramic tools in high speed machining operation under different cutting conditions.
4. Determination of wear behaviour under stable and unstable (chatter) cutting conditions and establishment of stability lobes for nickel based super-alloys.

5. Establishment of analytical models for milling process:

- (a) A mathematical model to permit a comparison of up and down milling methods based on resultant cutting speed.
- (b) An analytical model to determine uncut chip thickness for a given width of cut (w), radius of cutter (R) and feed (f_t).

1.5 Research approach

The research consists of experimentation with certain analytical works. Cutting tests were performed on a CNC milling machine. Special cutting tools (Whisker reinforced ceramic tools, Kyon 2100 ceramic tools, TiAlN coated and uncoated carbide tools) were used to machine Inconel 718. Those special cutting tools have good wear resistance, high hot hardness and adequate chemical stability at elevated temperatures. Therefore, the present study aims to establish analytical models for milling processes and detailed experimental works for milling Inconel 718 using ceramic and carbide tools. Since cutting experiments were carried out on a CNC milling machine, the experimental results will be extended to applicable for milling operation.

1.6 Contributions of thesis

A comprehensive analysis of wear and surface roughness in milling of Inconel 718 are presented. The analysis was based on an extended test matrix covering wet (coolant) and dry cutting conditions. Researchers [Rahman *et al* 2000] presented experimental results using coolant but it was not sufficient because the cutting speed was very low. Unfortunately, a much smaller volume of research has been done by previous researchers for milling operations on nickel material. The emphasis of the previous studies by researchers on nickel based super-alloys concentrated mainly on the turning operation

and the focus was only on tool wear analysis. The effect of coolant on surface roughness in the machining of nickel based alloys by carbide tools has never been investigated during milling operation. While machining nickel based alloy, the effect of coolant on surface roughness should not be neglected and it is the very purpose of this thesis to present the machinability of nickel based super alloys under wet (coolant) and dry cutting operation. The use of coolant could lengthen tool life greatly as a result of the formation of a chemically absorbed film between tool and work piece or chip. Tool life equations were established for wet (coolant) and dry cutting conditions. Those equations can be applied in the manufacturing industry to determine tool life for nickel based super-alloys (Inconel 718) machining operation. Due to the higher productivity, high speed cutting technology is commonly used in the aerospace industry. The literature search carried out by the author indicates that there is very little information in high speed milling of nickel based superalloys using a ceramic tool. The thesis work was carried out on machine nickel based super-alloys with special ceramic tools (Whisker reinforced and Kyon 2100). We studied tool wear and surface roughness under various cutting conditions for ceramic tools which performed well at high cutting speeds. Only a few researchers [Elbestawi *et al* 1998] have worked on wear mechanisms for ceramic tools in nickel based super-alloys milling operation. We examined wear mechanisms for the cutting tool using scanning metallographic microscope (SMM). Energy dispersive X-ray (EDX) analysis was done for ceramic tools. Machined surface roughness analysis was carried out in order to investigate surface defects in the form of scratch and short grooves which were noticed at higher feed rates.

The quality of the surface improved at higher cutting speeds. Therefore the experiment results of ceramic tools can be used in aerospace industry as well as other manufacturing industries to machine nickel based super alloys in high speed milling machine operations. We established stability lobes for nickel based super-alloys. This stability can be used for the aerospace industry in order to identify stable cutting conditions for nickel based super-alloys machining operations. Wear mechanisms were also determined under stable and unstable conditions. A mathematical model on change of resultant cutting with the change of contact angle of the cutting tooth with the work piece was established. An analytical model for uncut chip thickness was also established. These models can be used in high speed (higher speed and higher feed rate) machining operation. It is hoped that the results of this investigation will provide the data-base for aerospace and other manufacturing industries.

1.7 List of Publications

In this section is the list of journals and conference papers that I co-authored during my stay at Concordia University.

Referred Journal paper:

1. Sumit Kanti Sikdar and Mingyuan Chen, Relationship between tool flank wear and component forces, *Journal of Materials Processing Technology*, vol.128, pp.210-215, 2002.
2. Sumit Kanti Sikdar, Serafettin Engin and Mingyuan Chen, Machinability of nickel based super alloys, *Journal of Materials Processing Technology* (submitted).

Referred conference paper:

1. Sumit Kanti Sikdar and Mingyuan Chen, Tool flank wear during machining operation, *Proceedings of the International Conference on Multidisciplinary Design in Engineering-CSME*, 21-22 November 2001, Montreal, Canada.

Publications under preparation:

1. “High speed machining for ceramic inserts during nickel based superalloys machining”. A journal or conference paper including the mathematical model for resultant cutting speed in milling process and experimental works for high speed milling with ceramic tools.

2. “Wear mechanisms for nickel based superalloys machining operation”. A conference paper on the effect of cutting speed on wear mechanisms for nickel based superalloys machining operation.

1.8 Outline of thesis

The remainder of this thesis is organized as follows. In chapter 2, we present a review of literature regarding wear, surface quality, coolant effect, cutting forces, temperature, stress, wear mechanisms, machining dynamic's and high speed machining. Chapter 3 details the experimental instruments and cutting tools. Chapter 4 shows the results obtained in this research for carbide tools. Different aspects such as wear, coolant effects and surface roughness for different cutting conditions are also discussed. An experimental evaluation of wear and machined surface quality for ceramic tools in high speed machining is presented in Chapter 5. In this chapter wear and the effects of cutting conditions on ceramic tools performance are discussed in detail. Wear mechanisms for stable and unstable (chatter) conditions are presented in Chapter 6. In Chapter 7, we

established mathematical models regarding resultant cutting speed and uncut chip thickness. These models are extended to the milling operation. The summary, conclusions and future research are presented in Chapter 8.

CHAPTER 2

Literature review

The demand for increasing productivity when machining heat resistant superalloys has resulted in the use of advanced cutting tools such as ceramics and new carbide tools. Industrial demands for higher productivity and lower manufacturing cost have always urged improvements on cutting tool performance. Introducing more powerful machine tools and stronger heat resistant superalloys further emphasizes the demand on the machine tools ability to operate at higher cutting speeds. Inconel 718 is a family of heat resistant superalloys used in aerospace industries to increase energy efficiency in terms of fuel consumption. These materials reserve most of their strength at very high temperature, but are difficult to machine owing to their characteristics that make them high temperature materials. The investigation documented in this thesis involves machining of nickel based superalloys. In this chapter, a review of wear mechanisms, surface quality, cutting environment (coolant or dry), high speed machining and chatter vibration literature is given.

2.1 Wear and machined surface quality

In recent years there has been renowned interest in the technology of cutting tools primarily to meet the machining demands of new materials many of which are considered as “difficult-to-machine” materials (Inconel 718). Haron *et al* [2005] studied the machinability of titanium alloys using coated and uncoated carbide tools. They reported that coated carbide have good use in end milling operation. They compared the cutting tool performance based on wear. Dobrzanski and Golombek [2005] investigated cutting ability tests of carbides (coated and uncoated) in turning operation. The material was C45E steel. The tool life of insert was determined based on measurements of the wear and the width of the tool flank. It was observed that coated tool performed better than uncoated tool based on wear. On the other hand, the value of surface roughness was higher in coated tool than uncoated tool. Chowdhuri *et al* [2004] presented an experimental investigation to understand the wear characteristics of carbide tools during turning operation. It was observed that an increase in the feed rate has the same effect on tool life as that of the increase in cutting speed. Results of their tool life testing indicate that thermal softening of the tool point combined with abrasion is the predominant tool failure mechanism. Rocha *et al* [2004] reported the influence of cutting speed, feed rate and depth of cut on wear for PCBN tools during turning operation. They also studied surface roughness. Among the cutting parameters the cutting speed was the most influential on the wear of the cutting tool. Akasawa *et al* [2003] examined wear and surface roughness for machinability analysis of austenite stainless steels. Machining tests were carried out on a CNC lathe using carbide tools. It was observed that chips

occasionally impinged on the machined surface and scratched it thus leaving a rough machined surface. Chelule *et al* [2003] studied the machinability of CAPTAL90 material. The experimental work was based on milling technique and the machining variables were wear and surface roughness. It was found that wear was a result of the workpiece reacting with the tool material causing attrition wear of the tool. Dabade *et al* [2003] discussed the cutting performance of a face milling cutter for the machining of aluminum. It was found that surface roughness was greatly influenced by inclination angle. An increase in the inclination angle reduced the surface roughness. This could be due to an increase in the contact length between the workpiece and the cutting edge of tool. Kudou *et al* [2003] studied the wear characteristics of carbide cutting tools during turning operation. They reported that the strength of carbide tool was decreased by the mutual diffusion among binder and carbon of the cutting tool and workpiece material and this phenomenon leads to the increase of wear. The main role of coating material on the surface of cutting tool was to prevent cutting tool from suffering abrasive wear. Ozacatalbas and Ercon [2003] investigated the machinability of mild steel in turning operation. The machinability was characterized in terms of wear and surface roughness. It was observed that an excessive adhered layer and an abrasive wear effect were dominant on flank of the tool. On the other hand, it was observed that built-up edge (BUE) chip thickness reduced as the cutting speed increased. Paro *et al* [2001] examined the machinability of X5CrMnN1818 stainless steels (0.91% wt N and 0.57% wt N) in turning operation under different cutting conditions. Poulachon *et al* [2001] presented the various modes of wear and damage of the PCBN cutting tool under different loading conditions, in order to establish a reliable wear modeling. The tool-wear experiments (facing operation) were carried out on a high

speed lathe using PCBN inserts coated with a 2 micro meter TiN thin layer. All cutting tests were performed without coolant at constant cutting speeds. AISI 52100 was chosen as the workpiece material. The experimental results show that the main wear mechanism of the PCBN tools is abrasion by hard alloy carbide particle contained in the workpiece. Caroline *et al* [2000] presented the machinability of SiC-reinforced aluminum metal-matrix composite (MMC) with diamond inserts. A series of turning experiments was carried out on a CNC lathe. All of the turning tests were performed under dry conditions. The results indicate that crater wear may not be a main concern to the diamond inserts due to the very low coefficient of friction and the high thermal conductivity of diamonds. Flank wear plays a more important role in determining the tool life. Yanming and Zehua [2000] investigated the tool wear in the cutting of SiC particle reinforced aluminium matrix composites during turning operation. For the cutting of SiC particle reinforced aluminium matrix composites, the major wear form of conventional tools is abrasive wear on the tool flank; edge and corner breakage taking place chiefly on high hardness tools such as PCD and CBN. Ferreira *et al* [1999] reported the practical experiments in turning, to study the performance of different tool materials such as ceramics, cemented carbide, CBN and diamond (PCD). Experiments were conducted in a CNC lathe. Workpiece was carbon fiber reinforced composite materials (CFRP). Huang *et al* [1999] investigated the machinability of KOVAR (Ni-Fe alloy) bar in a lathe using four different cutting tools. Experimental results on the machinability of these tools, including flank wear, cutting force, surface roughness of the workpiece were studied. Rahman *et al* [1999] studied the machinability of carbon fiber reinforced composite (CFRP) material. All experiments were carried out on a CNC lathe under dry conditions. The purpose of

their study was to determine how best the CFRP could be machined using different cutting tool inserts such as tungsten carbide under varying machining parameters. Su *et al* [1999] presented the performance analysis of TiCN coated cemented carbide tool during milling process. All of the cutting tests were conducted in a vertical machining center under dry conditions. The workpiece material was AISI 1045 medium carbon steel. Nelson *et al* [1998] carried out research work with the objective of finding operating parameters providing extended tool life. Cutting tests were performed on the McMaster milling machine. The McMaster is a modified F.J. Lamb three axis-milling machine equipped with a vertical spindle and CNC controller. Micro grain carbide and PCBN tipped carbide round inserts in an off center ball nose end mill with a single cutting edge were considered for all experiments. Mode of milling was down milling. The experimental results show that satisfactory performance can be achieved using an off center ball nose end mill with a micro grain carbide or PCBN tipped insert in milling hardened H13 tool steel. Jawahir *et al* [1998] developed a new methodology for tool wear evaluation in machining with grooved tools through a parametric approach involving chip-groove features. They investigated the effects of chip flow, chip-groove features and cutting forces in the machining operation. Hasler [1998] described the advantages of high speed machining operation. He investigated cutting forces and tool wear. Arsecularatne *et al* [1998] measured the cutting forces and surface finish during machining operation and found that surface roughness decreases with increasing cutting speed. Smith *et al* [1998] presented the effect of tool length on the metal removal rate during machining operation.

Astakhov and Shuvets [1997] investigated the chip formation process during the orthogonal cutting process. They reported that chip thickness can be predicted for different cutting conditions. Armarego [1997] presented the cutting forces for orthogonal process. It was found that the tangential force was the largest among others. The effect of flank wear on cutting forces was analyzed Lister and Barrow [1996] studied the field of tool wear and tool failure-monitoring systems and discussed the relative merits of the techniques proposed. Both tool wear and tool failures were considered and the differences between direct and indirect methods were highlighted. Mackinnon *et al* [1996] studied multi-component force measurements for the purpose of tool condition monitoring during adaptively controlled metal cutting on a lathe. Katayama and Toda [1996] investigated the machinability of medium carbon graphitic steels (G1 and G2) during turning operation. The experimental analysis was based on wear. Agrawal *et al* [1995] assessed the relative performance of coated and uncoated carbide tools in the machining of austenitic stainless based on cutting force, tool rake face and chip characteristics. Lim [1995] presented the changes that can be detected in the cutting force signatures during machine turning operations. Tool wear is therefore a major factor in assessing the life of cutting tools and improving cutting performance. Lin and Chen [1995] studied various cutting characteristics of a CBN tool in cutting hardened steel. BZN tool inserts from General Electric™ company were used to cut 52100 bearing steel in the cutting experiments. Based on the experimental results, certain cutting characteristics, such as tool life, cutting forces, surface roughness and tool wear were analyzed. Tool wear and cutting force were also investigated by Milovic and Wise [1995]. The experiments were done using leaded 0.11%C free cutting tool with carbide,

uncoated high speed steel and titanium nitride coated high speed steel. The results showed that the higher the rake angle of tool the smaller built up edge and good surface finish. Zhou *et al* [1995] described the spontaneous failure of a cutting tool in a turning process. The system includes a high-speed data acquisition subsystem and a graphic presentation subsystem. The strategy for monitoring is based on the estimation of the stress in a cutting tool. Hamman *et al* [1994] pointed out that a displacement of the stable built up layer from the face to the flank of the tool as the cutting speed increases. Werthein *et al* [1994] discussed the effect of tool geometry on the machining process. They found that the rake angle has influence on cutting stress. Du *et al* [1994] carried out an investigation to establish a relationship between cutting force fluctuations and surface formation in face cutting using a sintered carbide cutting tool. It was found that cutting forces were sensitive with surface roughness. Burta *et al* [1994] investigated the stress distribution during machining operation. It was found that the highest stress occurred at the chip tool contact area. Rapier [1993] investigated the influence of cutting temperature during machining process. He conducted experiments for measurement of temperature for different conditions. On the other hand, Rubenstein [1993] described the chip formation process in machining operation. He discussed the importance of chip mechanism. Andreasen and Chiffre [1993] developed an automatic system for chip breaking detection in turning operation. The system utilizes a detection technique based on frequency analysis of the dynamic feed force component. The ability to identify chip breaking has been demonstrated using different cutting tools, workpiece materials and cutting data.

Masuda *et al* [1993] examined the influence of WC grain size and Co content on tool wear rate when carbon materials (sintered carbon and fiber reinforced composites) were machined. All cutting tests were carried out on a high-speed lathe. Cutting tools were tungsten carbide-cobalt alloy tools. Tomac and Tonnessen [1992] investigated the machinability of particulate aluminium matrix composite (PAIMC) reinforced with 14%SiC. Cutting force, tool wear and surface roughness were measured. Looney *et al* [1992] studied the influence of cutting speed on tool wear, surface finish and cutting force for various tool materials. It was found that cutting force can be used for wear monitoring operation. The tangential cutting was the highest cutting force among others. Nair *et al* [1992] developed a method for identifying chip formation in turning. They also conducted experiments for force analysis. Jhita and Jain [1992] investigated the wear behaviour of tool operating under accelerated cutting conditions. Experimentally it has been found that tool flank wear during face turning follows an exponential law instead of three stage flank wear normally observed in conventional turning. Posti and Nieminen [1989] investigated the effects of coating thickness on tool life and cutting forces. It was observed that coated tool performed better than uncoated based on cutting force and tool wear. Danai and Ulsoy [1987] discussed about tool wear and cutting forces. The observer was used for on-line tool wear sensing in turning based on force measurement. Giusti *et al* [1987] developed a sensor based on TV image analysis of a worn tool. The flank wear was measured by the active cutting part from a proper direction. The crater wear was visualized by imaging the tool with a laser system. From the obtained image, it is possible to extract the position and the dimensions of the crater to obtain a complete mapping.

Comment on literature

Akasawa *et al.* investigated machinability of stainless steel. The depth of cut was low (0.1mm). These experimental results can only be applicable for steel. Agarwal *et al.* described the performance analysis of coated and uncoated carbide tool for turning operation. They considered only tool wear and the cutting speed was low (50 m/min). Caroline *et al.* reported the machinability analysis of metal matrix composites for turning operation but the depth of cut was very low (0.5mm). Dobrzanski and Golombek presented experimental results of wear and surface roughness. But the cutting tests were done on lathe machine. Those experimental results are not applicable in milling operation. On the other hand, Debade *et al.* discussed the performance of milling cutter. But the effect of cutting parameters on surface roughness was not considered for their research work. A manufactured parts performance quality is determined by its surface quality resulting from the manufacturing process. For example, the design and manufacturing of products that may be subjected to cyclic fatigue such as aircraft parts are highly affected by surface quality. Therefore surface roughness analysis is important during the machining operation. But unfortunately other researchers [Chowdhuri *et al.*, Ferreira *et al.*, Haron *et al.*, Kudou *et al.*, Katayama and Toda, Masuda *et al.*, Nelson *et al.*, Paro *et al.*, Poulachon *et al.*, Rahman *et al.*, Su *et al.*, Yanming and Zehua] have not reported the effect of cutting parameters on surface quality. Only few researchers [Chelule *et al.*, Ozacatalbas and Ercon, Tomac and Tonnessen, Rocha *et al.*] studied surface roughness and obtained the high values of surface roughness. The high values of

the surface roughness parameters indicate that the phenomena which takes place on the chip-tool interface does not occur in continuous and homogeneous form and suggests the probable formation of built-up edge (BUE). From literature survey, it was found that previous researchers mainly focused on turning operation for examining of wear, mechanisms and roughness. Recently, the application of milling operation has grown more popularity in aerospace industry as well as other manufacturing industry due to their complex shaped of manufacturing parts. Therefore, very little work related to milling of nickel based superalloys (Inconel 718) can be found in open literature. This research aims at a comprehensive study on milling of nickel based superalloys using coated (TiAlN) and uncoated carbide tools.

2.2 Wet (coolant) and dry machining

During the machining of metals, a considerable quantity of heat is generated, mainly due to the high plastic deformation in the primary shear zone and due to the friction of the chip on the rake surface. These conditions of friction and temperature cause tool wear, resulting poor surface finish and an incorrect dimension. Cutting fluids are used to reduce detrimental effects of heat and friction on both tool and workpiece. Ezugwu *et al* [2005] presented the effect of coolant on wear and cutting forces. Lower cutting forces were recorded with increasing coolant supply pressure when machining Inconel 718. This is because coolant supply at high pressure is able to access the cutting interface, ensuring effective cooling, lubrication and reducing the cutting temperature. This will consequently result in uniform flank wear and gradual wear rate. Lacalle *et al* [2005] conducted experiments using minimum quantity of lubricant (MQL) for high speed steel. The experimental results showed that tool wear decreased. The MQL jet

works correctly penetrating in the cutting zone. Therefore, taking into account the impossibility of dry machining, a technique involving minimal consumption of cutting fluid called MQL can be applied. Su *et al* [2005] investigated the cutting performance of coated carbide tools in dry machining conditions. Experiments were performed with carbide tools in turning operation. The material of the workpiece was medium carbon steel. The results indicate that the coating thickness influences the wear resistance of coated carbide tools. During dry cutting operation, a large amount of workpiece material adhered to the flank face of the cutting tool. Arunachalam *et al* [2004] discussed the residual stress and surface roughness in the turning operation of Inconel 718 using CBN tools. Experiments were conducted at cutting speeds from 150 to 375 m/min. From this investigation, it could be suggested that in the turning of Inconel 718 components, use of CBN tools at low cutting speed (150 m/min) under wet conditions will result in minimal residual stresses. Good surface finish was achieved at cutting speed of 375 m/min. Wakabayashi *et al* [2003] investigated the behavior of lubricants for semi-dry application in connection with their cutting performance during turning operation. It was found that coolant has significant influence on machining operation. Aoyama *et al* [2003] described the developments of mixture supply system for machining with minimal quantity lubrication (MQL). Jawaid *et al* [2001] reported the wear behaviors of two different grades of single layer PVD-TiN coated and uncoated tungsten carbide inserts during face milling of Inconel 718 at various cutting conditions. Tests were carried out on a CNC milling machine. A general purpose of emulsion with 6% concentration was used as a coolant through the tests. Barry and Byrne [2001] examined the tool wear behavior in the machining of hardened steel for cubic boron nitride cutting tool. Sreejith and Ngoi [2000]

described some examples of recent developments in the dry machining operation. They also concluded that dry machining is ecologically desirable. Further research was conducted by Rahman *et al* [2000] to describe the performance of high pressure coolant and compare with conventional coolant during machining operation. EI-Gallab and Sklad [1998] carried out a series of dry high speed turning (248 m/min - 894 m/min) tests to select the optimum tool material, tool geometry and cutting parameters for the turning of 20% SiC/Al metal matrix composites. The results showed that PCD tools sustained the least tool wear compared to TiN coated carbide tools and Al₂O₃ /TiN tools. Further research was carried out by EI-Gallab and Sklad [1998] to investigate surface integrity of machined Al/20%SiC particulate metal matrix composites (PMMC). Alauddin *et al* [1998] studied the tool deterioration in the form of flank wear in the full immersion and half immersion end milling of Inconel 718 using uncoated carbide inserts under dry conditions. Kustas *et al* [1997] presented novel material systems for coatings on cutting tools, towards accomplishing clean manufacturing i.e. without the use of a cutting fluid. Further research was conducted by Narutaki *et al* [1997] to describe the performance of cutting tools during dry machining operation. They reported that tool wear increased substantially in dry cutting operation. Rahman *et al* [1997] discussed the effect of cutting conditions on the machinability of Inconel 718. Experiments were conducted on a CNC lathe machine under wet conditions. The experimental results showed that tool life of the inserts decreased when the speed or the feed was increased. This was due to the commonly experienced high cutting forces, low conductivity, abrasiveness and hardness, tendencies of Inconel 718 resulting in high heat generated at the cutting edge. Of the cutting three forces measured, the tangential force was the largest and the smallest was

the radial force. Abrao and Aspinwall [1996] described the surface integrity for the machining of hardened steel. Further research was conducted by Brandt [1996] to identify wear mechanisms in machining operation. Liao and Shiue [1996] investigated the wear mechanism of carbide tool in cutting of Inconel 718. The experiments were carried out on a lathe machine under dry conditions. Cutting forces were measured by dynamometer. The experimental results showed that cutting forces and flank wear were larger when uncoated tool was used. Konig and Essel [1996] investigated the wear mechanisms during machining process. They mentioned that adhesive and abrasive mechanisms were found for carbide tools under different cutting conditions. Kovacevic *et al* [1995] discussed the influence of coolant during milling operation. They reported that good surface finish was achieved at higher cutting speeds. Locasto *et al* [1991] discussed the performance of carbide tools based on tool wear during machining operation

Comment on literature

Arunachalam *et al* conducted experiments using CBN tools in dry and wet cutting operation. Lower values of surface roughness were obtained when coolant was used while dry cutting resulted in higher values of surface roughness. The higher values of surface roughness in dry cutting were due to the built-up edge deposited over the machined surface. They carried out all cutting tests on the CNC lathe and the depth of cut was very low (0.05 mm). Alauddin *et al* conducted tool wear analysis in dry machining operation. The cutting speed was low (20 to 35 m/min). Coolant was not used for their research work. Abrao and Aspinwall studied surface integrity but the effect of cutting parameters on surface integrity was not considered. Experiments have been done with minimal quantity of lubrication by previous researchers [Aoyama and Lacalle *et al*]. They

investigated only tool wear and surface roughness was not measured during their study. Previous researchers [Berry and Byrne, Brandit, EI-Gallab and Sklad, Ezugwu *et al*, Jawaid *et al*, Kustas *et al*, Kovacevic *et al*, Konig and Essel, Locasto *et al*, Liao and Shieu, Narutaki *et al*, Rahman *et al*, Sreejith and Ngoi, Su *et al*, Wakabayashi *et al*] refer to the advantages of the use of a coolant system and there are several successful experiences when it is used in the machining of different materials. As the research works done so far discussed in the literature review, it was either dry cutting or coolant. Moreover, none of the above studies have compared the effect coolant and dry cut during nickel based super alloys machining operation. Therefore an attempt has been made in this thesis work to compare wet cut (coolant) and dry cut based on wear and surface finish using carbide tools under different cutting condition.

2.3 High speed machining operation

It is well known fact that high speed machining became wide spread in production practice with many benefits. Among these benefits are high productivity, good surface finish quality and high dimensional tolerances. Almost every cutting operation can be enhanced using higher cutting speeds but most frequently application of high speed machining is found in milling. Ekinovic *et al* [2005] investigated the machinability of steel at high speed milling operation. Surface roughness was the machinability indicator used in this study. Results of this investigation confirmed statement that there are some differences in behavior of same material at different states. The cutting parameters (cutting speed and feed) showed significant influence on surface roughness. Increasing in feed, according to obtained results, produce different effect on surface roughness value

for different cutting speeds. Such behavior may be product of materials plasticity and existing of slip-stick effect between tool and machined surface connected with softness of machined materials as well as the differences in process of generating chip in conventional and high speed machining. Hussein and Yahya [2005] conducted cutting tests in end milling operation. The length of chip-tool contact is small for these cutting tools as they contain a chip breaker that restricts the chip-tool contact area. In their study, the possible failure modes of wear were discussed and the effect of cutting speed and feed rate variation on tool life was investigated. An increase in tool life was noticed with increasing the cutting speed. Schroeter *et al* [2005] carried out experiments at high cutting speeds. The wear phenomenon was different for cutting speeds of 200 to 400 m/min. The entrance of the tool from the workpiece in up milling cuts causes breaks in the workpiece edge. On the other hand, the exit of the tool from the workpiece for the down milling direction caused micro breaks regardless of the programmed radial depth of cut. Coelho *et al* [2004] studied the wear behavior of ceramic tools when turning of Inconel 718 at high cutting speed. The alumina-based ceramic was the best in terms of wear. Microscopic examinations on several points and different workpieces cut with the ceramic tool used did not show any significant alterations in the microstructure. Vivancos *et al* [2004] conducted experiments in high speed milling operation. Their study was mainly focused on aspects related to surface quality and dimensional precision, which are the most important parameters from the point view of selecting the cutting conditions of processes, as well as economical aspects. From the results obtained, it follows that down milling leads to better surface finish than up milling. Chenping [2001] conducted experiments during machining operation. The

workpiece was aluminum composite. It is reported that ceramic tool is capable of high speed machining especially at high cutting speed and high feed rate cutting. Moreover, the tool bears neither built-up-edge nor flank build-up which appears with conventional tools in cutting the aluminum composite. Ng *et al* [2000] investigated tool life, cutting forces and workpiece surface roughness during high-speed milling. The workpiece material was Inconel 718. The effect of cutter orientation and tool coating on resultant cutting forces was investigated. Narutaki *et al* [1999] studied the wear characteristics of TiC added ceramic tools, square type 120408 and button type 120400 inserts under high speed turning of Inconel 718. Turning tests were conducted in the presence of a 10% water based coolant. The TiC added showed the best performance in terms of wear at the cutting speed of under 300 m/min. However when the cutting speed exceeded 400 m/min, the TiC added ceramic tool showed the higher value of wear. Zhao *et al* [1998] investigated the machinability of Inconel 718 using the SiC whisker reinforced Al₂O₃ ceramic tool. All the machining experiments were carried out on a CNC lathe under wet conditions. The results show that the SiC whisker reinforced Al₂O₃ ceramic tool can be used to machine nickel based alloys over a wide range of cutting conditions. Tool life was estimated in terms of the cutting length that the tool can endure before the maximum flank wear width reaches its limit of 0.70 mm. El-bestawi *et al* [1998] examined the cutting performance of Whisker reinforced ceramic inserts of round and square shapes during end milling of Inconel 718. The dominant of wear mechanisms and tool failure modes were studied and the effects on the cutting forces were also investigated. Experiments were conducted on a CNC milling machine under dry conditions. Gatto and Iuliano [1997] described the machining of Inconel-718. They carried out all experiments

using uncoated and coated ceramic tools (CrN) during milling operation. In their study, the results obtained in the machining of nickel based superalloys using coated and uncoated tools are presented. The coating was adopted to increase the tool life of coated tools by minimizing the temperature effects on composite reinforcement mechanisms.

Comment on literature

Chenping conducted experiments at cutting speeds from 100 to 400 m/min. On the other hand Coelho et al studied the wear behavior of ceramic tools at cutting speeds from 100 to 500 m/min. El-bestawi *et al* examined the performance of whisker ceramic tools in milling operation. The cutting speed was 200 to 700 m/min. Surface quality was not considered for their study. Ekinovic *et al* investigated the machinability of steel at cutting speeds from 120 to 300 m/min. Gatto and Iuliano investigated the performance of ceramic tools based on wear at cutting speeds from 300 to 530 m/min. Other researchers [Hussein and Yahua, Narutaki *et al* and Ng *et al*] studied the wear characteristics at cutting speed from 150 to 550 m/min. Schroeter et al carried out experiments at cutting speeds from 200 to 400 m/min. Vivancas *et al* conducted experiments at cutting speeds from 150 to 300 m/min. Zhao *et al* investigated the machinability of Inconel 718 in turning operation. Cutting tests were performed using ceramic tools at cutting speeds from 100 to 280 m/min. To date limited work has been published dealing with high speed milling of Inconel 718 using ceramic tools. The characteristics of ceramic materials that affect their performance include hot hardness, thermal shock resistance, abrasion resistance and chemical stability. The latest ceramic tools material to come into the market are Sialon (Kyon 2100) and whisker-reinforced composite ceramics. Sialon ceramics is a complex mixture of the elements silicon, aluminum, oxygen and nitrogen.

The high thermal resistance of sialon (Kyon 2100) makes it particularly suitable for heavy feed rate or interrupted cutting. Sialon retains its hardness at high temperature, which gives it excellent abrasion resistance. On the other hand whisker-reinforced composite ceramic is made by adding uniformly 25% in volume of silicon carbide whiskers into plain alumina, to improve prominently the fracture toughness and wear resistance of the compact. The whisker reinforced aluminum oxide is extremely tough, because microscopic silicon carbide whiskers are distributed randomly through the matrix. Whisker-reinforced composite ceramic has good thermal shock resistance capability. As a result, machining at very high cutting speeds, even the interrupted cutting such as milling can be performed. The whisker toughening effect first prevents catastrophic failures and second the wear resulted from micro-fracture and particles removal. We used ceramic tools for nickel based superalloys (Inconel 718) machining operation. Inconel 718 is known as a difficult-to-machine material especially at high speed owing to several inherent properties. The aerospace industry produces both airframe and engine components from nickel based superalloys. Typically, more than 90% of the material must be removed to reach the final workpiece shape, thus machining time becomes a substantial factor in the final product cost. Therefore the effect of high speed cutting (ceramic tools) conditions on wear, mechanisms and surface quality was evaluated in this thesis research work.

2.4 Wear mechanisms under stable and unstable (chatter vibration)

Chatter is a self-excited vibration, which occurs during machining operation. The occurrence of chatter is dependent on many factors such as cutting conditions, workpiece properties and dynamics of machine tool systems. Chatter is an undesirable phenomenon because it creates different effects during machining operation. Chatter vibrations result in unstable cutting process, reduced tool life and damage to the machined surface. The occurrence of tool wear mechanism is strongly influenced by chatter vibration. Wear mechanisms will be different due to unstable (chatter) condition. Understanding the wear mechanisms in the machining process will enable us to know the progression of tool wear or failure. Therefore it is important to know the behaviour of wear mechanisms in both cases (stable and unstable) in order to select proper cutting conditions. So far very little research has been done on the behaviour and comparison of tool wear analysis under stable and unstable cutting conditions. Weingaertner *et al* [2006] studied the influence of cutting parameter on the high speed milling of aluminium alloy. Cutting tests were conducted using carbide tool. The stability evaluation was based on the workpiece surface finish and the audio signal measured during the cutting process. They used microphone to detect vibrations during the cutting process. They reported that machined surface was deteriorated at higher depth of cut and process was unstable. Movahhedy *et al* [2006] studied the spindle dynamics during milling operation. The cutting tool was attached to the spindle through a standard tool holder. The signal of the machine at the tool tip was mostly affected by the dynamics of the spindle. Further research was carried out by Movahhedy *et al* [2006] for establishment of stability lobes in milling operation. In their research, they reported that proper cutting conditions could be

determined for aluminium alloy using stability lobes. Minson *et al* [2006] investigated the effect of vibration on cutting parameters and chip thickness. All experiments were conducted on aluminium and brass. The cutting tool was diamond tool. The results show that the cutting process was efficient for smaller value of depth of cut and chip thickness. Budak [2006] discussed about structural deformation in milling operation. He performed experiments for steel using carbide tool. He reported that surface defects occurred when the vibration appeared during machining operation. Further research carried out by Budak [2006] in order to establish stability lobes for aluminum alloy. The transfer function was determined by impact hammer test. The results show that cutting process was stable for different cutting speeds under a particular depth of cut. Erturk *et al* [2006] analyzed the dynamics of tool point in machining operation. They also studied the effects of contact parameters (stiffness and damping) at the spindle-holder and holder-tool point. Erturk *et al* [2006] carried out further research for establishment of stability lobes. They performed experiments for aluminium using high speed steel (HSS) cutting tool. Different feed rates were used in order to identify cutting coefficients. They identified unstable conditions using the spectrum analysis of the sound signal during cutting operation. It was found that stable depth of cut could eliminate chatter vibration. Chen *et al* [2006] discussed about stability analysis in turning operation. They performed tests using steel and bronze. The relationship between the depth of cut and spindle speed was investigated under a range of cutting conditions. The result shows that the deflection of the tool holder affects the cutting process. Castro *et al* [2006] presented a method for measurement of dynamic forces using a commercial piezoelectric dynamometer. They discussed about experimental devices and procedures for experimental tests. They

reported that the geometry and the properties of the cutting tool could change the dynamic characteristics of the system. Moufi *et al* [2006] studied the effect of cutting conditions on stability lobes and surface roughness. All cutting tests were performed on a lathe under dry condition. They indicated that the process damping could induce an increase of the machined surface roughness. It was also found that good surface finish occurred under stable condition. Rashid *et al* [2006] carried out tests in order to investigate surface roughness and tool wear for aluminium and steel. The cutting tool was carbide. The improved surface finish and the reduced tool wear provide evidence that chatter vibration was not present under stable depth of cut. Zaharnah [2006] investigated surface roughness, vibration and cutting forces in milling operation. His main objective was to maintain a constant relative position between the cutting tool and workpiece during cutting operation. He reported that surface roughness improved, when the acceleration or vibration in both the feed and radial directions reduced. Schmitz *et al* [2006] studied surface roughness and stability in milling operation. Different cutting tests were used for machined surface roughness measurement. Surface roughness is seen to increase for larger depth of cut. This could be due to the presence of chatter during cutting process. Cao *et al* [2006] discussed about stability lobes in milling operation. They reported that spindle speed, depth of cut, tool material and workpiece material properties could affect the amplitude of the vibration during machining operation. Kim *et al* [2006] investigated cutting forces for ball end milling operation. The workpiece material was aluminium. They used carbide tools and determined average cutting force coefficients. Liming *et al* [2006] presented an experimental study of the tool wear and cutting forces in milling of Inconel 718 with carbide tools. The results showed that

significant flank wear was the predominant failure mode for cutting tool during machining operation.. The tool wear progression in the up milling operation was more rapid than that in the down milling operation. They also analyzed cutting forces. It was found that for each cutting pass, the values of the cutting force components showed a steady increase within a certain range. Omar *et al* [2006] investigated cutting forces, tool wear, surface roughness and vibration in milling operation. It was found that the surface became rougher when the flank wear increased. This was due to the broken of cutting tool material on the machined surface. The cutting forces increase linearly with an increase of feed rate. Wan *et al* [2006] discussed about cutting force and cutting force coefficient in milling of aluminium (Al 2618). Cutting force coefficients were determined using average cutting forces from a number of experimental tests under different conditions. Hung *et al* [2006] studied tool wear and cutting forces in milling operation. The objective of their study was to monitor tool wear in order to replace a tool before failure. The results show that all cutting forces increase with an increase of flank wear. It is also found that cutting tool fails at larger depth of cut due to the presence of chatter in machining operation. Li and Kishawy [2006] used a self-propelled rotary tool for determination of cutting forces in turning operation. The workpiece material used in their investigation was carbon steel. Among all cutting forces, the tangential cutting force was found to be more sensitive to the changes with feed rate. There was only a slight difference in the value of cutting forces for a given feed at different cutting speed. Reddy and Rao [2006] studied cutting force, tool wear and surface roughness in milling operation. They reported that cutting force increased when the tool wear increased. This could be due to the increase in contact area between the tool and workpiece. It was

observed that as the feed rate increased, cutting forces increased. Surface roughness was found to be increase with the increase of feed rate and depth of cut. Pramanick *et al* [2006] conducted tests for cutting force measurement during composite material turning operation. The experimental results show that the tangential and thrust forces increase with an increase of feed rate. However, the rate of increase in tangential force was higher than that of the thrust force. It was also mentioned that the tangential and thrust forces decrease with an increase of cutting speed. Fontaine *et al* [2006] investigated cutting forces for steel in milling operation. The experimental results show that the cutting force increases at the beginning of contact of the cutting tool with the workpiece. This could be due to the rubbing action of the tool during machining operation. They also reported that the cutting process was more stable at higher cutting speed. Further research was carried out by Ming and Liang [2006] in order to study tool wear and cutting forces in turning operation. They reported that all cutting forces (tangential, axial and radial) increased with the increasing of flank wear. Moreover, the predicted force in tangential direction increased significantly than the forces in the other two directions. Ozturk *et al* [2006] determined cutting force coefficients for aluminium in ball end milling operation. It was shown in their research that the inclination angle had a great influence on cutting forces. Their experimental results were only useful for slot cutting of aluminium material. They did not consider vibration for their research. Araujo *et al* [2006] investigated the effect of tool geometry and cutting forces in machining operation. The results show that cutting force magnitude changed as the depth of cut was increased. They also reported that for a given helix angle, as the contact angle

of cutting tool increased, the average cutting forces increased significantly. Hamade *et al* [2006] performed cutting tests in order to determine cutting force coefficient in machining operation. It is found that the feed seems to have more pronounced effect on cutting forces among other cutting parameters. Gradisek *et al* [2005] conducted cutting tests for stability analysis in milling operation. They determined transfer function for stability lobes. The results show that the frequency of the dominant vibration mode decreases as spindle speed increases. Bravo *et al* [2005] presented stability lobes for proper cutting condition selection. Machining tests were carried out for different conditions. They did not perform tests under larger depth of cut. The experimental results showed that the cutting process was stable when the depth of cut was 2.5 mm. Liu *et al* [2005] studied machining dynamics in milling operation. They determined cutting forces, vibration and surface roughness. It is found from their study that the dynamic cutting force oscillates and excites vibration due to the improper selection of cutting parameters. The results show that cutting process has impact on surface profile. Mohdavinejad [2005] discussed about dynamic characteristics for turning operation. He performed cutting tests for acoustic emission and chatter vibration. The variations of acoustic emission signal were analyzed. It was found from his experimental tests that chatter vibration could be detected using acoustic emission signal under different cutting conditions. Baro *et al* [2005] studied cutting forces in milling operation using self-propelled cutter. It is observed from their research that the inclination angle influences on tangential and axial forces. Albrecht *et al* [2005] conducted cutting tests for cutting force and vibration analysis in milling operation. The workpiece materials were steel and aluminium. They used microphone in the cutting zone in order to determine stable cutting conditions. They

reported that stable cutting conditions could be achieved by changing depth of cut and spindle speed. Polini and Turchetta [2004] investigated cutting forces under different parameters such as depth of cut and feed rate. A diamond tool was used for their investigation. They determined cutting force coefficient from cutting force data. Peigne *et al* [2004] studied vibration and surface roughness in milling operation. Their experiments confirmed the existence of a domain in which cutting conditions were unstable at high cutting speed. They also mentioned that machined surface was deteriorated under unstable conditions. Lamikiz *et al* [2004] carried out cutting tests on sculptured aluminium workpiece in order to determine cutting forces in milling operation. All tests were conducted using carbide tool. They estimated cutting force coefficient for different cutting conditions. Solis *et al* [2004] conducted tests for vibration. They increased cutting speed for their tests to reduce chatter. The results show that chatter occurs due to the interaction between the tool and workpiece and larger depth of cut.

Comment on literature

Researchers [Weingaertner and Movahhedy] established stability lobes for aluminum alloy. Therefore their experimental results will not be useful for nickel based superalloys. Minson *et al* reported about tool vibration and chip thickness. They did not consider stability analysis for their research work. Budak and Erturk discussed about stability analysis. They conducted tests at high cutting speed (above 10000 rpm) for steel and aluminium. But it will be very difficult to perform test at high cutting speed for nickel based superalloys using carbide tool. Chen and Castro investigated dynamic characteristics in turning operation. The common point of their study was system dynamics information at the tool point. They did not study wear mechanisms or surface

roughness in order to select proper cutting conditions. Moufki *et al* investigated vibration in feed direction under orthogonal cutting operation. Their analysis can not provide sufficient information about milling process. Although Rashid and Zaharnah addressed about vibration, cutting force, tool wear and surface roughness. But they did not focus on wear mechanisms, which was essential in order to obtain the information about wear progression during machining operation. Schmitz *et al* studied only roughness for different conditions. Kim *et al* did not consider stable cutting conditions for their research. Liming *et al* reported that the variation of the cutting forces occurred during machining operation. This could be due to the thermal effect for the cutting force variation within a single cutting pass. Omar *et al* discussed about dynamic behaviour in machining operation but they did not consider stability in their work. Hung *et al* studied about tool wear monitoring system. However the variation of cutting forces was not reported in their research work. Li and Kishawy determined cutting forces for different cutting conditions in turning operation. Their research was based on self-propelled rotary tool. Therefore, the cutting force data does not provide useful information for other cutting tool. Reddy and Rao reported that the machined surface was deteriorated at larger depth of cut. This might be the presence chatter vibration during machining operation, which was responsible for damage of machined surface. Pramanick *et al* investigated cutting forces but they did not consider stable depth of cut for their experimental work. Fontaine *et al* reported that cutting process was stable at higher cutting speed. They did not investigate machining dynamics for their research work. Ozturk *et al* did not consider vibration under stable and unstable conditions. Gradisek *et al* reported about chatter vibration. The effect of wear under stable and unstable was not analyzed during their

research work. Bravo and Liu discussed about machining dynamics and cutting forces for aluminum and carbon steel. The stable depth of cut was found to be 3.5 mm. It will not be possible to use this depth of cut for other workpiece material such as nickel based superalloys. Mohdavinejad *et al* reported machining dynamics and stability lobes. Their research was focused on the effect of structural parameters in machine instability, so no efforts were made to assess the stable and unstable cutting conditions. Peigne *et al* discussed about vibration and surface roughness but the analysis of wear mechanism was not reported in their research work.

CHAPTER 3

Equipment and instrumentation

The first benefit offered by all forms of CNC machine tools is improved automation. CNC machine was used in this research to machine nickel based superalloys (Inconel 718) material. Inconel 718 is a high strength, thermal resistant nickel based super alloys and it is difficult to machine. The primary use of these alloys is in aircraft gas turbines, space vehicles and nuclear power systems. We describe about instruments and cutting tools in this chapter.

3.1 Equipment for machining experiments

The cutting tests were performed using a five axis CNC milling machine. The inspection of the surface roughness was carried out using a stylus-type surface roughness machine. Tool maker's microscope was used to measure wear. Wear mechanism were examined using scanning metallographic microscope. The equipment and instrumentation are discussed below.

3.1.1 CNC milling machine

The characteristic features of most workpieces to be processed in tools, forms and models include large dimensions, increasingly complex free form surfaces and highest quality when it comes to surfaces and precision.

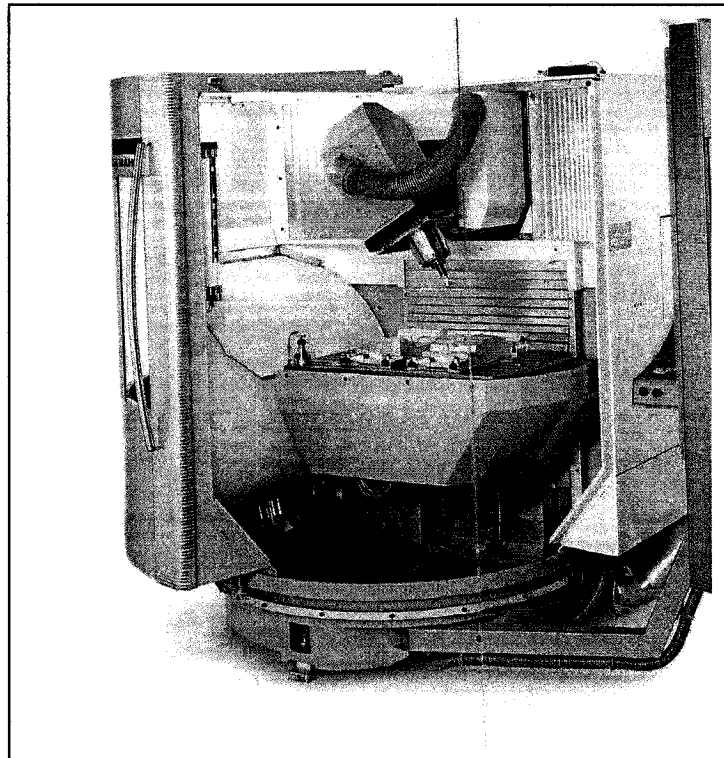


Figure 3.1: CNC milling machine

The CNC milling (DECKEL-MAHO) machine is the new class of compact universal milling machines. The maximum spindle speed is 12000 rpm. The enhanced DMU range provides accuracy, precision and high service finish. It has five axis, a new swivel cutting head with B-axis for negative angles up to 30°, choice of different spindles and the large range of options. The modular concept of this CNC machine ensures the necessary rigidity and also offers optimum ergonomics and user-friendliness. These innovative easy access and user-friendly machines open up a new range of production for efficient universal applications. Figure 3.1 shows the CNC milling (DECKEL-MAHO) machine.

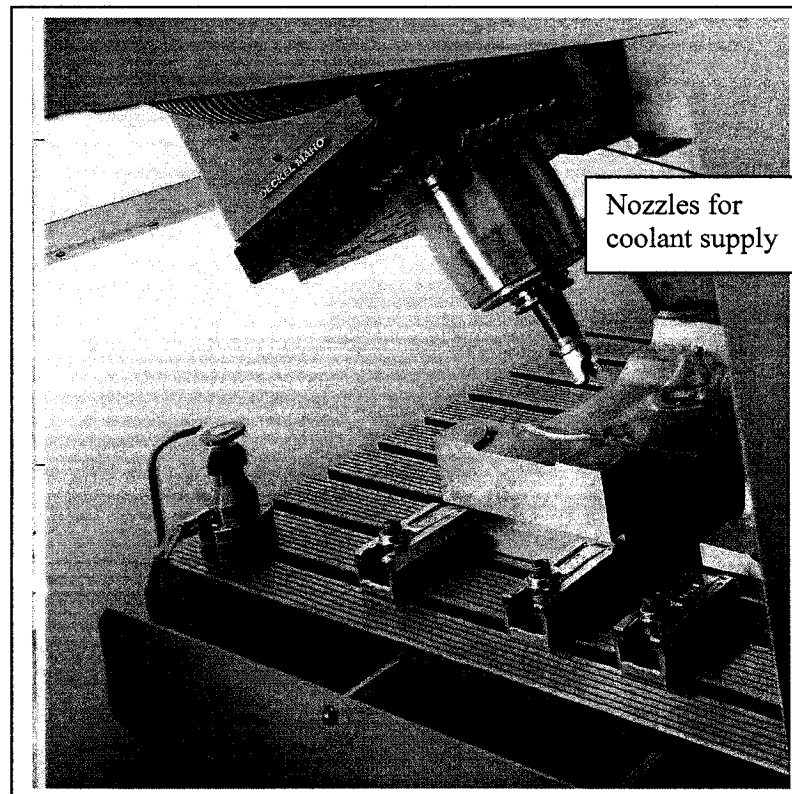


Figure 3.2: Coolant supplied through nozzles in CNC milling machine

Figure 3.2 shows nozzles for coolant supply during machining operation. The milling machines and machining centres are universal both in respect of 5-sided and 5-axis integrated machining by one machine and in respect of the modular machine design from various lines of product and their technological solutions in the hardware and software field. A wide range of technologies and equipment variations, such as 5-axis simultaneous machining or high-speed cutting, complement the features of the basic machines. The vertical machining centres for flexible serial production stand out due to their high availability in day-to-day use and high constant precision even at extreme loads. The vertical machining centres therefore ensure an economic production. The new generation of vertical machines uses state-of-the-art linear drive technology, offering extra dynamics and efficiency.

3.1.2 Surface roughness machine

The Mitutoyo Surftest is portable for measurement of surface roughness during machining operation.



Figure 3.3: Surface roughness machine

This surface roughness instrument shown in Figure 3.3 is rugged and lightweight, with a detachable drive unit for tight spots, easy-to-view LCD screen, and wide range of evaluation methods that make it an efficient portable roughness tester. in its class.

3.1.3 Microscope

The viewing and measuring unit of the microscope is mounted within a robust steel casting which is webbed to give the maximum rigidity between the end plates, the base and the microscope carriage supports as shown in Figure 3.4. The microscope carriage is mounted between the end plates of the casting and which with the casting form a rigid box construction. The sliding carriage carries a scale which butts against a gradual bar running the full length of the microscope. A swiveling focusing magnifier is mounted on the carriage for reading the scale. The microscope carriage slides freely over a third central rod which is spring loaded via a thrust bearing against a micrometer screw fitted with a calibrated drum, which is mounted on one end of the casting. The sliding carriage

can be readily and firmly clamped to the central rod and when clamped can therefore be moved by means of the micrometer drum. Since the microscope carriage is spring loaded against the micrometer screw, the microscope can be used in any position and the microscope body and focusing mechanism can be pivoted on its axis for the measurement of tool wear.

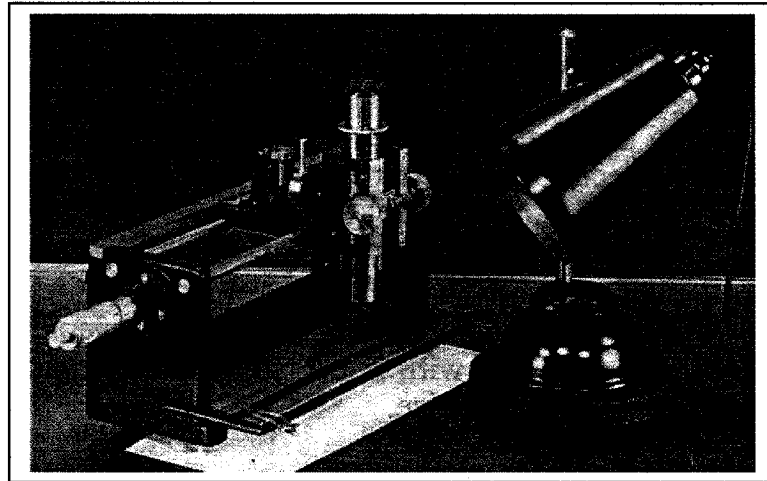


Figure 3.4: Microscope for tool wear measurement

The microscope body accepts any objective or eyepieces of standard specification used with ordinary microscope. The eyepiece tube is fitted with a clip restraint so that eyepiece will not easily rotate or fall out. The eye tube is attached to a sliding tube graduated with millimeters for the variation of the initial magnification of any object. Cutting tools were examined under microscope to measure the tool wear. Average and maximum flank wear were recorded. Figure 3.4 shows tool wear measuring microscope. It can be used for the tool room or production inspection of screws, thread gauges, taps and for the measurement of form tools, templates and castings. Scanning metallographic microscope can improve conventional images by recording fluorescence generated from the focal plane within the sample, while rejecting all other light coming from above or below the focal. The microscope system is a fully integrated workstations that incorporate user-

friendly image acquisition and image analysis software with high-resolution confocal optics that require no user alignment. A windows based graphic user interface allows new users to quickly generate images in various scan modes. Multi-parameter experiments can be quickly designed and executed through the powerful software package. With this software, new images involving multi-location acquisition can be easily generated and saved into the computer. The microscope is equipped with several efficient scanning modes, including point, line, and free line, and rectangle, which are especially suited for detection of material structure information.

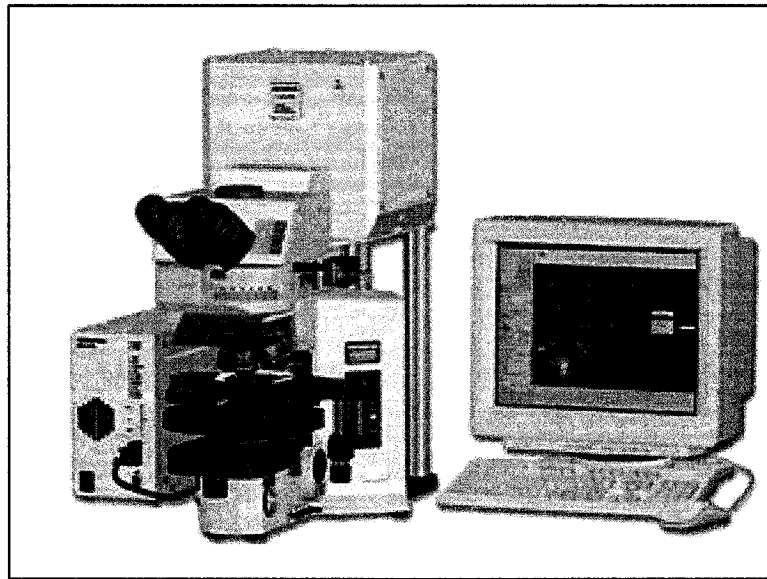


Figure 3.5: Scanning metallographic microscope for wear mechanisms examination

The cross section image may also be rotated 360° or drawn as a free line (free line-Z). It acquires a single XY confocal optical image over time, at an interval that can be arbitrarily chosen. It acquires a single line image over time for time-lapse analysis with high temporal resolution. The cross section image may also be rotated 360° or drawn as a free line (free line). Figure 3.5 shows scanning metallographic microscope (SMM).

3.2 Cutting tool materials

Friction and wear of cutting tools often detrimentally limit the performance of cutting processes. To ensure a good performance and a high wear resistance, the cutting tool materials have to fulfill certain requirements regarding their physical properties. Important criteria, in addition to the dimensional quality in terms of size and shape are the mechanical properties of the cutting material, for example high hardness and toughness at elevated temperatures. The toughness is indicated by the critical stress intensity factor, which describes the stress concentration required at the end of crack to extend that crack.

3.2.1 Carbide tools

Micrograin carbides are considered reliable tools being relatively insensitive to changes in cutting parameters due to their smaller grain size. These tools have a lower affinity with Inconel 718 compared to tungsten carbides thus exhibiting a good resistance to wear. Four types of carbide inserts were used for this study. The carbide inserts are as follows:

- APKTIC28: uncoated micrograin carbide
- APCTIC28: uncoated micrograin carbide
- APKTIC928: TiAlN coated micrograin carbide
- HM90APKT: TiAlN coated micrograin carbide

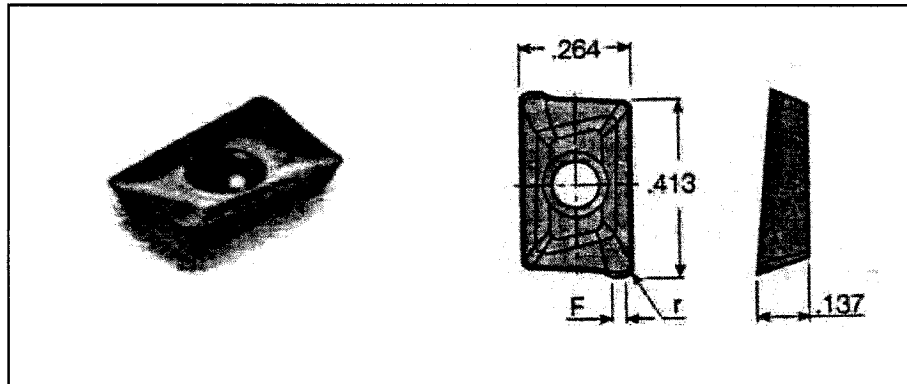


Figure 3.6: Carbide inserts (APKT and APCT)

The insert was rigidly clamped in a specially designed tool holder to present the required tool geometry. The cutter diameter was 19.05 mm. Figure 3.6 shows carbide inserts (APKT and APCT). The nose radius of each insert is 0.51 mm. On the other hand, HM90APKT has different nose radius (0.79mm). Figure 3.7 shows HM90APKT coated carbide insert.

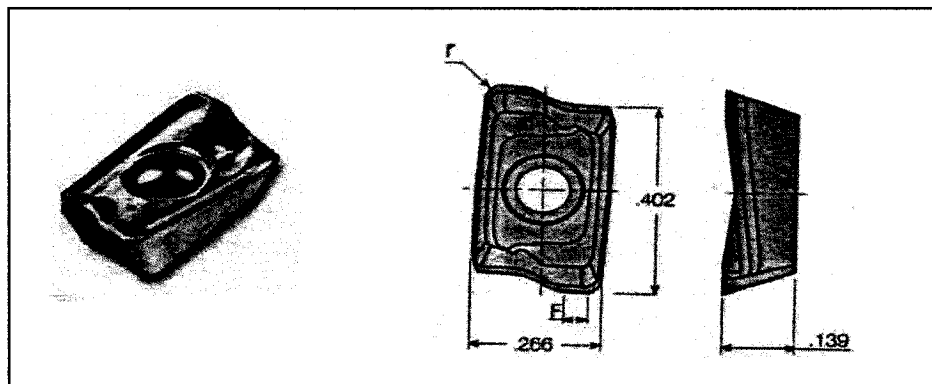


Figure 3.7: Carbide insert (HM90APKT)

3.2.2 Ceramic tools

Ceramics for cutting purposes can be either aluminium oxide or silicon nitride ceramics. Due to the high hardness at elevated temperatures and the reduced resistance against

thermal shock, ceramics are often used without a cooling lubricant supply. Figure 3.8 shows a Whisker reinforced ceramic tool holder. The cutter diameter was 50.8 mm.

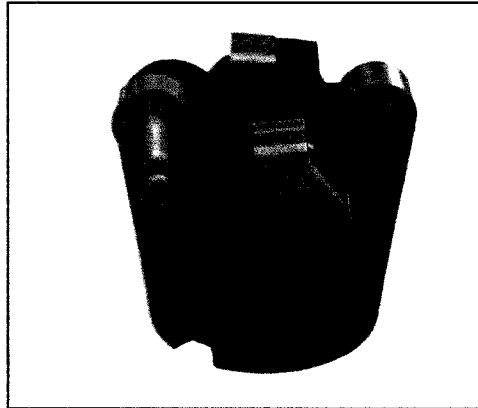


Figure 3.8: Tool holder for Whisker reinforced ceramic

The ceramics were Whisker-reinforced ceramic composite (WG-300) and silicon nitride based Kyon 2100 tool. They were used with two different tool holders. The round inserts were 12.7 mm in diameter and 7.94 mm thick. Tool holder for Kyon 2100 insert is shown in Figure 3.9

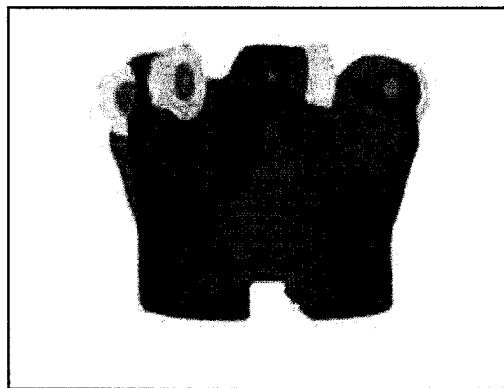


Figure 3.9: Tool holder for Kyon 2100

CHAPTER 4

Wear and surface quality for carbide tools

At present only few research findings have been published on milling performance of Inconel718 with carbide tools during wet (coolant) cutting. Recently with intensive research in machining technology, new tool materials such as micro grain carbides are becoming popular. We studied the performance of coolant in the milling of Inconel 718 with carbide tools. Cutting fluids are used to improve the machinability during machining. Cutting fluid improves machinability by reducing tool wear and improving surface finish. Cutting fluid performs the following functions: cooling, lubrication and chip flushing. Cooling and chip flushing are the most important functions during machining operation. In this chapter the author has focused on tool wear and surface quality using micrograin TiAlN coated and uncoated carbide tools. The effect of cutting conditions such as speed, feed rate and coolant on tool wear and surface roughness will be discussed.

4.1 Carbide tools for machining operation

Wide choice of coatings available now a days and technologies are growing in the last years demanding for the state-of-the-art surface modification methods. Cutting tools represent one of the fundamental links in any machining process. Tool life and behaviour often sets the machining process limits and greatly influence the machining economics and machine tool development. One of the principal characteristics of nickel based super alloys machining is given by the cutting temperatures generated. The thermal load on the cutting edge rises considerably when increasing the cutting speed, drastically reducing the tool life when attempting to use conventional, high speed steel cutting tools, thus new tool materials and/or coatings need to be developed in order to assure the feasibility of nickel based super alloys machining. This aspect is very important in milling, where special demands regarding the edge toughness and resistance to thermal fatigue are placed on the cutting tool. Therefore micro grain coated carbide are now the materials of choice in milling operation. As presented by Nelson *et al* [1998], often the cutting speed range has been limited by the tool material capability. A comparison between cemented carbide tool and PCBN one demonstrates that, for specific applications the tools have complementary ranges of cutting speeds, the carbide tool being suitable for applications when cutting speed will not exceed 80 m/min. In a study published by Alauddin *et al* [1998], cutting results were obtained when uncoated tools were used in end milling of Inconel 718. In their research the cutting speed was considered as the essential parameters regarding the tool wear. Currently, it is estimated that 75% of all cutting tools sold are carbide. The composition and range of coatings is extremely diverse; for example recent coated products comprise of individual layers of 1 to 4 mm thick. In

contrast to turning, there is relatively little published information on milling of nickel based super alloys and in particular Inconel 718 with carbide cutting tools. The maximum temperature reached during machining of Inconel 718 can be extremely high. Resistance to softening at elevated temperature represents a crucial factor in machining with carbide tools thus has to be taken in consideration when assessing the machinability of Inconel 718. Dobrzanski and Golombek [2005] showed that multilayer coatings reduced the extent of thermal cracking when a base coating with a low co-efficient of thermal expansion was used. Currently TiAlN coatings have proved increasingly useful in the cutting tool industry. The literature shows that new coated carbide may offer the greatest potential achieving a robust and reliable process that can be used in nickel based super alloys machining operation. Coated carbides have good wear resistance and strength. The properties of carbides are mainly on the ratio of tungsten carbide to cobalt binder and the grain size of the compound. In general, the finer the grain size, the more wear resistant of the cutting tool material. On the one hand, micrograin cutting materials possess high strengths at elevated temperatures. On the other hand, the very fine and homogeneous structure of the cutting materials leads to satisfactory tensile strengths. The high strength and hot hardness of the micrograin carbide cutting material resulted in excellent process operation. The introduction of micrograin TiAlN coated carbide tools has made it possible to machine Inconel 718 at higher cutting speeds. To date very few tests on milling have incorporated with carbide tools under wet (coolant) and dry conditions. The cutting material used in this investigation was micrograin TiAlN coated and uncoated carbides. Therefore the following experimental work was undertaken to assess the

performance of coolant using micrograin TiAlN coated and uncoated carbide tools during milling of Inconel 718.

4.1.1 Selection of cutting conditions

Cutting conditions and machining parameters should be selected from the most advantageous ranges. Jawaid *et al* [2001] performed tests at cutting speeds from 30 to 50 m/min for uncoated carbide tools and at cutting speeds of 70 to 100 m/min for TiN coated carbide tools. The tool life was less than 1 (one) min at cutting speed of 100 m/min. He suggested that coatings act as thermal barriers due to their high heat resistant capability and thus prevent high cutting temperatures acting on the substrate. Kudou *et al* [2003] put forward the same argument to explain the improved performance of coatings for machining operation. We carried out tests at cutting speeds from 40 to 70 m/min for uncoated carbides and at cutting speeds from 40 to 100 m/min for TiAlN coated carbide tools. Attempts to increase cutting speeds over 70 m/min resulted in rapid wear for uncoated carbide tools. Therefore the cutting speed was raised up to 70 m/min for uncoated tools. On the other hand, TiAlN coated carbide tools can not be used for nickel based super alloys machining at cutting speed of 110 m/min because they can not withstand the high temperature and stress in the cutting zone during machining operation. For this reason, we selected cutting speeds from 40 to 100 m/min for coated carbides. A larger feed can produce a rough surface consequently deteriorating the machined surface quality. Feed rates were chosen between 0.025 to 0.04 mm/tooth for better surface finish. Rahman *et al* [2000] mentioned that higher depth of cut can damage tool surface. A higher change in depth of cut does contribute directly to the change in height of surface irregularities and hence the surface finish. Thus we maintained the depth of cut of 1.5

mm throughout the cutting test. Down milling operation was conducted for longer tool life. Therefore it may be concluded that the test matrix prepared for this experimentation can be safely used in the chosen range of cutting parameters.

4.2 Tool wear criteria

Nickel based super alloys are generally difficult materials to machine since they have low thermal conductivity and high strength. Tool failure modes could be classified in two principal categories: catastrophic failure and gradual wear. Obviously gradual wear can ultimately lead to catastrophic failure but this effect could be avoided by monitoring the stages of tool wear. Often the tool life is determined not by the tool failure but due to poor surface finish to the point where catastrophic failure is imminent due to a high degree of tool wear. Types of catastrophic failure include plastic deformation of the tool edge to the point where the tool geometry is altered, cutting edge breakage or chipping and the extreme situation of complete tool fracture. Due to the possibility of Injury and workpiece and machine tool damage, the complete fracture is the most unwanted and costly tool failure. Jawaid *et al* [2001] showed that tool life of carbide tools when machining Inconel 718 was dominated by flank wear and fracture caused by a combination of plastic deformation, diffusion, abrasion and adhesion. They determined the tool life based on maximum flank wear of 0.7 mm according to ISO when flank wear occurred on the tool surface. The major regions of tool wear (Figure 4.1) are firstly, flank wear, secondly, crater wear and thirdly, notch wear. It is seen that one of these dominates the rest depending on the cutting condition. Tool life is not very much influenced by the other secondary types of tool wear such as inner and outer chip notch on the rake face, the primary groove on the side of the flank and the secondary groove on the flank end.

Each set of parameters chosen will give rise to a specific type of tool wear on the cutting tool. Flank wear plays a more important role in determining tool life. Flank wear occurs due to frictional contact between the workpiece and the flank of the cutting tool. It starts at the cutting tip and then widens as the contact area increases, thus forming the wear land. The width, shape and growth rate of the wear land depends on the depth of cut, the material of the tool and workpiece and the cutting parameters respectively. The friction between the cutting tool and workpiece material during the machining process would raise the temperature of the tool at the cutting edge. This increase in temperature further influences the properties of the material and the formation of the wear land. In the initial phase, the flank wear affects only the coating, then, with the cutting progression, the uniform wear phase reached. Because of the lower wear resistance of the tool material relative to the coating the flank wear is more accentuated in the areas where the coating was spalled thus the progression be continuously and gradually.

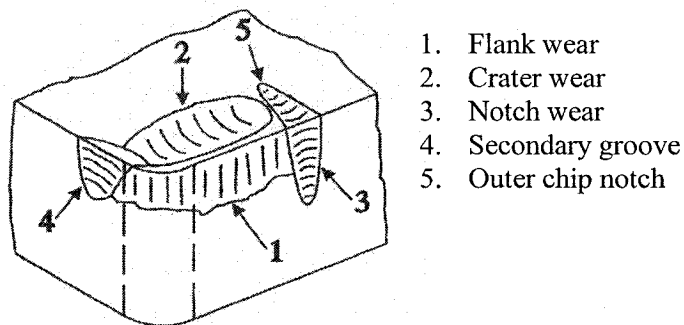


Figure 4.1: Different forms of tool wear on cutting tool

Tool wear depends upon many factors: - physico mechanical properties of the material being machined and of the tool material, conditions of the surfaces and cutting edges of the tool, type of cutting fluid and its physico chemical properties, cutting variables, condition of the machine tool, rigidity of the machine tool-workpiece complex and other

machining factors. The performance of a cutting tool is one of the most critical elements in automated production. Any cutting tool engaged in a machining operation is subjected to wear. It occurs in several major forms and often more than one mechanism operates simultaneously. If the cutting tool is allowed to wear excessively, the quality of the workpiece will deteriorate or may even be damaged. In addition, it can also be detrimental to the machine tool itself. This is obviously undesirable, as it will increase production costs. Therefore, it is important to change the cutting tool at the right time to have an optimal utilization of the cutting tool. In up milling the tooth of the cutter is subjected to heavy friction in sliding over the cut surface. Therefore intense flank wear occurs in up milling whereas in down milling, the tooth of the cutter enters into the workpiece without sliding. For this reason tool wear should be less in down milling than in up milling. Tool life is defined as the cutting time (the start of cut to the end of cut) required to reach the value of maximum flank wear.

4.3 Experimental work

This work presents a comparative experimental study on the performance of TiAlN coated and uncoated carbide tools during milling of Inconel 718 under wet (coolant) and dry conditions. Several critical issues such as wear mechanisms, tool life and surface roughness were investigated as well as the influence of various cutting parameters on tool performance. Dry and wet (coolant) cutting conditions were used and the influence of coolant on tool life and surface roughness was also examined. The experiments were planned to provide a comprehensive assessment of the use of carbide tools in milling of Inconel 718. Cutting tests were performed on a CNC milling machine to obtain tool wear and surface roughness information during nickel based super alloys machining operation.

The work pieces (Inconel 718) were prepared in the form of 170 x 110 x 110 mm rectangular blocks. Water based cutting fluid (Blasocut 2000 universal) was used as a lubricant during milling of Inconel 718 using carbide inserts. The cutting fluid was delivered to the cutting zone through nozzles. Depth of cut (d) was 1.5 mm constant for carbide inserts. The processes utilized for tool-life testing were half-immersion (down cut) milling operations. Average flank wear (VB) and maximum flank wear (VB_{max}) were measured by microscope. The tool life tests were carried out for carbide inserts accordance with ISO. Tests were stopped when the maximum flank wear (VB_{max}) reached at 0.70 mm. Surface roughness parameters (R_a,R_t) were measured by a portable stylus type surface roughness tester (Mitutoyo). The measured surface roughness was obtained by averaging the surface roughness values at a minimum of four (4) location points along the length of the machined workpiece. A cut-off value of 0.8 mm was used when measuring the surface roughness of the workpiece. Wear mechanisms were examined using scanning metallographic microscope (SMM). Table 4.1 shows the test matrix up to cutting speed of 70 m/min for uncoated (APKTIC28) carbide inserts and tick indicates the same cutting parameters used for each set of cutting conditions.

Table 4.1: Test matrix for uncoated carbide (APKTIC28)

	v (m/min)	f (mm/tooth)	Environment	Immersion
Condition 1	40	0.025 0.030 0.035 0.040	coolant dry	half
Condition 2	50	√	√	√
Condition 3	60	√	√	√
Condition 4	70	√	√	√

We found that tool wear increased when cutting speed exceeds over 70 m/min for uncoated carbide inserts. Table 4.2 shows the test matrix for uncoated (APCTIC28) carbide inserts.

Table 4.2: Test matrix for uncoated carbide (APCTIC28)

	v (m/min)	f (mm/tooth)	Environment	Immersion
Condition 1	40	0.025 0.030 0.035 0.040	coolant dry	half
Condition 2	50	√	√	√
Condition 3	60	√	√	√
Condition 4	70	√	√	√

The tool wear is a direct function of the carbides grain size. Micrograin carbide tools are more resistant to wear. Table 4.3 lists the cutting parameters and their respective value for coated (APKTIC928) carbide inserts.

Table 4.3: Test matrix for coated carbide (APKTIC928)

	v (m/min)	f (mm/tooth)	Environment	Immersion
Condition 1	40	0.025 0.030 0.035 0.040	coolant dry	half
Condition 2	50	√	√	√
Condition 3	60	√	√	√
Condition 4	70	√	√	√
Condition 5	80	√	√	√
Condition 6	90	√	√	√
Condition 7	100	√	√	√

The coating layer properties should be such as to improve the tool life and minimize the negative influence of cutting parameters. Table 4.4 shows the cutting conditions for coated (HM90APKT) carbide.

Table 4.4: Test matrix for coated carbide (HM90APKT)

	v (m/min)	f (mm/tooth)	Environment	Immersion
Condition 1	40	0.025 0.030 0.035 0.040	coolant dry	half
Condition 2	50	√	√	√
Condition 3	60	√	√	√
Condition 4	70	√	√	√
Condition 5	80	√	√	√
Condition 6	90	√	√	√
Condition 7	100	√	√	√

4.4 Experimental results

During the milling test, wear gradually developed on the flank faces of cutting tool. For the cutting of Inconel 718, flank wear was the primary concern; therefore, its width was taken as the criterion of tool life. In order to understand the development of tool wear, the worn tools were examined thoroughly under tool wear measuring microscope.

4.4.1 Tool wear for uncoated and coated carbides

The combination of cutting parameters and coolant has significant influence on the value of tool wear. In the cutting tests performed on Inconel 718, the increase in cutting speed at a constant feed caused a noticeable reduction of tool life. Alauddin *et al* [1998] reported that tool life was found to be greater when the cutting speed increased. They also reported that tool life was longer in down milling than up milling. Therefore, the down milling operation was conducted for all our experiments.

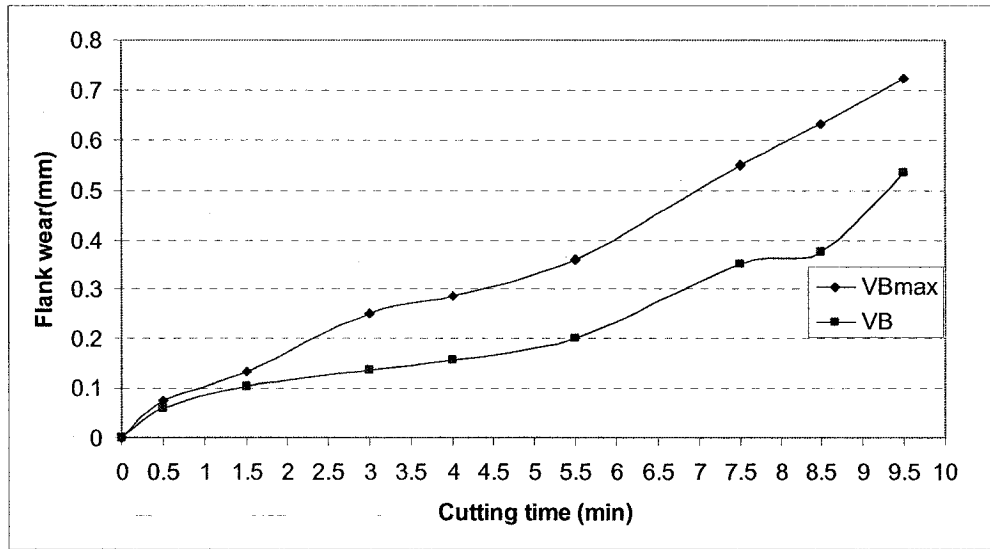


Figure 4.2: Flank wear vs. Cutting time (APKT, uncoated insert
 $v = 50$ m/min, $f = 0.025$ mm/tooth, wet (coolant) cutting)

Figure 4.2 shows the variation of flank wear with time for uncoated (APKT) carbide tool at the cutting speed of 50 m/min under wet cutting. The tool life is 9.5 min based on maximum flank wear.

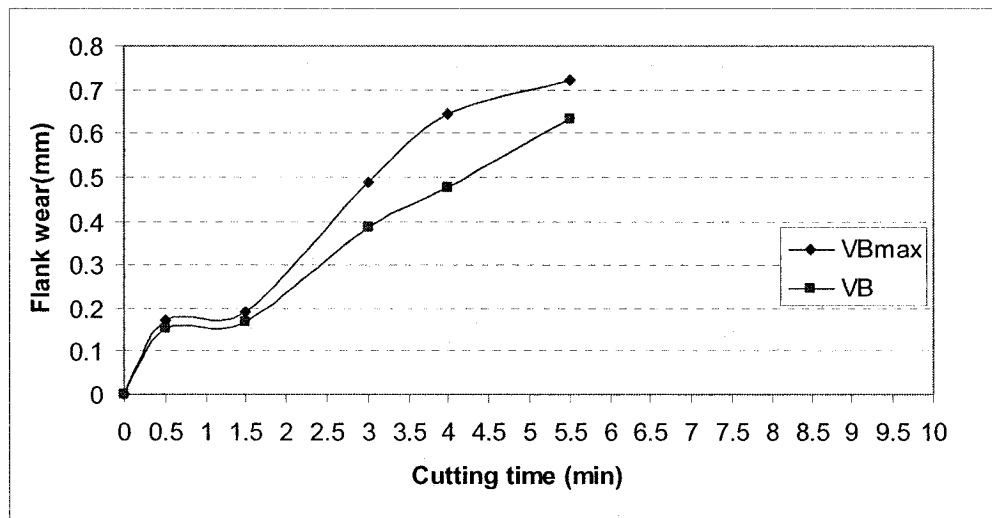


Figure 4.3: Flank wear vs. Cutting time (APKT, uncoated insert
 $v = 50$ m/min, $f = 0.025$ mm/tooth, dry cutting)

Figure 4.3 shows the variation of flank wear for uncoated (APKT) carbide at the cutting speed of 50 m/min under dry cutting. The tool life is 5.5 min.

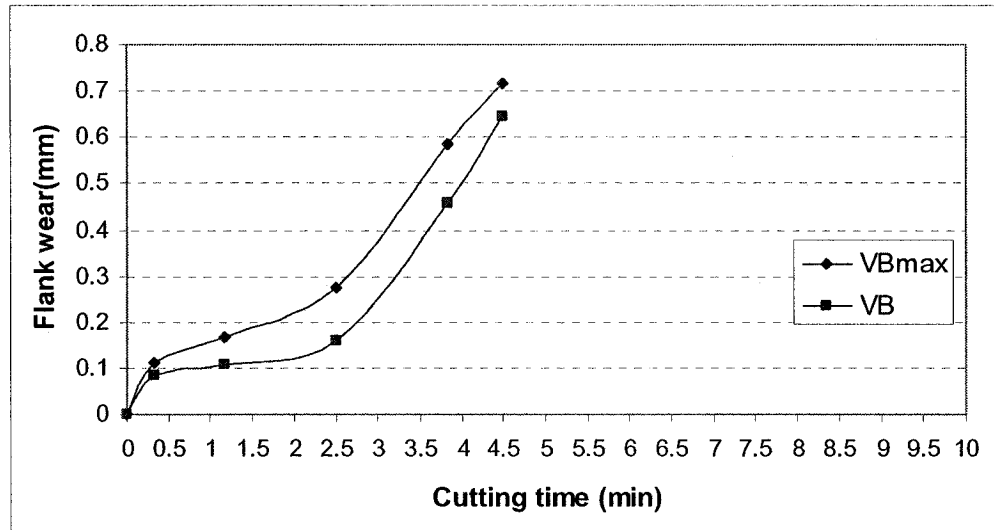


Figure 4.4: Flank wear vs. Cutting time (APKT, uncoated insert $v = 70$ m/min, $f = 0.025$ mm/tooth, wet cutting)

Figure 4.4 shows the variation of flank wear for uncoated (APKT) carbide at the cutting speed of 70 m/min under wet cutting. The tool life is 4.5 min.

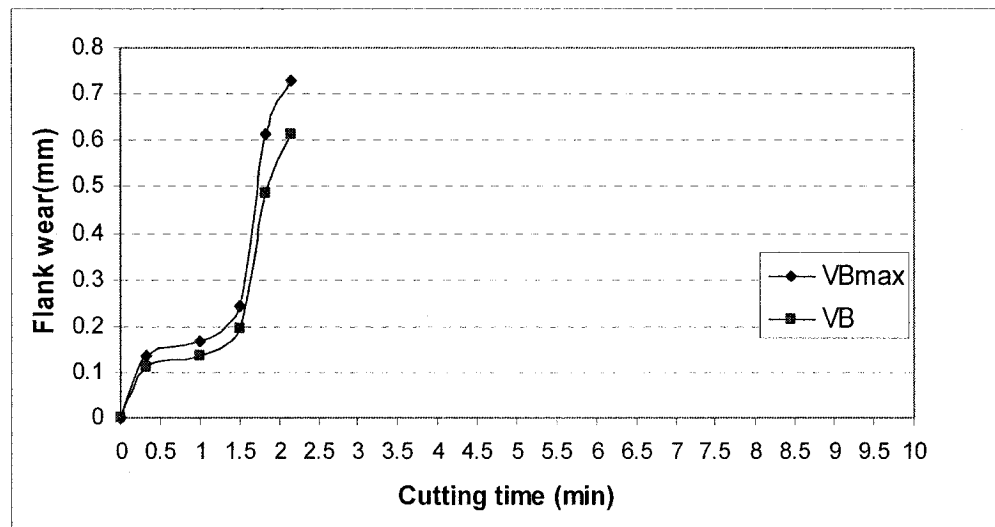


Figure 4.5: Flank wear vs. Cutting time (APKT, uncoated insert $v = 70$ m/min, $f = 0.025$ mm/tooth, dry cutting)

Figure 4.5 shows the variation of flank wear for uncoated (APKT) carbide at the cutting speed of 70 m/min under dry cutting. The tool life is 2.1 min.

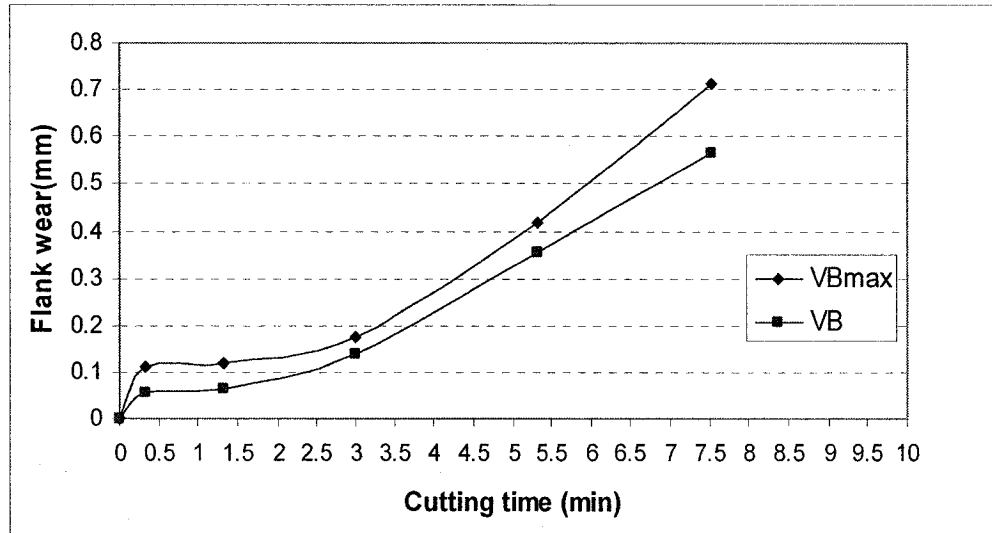


Figure 4.6: Flank wear vs. Cutting time (APCT, uncoated insert $v = 50$ m/min, $f = 0.025$ mm/tooth, wet cutting)

Figure 4.6 shows the variation of flank wear for uncoated (APCT) carbide at the cutting speed of 50 m/min under wet cutting. The tool life is 7.5 min.

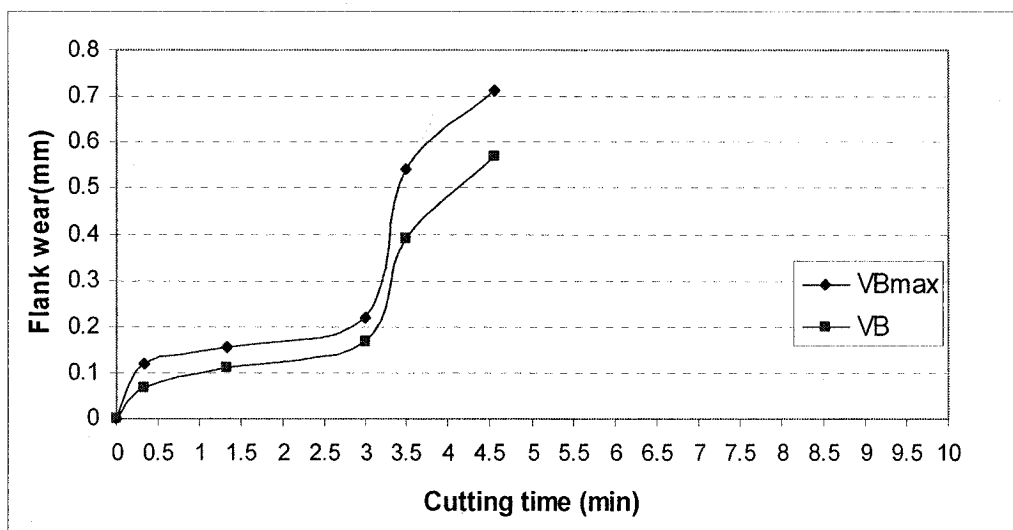


Figure 4.7: Flank wear vs. Cutting time (APCT, uncoated insert $v = 50$ m/min, $f = 0.025$ mm/tooth, dry cutting)

Figure 4.7 shows the variation of flank wear for uncoated (APCT) carbide at the cutting speed of 50 m/min under dry cutting. The tool life is 4.5 min.

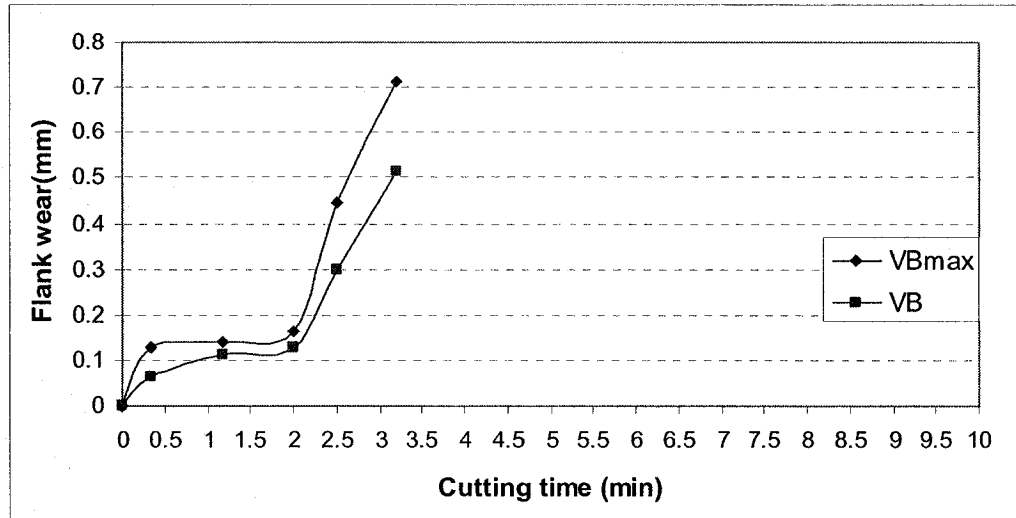


Figure 4.8: Flank wear vs. Cutting time (APCT, uncoated insert $v = 70$ m/min, $f = 0.025$ mm/tooth, wet cutting)

Figure 4.8 shows the variation flank wear for uncoated (APCT) carbide at the cutting speed of 70 m/min under wet cutting. The tool life is 3.2 min.

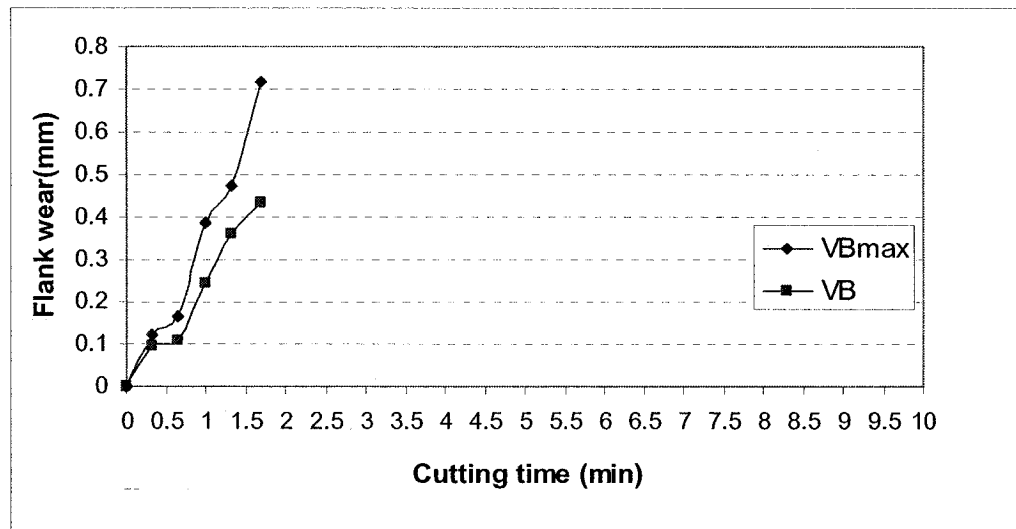


Figure 4.9: Flank wear vs. Cutting time (APCT, uncoated insert $v = 70$ m/min, $f = 0.025$ mm/tooth, dry cutting)

Figure 4.9 shows the variation flank wear for uncoated (APCT) carbide at the cutting speed of 70 m/min under dry cutting. The tool life is 1.7 min. Two types of uncoated carbide inserts (APKT and APCT) were used. The flank wear rate at various cutting conditions when milling with uncoated carbide tools were shown in figures 4.2 to 4.9. The difficulties in machining of nickel based super alloys are usually its high temperature, high resistance to plastic deformation and severe work hardening. The requirements for tool material for machining nickel based super alloys are regarded as high strength and toughness at high temperatures, especially high thermal conductivity and resistance to thermal shock. With an increase in cutting speed more heat is generated causing thermal considerations to reduce tool life. Both uncoated inserts exhibit decreased tool life with increasing cutting speed. The APKT tool performs slightly better than APCT tool. Occurrence of built-up edge (BUE) on the tool face was found to be very common while machining at low cutting speed (35 m/min). On the other hand uncoated tools experienced breakage when cutting speed was raised to 80 m/min, generating a short tool life of under less than 1 min. Therefore cutting conditions were chosen at cutting speeds from 40 to 70 m/min for uncoated carbide tools.

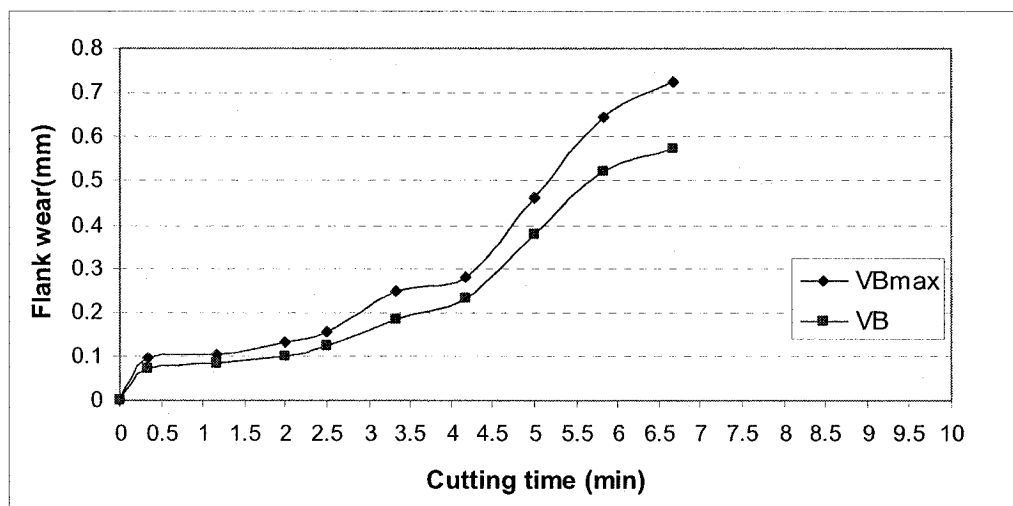


Figure 4.10: Flank wear vs. Cutting time (HM90APKT, coated insert $v = 70$ m/min, $f = 0.025$ mm/tooth, wet cutting)

Figure 4.10 shows the flank wear variation with time at the cutting speed of 70 m/min for coated (HM90APKT) carbide tool under wet condition. The tool life is 6.7 min.

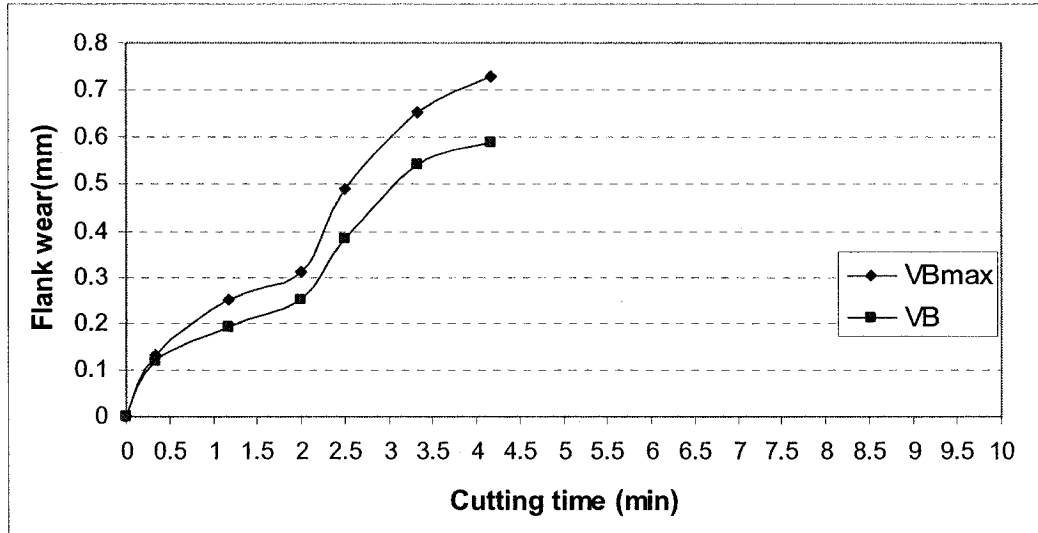


Figure 4.11: Flank wear vs. Cutting time (HM90APKT, coated insert $v = 70$ m/min, $f = 0.025$ mm/tooth, dry cutting)

Figure 4.11 shows the flank wear variation with time at the cutting speed of 70 m/min for coated (HM90APKT) carbide tool under dry condition. The tool life is 4.2 min.

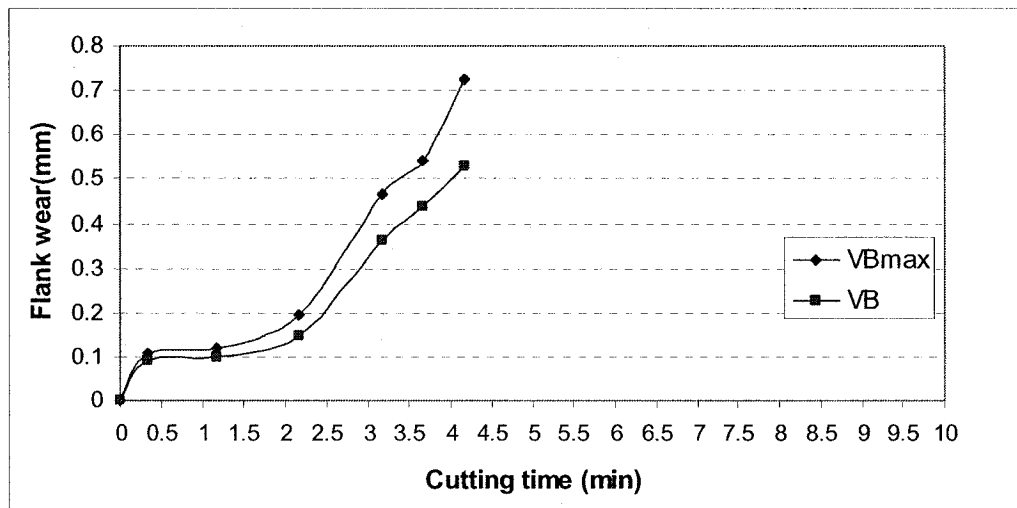


Figure 4.12: Flank wear vs. Cutting time (HM90APKT, coated insert $v = 90$ m/min, $f = 0.025$ mm/tooth, wet cutting)

Figure 4.12 shows the flank wear variation with time at the cutting speed of 90 m/min for coated (HM90APKT) carbide tool under wet condition. The tool life is 4.1 min.

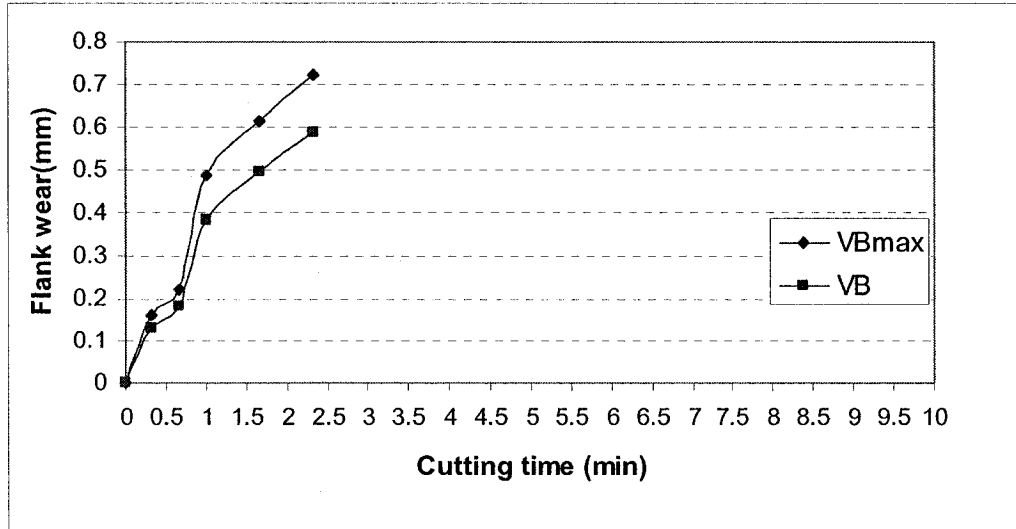


Figure 4.13: Flank wear vs. Cutting time (HM90APKT, coated insert $v = 90$ m/min, $f = 0.025$ mm/tooth, dry cutting)

Figure 4.13 shows the flank wear variation with time at the cutting speed of 90 m/min for coated (HM90APKT) carbide tool under dry condition. The tool life is 2.3 min.

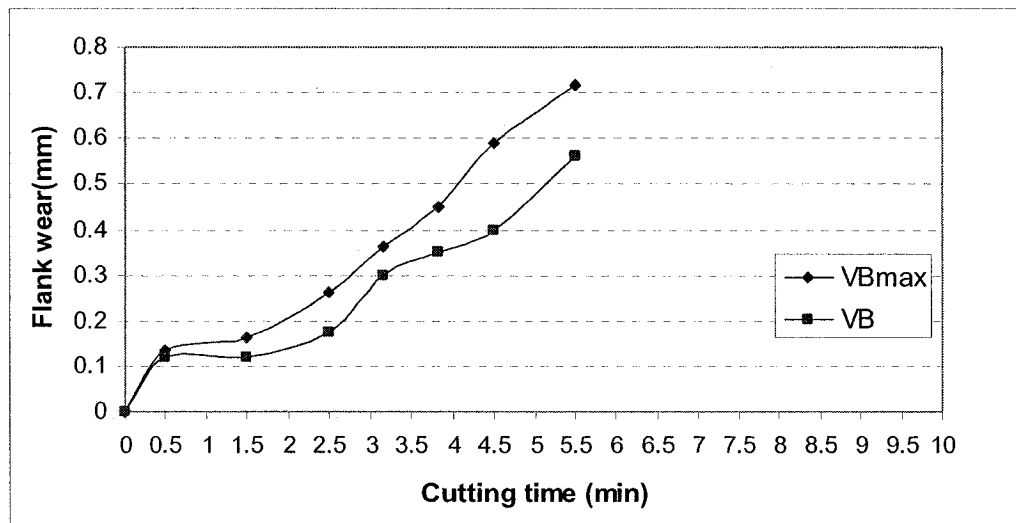


Figure 4.14: Flank wear vs. Cutting time (APKTIC928, coated insert $v = 70$ m/min, $f = 0.025$ mm/tooth, wet cutting)

Figure 4.14 shows the flank wear variation with time at the cutting speed of 70 m/min for coated (APKTIC928) carbide tool under wet condition. The tool life is 5.5 min.

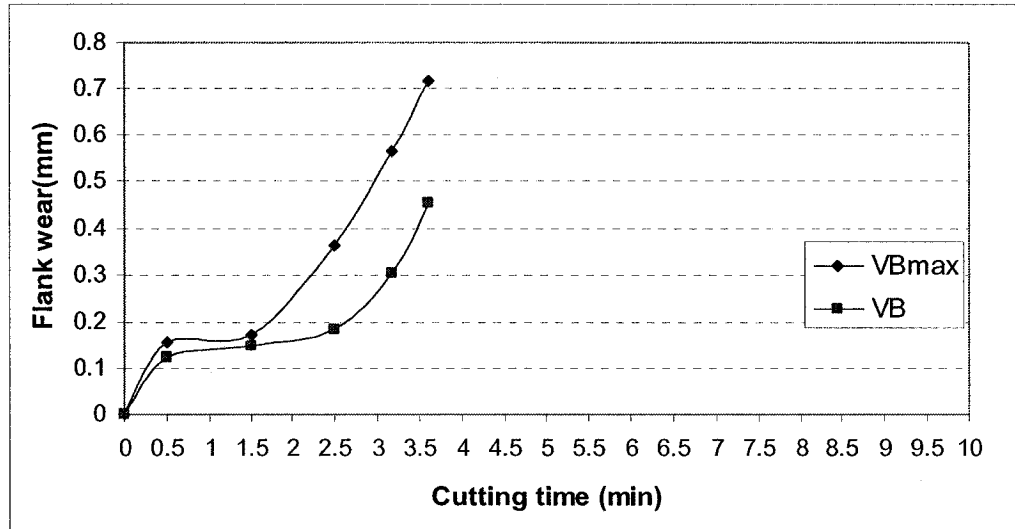


Figure 4.15: Flank wear vs. Cutting time (APKTIC928, coated insert $v = 70$ m/min, $f = 0.025$ mm/tooth, dry cutting)

Figure 4.15 shows the flank wear variation with time at the cutting speed of 70 m/min for coated (APKTIC928) carbide tool under dry condition. The tool life is 3.6 min.

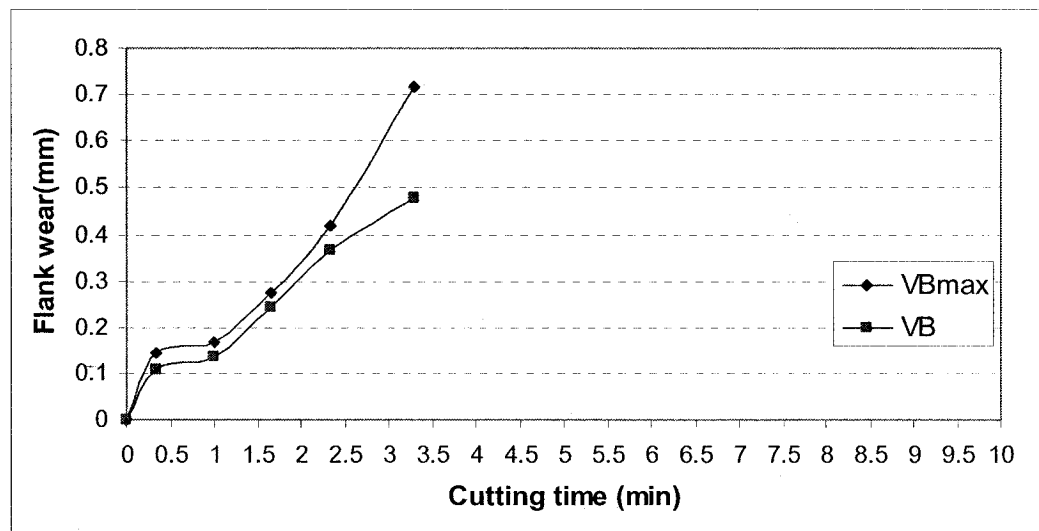


Figure 4.16: Flank wear vs. Cutting time (APKTIC928, coated insert $v = 90$ m/min, $f = 0.025$ mm/tooth, wet cutting)

Figure 4.16 shows the flank wear variation with time at the cutting speed of 90 m/min for coated (APKTIC928) carbide tool under wet condition. The tool life is 3.3 min.

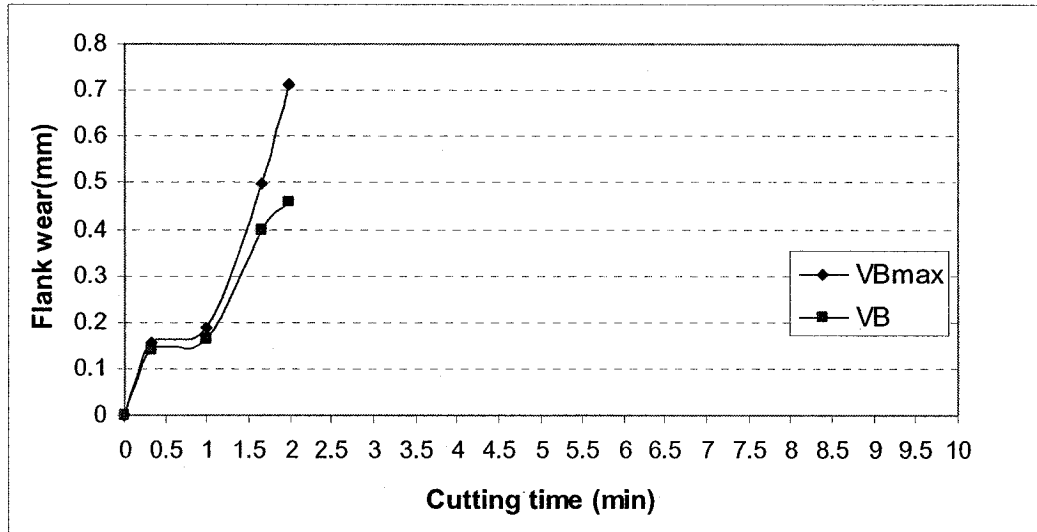


Figure 4.17: Flank wear vs. Cutting time (APKTIC928, coated insert
 $v = 90$ m/min, $f = 0.025$ mm/tooth, dry cutting)

Figure 4.17 shows the flank wear variation with time at the cutting speed of 90 m/min for coated (APKTIC928) carbide tool under dry condition. The tool life is 1.9 min. The tool life was determined according to ISO when the maximum flank wear of the carbide tool reaches the 0.70 mm limit. Tool wear for TiAlN coated carbide tools are shown in figures 4.10 to 4.17. Two types of TiAlN coated (APKTIC928 and HM90APKT) tools were tested for wide range of cutting conditions. Both tools showed severe breakage when the cutting speed was raised to 110 m/min. For this reason cutting tests were conducted at cutting speed from 40 to 100 m/min. In general fine grain carbide tools are known for better wear resistance, cutting edge strength and higher toughness compared to regular grades. The results indicate that carbide sizes have a decisive influence on tool wear. The experimental results suggested that HM90APKT tool demonstrated better than APKTIC928 tool based on tool life. Of the fact as tested, tool coating had the biggest

influence on tool life. During machining, the coated tool performed better than uncoated tool. TiAlN coating gave the longest tool life because high temperatures were generated and the TiAlN coating formed a protective layer of Al_2O_3 and an intermediate layer containing Ti, Al, O and N, which provided higher oxidation resistance.

4.4.2 Effect of cutting speed on tool wear

Cutting speed is the most important factor that affects tool life. In studying the machining processes, it is necessary to know the behaviour of tool wear at different cutting speeds. When machining nickel based super alloys the region of high temperature will be situated close to the cutting edge. Coolant reduces temperature and tool wear. An increase in the cutting speed will increase the cutting tool temperature which subsequently increases tool wear.

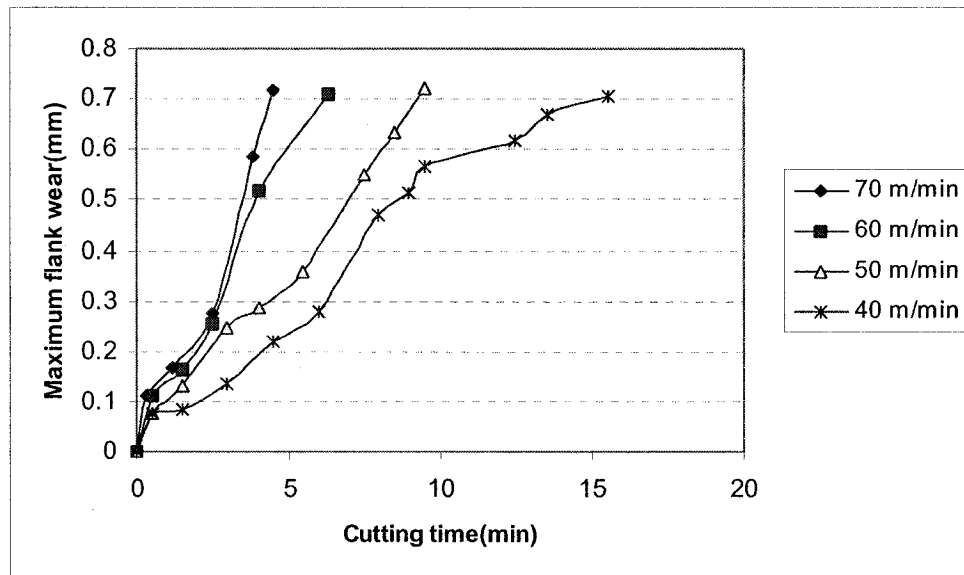


Figure 4.18: Maximum flank wear vs. cutting time (APKT, uncoated insert, $f=0.025$ mm/tooth, wet (coolant) cutting)

The maximum flank wear rate at various cutting speeds when milling Inconel 718 with uncoated (APKT) tool under wet condition is shown in figure 4.18.

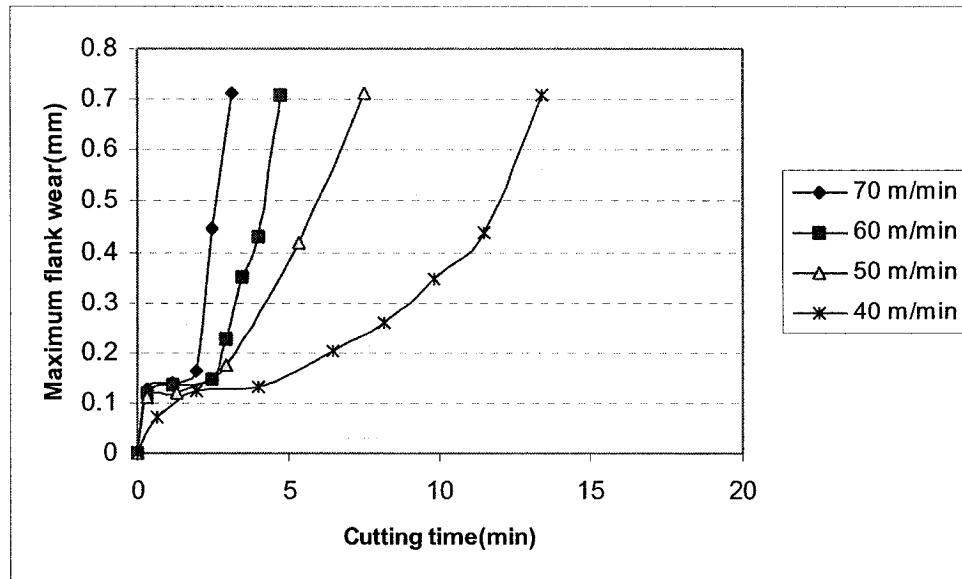


Figure 4.19: Maximum flank wear vs. cutting time (APCT, uncoated insert, $f=0.025$ mm/tooth, wet (coolant) cutting)

The effect of cutting speed on tool wear for uncoated (APCT) tool can be seen in figure 4.19. Increasing cutting speed to 80 m/min, results in excessive heating of the insert. Wear was dominated by thermal cracking of the cutting edge which quickly failed. Therefore the cutting speed range was 40 to 70 m/min. Cutting speeds around 40 m/min seem to be the best range for uncoated tools. Between 60 to 70 m/min, a significant reduction of tool life is observed.

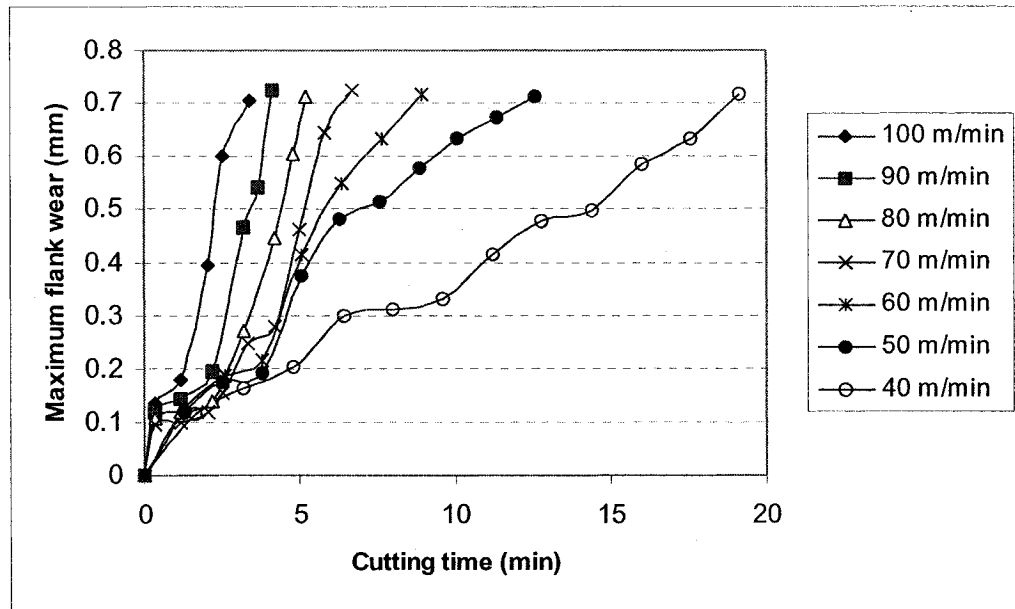


Figure 4.20: Maximum flank wear vs. cutting time (HM90APKT, coated insert, $f=0.025$ mm/tooth, wet (coolant) cutting)

By increasing the cutting speed the tool life dropped sharply. Figure 4.20 (HM90APKT) shows that as the cutting speed increases from 40 m/min to 100 m/min flank wear increased significantly. The main effects plot for cutting speed (Figure 4.19) shows that the tool life was longer at 40 m/min than at 100 m/min which was most likely a result of lower cutting temperature. This is due to the commonly experienced abrasiveness and work hardening tendencies of Inconel 718, resulting in high heat generated at the cutting edge. The TiAlN coating imparts wear resistance to the carbide substrate increasing its tool life overall cutting speed considered. There is evidence that TiAlN forms an Al_2O_3 skin at elevated temperatures and that this functions act as a chemical barrier layer to protect the underlying coating and slow wear. Overall, the TiAlN coated insert appear to be stronger than uncoated insert under the same cutting conditions.

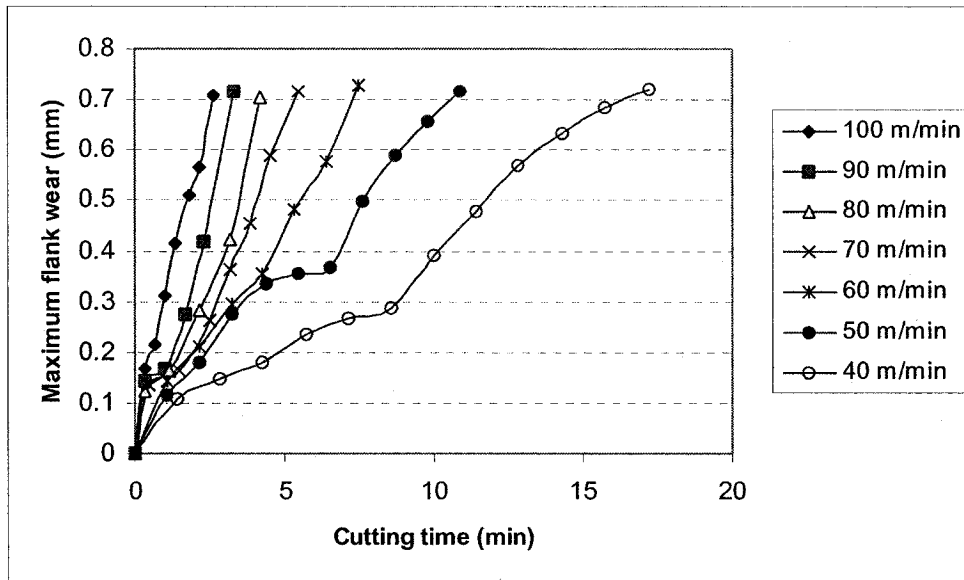


Figure 4.21: Maximum flank wear vs. cutting time (APKTIC928, coated insert, $f = 0.025$ mm/tooth, wet (coolant) cutting)

Figure 4.21 suggests that a sharp increase occurred in the wear rate when at cutting speed 80 m/min and above.

4.4.3 Effect of coolant on tool wear

Coolant has been used to reduce tool wear during machining operation. Use of cutting fluids was always considered a solution rather than a problem in machining, at least till recently. They serve many useful functions, including cooling of the cutting tool at higher cutting speeds, lubrication at low speeds and high loads, increasing tool life, improving surface finish, reducing cutting forces, power consumption, reducing the distortion due to temperature rise in the workpiece, providing a protective layer on the machined surface from oxidation and protection of the machine tool components from rust. Many new coolants have been developed to meet the needs of new materials and new cutting tools.

The goal of machining operation is to improve productivity and reduce costs. This is accomplished by machining at the highest practical speed while maintaining practical tool life, reducing scrap and producing parts with the desired surface quality. Proper selection and use of cutting fluids can help achieve all of these goals. In machining almost all of the energy during cutting is transformed into heat. The deformation of the metal to create chips and the friction of the chip sliding across the cutting tool produce heat. At the contact between the chip and tool, cooling can reduce the chip temperature and thus, affect directly the friction force between the chip and tool. However, temperature of the tool below the contact may be reduced at all cutting speeds by cooling the tool.

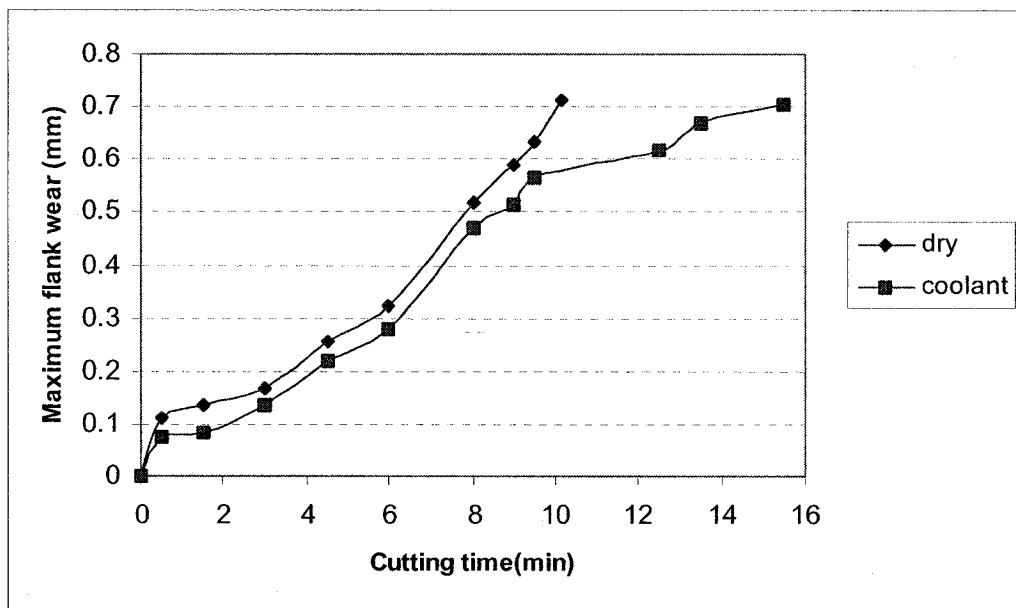


Figure 4.22: Maximum flank wear vs. cutting time (APKT, uncoated insert, $v=40$ m/min, $f=0.025$ mm/tooth)

Figure 4.22 shows gradual improvement in tool life when machining with coolant. . Remote from the cutting edge, the coolant always plays a major role in maintaining the

machine and machined material at ambient temperature, reducing errors of size resulting from thermal expansion.

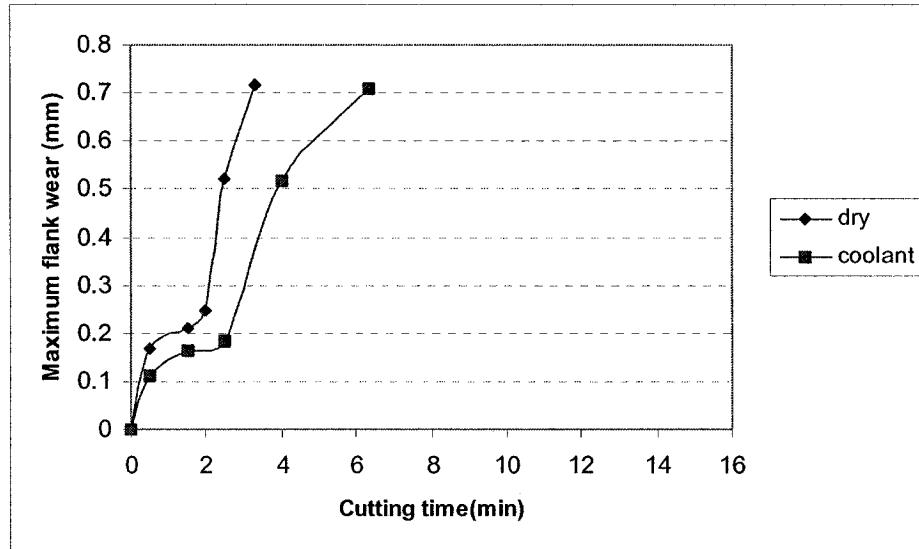


Figure 4.23: Maximum flank wear vs. cutting time (APKT, uncoated insert, $v= 60$ m/min, $f= 0.025$ mm/tooth)

Figure 4.23 shows that coolant has decreased the flank wear rate. Coolant takes heat from the tool and workpiece.

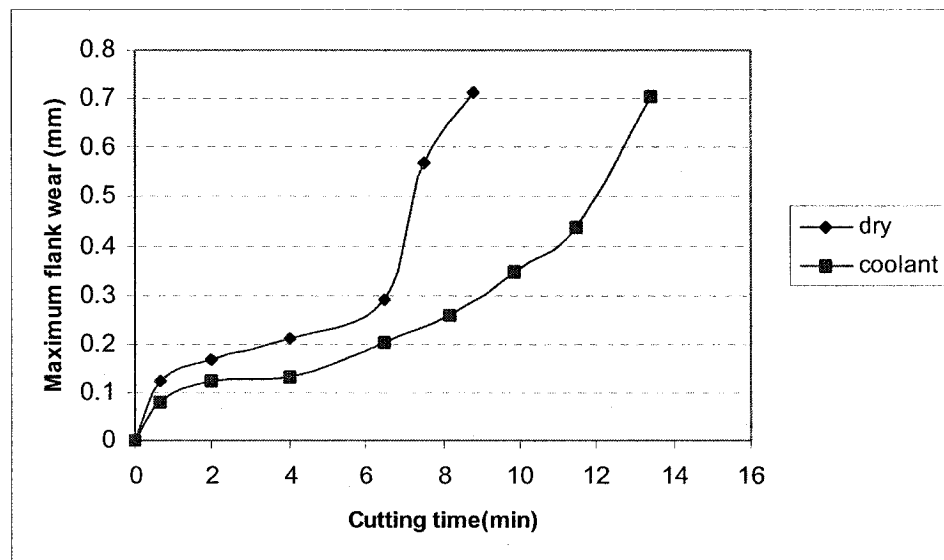


Figure 4.24: Maximum flank wear vs. cutting time (APCT, uncoated insert, $v= 40$ m/min, $f= 0.025$ mm/tooth)

The effect of coolant on apparent flank wear progression is shown in figure 4.24. Under dry conditions, flank wear progression was rapid. The removal of the heat prevents the workpiece from expanding during the machining operation, which would cause variation as well as damage to the material's microstructure.

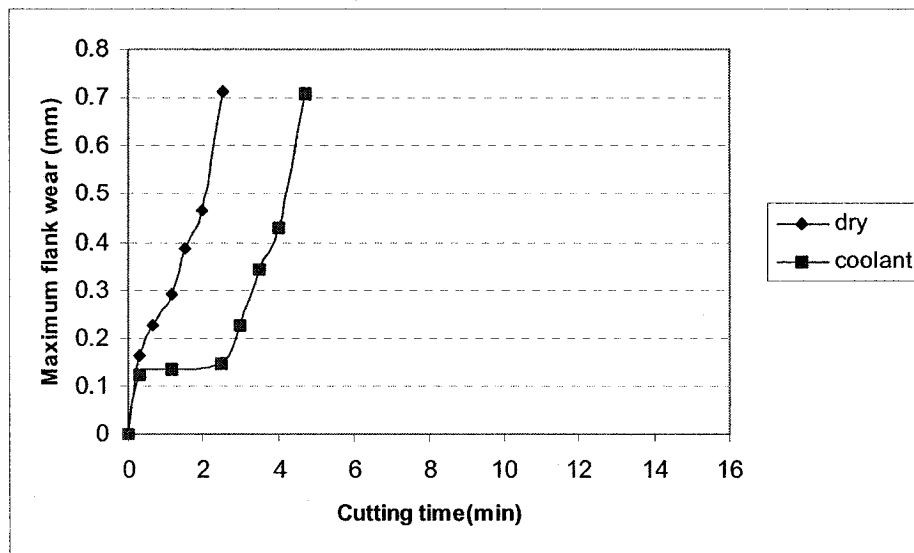


Figure 4.25: Maximum flank wear vs. cutting time (APCT, uncoated insert, $v= 60$ m/min, $f= 0.025$ mm/tooth)

Figure 4.25 shows that flank wear variation for uncoated carbide (APCT). It was found that wear rate was high in dry cutting operation at the cutting speed of 60 m/min.

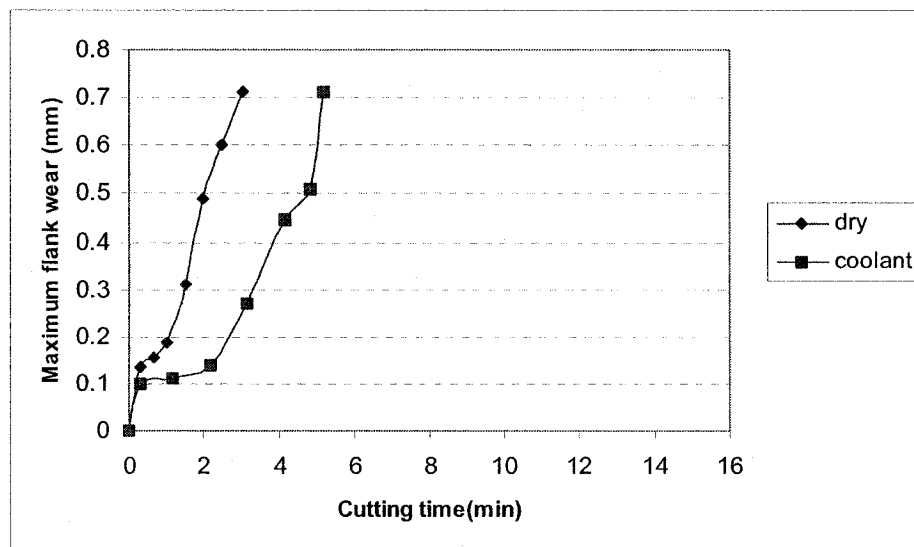


Figure 4.26: Maximum flank wear vs. cutting time (HM90APKT, coated insert, $v= 80$ m/min, $f= 0.025$ mm/tooth)

Generally, during dry cutting a large amount of workpiece material will adhere to the flank face, accumulate and then detach accompanied by the underlying material due to strong adhesion. Figure 4.26 shows the comparative study of flank wear at the cutting speed of 80 m/min for coated tool (HM90APKT) under wet and dry conditions.

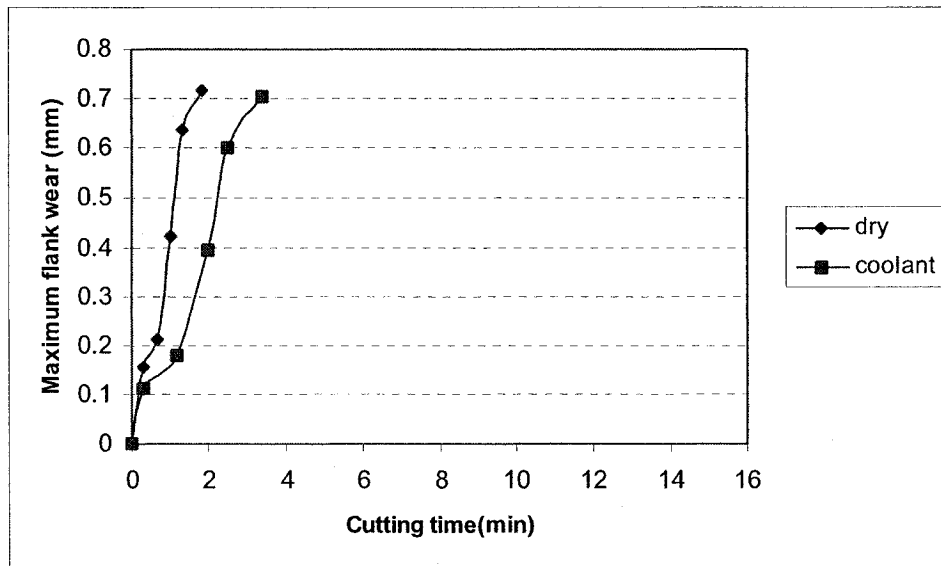


Figure 4.27: Maximum flank wear vs. cutting time (HM90APKT, coated insert, $v= 100$ m/min, $f= 0.025$ mm/tooth)

Figure 4.27 shows the wear progression at the cutting speed of 100 m/min. Although coolant has influence on tool wear but it does not show any significant influence at the cutting speed of 100 m/min.

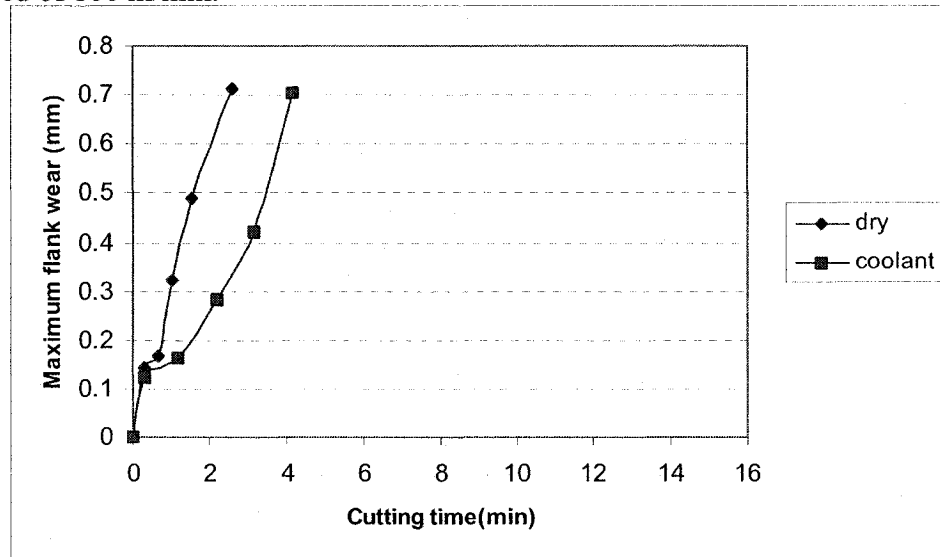


Figure 4.28: Maximum flank wear vs. cutting time (APKTIC928, coated insert, $v= 80$ m/min, $f= 0.025$ mm/tooth)

APKTIC928 tool (Figure 4.28) also shows that higher wear rate occurs at cutting speed of 80 m/min under dry condition.

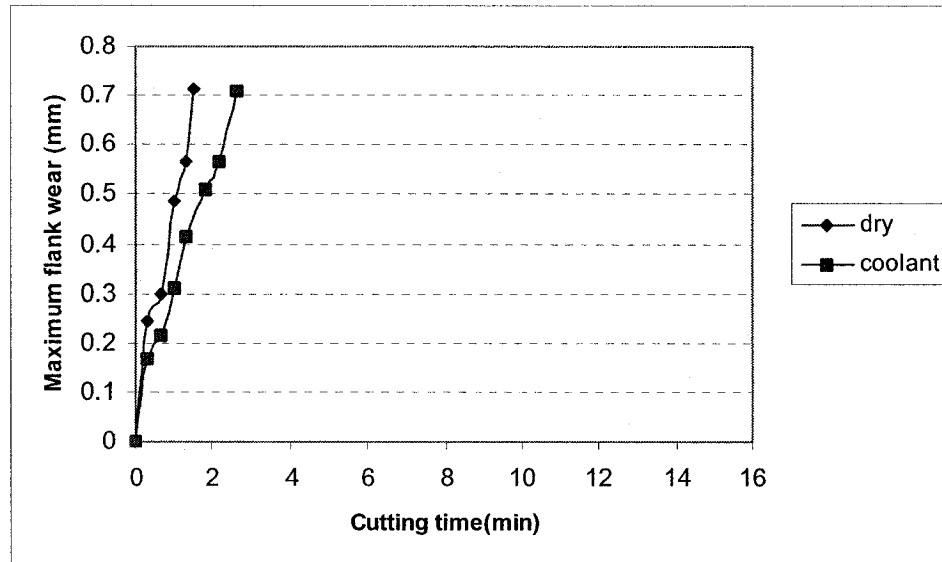


Figure 4.29: Maximum flank wear vs. cutting time (APKTIC928, coated insert, $v=100$ m/min, $f=0.025$ mm/tooth)

Figure 4.29 shows that wear rate is significantly higher at the cutting speed of 100 m/min. Compared to results obtained when milling of Inconel 718 under dry condition, the performance of uncoated tool reduced significantly due to excessive heating at the cutting edge region. On the other hand, the TiAlN coated tool performed better than uncoated due to the former having higher oxidation resistance and higher room temperature capability. The advantage of cooling technology include significant improvement of tool life, efficient cooling and lubrication. The penetration of the high energy jet in to the tool-chip interface reduces the temperature gradient and eliminates the seizure effect, offering adequate lubrication at the tool-chip interface with significant reduction in friction in addition to alternation of the chip flow conditions resulting in the lowering of cutting temperature and consequently tool wear rate. Ezugwu *et al* [2005] reported that coolant

has significant influence on tool wear during nickel based super alloys machining operation.

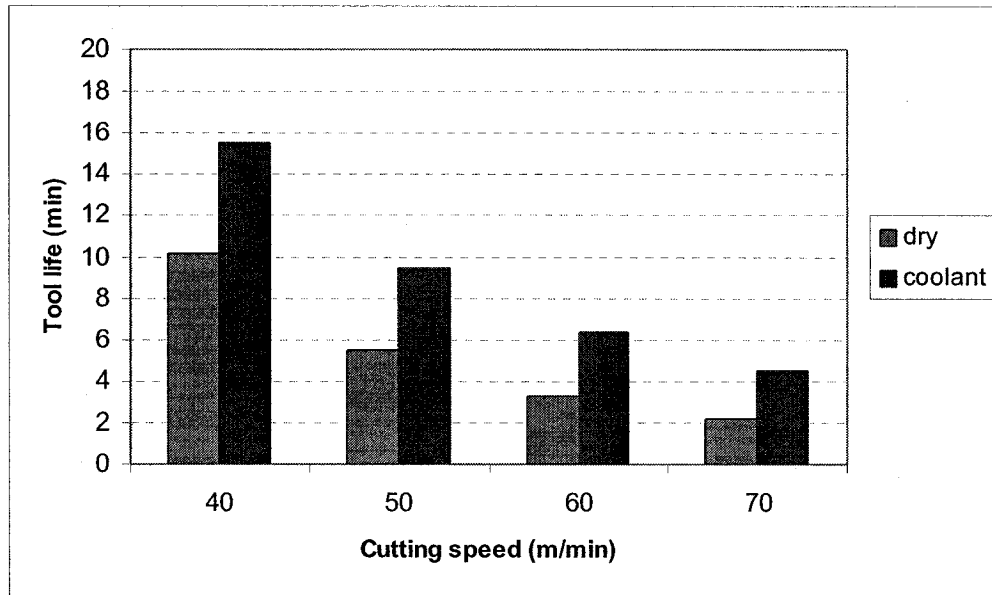


Figure 4.30: Tool life vs. cutting speed (APKT, uncoated insert, $f=0.025$ mm/tooth)

When tool life is compared in the cases of coolant and dry, it is found that tool life is always longer in wet condition than dry condition (Figure 4.30)

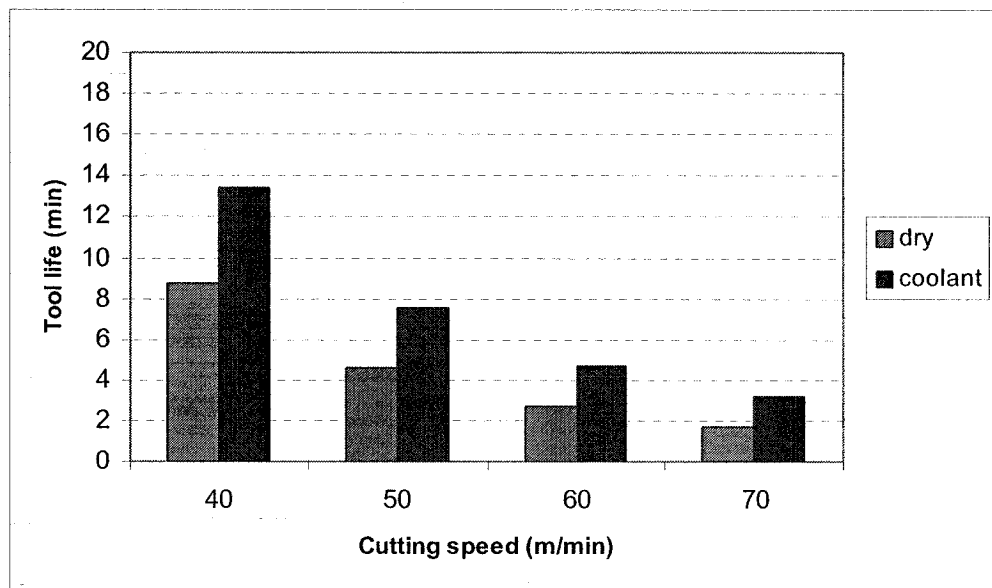


Figure 4.31: Tool life vs. cutting speed (APCT, uncoated insert, $f=0.025$ mm/tooth)

The effect of cutting environment on tool life is shown in figure 4.31 for uncoated carbide tools. It was found that uncoated tool shows smaller tool life at the cutting speed of 70 m/min under dry condition. As the cutting speed increases the temperature was high when machining under dry condition. It was also observed that coolant reduced temperature. This cooling effect is likely to account for the increased tool life values and indicates the importance of maintaining low cutting temperature when machining Inconel 718 with carbide tools. Rahman *et al* [2000] also reported that tool life increased for carbide tools under wet (coolant) cutting operation.

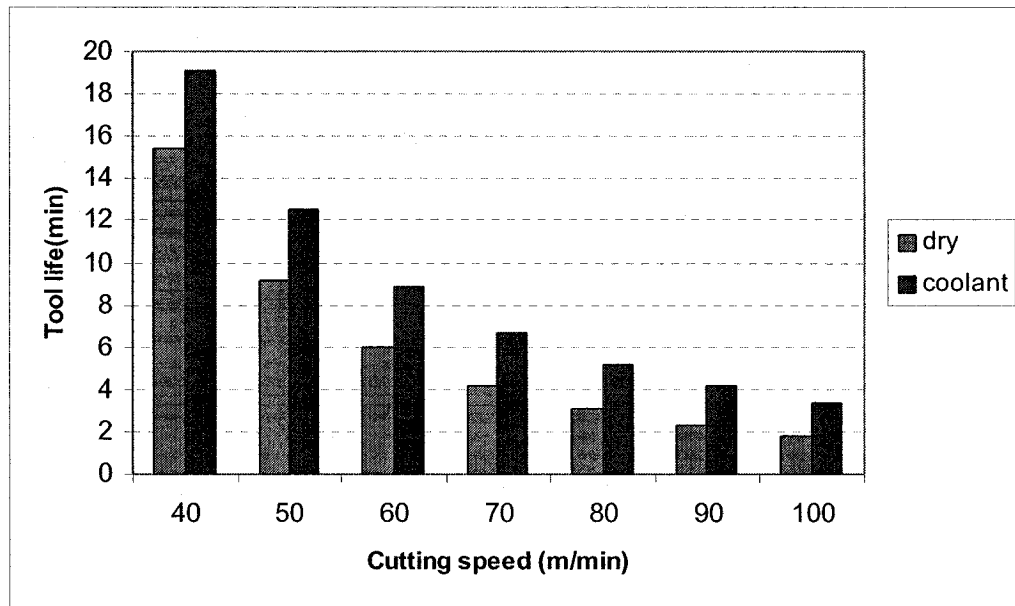


Figure 4.32: Tool life vs. cutting speed (HM90APKT, coated insert, $f=0.025$ mm/tooth)

Figure 4.32 also illustrates the decrease in tool life with increasing cutting speed for coated tool (HM90APKT) under wet and dry conditions. The result indicates that the cutting fluid does not accomplish the simultaneous action of cooling and lubrication at the higher cutting speed (100 m/min).

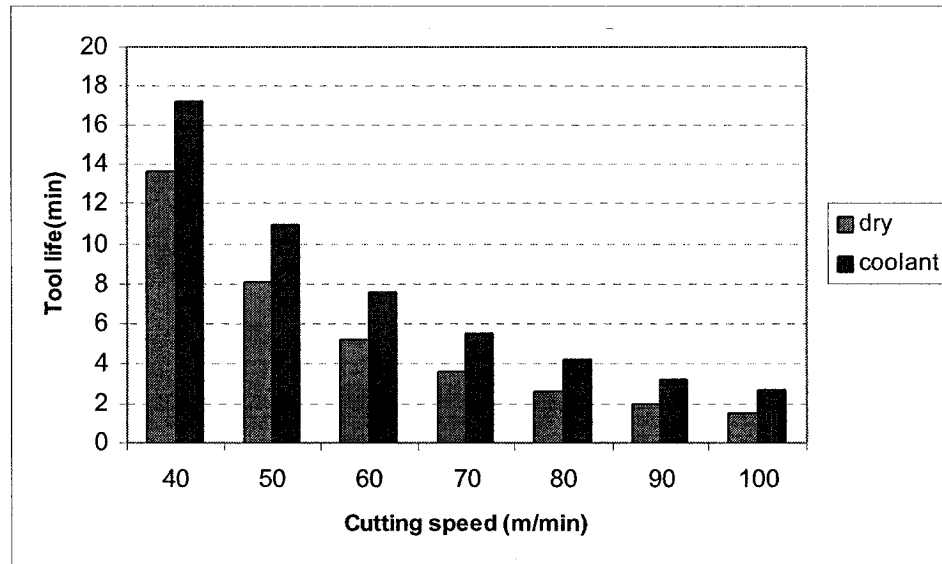


Figure 4.33: Tool life vs. cutting speed (APKTIC928, coated insert, $f=0.025$ mm/tooth)

From figure 4.33, it was found that tool life increased for coated carbide (APKTIC928) during wet (coolant) cutting operation. When dry machining, the absence of coolant leads to temperature increases that could affect the tool wear progress within the part being machined and could induce dimensional errors and chip buildup on both tool and workpiece. Water based cutting fluids provide the best cooling action. Water, the major component of water based fluids, has better heat transfer characteristics than oils. Extreme temperature additives are used to improve lubrication. Chemically inactive additives are used to reduce friction and surface tension that improve surface finish; these include surface adsorption types (such as fatty oils, and fatty soaps) and physical separation types (such as inorganic and organic salts). Chemically active additives (such as sulfur, chlorine or prosperous compounds) are used to produce a chemical reaction either in the lubricant or on the metallic surface. The reaction product is intended to act as

a solid lubricant to reduce friction. Blasocut universal 2000 cutting fluid was used during this nickel based machining operation. Blasocut universal 2000 is water based coolant. It has good lubrication, non-toxic and non bacterial degradation property that extends tool life, reduces friction, heat and tool failure during machining operation. When evaluating economic cutting conditions there are obvious advantages in using tool life equation.

The Figure 4.33 is plotted using a logarithmic scale in Figure 4.34, showing a linear relation between $\log T$ and $\log V$. This result is reminiscent of the fatigue life of materials subjected to repeated cyclic loading [William 1963]. Fatigue is the progressive and localized structural damage that occurs when a material is subjected to cyclic or fluctuating strains at nominal stresses that cause structural failure. For many materials, the number of cycles to failure decreases continuously with increasing stress. The fatigue life of materials can be expressed by the following equation.

$$NS^b = C \quad (4.1)$$

$$\log S + a \log N = \log K \quad (4.2)$$

where:

S = Stress

N = Number of cycles

It should be possible to relate tool life with cutting speed in a similar fashion.

Taylor showed that tool life varied with the cutting speed, which was expressed by following equation [Altintas 2000]:

$$VT^n = C \quad (4.3)$$

$$\log V + n \log T = \log C \quad (4.4)$$

$$\log T = \frac{1}{n} [\log C - \log V] \quad (4.5)$$

where:

V = Cutting speed

T = Tool life in minutes

n = Exponent

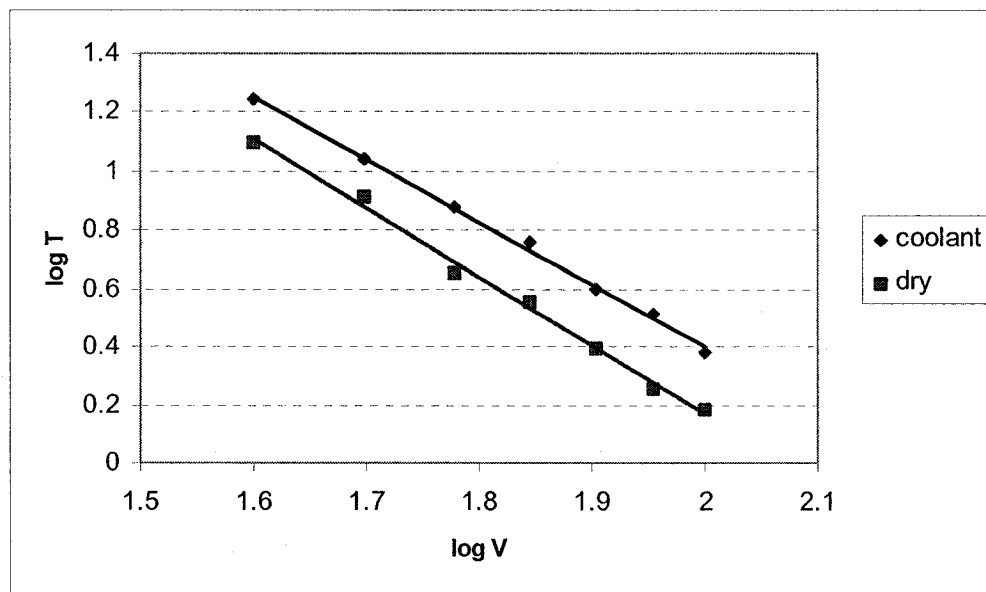


Figure 4.34: Tool life, APKTIC928 coated insert, $f = 0.025$ mm/tooth

From figure 4.30, the tool life equations for uncoated carbide tool (APKT) under wet and dry conditions can be expressed as follows:

$$VT^{0.45} = 137.7 \quad (4.6)$$

$$VT^{0.36} = 92.36 \quad (4.7)$$

From figure 4.31, the tool life equations for uncoated carbide tool (APCT) under wet and dry conditions can be expressed as follows:

$$VT^{0.39} = 110.02 \quad (4.8)$$

$$VT^{0.34} = 83.79 \quad (4.9)$$

From figure 4.32, the tool life equations for coated carbide tool (HM90APKT) under wet and dry conditions can be expressed as follows:

$$VT^{0.53} = 191.37 \quad (4.10)$$

$$VT^{0.43} = 129.35 \quad (4.11)$$

From figure 4.33, the tool life equations for coated carbide tool (APKTIC928) under wet and dry conditions can be expressed as follows:

$$VT^{0.49} = 161.38 \quad (4.12)$$

$$VT^{0.42} = 119.87 \quad (4.13)$$

Tool life equations were established only for particular feed rate ($f= 0.025\text{mm/tooth}$) because both carbide tools showed good results at feed rate (f) of 0.025mm/tooth . From our experiments, tool-life equations (4.6) to (4.13) were established. For constant feed rate ($f=0.025\text{mm/tooth}$) and depth of cut ($d=1.5\text{mm}$), those equations can be used for

appropriate selection of cutting speeds for a desired tool life performance. Table 4.5 shows the different values of " n " and " C " for uncoated and coated carbide tools. The magnitude of cutting parameters will have to be determined experimentally and knowing the effect of key variables on tool life will also give some indication of what failure mechanisms to expect or avoid. Experimental tests should be required to interpolate the response over a range of cutting conditions.

Table 4.5: Different values of " n " and " C "

Carbide tools	Workpiece	n	C	Environment	Speed (m/min)
APKT uncoated	Inconel 718	0.45	137.70	coolant	40 - 70
APKT uncoated	Inconel 718	0.36	92.36	dry	40 - 70
APCT uncoated	Inconel 718	0.39	110.02	coolant	40 - 70
APCT uncoated	Inconel 718	0.34	83.79	dry	40 - 70
HM90APKTcoated	Inconel 718	0.53	191.37	coolant	40 - 100
HM90APKTcoated	Inconel 718	0.43	129.35	dry	40 - 100
APKTIC928coated	Inconel 718	0.49	161.38	coolant	40 - 100
APKTIC928coated	Inconel 718	0.42	119.87	dry	40 - 100

Table 4.6 shows the tool life for coated carbide tools at feed rate of 0.03mm/tooth under wet and conditions. The tool life was longer at cutting speed of 40 m/min.

Table 4.6: Tool life for coated carbide tools

Cutting speed (m/min)	Feed (mm/tooth)	Tool life (min) for HM90APKT coolant	Tool life (min) for HM90APKT dry	Tool life (min) for APKTIC928 coolant	Tool life (min) for APKTIC928 dry
40	0.03	17.5	13.6	15.3	11.6
50	0.03	11.2	7.8	9.3	6.6
60	0.03	7.6	4.7	6.4	4.1
70	0.03	5.65	3.2	4.3	2.8
80	0.03	4.2	2.9	3.4	2.5
90	0.03	3.5	2.1	2.6	1.8
100	0.03	2.9	1.9	2.1	1.4

Table 4.7 shows the tool life for coated carbide tools at feed rate of 0.035mm/tooth under wet and dry conditions. It can be found that tool life was deteriorated at the cutting speed of 100 m/min.

Table 4.7: Tool life for coated carbide tools

Cutting speed (m/min)	Feed (mm/tooth)	Tool life (min) for HM90APKT coolant	Tool life (min) for HM90APKT dry	Tool life (min) for APKTIC928 coolant	Tool life (min) for APKTIC928 dry
40	0.035	16.2	12.2	13.8	10.5
50	0.035	10.3	6.8	8.1	5.4
60	0.035	6.9	4.1	5.3	3.9
70	0.035	5.1	2.8	3.8	2.5
80	0.035	3.8	2.5	2.7	1.9
90	0.035	3.1	1.9	2.2	1.6
100	0.035	2.4	1.5	1.8	1.1

Table 4.8 shows the tool life for coated carbide tools at feed rate of 0.04 mm/tooth under wet and dry conditions.

Table 4.8: Tool life for coated carbide tools

Cutting speed (m/min)	Feed (mm/tooth)	Tool life (min) for HM90APKT coolant	Tool life (min) for HM90APKT dry	Tool life (min) for APKTIC928 coolant	Tool life (min) for APKTIC928 dry
40	0.04	13.5	9.8	10.2	8.6
50	0.04	8.2	5.2	6.0	4.6
60	0.04	5.6	3.4	3.9	2.8
70	0.04	3.9	2.4	2.7	1.6
80	0.04	2.8	2.1	1.9	1.4
90	0.04	2.3	1.5	1.7	1.1
100	0.04	1.9	1.2	1.4	0.6

Table 4.9 shows the tool life for uncoated carbide tools at feed rate of 0.03 mm/tooth under wet and dry conditions.

Table 4.9: Tool life for uncoated carbide tools

Cutting speed (m/min)	Feed (mm/tooth)	Tool life (min) for APKT coolant	Tool life (min) for APKT dry	Tool life (min) for APCT coolant	Tool life (min) for APCT dry
40	0.03	12.5	7.6	10.8	6.6
50	0.03	7.4	3.8	5.8	3.1
60	0.03	4.8	2.7	3.6	2.3
70	0.03	3.4	2.2	2.4	1.9

Table 4.10 shows the tool life for uncoated carbides at feed rate of 0.035 mm/tooth under wet and dry conditions.

Table 4.10: Tool life for uncoated carbide tools

Cutting speed (m/min)	Feed (mm/tooth)	Tool life (min) for APKT coolant	Tool life (min) for APKT dry	Tool life (min) for APCT coolant	Tool life (min) for APCT dry
40	0.035	10.2	5.17	8.4	4.1
50	0.035	5.8	2.9	4.4	2.4
60	0.035	3.7	1.8	2.7	1.6
70	0.035	2.5	1.2	1.7	1.3

Table 4.11 shows the tool life for uncoated carbide tools at cutting feed of 0.04 mm/tooth.

Table 4.11: Tool life for uncoated carbide tools

Cutting speed (m/min)	Feed (mm/tooth)	Tool life (min) for APKT coolant	Tool life (min) for APKT dry	Tool life (min) for APCT coolant	Tool life (min) for APCT dry
40	0.04	8.5	4.3	6.8	3.7
50	0.04	4.9	2.1	3.3	1.9
60	0.04	3.1	1.6	1.9	1.2
70	0.04	2.0	1.0	1.2	0.8

4.4.4 Wear mechanisms for carbide tools

Tool life is often the most important practical consideration in selecting cutting tools and cutting conditions. Tool wear and fracture rates directly influence tooling costs and part quality. Cutting tools which wear slowly have a low per part cost and produce predictable tolerances and surface finishes. For these reasons tool life is the most common criteria used to rate cutting tool performance and the machinability of materials. An understanding of tool life requires an understanding of the ways in which tools fail. Broadly, tool failure may result from wear, plastic deformation or fracture. A primary goal of metal cutting research has been to identify wear mechanisms of cutting tool. The problem is complicated by the fact that wear is not a process involving one unique mechanism; there are several alternative mechanisms which are known to be operative, depending on the physical conditions existing.

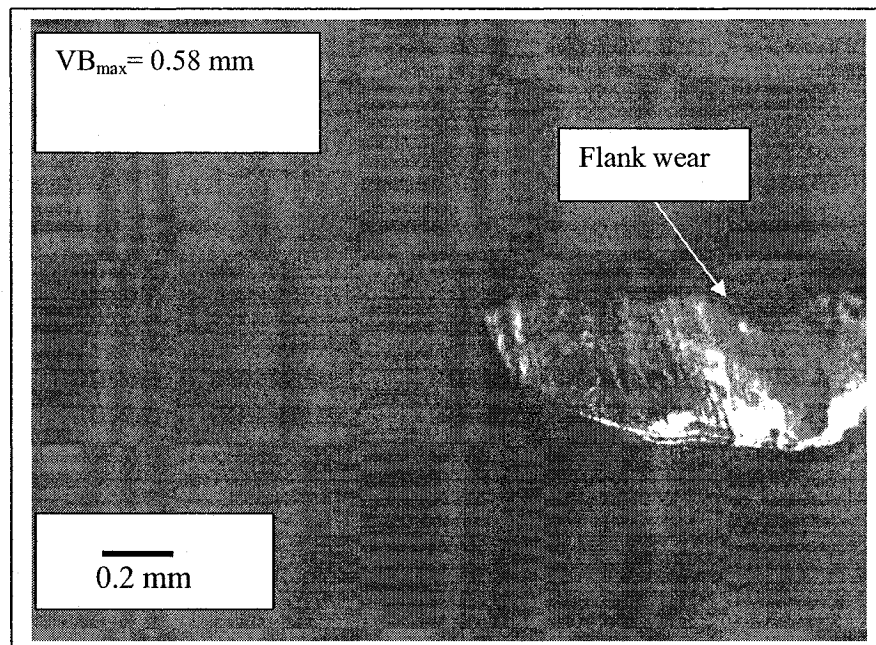


Figure 4.35: SMM micrograph of wear surface (APKT, uncoated carbide insert, cutting speed= 70 m/min, feed= 0.025 mm/tooth, wet cutting)

Adhesive wear was found to play an important role in rake face cratering especially when machining Inconel 718 with uncoated tools at the cutting speed of 70 m/min, as is shown in Figures 4.35 to 4.36.

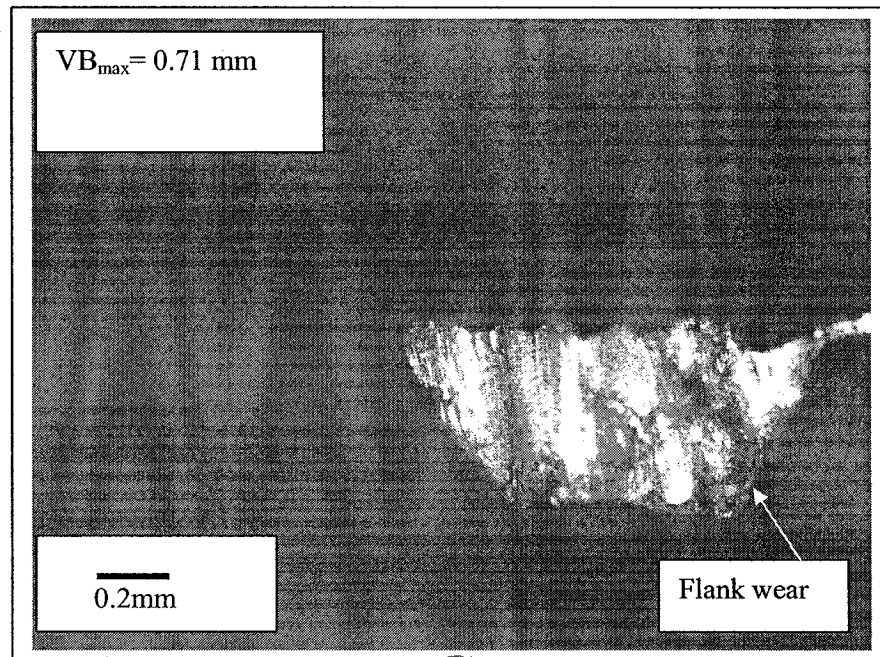


Figure 4.36: SMM micrograph of wear surface (APCT, uncoated carbide insert, cutting speed= 70 m/min, feed= 0.025 mm/tooth, wet cutting)

By applying a hard coating, the frictional behaviour between chip and tool is influenced. The friction is reduced by the coating, which has the consequence that the chip can glide faster over the tool. Thereby a smaller contact zone between chip and workpiece develops. This has the consequence that the smaller contact length reduces the thermal loading on the tool. Multi-layer coatings enable the generation of more favorable characteristics combinations. TiAlN coated carbide tool shows advantage at high process temperatures and forms a thin passive layer at the tool surface, which prevents a past progressing diffusion or oxidation wear. The loss of tool particles can be seen in figure

4.37. The wear of the coatings then proceeded by an adhesive wear mechanism. It shows evidence for this mechanism with regions of exposed substrate and areas when the coating has started to peel away. The edge of the coating is fragmented, highlighting the brittle nature of coating fracture. For the TiAlN coating the wear at 70 m/min cutting speed is minimal in comparison to uncoated tool.

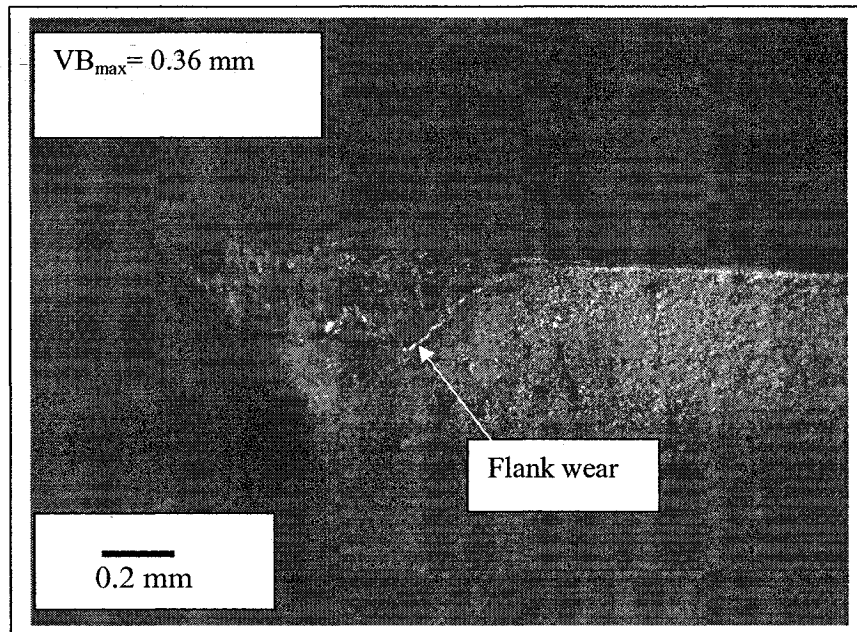


Figure 4.37: SMM micrograph of wear surface (APKTIC928, coated carbide insert, cutting speed= 70 m/min, feed= 0.025 mm/tooth, wet cutting)

SMM micrograph in figures 4.35 to 4.36 clearly show the presence of wear on the flank faces in addition to the adherence of small chip particles at the section of the cutting edge of coated and uncoated carbide tools. The wear rate was lower in coated carbide than uncoated carbide. Figure 4.37 shows that wear consists of a few thin layers of smeared work-piece material, which were formed on the flank face. These layers were easily distinguished by the position of their edges next to the border of a pitted area on the flank face of the coated tool. In the coated tool, adhesion occurs, which was the welding of

relatively small chip particles on the flank face of the cutting tool. Since coated tools were used at higher cutting speeds than uncoated tools, rapid cratering of the substrate due to diffusion or chemical wear usually following coating failure.

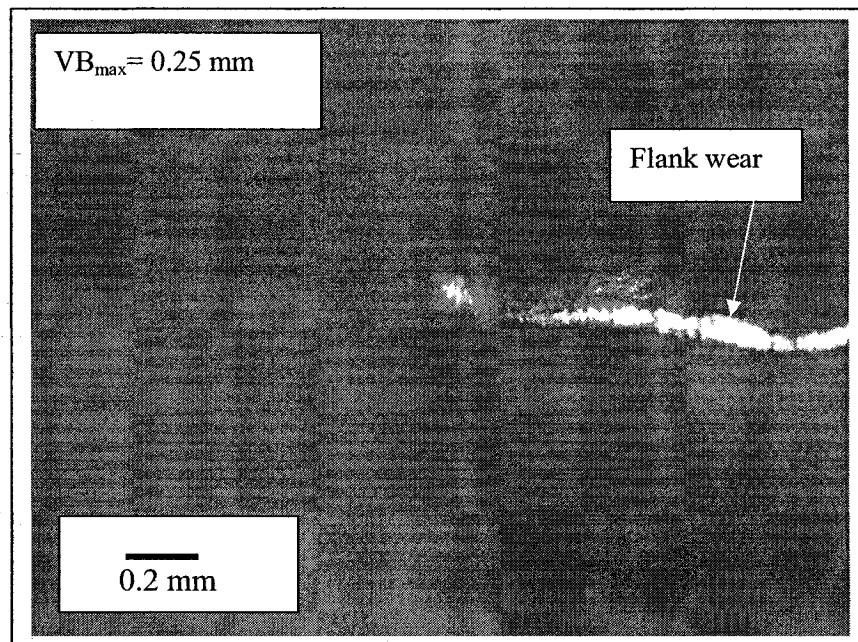


Figure 4.38: SMM micrograph of wear surface (HM90APKT, coated carbide insert, cutting speed= 70 m/min, feed= 0.025 mm/tooth, wet cutting)

The results of the micro analysis using SMM (Scanning metallographic microscope) indicate that adhesion and abrasion are the wear mechanisms for both uncoated and coated tools when milling of Inconel 718. As the cutting speed increases from 70 m/min to 110 m/min, the contribution of the coating layer on the tool flank to resist wear was not significant. Figure 4.39 shows that cutting edge breaks away at the cutting speed of 110 m/min. It was found that the strength of the cutting edge was significantly reduced when cutting at higher cutting speed so that the cutting edge breaks at the cutting speed of 110m/min. The most likely causes of the premature failure are believed to be the high

mechanical impact induced due to intermittent cutting and high temperature generated at the vicinity of the cutting edge. The removal of coatings and the substrate material in this manner was probably due to the cyclic thermo-mechanical stresses, which are inherent in the milling process. Jawaid *et al* [2001] reported that abrasive and adhesive mechanisms were dominated for carbide tools during nickel based super alloys machining operation. They also found that irregular adhesion wear occurred.

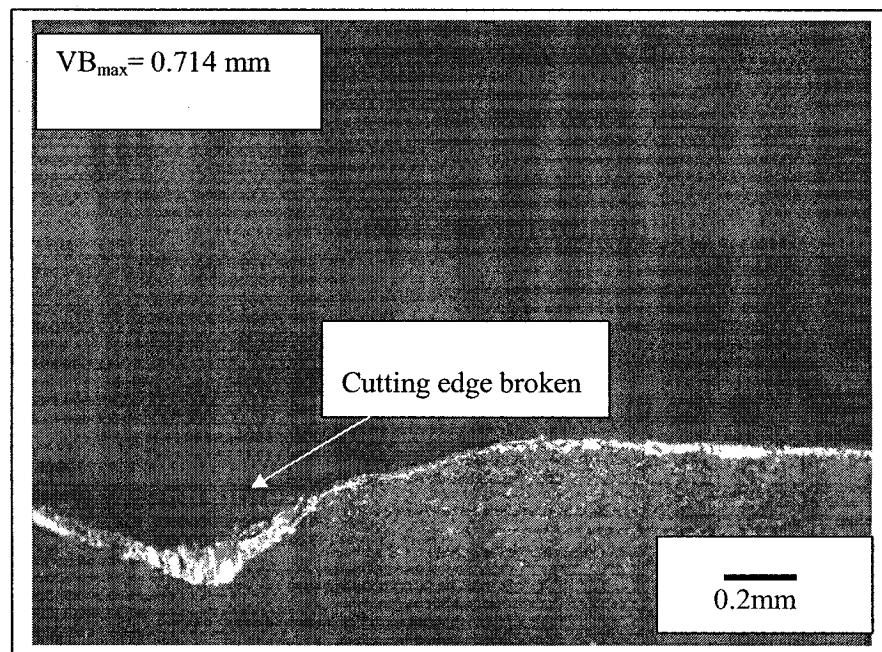


Figure 4.39: SMM micrograph of wear surface (APKTIC928, coated carbide insert, cutting speed= 110 m/min, feed= 0.025mm/tooth, dry cutting)

In their study, the irregular adhesion was due to the interrupted cutting which makes a periodic attachment and detachment of the workpiece material on the tool surface. Figures 4.35 to 4.39 show that the dominant wear mechanisms which resulted on carbide flank surface were a combination of alternating occurrence of adhesion and a degree of abrasion.

4.4.5 Surface roughness parameters

The principal consideration of a surface condition produced during manufacturing is concerned with safety, reliability and service life. It requires the study of surface alternations resulting from specific machining operations. This concerns the geometric irregularities of the surface and the metallurgical alternations of the surface and surface layer. Most alternations occur on the surface which is very undesirable. Thus such defects may result in component failure. The surfaces produced by machining generally are irregular and complex. Despite this, the majority of machined parts can be satisfactorily performed their functions with general, uncomplicated surface texture specifications. Surface roughness is colloquial term widely used to denote the general quality of a surface. Surface finish is not specifically tied to the texture or characteristics pattern of the surface however good finish implies low roughness value. Roughness is of significant interest in manufacturing because it is the roughness of a surface that determines its friction in contact with another surface. The roughness of a surface defines how that surface feels, how it looks, how it behaves in a contact with another surface, and how it behaves for coating or sealing. " R_a " is the universally recognized parameter of roughness (Figure 4.40). It is the arithmetic mean of the departures of the roughness profile from the mean line.

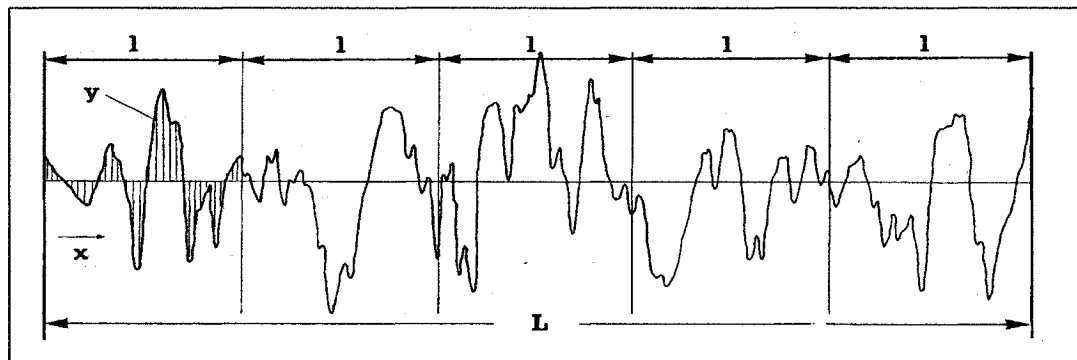


Figure 4.40: Surface roughness (R_a)

On the other hand, the peak to valley roughness height (R_t) can be used for assessing the tooth mark during milling operation. " R_t " is the maximum peak to valley height of the profile in the assessment surface (Figure 4.41). " R_p " is the maximum height of the profile above the mean line within the assessment line. " R_v " is the maximum depth of the profile below the mean line within the assessment line. Roughness parameters of machined surface were measured by portable surface roughness machine.

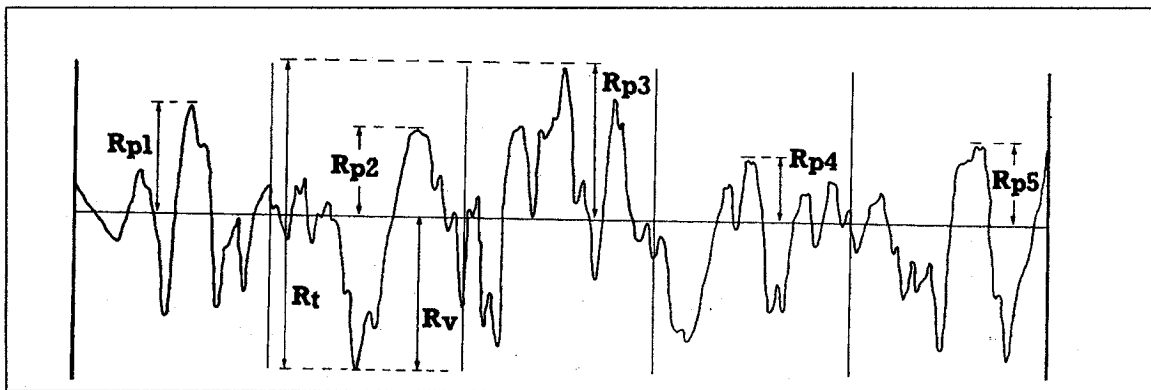


Figure 4.41: Peak to valley roughness height (R_t)

4.4.6 Surface roughness in wet and dry conditions

It is well understood that the quality of the surface plays a very important role in the performance of such parts as airfoils machined by milling. Although many factors affect the surface condition of a machined part, cutting parameter such as feed, has a significant influence on the surface roughness for a given machine tool and workpiece set-up. A good quality milled surface significantly improves fatigue strength, corrosion resistance or creep life.

Thus it is necessary to know how to control the machining parameters to produce a fine surface quality for machined workpiece.

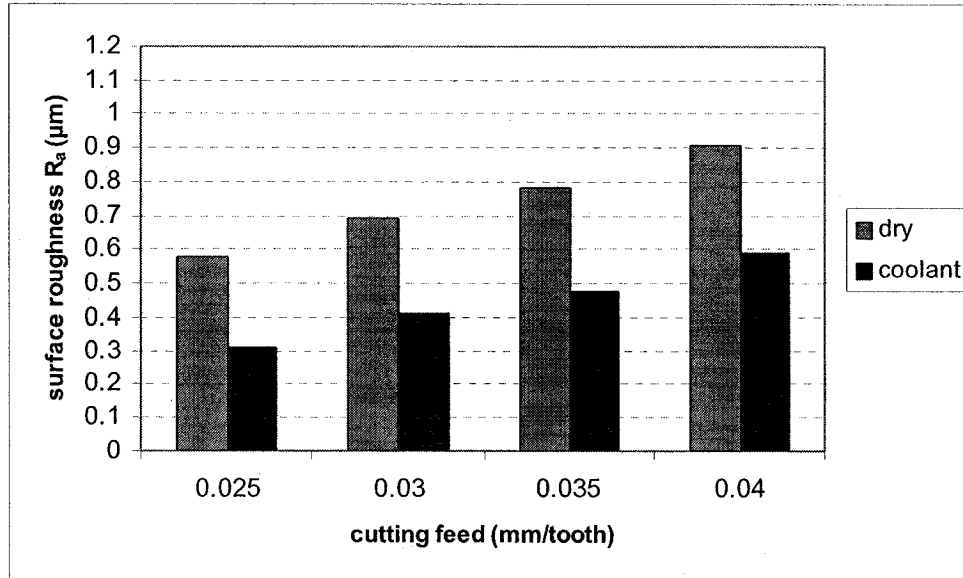


Figure 4.42: Surface roughness (R_a) for wet and dry conditions (HM90APKT, coated insert, $v = 70$ m/min)

Figure 4.42 shows surface roughness values recorded when milling Inconel 718 with coated carbide at cutting speed of 70 m/min under wet and dry conditions.

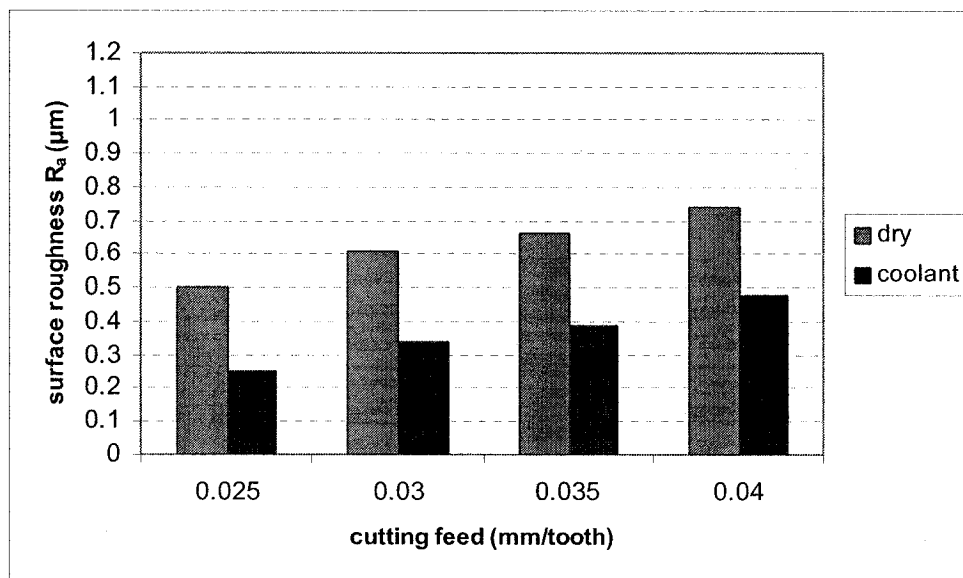


Figure 4.43: Surface roughness (R_a) for wet and dry conditions (HM90APKT, coated insert, $v = 90$ m/min)

Generally improved surface roughness values were obtained in wet (coolant) cutting operation. From figures 4.42 to 4.43, it was observed that the higher value of feed rate (0.04 mm/tooth) increased surface roughness.

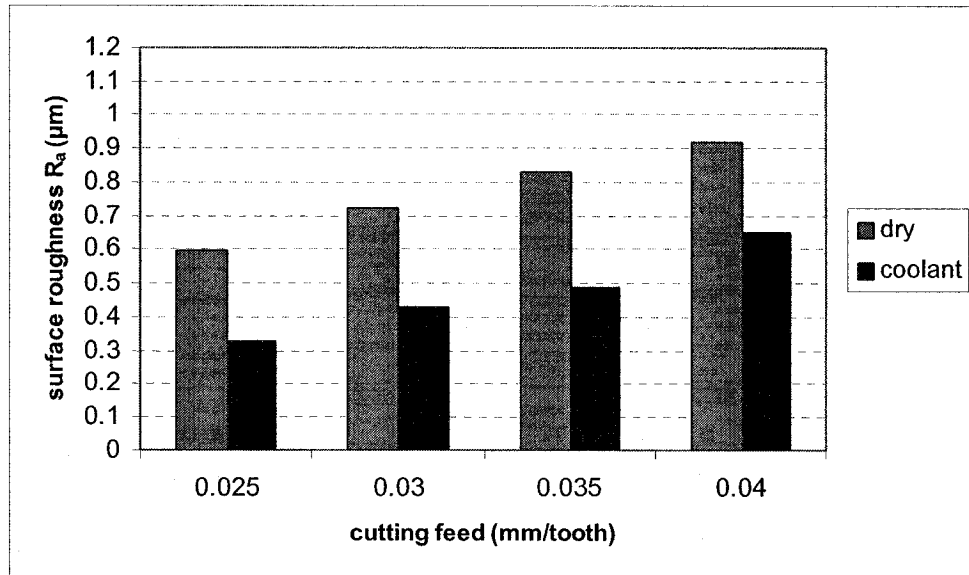


Figure 4.44: Surface roughness (R_a) for wet and dry conditions (APKTIC928, coated insert, $v = 70$ m/min)

Figure 4.44 shows surface roughness of coated carbide (APKTIC928) under wet and dry conditions.

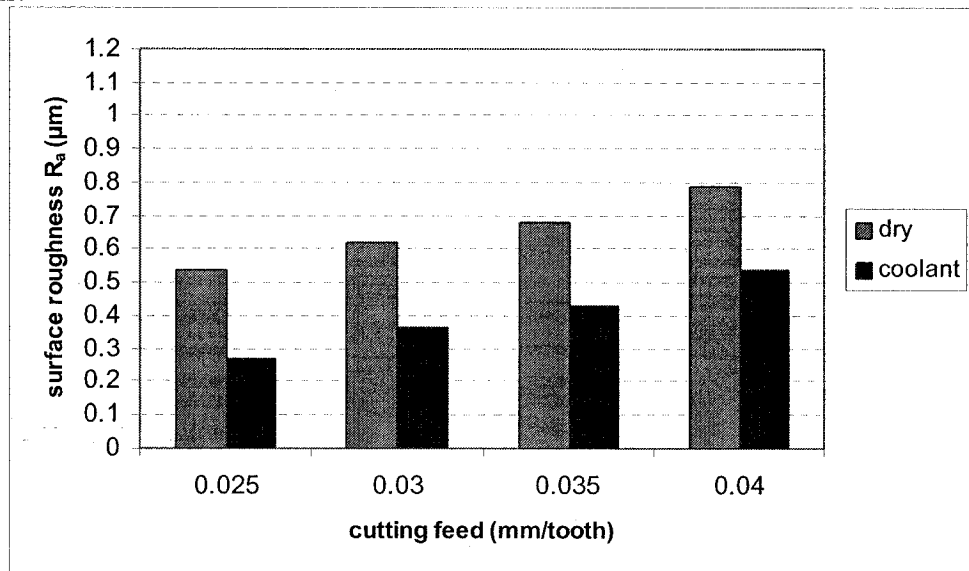


Figure 4.45: Surface roughness (R_a) for wet and dry conditions (APKTIC928, coated insert, $v = 90$ m/min)

Figure 4.45 shows the surface roughness for coated carbide (APKTIC928) at cutting speed of 90 m/min under wet and dry conditions.

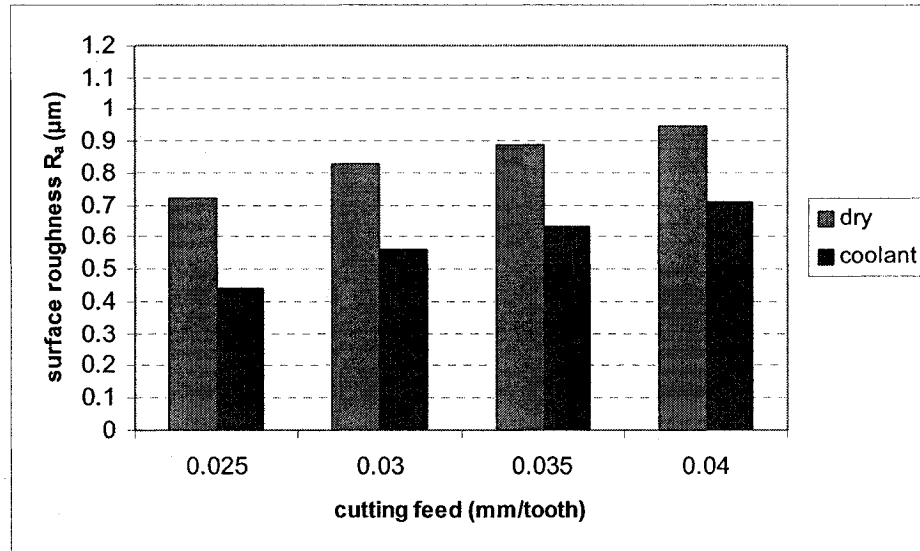


Figure 4.46: Surface roughness (R_a) for wet and dry conditions (APKT, uncoated insert, $v = 40$ m/min)

Figure 4.46 shows the surface roughness for uncoated carbide (APKT) under wet and dry conditions.

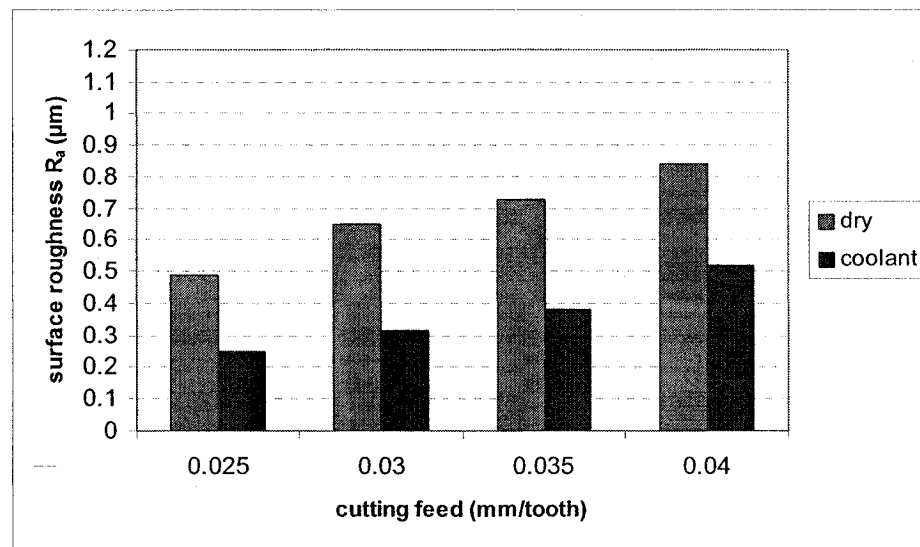


Figure 4.47: Surface roughness (R_a) for wet and dry conditions (APKT, uncoated insert, $v = 70$ m/min)

It can be observed in figure 4.47, at a constant depth of cut and cutting speed that an increase in feed rate accelerates the higher values of roughness. It was found that the larger values of roughness at the feed rate of 0.04 mm/tooth. The chip load (feed) must be kept below a maximum value to avoid mechanical overload and above a minimum value to avoid rubbing. Arunachalan *et al* [2004] also reported that surface roughness increased with higher cutting feeds. On the other hand, increased cutting speeds will decrease surface roughness. The softening of the material due to increased temperature results in a smoother surface and so lower roughness.

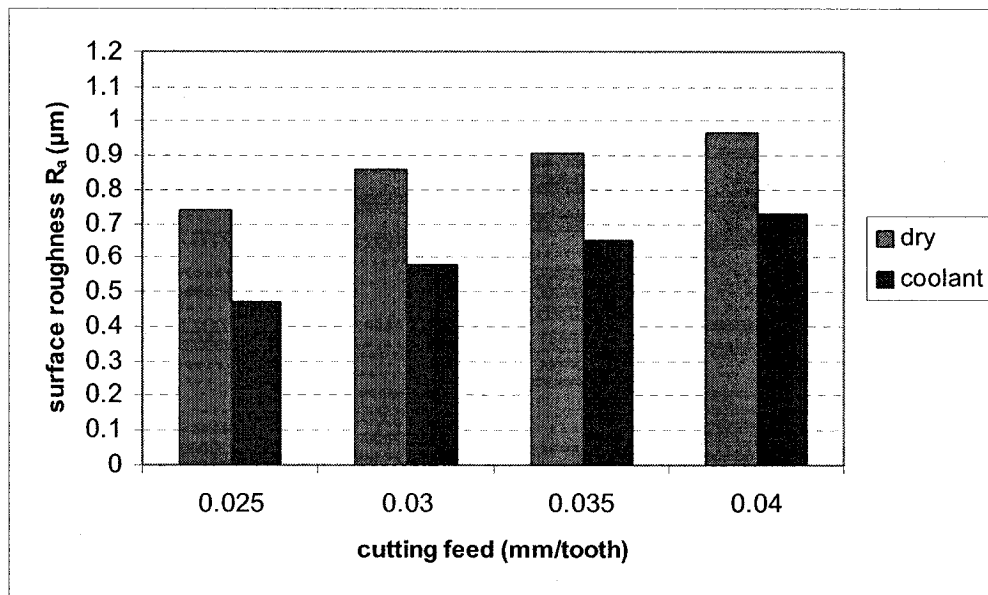


Figure 4.48: Surface roughness (R_a) for wet and dry conditions (APCT, uncoated insert, $v = 40$ m/min)

Figures 4.42 to 4.48 show that the surface roughness value for particular feed rate (0.025 mm/tooth) was not high because it could be due to the relatively closer levels of feed rate employed during present experiment. It was earlier thought that an increase in the depth of cut might lead to vibrations during machining consequently influencing surface

roughness. Therefore, it may be concluded here that the cutting parameters selected for this experimentation can be safely used in the chosen range of depth of cut.

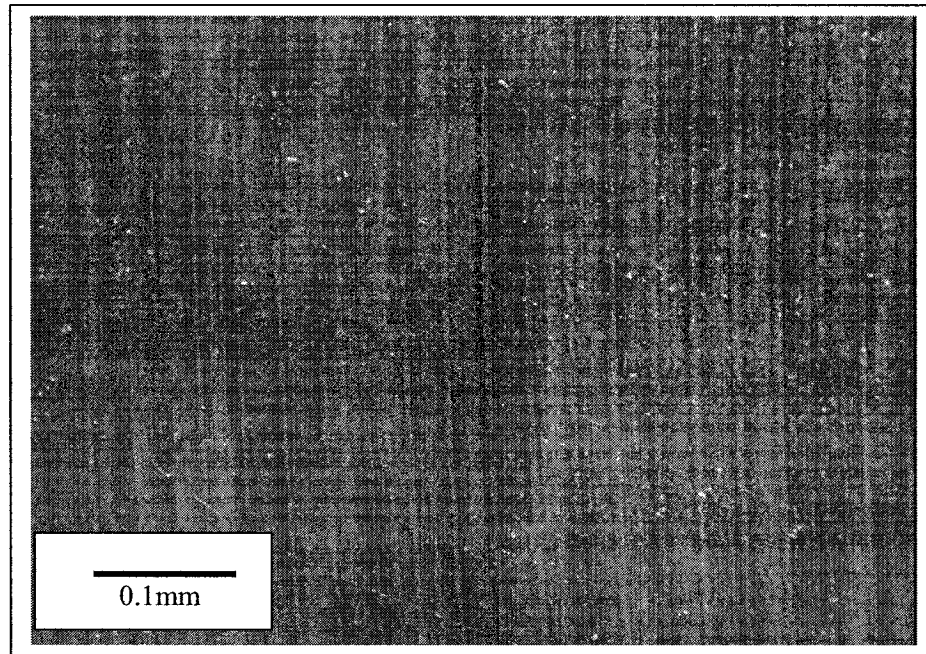


Figure 4.49: Microscopic examination of machined surface for wet condition (HM90APKT, coated insert, $R_a = 0.31 \mu\text{m}$, $R_t = 1.2 \mu\text{m}$, $v = 70 \text{ m/min}$, $f = 0.025 \text{ mm/tooth}$)

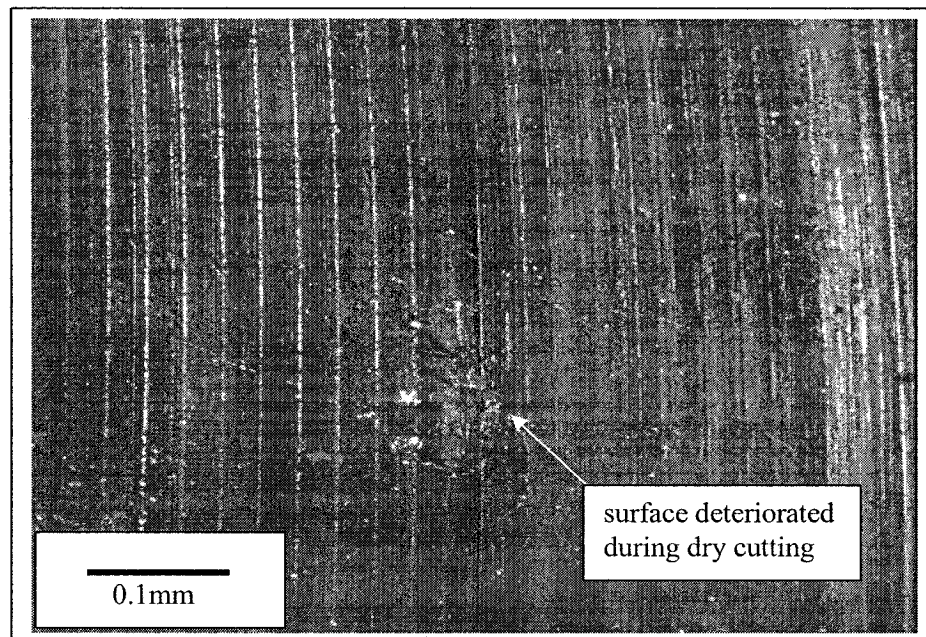


Figure 4.50: Microscopic examination of machined surface for dry condition (HM90APKT, coated insert, $R_a = 0.78 \mu\text{m}$, $R_t = 2.6 \mu\text{m}$, $v = 70 \text{ m/min}$, $f = 0.035 \text{ mm/tooth}$)

Figures 4.49 to 4.50 show the micrograph of machined surface for coated carbide (HM90APKT) at the cutting speed of 70 m/min under wet and dry conditions.

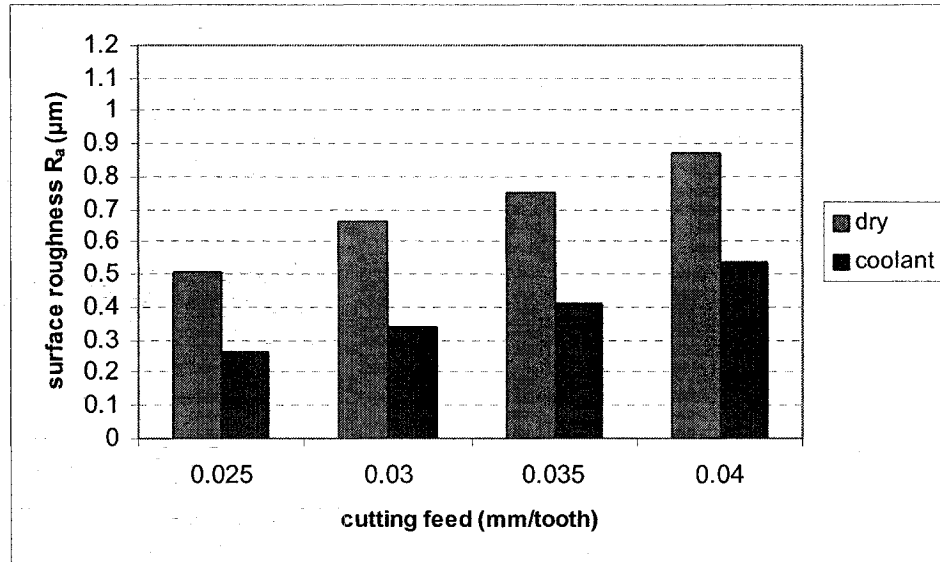


Figure 4.51: Surface roughness (R_a) for wet and dry conditions (APCT, uncoated insert, $v = 70$ m/min)

Figure 4.51 shows the surface roughness for uncoated carbide (APCT) at the cutting speed of 70 m/min.

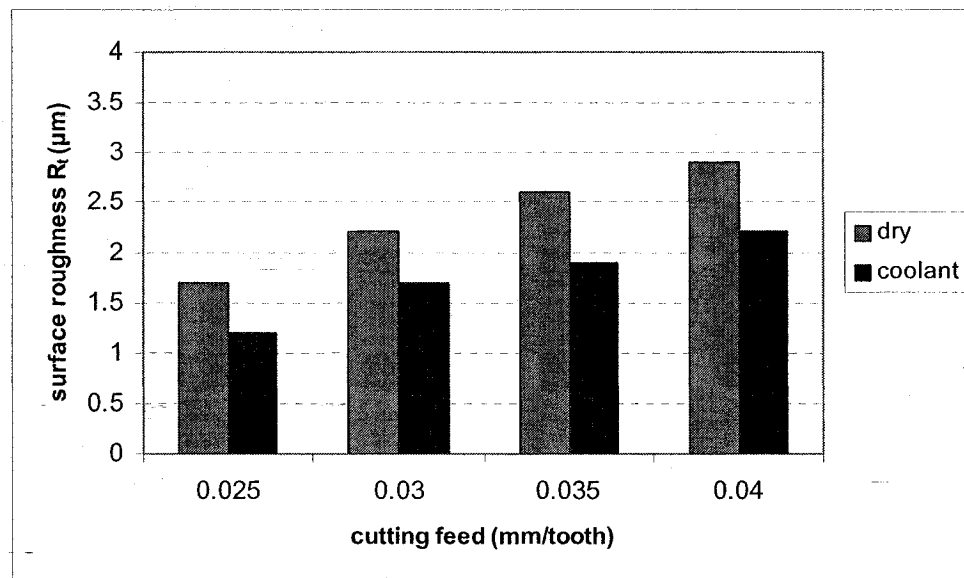


Figure 4.52: Surface roughness (R_t) for wet and dry conditions (HM90APKT, coated insert, $v = 70$ m/min)

When the Inconel 718 was machined with the cutting fluid, the surface roughness height (R_t) improved considerably. Figures 4.52 to 4.53 show the effect of cutting feed on roughness height (R_t). The roughness parameter is slightly larger for coated carbides than that of other uncoated carbides. This could be due to the breaking away of coating particle of tool since the wearing of the coated tool corner.

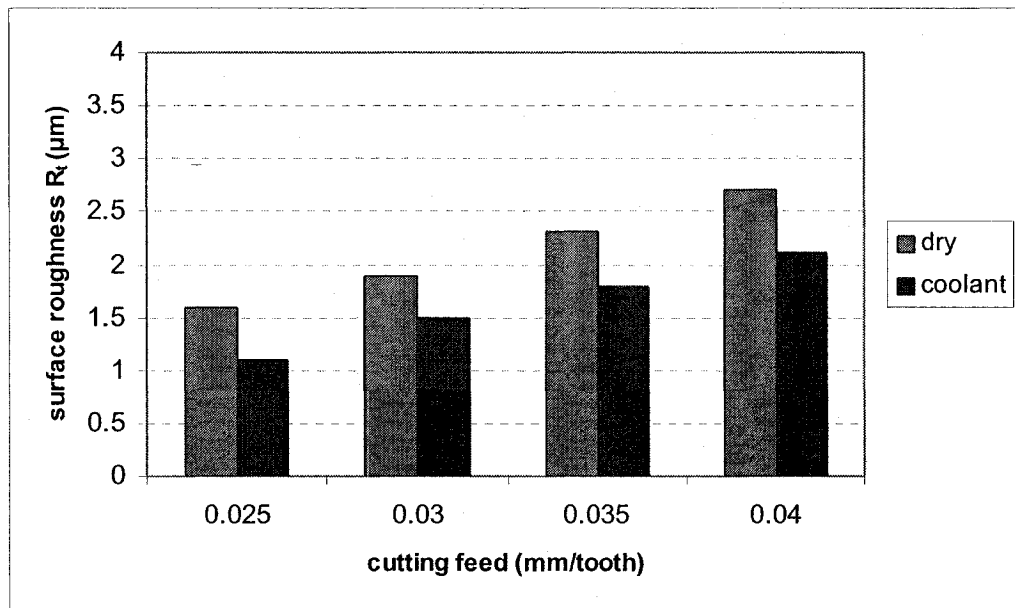


Figure 4.53: Surface roughness (R_t) for wet and dry conditions (APKT, uncoated insert, $v = 70$ m/min)

The greater the feed rates, the higher the value of roughness height (R_t) so that quality of machined surface will be deteriorated. The presence of one or the other or both types of tooth marks alters the geometric conditions of the machined surface and consequently, the quality of surface. When in milling with cutter, the tooth mark depends on the cutter radius and on the effective feed per tooth. Generally, surface finish improves as the tooth mark decreases under a given set of cutting conditions. In machining operation, especially in the finishing operation, the surface finish requirement restricts the range of feed rates which can be used. Moreover, since tooth marks occur on the surface, it will

deteriorate the machined surface quality and ultimately reduce the machining productivity.

4.5 Discussion

Tool materials with improved room and elevated temperature hardness like carbides can be used for machining of nickel based super alloys. In machining nickel based super alloys operation the wear of the flank of the cutting tool is not uniform along the active cutting edge; therefore it is necessary to specify the locations and degrees of the wear when deciding on the amount of wear allowable before regrinding the tool. The width of the wear land is usually taken as a measure of the amount of wear and can be readily determined by means of a toolmaker's microscope. Tool life is one of the most important economic considerations in metal cutting operation. Increased cutting speeds will generally decrease tool life (Taylor equation). In uncoated tool materials there may be cutting speed below which thermal over all (decrease tool life diminished material characteristics) may occur. Similarly, a local tool life maximum may exist at a particular cutting speed if there a phase changes in the workpiece material. Increased chip load (0.025 to 0.04 mm/tooth) will generally decrease tool life. But the impact of chip load (feed) on tool life in comparison to cutting speed was not significant. As previous researchers Rahman *et al* [2000] reported that feed did not show significant influence on tool life during Inconel 718 machining. The performance difference based on tool life between TiAlN coated and uncoated micro grain carbide inerts was more significant. Although TiAlN coated carbide inserts performed the best than uncoated but it did not perform well over cutting speed of 100 m/min. Despite this micro grain carbide is the most attractive from an application view point in that it may be applied to a wide range of

cutting conditions. Tool wear mechanisms are generally influenced by thermal softening, diffusion and abrasion. Nickel based super alloys have a tendency to work harden and retain the major part of their strength during machining. This generates high heat at the interface of the cutting tool and the workpiece giving rise to thermal stress. Moreover, the tip of the cutting edge was the hottest spot in machining of nickel based super alloys. At the cutting speed of 110 m/min, coated carbide tools failed due to thermal softening of the cobalt binder phase and subsequent plastic deformation of the cutting edge. Previous researcher [Jawaid *et al* 2001 and Alauddin *et al* 1998] have indicated that the breaking down of the cutting edge of carbide tools is due to the heat generation in the primary deformation zone. For any material, elements enter the secondary deformation zone after having been strain hardened in the primary deformation zone. Material in the secondary deformation zone is then subjected to very high rate of shear strain. In the case of nickel based super alloys, the combination of a large primary deformation zone heat source and a large secondary deformation zone shear stress applied immediately behind the cutting edge gives rise to high temperature and stress in the region. More over, the normal stresses on the cutting tool are usually twice as high as for machining of nickel based super alloys as for machining steel at the same cutting speed. Under the conditions tested, the removal of coating layer from the rake face of the coated tools indicated that the bond between the adhered material and the rake face was stronger than one between the coating and carbide substrate. As a result, separation of the coating layer took place when the adhered workpiece was forced and pushed away by the shearing action due to the chip flow or by detachment of the chip at cutter exit or entry. The interface between the coating and substrate was disturbed due to the differences in thermal expansion co-

efficient of the substrate and coating and also due to the fluctuating of thermal stress. The use of cutting fluid reduces friction and heat. Cutting fluid reduces friction and heating in machining operation. This allows good cutting conditions. Effective use of coolant helps remove the chips during machining operation. This prevents the chip from being caught between the tool and workpiece where it causes scratches and poor surface finish. Coolant also protects the tool, machine and workpiece against rust and corrosion. Utilizing flood coolant at high pressure enables the coolant stream to penetrate even closer to the edge and improves the heat dissipation into the cutting zone. In addition to heat dissipation coolant substantially improved chip evacuation. Compared to dry tests, wet (coolant) cutting tests had much longer tool life under same cutting conditions. It was noticed early that especially when milling at high cutting speed (100 m/min), the standard cooling did not effectively reach the tip of the tool so that tool life was not as high as estimated. In all cases, dry cutting was not the preferred option due to excessive flank wear (some cooling should be required to reduce flank wear). An attempt has been made here for evaluating the performance of coolant with respect to dry cutting. The surface finish produced by coolant was found to be better compared to that produced by dry cutting. In the case of wet cutting, the micron size ultra fine particle of coolant was capable of providing better lubrication by penetrating deeper into the chip tool interface so that it could reduced temperature generated during machining. An improvement in surface quality indicates an enhanced dimensional accuracy which is essential while machining nickel based super alloys. On the other hand, cutting speed was increased to prevent built-up edge (BUE) formation during cutting operation. All cutting tests have been performed under stable cutting conditions; otherwise surface roughness would be

rough. With an increase in the cutting feed, it was observed that surface roughness parameters increased.

CHAPTER 5

High speed machining: wear and surface roughness for ceramic tools

High speed machining is a technique that combines high spindle speeds with increased feed rates. It can be successfully used in the aerospace industry to manufacture a variety of structural parts. The benefits of high speed machining are increased productivity and improved surface finish [Arunachalam *et al* 2004]. High speed machining technology has been extended to encompass the machining of nickel based superalloys. Nickel based superalloys are used extensively for applications in the aerospace industry for components in the hot sections of gas turbine engine. Whisker reinforced and Kyon 2100 ceramic tools can be used in high speed machining operations. These ceramic tools can withstand higher temperatures during nickel based machining operation. An experimental evaluation of tool wear, wear mechanisms and machined surface roughness for ceramic tools under different cutting conditions is presented in this chapter.

5.1 High speed machining operation

In today's aerospace industry part machining is more exigent and competitive and presents greater requirements in dimensional precision and surface finish as well as in costs and manufacturing times. Vivancos *et al* [2004] discussed in advantages of high speed machining operation. They also reported that good surface finish was achieved in high speed machining. High speed machining is a technique that combines high spindle speeds with increased feed rates. Machining with high speeds increases efficiency, accuracy and quality of workpieces and at the same time to decrease machining time. The use of high speed machining allows us to shorten production time and to increase accuracy of machined parts. High speed machining is used in manufacturing industry due to specific requirements. An increase of cutting speed gives several benefits such as enlarging of the removal rate and improving of the final machined surface. The productivity of machining operations can be increased and the quality of machined surface can be improved by higher cutting speeds than conventional method. Introducing stronger, tougher and more heat resistant cutting tools leads to higher productivity by means of higher cutting speeds and heavier machining loads. The development of ceramic tool materials has enabled high speed milling of nickel based superalloys.

5.2 Ceramic tools for nickel based superalloys machining

The individual branches drive the specific demands for new innovation using different engineering materials. However, the workpiece materials in many applications are very difficult or even impossible to machine with conventional cutting technology. Nickel based super alloys are generally known to be one of the most difficult materials to machine because of their high hardness, high strength at high temperature, affinity to

Chapter 5. High speed machining: wear and surface roughness for ceramic tools

react with tool materials and low thermal diffusivity. Only a few reports have been published on machining nickel based superalloys with ceramic tools. The high temperatures generated in machining of nickel based superalloys especially at high cutting speeds, necessitate the use of a refractory cutting tool that can withstand the high temperatures and to provide longer tool life. It is well known that grain size and impurities segregating at the grain boundaries have great influence on strength and performance of ceramic tool. For cutting tools, two kinds of ceramic tool materials (aluminium oxide and silicon nitride) are used, which can be differentiated according to the matrix materials. Aluminium oxide, commonly referred to as alumina possesses strong ionic interactions bonding giving rise to its desirable material characteristics. .Ezugwu *et al* [2005] conducted experiments for turning of Inconel 718 with ceramic tools. They reported that ceramic tool materials exhibited superior cutting performance in terms of wear resistance and fracture resistance. Elbestawi *et al* [1998] reported that whisker ceramic tool showed good performance during machining of Inconel 718. The whisker reinforced ceramic tool material consists of aluminium silicon carbide whiskers. Whisker reinforced ceramic tool is more wear resistant and fracture resistant than other tool materials. Silicon nitride based ceramic (Kyon 2100) has also good high temperature strength, creep resistance and oxidation resistance. Due to superior mechanical and thermal properties, these ceramic tools can be employed to machine nickel based superalloys at higher cutting speeds and feeds. Whisker reinforced and Kyon 2100 possess valuable hot hardness and may increase productivity. Therefore, we used whisker reinforced and kyon 2100 ceramic tools for the machining of nickel based superalloys.

5.3 Selection of cutting conditions for ceramic tools

Cutting parameters such as cutting speed and feed should be chosen properly in order to achieve longer tool life and good surface finish. Ezugwu *et al* [2005] conducted experiments with ceramic tools. They selected cutting speed from 100 to 500 m/min. Arunachalam *et al* [2004] carried out experiments with ceramic tools at the cutting speeds of 250 to 450 m/min. On the other hand, Elbestawi *et al* [1998] investigated failure characteristics and cutting performance of ceramic tools for machining of Inconel 718. They performed cutting tests at cutting speeds from 200 to 700 m/min and feeds from 0.05 to 0.10 mm/tooth. They also reported that tool wear increased at low cutting speed of 200 m/min. In this thesis work, we selected cutting speeds from 250 to 1450 m/min for ceramic tools. The cutting speed was not raised above 1450 m/min because of the limited capacity of machine spindle speed. Feeds were chosen between 0.03 to 0.12 mm/tooth for better surface finish. Above a feed of 0.12 mm/tooth, the machined surface quality was deteriorated. Therefore, the test matrix prepared for this experiment can be safely used in the chosen range of cutting parameters.

5.4 Experiments with ceramic tools in high speed machining

The purpose of the experiments was to investigate of tool wear and surface roughness for Whisker reinforced and Kyon 2100 ceramic tool materials. The experiment was conducted to find the optimum range of cutting conditions in this application and to identify wear mechanisms under various cutting conditions. The cutting speed levels were chosen by making use of the full capacity of the CNC milling machine. Since large depth of cut will increase the impact force and cause damage to the tool during interrupted cutting, the level of depth of cut was kept constant at 0.50 mm.

Chapter 5. High speed machining: wear and surface roughness for ceramic tools

All the tests were conducted in half immersion down milling process. Tool wear was observed periodically using a microscope. Tests were stopped for that cutting condition when the maximum flank wear reached a value of 0.70 mm. Zhao *et al* [1998] conducted experiments with ceramic tools. They determined tool life based on maximum flank wear (0.70 mm). Table 5.1 shows the cutting conditions for Whisker ceramic tool and tick indicates the same cutting parameters used for each set of cutting conditions.

Table 5.1 Test matrix for Whisker reinforced and Kyon 2100 ceramic tools

	v (m/min)	f (mm/tooth)	Environment	Immersion
Condition 1	250	0.03,0.04,0.05,0.06,0.07,0.08 0.09,0.10,0.11,0.12	dry	half
Condition 2	350	√	√	√
Condition 3	450	√	√	√
Condition 4	550	√	√	√
Condition 5	650	√	√	√
Condition 6	750	√	√	√
Condition 7	850	√	√	√
Condition 8	950	√	√	√
Condition 9	1050	√	√	√
Condition 10	1150	√	√	√
Condition 11	1250	√	√	√
Condition 12	1350	√	√	√
Condition 13	1450	√	√	√

Surface roughness was measured using a portable surface roughness instrument. A surface roughness measurement was taken each time tool wear measurements were taken. Wear mechanisms were examined by using a scanning metallographic microscope. All of the cutting tests were conducted under dry condition.

5.5 Experimental results

All the cutting tests were carried out using ceramic tools (Whisker reinforced and Kyon 2100) in milling operation. Each test was repeated at least twice in order to check the consistency of the results. From the experimental results, tool wear under different cutting conditions are presented.

5.5.1 Tool wear for ceramic tools

Flank wear was prevalent along the cutting edge during ceramic milling operation. Flank wear was measured using tool wear measuring microscope. Maximum flank wear (VB_{max}) and average flank wear (VB) were recorded for each cutting test. The flank wear rate changes with cutting length (Figure 5.1).

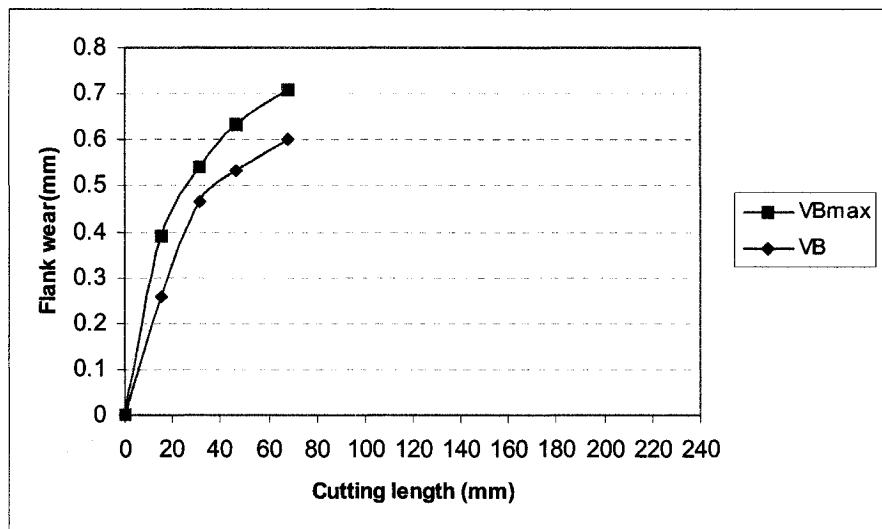


Figure 5.1: Flank wear vs. Cutting length (Whisker reinforced ceramic tool, $v = 250$ m/min, $f = 0.03$ mm/tooth, dry cutting)

Chapter 5. High speed machining: wear and surface roughness for ceramic tools

Figure 5.1 shows the variation of flank wear for Whisker reinforced ceramic tool at the cutting speed of 250 m/min and feed of 0.03 mm/tooth.

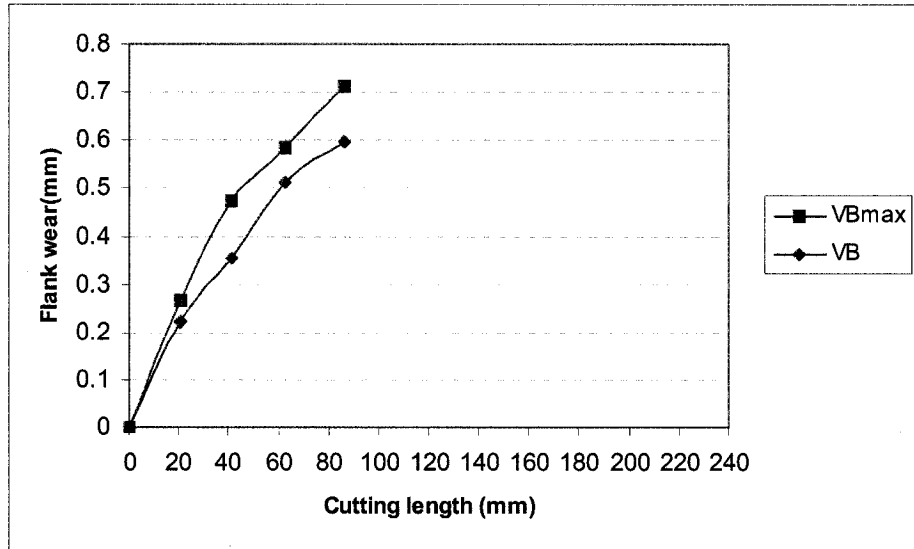


Figure 5.2: Flank wear vs. Cutting length (Whisker reinforced ceramic tool, $v = 350$ m/min, $f = 0.03$ mm/tooth, dry cutting)

Figure 5.2 shows the variation of flank wear for Whisker reinforced ceramic tool at the cutting speed of 350 m/min and feed of 0.03 mm/tooth.

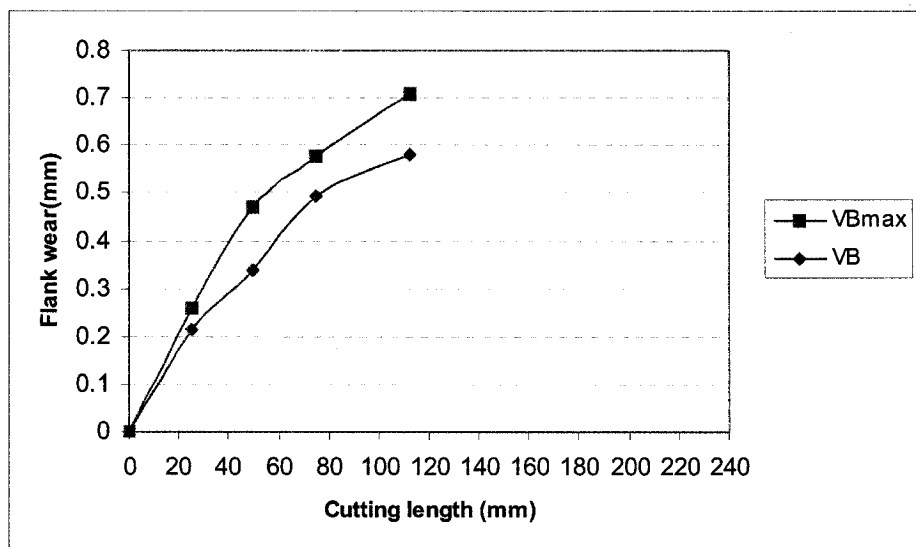


Figure 5.3: Flank wear vs. Cutting length (Whisker reinforced ceramic tool, $v = 450$ m/min, $f = 0.03$ mm/tooth, dry cutting)

Chapter 5. High speed machining: wear and surface roughness for ceramic tools

Figure 5.3 shows the variation of flank wear for Whisker reinforced ceramic tool at the cutting speed of 450 m/min and feed of 0.03 mm/tooth.

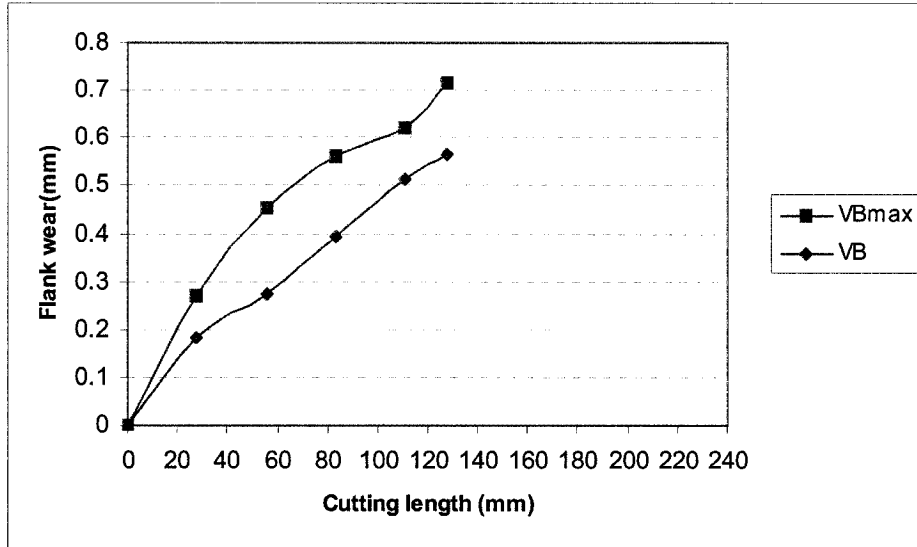


Figure 5.4: Flank wear vs. Cutting length (Whisker reinforced ceramic tool, $v = 550$ m/min, $f = 0.03$ mm/tooth, dry cutting)

Figure 5.4 shows the variation of flank wear for Whisker reinforced ceramic tool at the cutting speed of 550 m/min and feed of 0.03 mm/tooth.

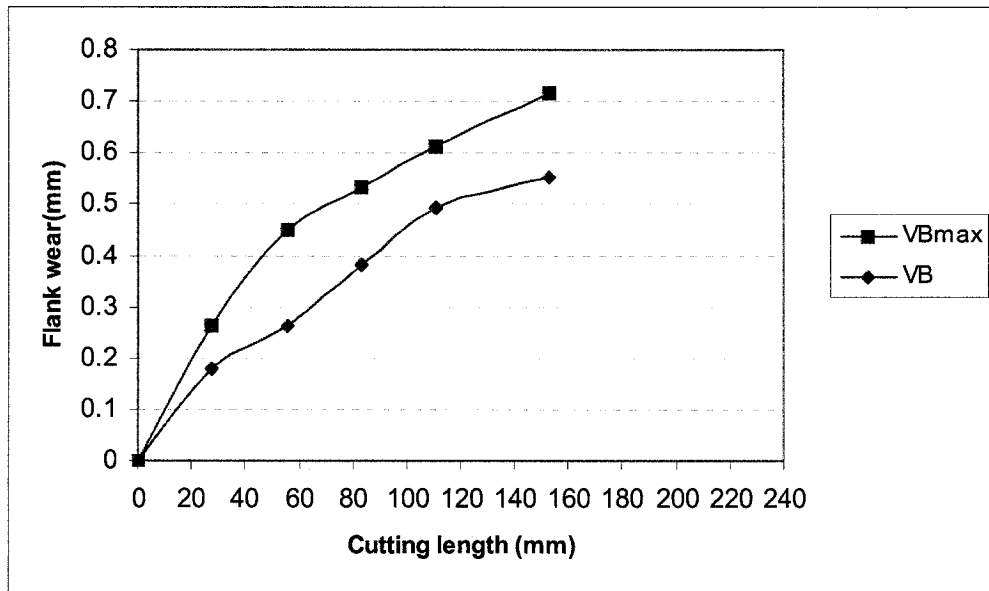


Figure 5.5: Flank wear vs. Cutting length (Whisker reinforced ceramic tool, $v = 650$ m/min, $f = 0.03$ mm/tooth, dry cutting)

Chapter 5. High speed machining: wear and surface roughness for ceramic tools

Figure 5.5 shows the variation of flank wear for Whisker reinforced ceramic tool at the cutting speed of 650 m/min and feed of 0.03 mm/tooth.

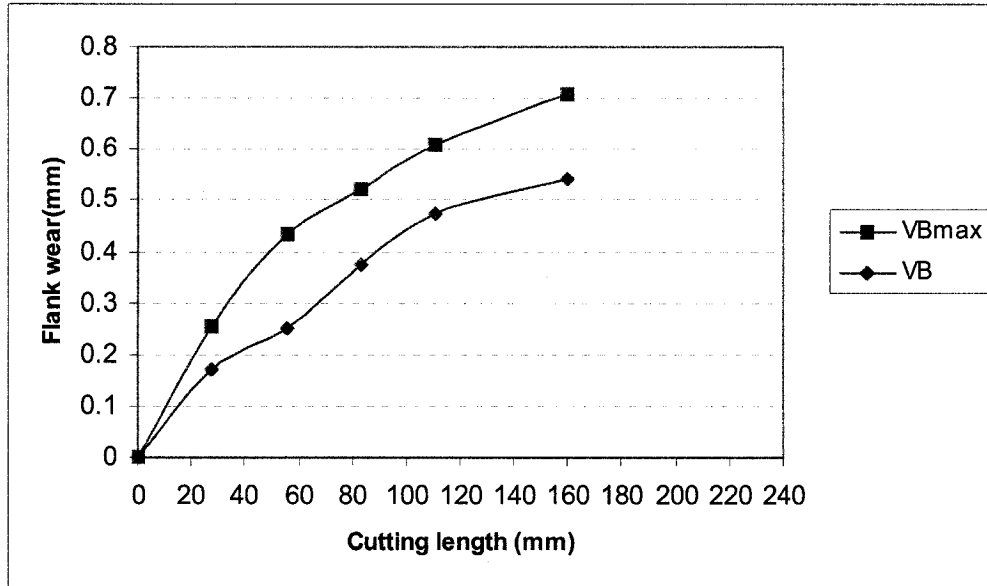


Figure 5.6: Flank wear vs. Cutting length (Whisker reinforced ceramic tool, $v = 750$ m/min, $f = 0.03$ mm/tooth, dry cutting)

Figure 5.6 shows the variation of flank wear for Whisker reinforced ceramic tool at the cutting speed of 750 m/min and feed of 0.03 mm/tooth.

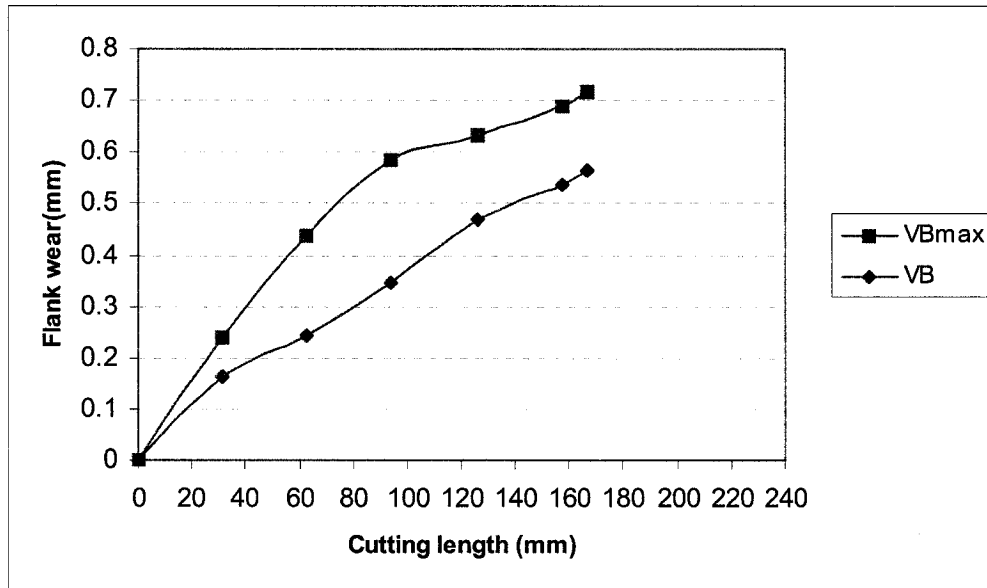


Figure 5.7: Flank wear vs. Cutting length (Whisker reinforced ceramic tool, $v = 850$ m/min, $f = 0.03$ mm/tooth, dry cutting)

Chapter 5. High speed machining: wear and surface roughness for ceramic tools

Figure 5.7 shows the variation of flank wear for Whisker reinforced ceramic tool at the cutting speed of 850 m/min and feed of 0.03 mm/tooth. At a constant depth of cut of 0.5mm and a constant feed of 0.03 mm/tooth, the flank wear seemed to be more severe at the lowest cutting speed of 250 m/min. The rate of wear started to decrease as the cutting speed increased and longer tool life or cutting length was recorded at the cutting speed of 850 m/min. The refractory characteristics of whisker ceramic tools enable them to retain high hot hardness and wear resistance. It was also found that the portion of the cutting edge affected by flank wear increased with increasing cutting speed (950 m/min).

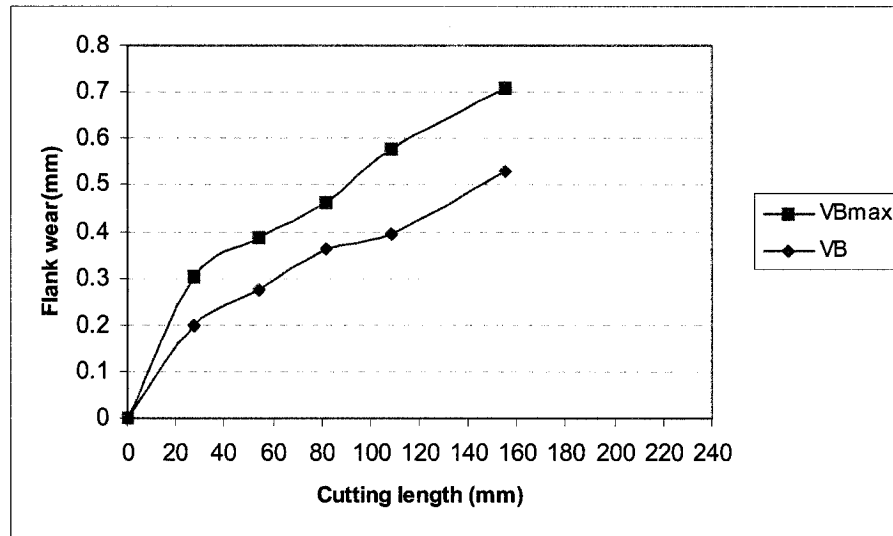


Figure 5.8: Flank wear vs. Cutting length (Whisker reinforced ceramic tool, $v = 950$ m/min, $f = 0.03$ mm/tooth, dry cutting)

Chapter 5. High speed machining: wear and surface roughness for ceramic tools

Figure 5.8 shows the variation of flank wear for Whisker reinforced ceramic tool at the cutting speed of 950 m/min and feed of 0.03 mm/tooth.

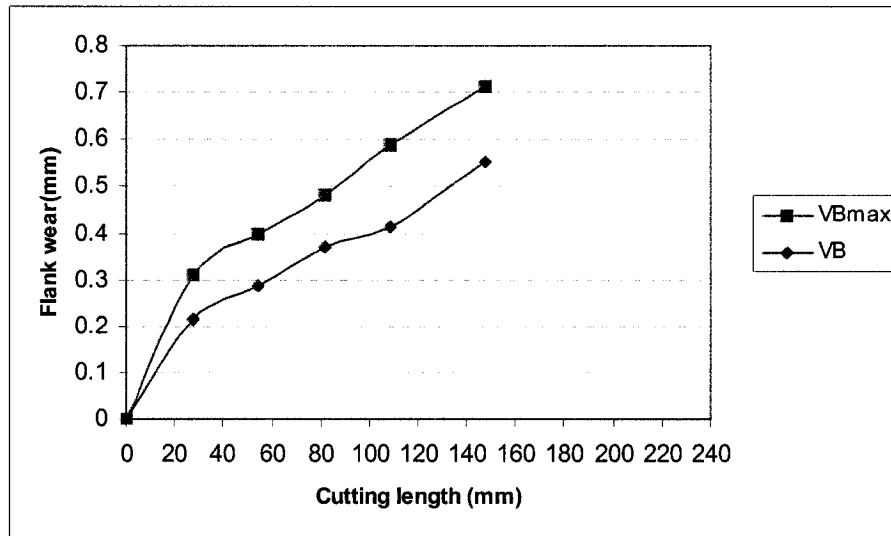


Figure 5.9: Flank wear vs. Cutting length (Whisker reinforced ceramic tool, $v = 1050$ m/min, $f = 0.03$ mm/tooth, dry cutting)

Figure 5.9 shows the variation of flank wear for Whisker reinforced ceramic tool at the cutting speed of 1050 m/min and feed of 0.03 mm/tooth.

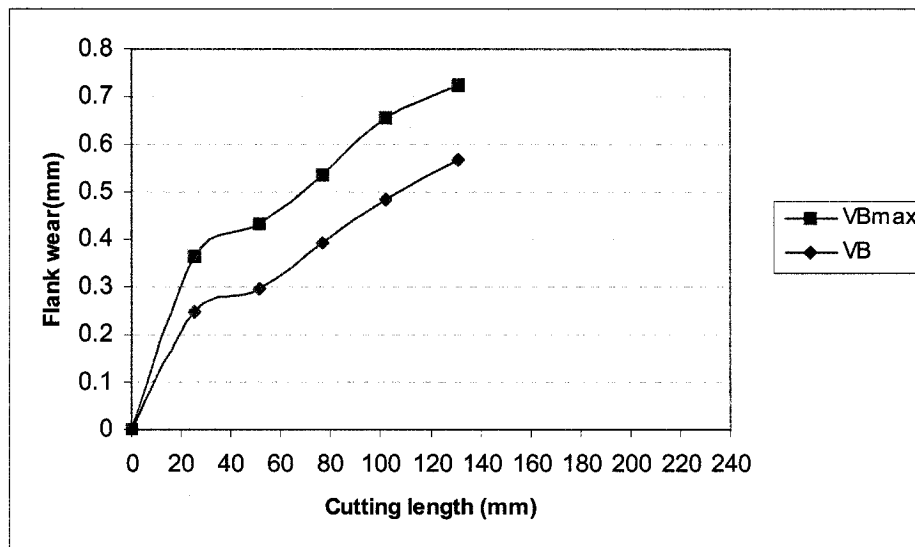


Figure 5.10: Flank wear vs. Cutting length (Whisker reinforced ceramic tool, $v = 1150$ m/min, $f = 0.03$ mm/tooth, dry cutting)

Chapter 5. High speed machining: wear and surface roughness for ceramic tools

Figure 5.10 shows the variation of flank wear for Whisker reinforced ceramic tool at the cutting speed of 1150 m/min and feed of 0.03 mm/tooth.

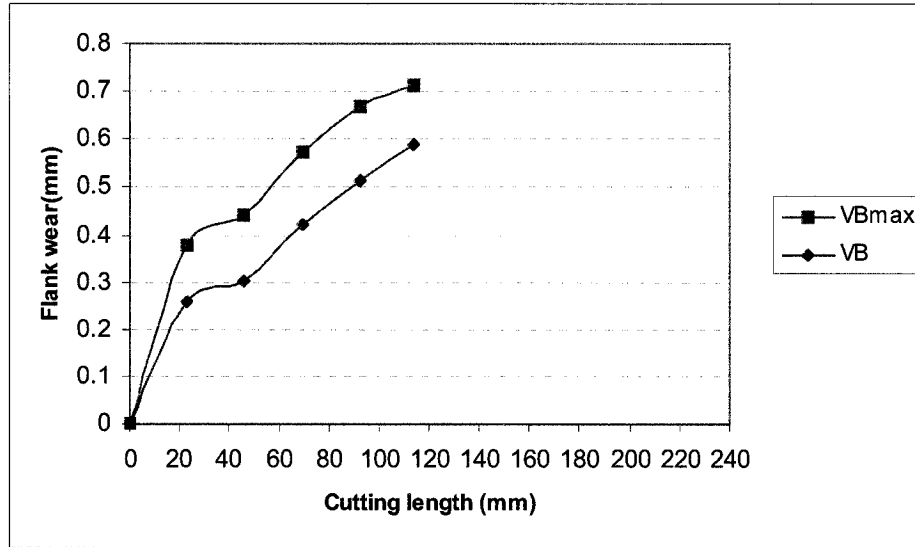


Figure 5.11: Flank wear vs. Cutting length (Whisker reinforced ceramic tool, $v = 1250$ m/min, $f = 0.03$ mm/tooth, dry cutting)

Figure 5.11 shows the variation of flank wear for Whisker reinforced ceramic tool at the cutting speed of 1250 m/min and feed of 0.03 mm/tooth.

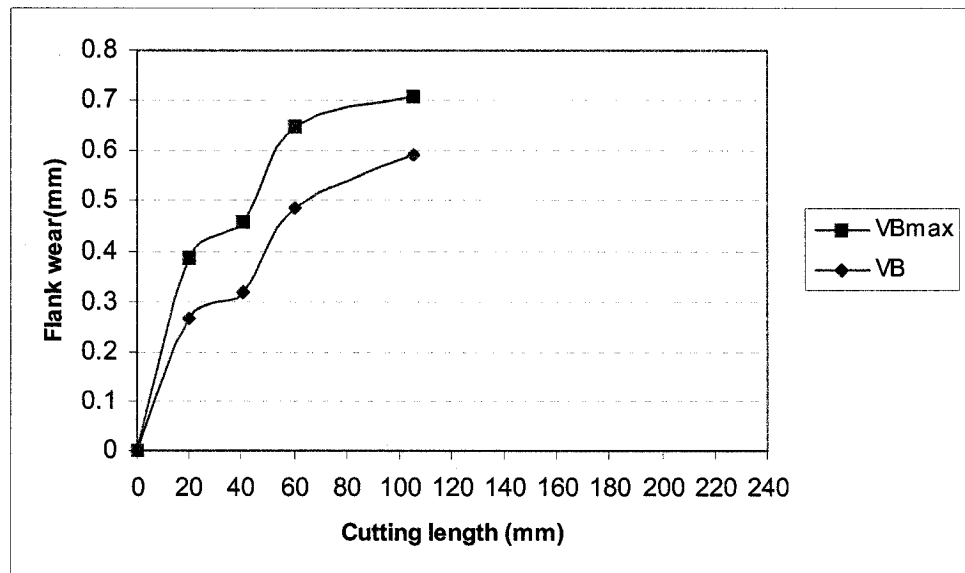


Figure 5.12: Flank wear vs. Cutting length (Whisker reinforced ceramic tool, $v = 1350$ m/min, $f = 0.03$ mm/tooth, dry cutting)

Chapter 5. High speed machining: wear and surface roughness for ceramic tools

Figure 5.12 shows the variation of flank wear for Whisker reinforced ceramic tool at the cutting speed of 1350 m/min and feed of 0.03 mm/tooth.

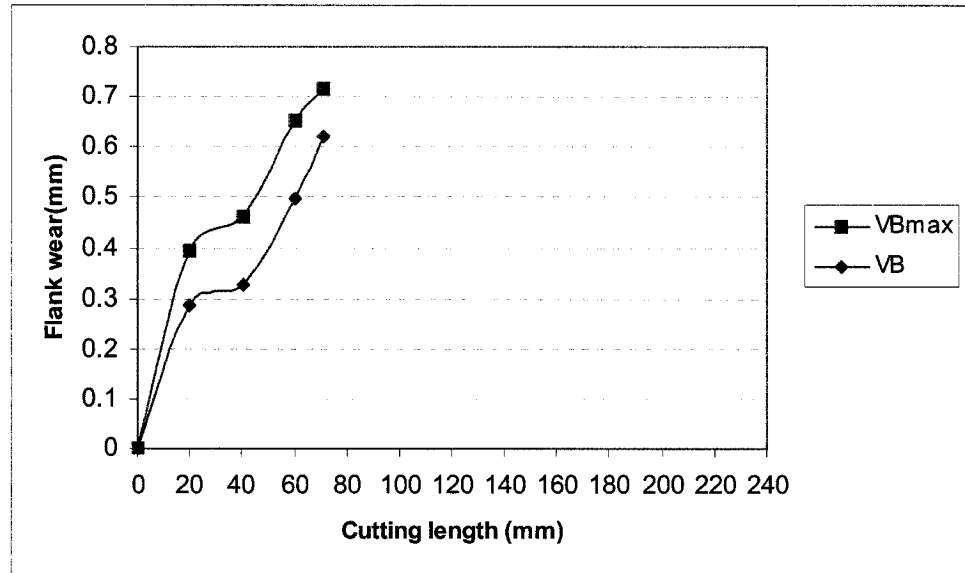


Figure 5.13: Flank wear vs. Cutting length (Whisker reinforced ceramic tool, $v = 1450$ m/min, $f = 0.03$ mm/tooth, dry cutting)

Figure 5.13 shows the variation of flank wear for Whisker reinforced ceramic tool at the cutting speed of 1450 m/min and feed of 0.03 mm/tooth. Since ceramic cutting tool is much more resistant towards chemical reactions with Inconel 718, the flank wear was mainly determined by adhesion and abrasion of workpiece material on the tool surface followed by grain pullout. Most of the flank surface appeared rather non uniform especially when machining Inconel 718 with ceramic tools. Reducing cutting speed (250 m/min) caused the tool to wear faster for the machining of Inconel 718 with ceramic tools. Ezugwu *et al* [2005] reported that wear on the flank face of the ceramic tool was pronounced when machining Inconel 718. On the other hand, Coelho *et al* [2004] also reported that thermal cracking was a major problem when coolant was used for ceramic tools. For this reason coolant was not used during milling with ceramic tools. It can be observed that tool life or cutting length was shorter at the cutting speed of 950 m/min

Chapter 5. High speed machining: wear and surface roughness for ceramic tools

The temperature generated during cutting is dependent on the property of the material (Inconel 718) being machined. An increase in the cutting speed will increase the cutting tool temperature which subsequently reduces its yield strength. The reduction of strength of the cutting tool can result in excessive tool wear. For this reason tool life or cutting length was found to be shorter as the cutting speed was increased from 950 to 1450 m/min. Tool life or cutting length was found to be shorter at the cutting speed of 250 m/min for Kyon 2100 ceramic tool.

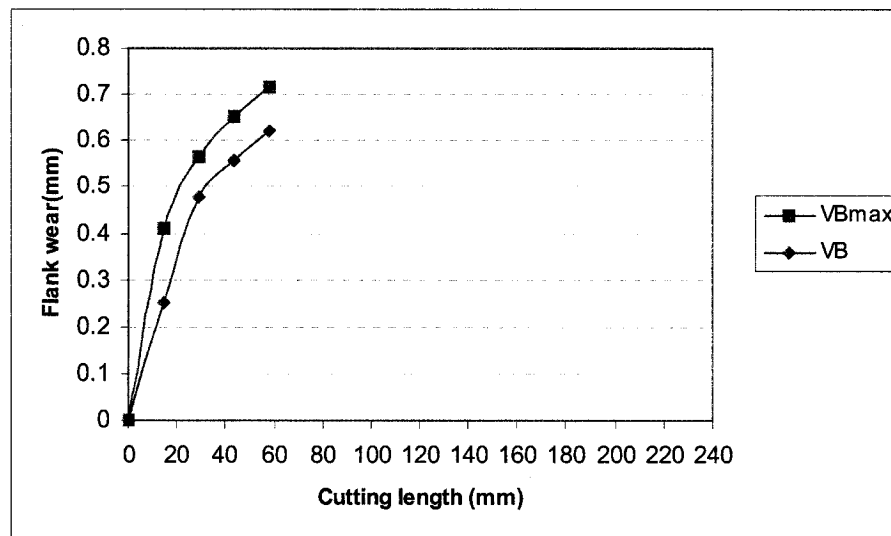


Figure 5.14: Flank wear vs. Cutting length (Kyon 2100 ceramic tool, $v = 250$ m/min, $f = 0.03$ mm/tooth, dry cutting)

Figure 5.14 shows flank wear for Kyon 2100 ceramic tool at the cutting speed of 250 m/min and feed of 0.03 mm/tooth. The Kyon 2100 ceramic tool material facilitated a substantial increase of tool life (cutting length) when machining nickel based superalloys. It is found that tool life increases as the cutting speed increases (250 to 850 m/min). Further increase in cutting speed (950 to 1450 m/min) accelerated the flank wear resulting in shorter tool lives. The maximum tool life or cutting length was achieved at the cutting speed of 850 m/min.

Chapter 5. High speed machining: wear and surface roughness for ceramic tools

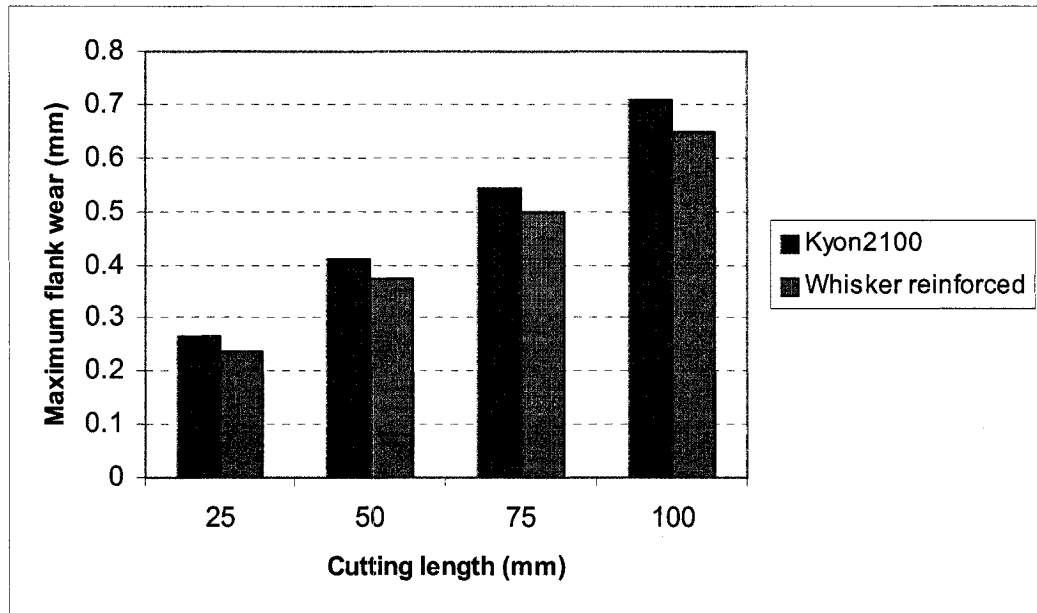


Figure 5.15: Maximum flank wear vs. Cutting length ($v = 450$ m/min, $f = 0.04$ mm/tooth, dry cutting)

Figure 5.15 shows maximum flank wear at the cutting speed of 450 m/min and feed of 0.04 mm/tooth. In our experiments, Whisker ceramic insert shows slightly better result than Kyon2100 based on tool wear. A whisker reinforced tool is inherently strong and able to withstand interruptions at high speed. This is due to the Whiskers toughening effect related to debonding and bridge between matrix grains mechanisms. Additionally, the Whisker reinforced ceramic is more chemically stable to nickel based super alloys than Kyon 2100 tool, so that the wear is slightly less than Kyon 2100 ceramic tool

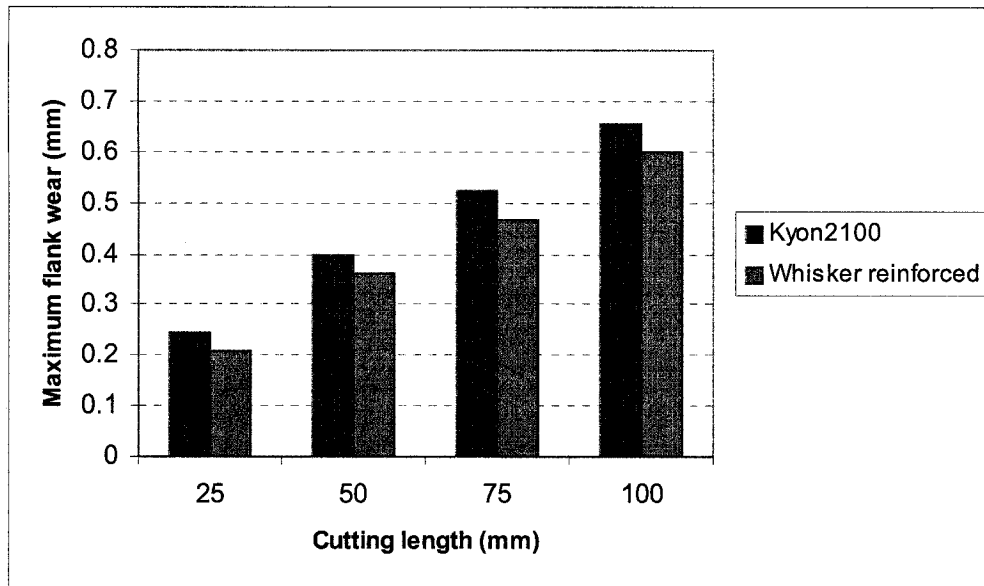


Figure 5.16: Maximum flank wear vs. Cutting length ($v = 550$ m/min, $f = 0.04$ mm/tooth, dry cutting)

Figure 5.16 shows maximum flank wear at the cutting speed of 550 m/min and feed of 0.04 mm/tooth.

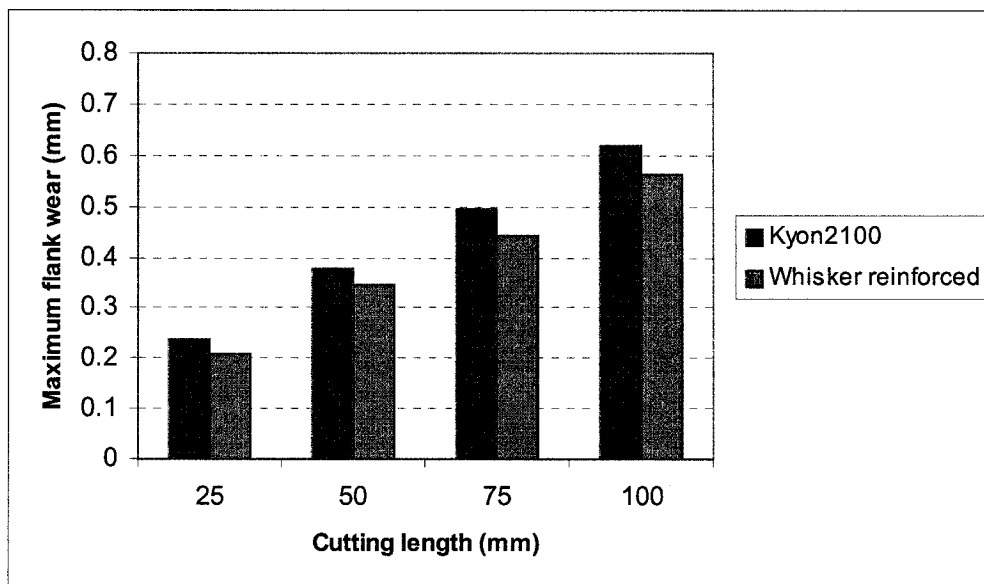


Figure 5.17: Maximum flank wear vs. Cutting length ($v = 650$ m/min, $f = 0.04$ mm/tooth, dry cutting)

Chapter 5. High speed machining: wear and surface roughness for ceramic tools

Figure 5.17 shows maximum flank wear at the cutting speed of 650 m/min and feed of 0.04 mm/tooth.

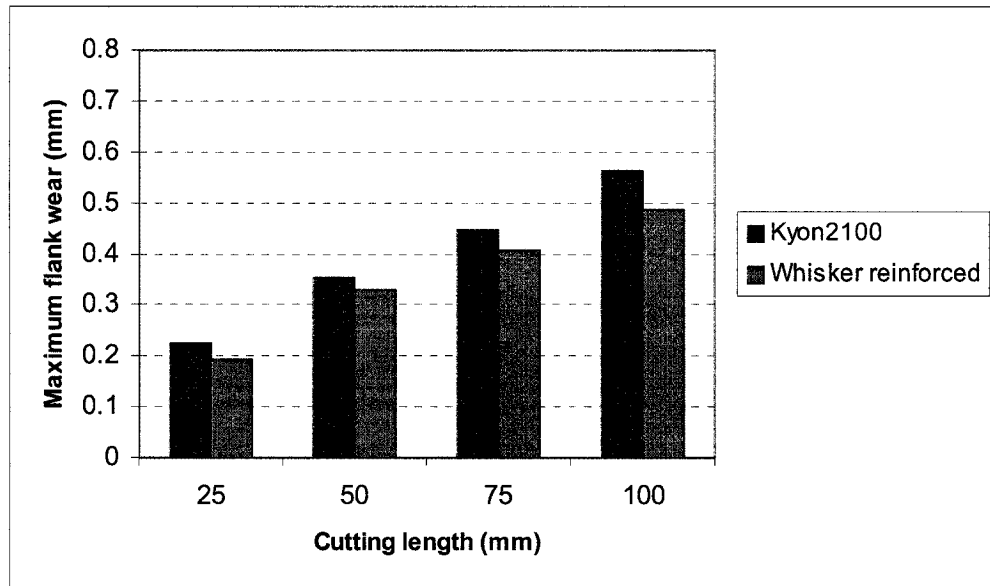


Figure 5.18: Maximum flank wear vs. Cutting length ($v = 750$ m/min, $f = 0.04$ mm/tooth, dry cutting)

Figure 5.18 shows maximum flank wear at the cutting speed of 750 m/min and feed of 0.04 mm/tooth.

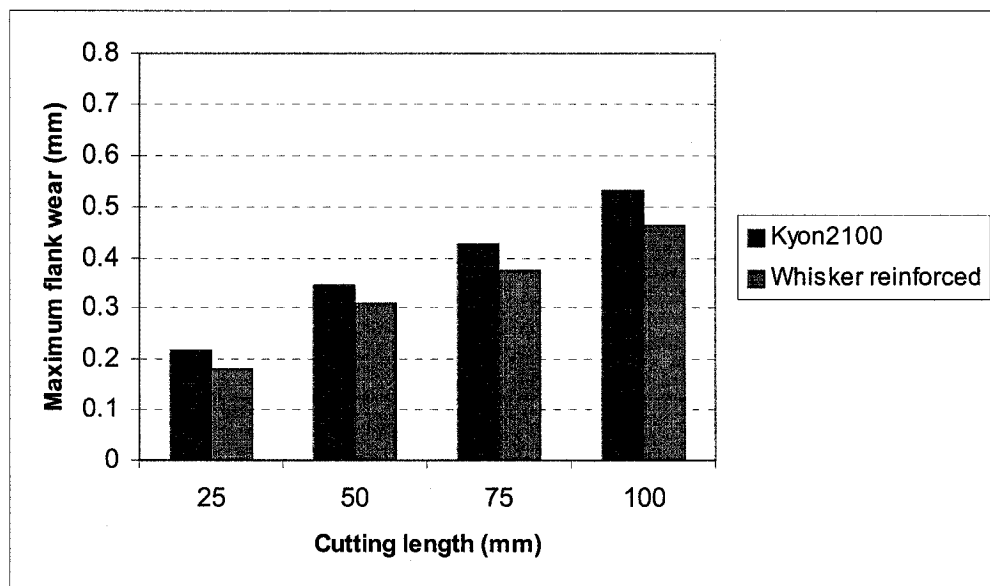


Figure 5.19: Maximum flank wear vs. Cutting length ($v = 850$ m/min, $f = 0.04$ mm/tooth, dry cutting)

Chapter 5. High speed machining: wear and surface roughness for ceramic tools

Figure 5.19 shows maximum flank wear at the cutting speed of 850 m/min and feed of 0.04 mm/tooth.

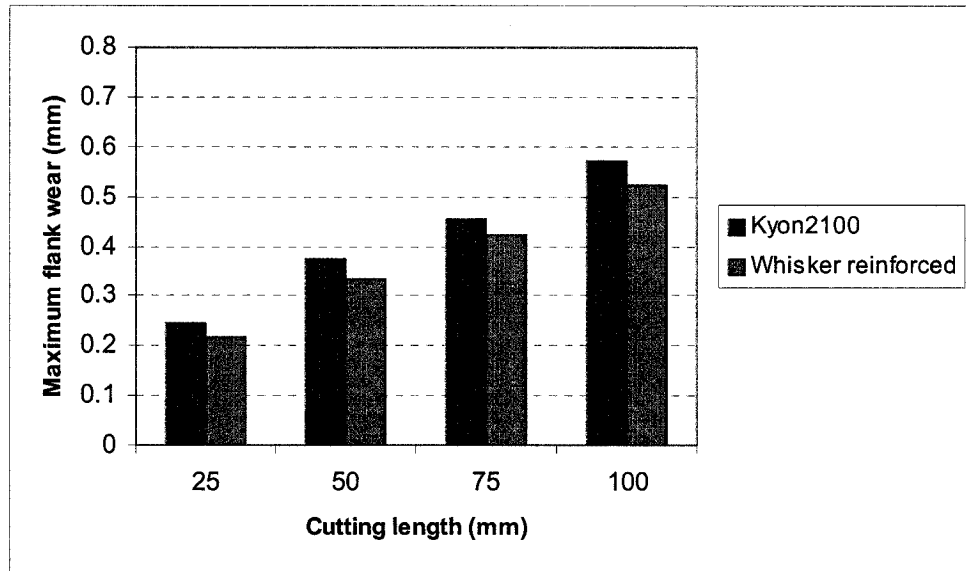


Figure 5.20: Maximum flank wear vs. Cutting length ($v = 950$ m/min, $f = 0.04$ mm/tooth, dry cutting)

Figure 5.20 shows maximum flank wear at the cutting speed of 950 m/min and feed of 0.04 mm/tooth

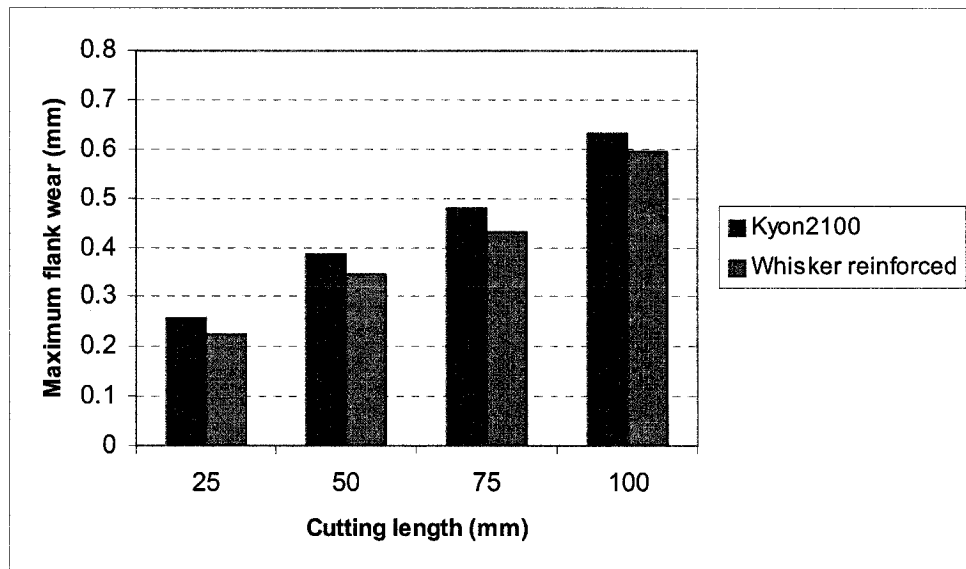


Figure 5.21: Maximum flank wear vs. Cutting length ($v = 1050$ m/min, $f = 0.04$ mm/tooth, dry cutting)

Chapter 5. High speed machining: wear and surface roughness for ceramic tools

Figure 5.21 shows maximum flank wear at the cutting speed of 1050 m/min and feed of 0.04 mm/tooth. Kyon 2100 shows slightly greater flank wear than Whisker reinforced ceramic tool when machining nickel based superalloys. Elbestawi *et al* [1998] reported that Whisker ceramic shows smaller flank wear than Kyon 2100 under same cutting conditions. Tests on Inconel 718 using ceramic tools showed that the cutting edge suffered from flank wear.

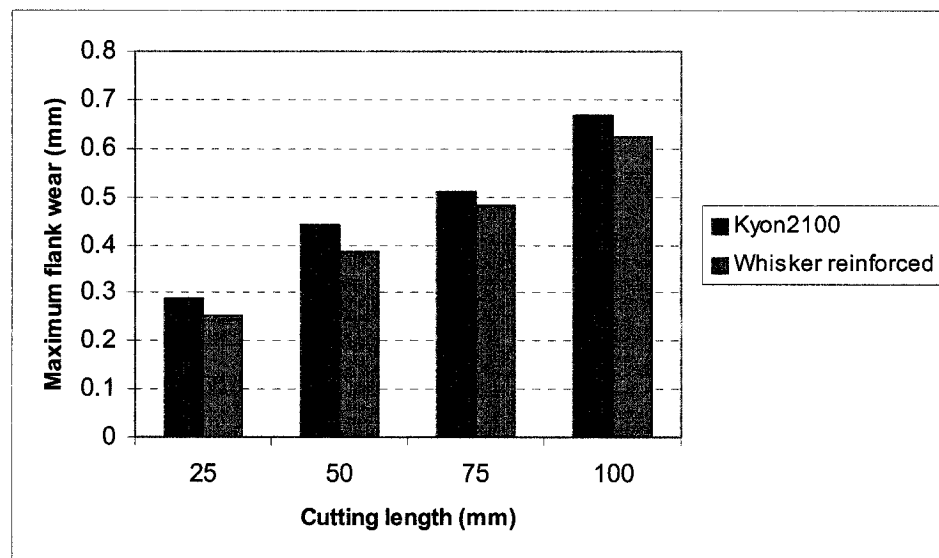


Figure 5.22: Maximum flank wear vs. Cutting length ($v = 1150\text{m/min}$, $f = 0.04\text{mm/tooth}$, dry cutting)

Figure 5.22 shows maximum flank wear at the cutting speed of 1150 m/min and feed of 0.04 mm/tooth. As for the flank wear it has been found that increasing the cutting speed (above 850 m/min) caused the tool to wear faster, however the portion of the cutting edge affected by the flank wear decreases as cutting speed was increased up to 850 m/min. The above mentioned results suggest a change in wear mechanisms, which is most likely due to substantial workpiece and tool softening.

Chapter 5. High speed machining: wear and surface roughness for ceramic tools

Since the sliding contact between the tool and workpiece reduces proportional to the increase in feed, then the tool wear is also expected to be reduced. The reinforced ceramic based on Al_2O_3 but contains silicon carbide (SiC) Whiskers which gives it better thermal conductivity and improves its bulk toughness considerably. On the other hand, silicon nitride based ceramic (Kyon 2100) has also better thermal properties and toughness. Therefore, the introduction of these ceramic cutting tools has enabled higher cutting speeds to be achieved.

5.5.2 Effect of cutting speed on cutting length (tool life)

Cutting speed generates the heat needed for ceramic tools to work properly. Whisker reinforced and kyon 2100 ceramic tools have capability to prevent thermal and mechanical shock and notching that make them suitable insert for milling of nickel based superalloys at higher cutting speeds. High-speed machining of nickel based superalloys is a typical application for ceramic cutting tools. We presented experimental results for ceramic milling for better understanding of high speed machining operation. The cutting length can be expressed in terms of tool life. Cutting tests were performed in this research work to find the optimum cutting speed. During the machining of Inconel 718, the temperature of the cutting edge increases rapidly with the increase of the cutting speed. At the higher cutting speeds, the cutting tip temperature approached the melting temperature of the workpiece material. The maximum temperature on the cutting tool is high and much closer to the cutting edge for nickel based superalloys machining operation than it is for other materials such as steel, due to the deformation in the primary shear zone combined with the tool-chip sticking condition in the secondary shear zone.

Chapter 5. High speed machining: wear and surface roughness for ceramic tools

On the other hand increasing the cutting speed will shorten the heating period within each cycle and the heating interval will be interrupted before the end of a transient phase of heat transfer between the formed chips and the cutting tools. Higher cutting speed leads to shorter heating interval and more obvious cooling effect. It was observed that tool life length increased with the increase of cutting speed due to the ceramics high temperature withstands capability. Tool life was estimated in terms of the cutting length that the tool can endure when the maximum flank wear reaches its limit of 0.70 mm. Figure 5.23 shows the variation of cutting length for whisker reinforced ceramic tools under different cutting speeds. Increasing the cutting speed will firstly make the machined workpiece softer due to more heat generated during faster plastic deformation and to maintain the desired properties of the ceramic tool.

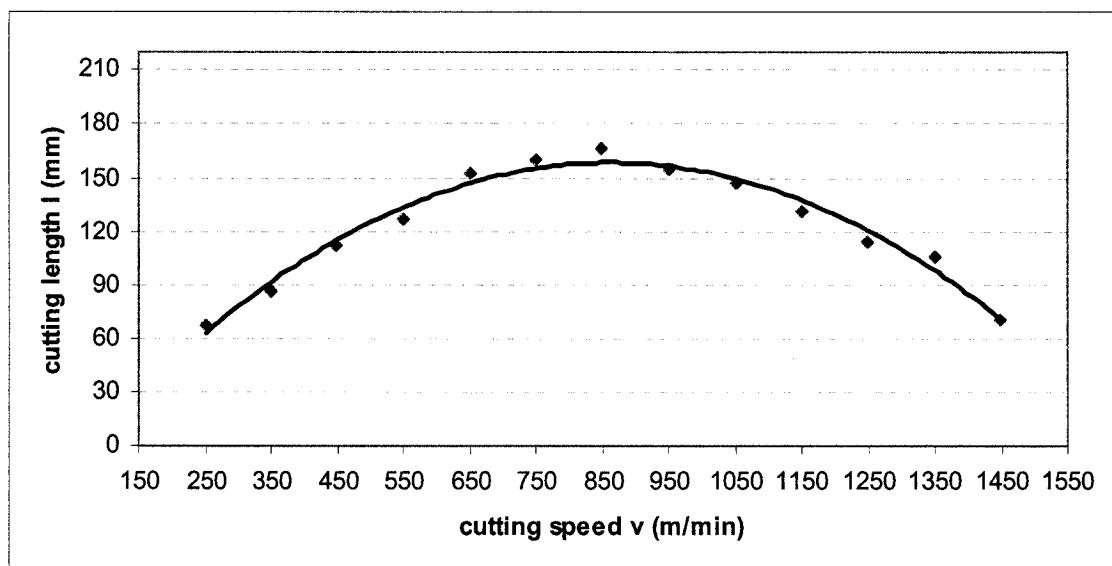


Figure 5.23: Cutting length vs. cutting speed (Whisker reinforced ceramic tool, $f=0.03$ mm/tooth, dry cutting)

Chapter 5. High speed machining: wear and surface roughness for ceramic tools

It was found (Figure 5.23) that as the cutting speed increased up to 850 m/min, the tool performance improved significantly i.e. the value of cutting length or tool life was found to be longer. This is due to the more favourable heat flow and workpiece softening at higher cutting speeds. On the other hand, ceramic tools have the capability of wear resistance and chemical stability than other tool materials. Therefore ceramic tools are inherently strong and able to withstand interruption at higher cutting speeds. Elbestawi *et al* [1998] reported that tool life increased as the cutting speed increased for ceramic tools. Ceramic tool material still keeps very high hardness and strength at the cutting speed of 850 m/min. A similar trend was observed in the feed range of 0.03 to 0.12 mm/tooth. The ceramic tool material showed not only superior wear resistance but also fracture resistance.

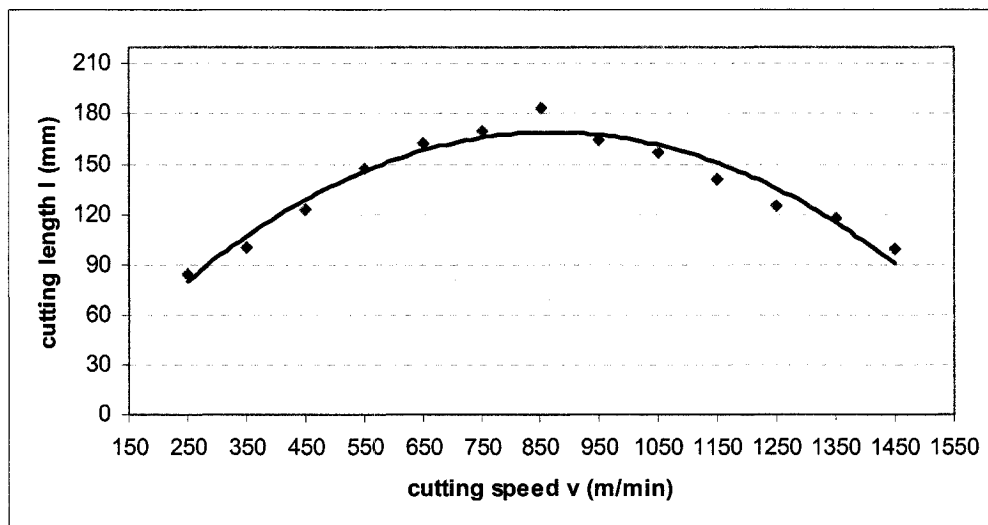


Figure 5.24: Cutting length vs. cutting speed (Whisker reinforced ceramic tool, $f=0.07$ mm/tooth, dry cutting)

Figure 5.24 shows the variation of cutting length for Whisker reinforced ceramic tool at the cutting feed of 0.07 mm/tooth.

Chapter 5. High speed machining: wear and surface roughness for ceramic tools

The wear rates of these ceramic tool materials suggest that the superior wear resistance is not only due to the higher hardness but also due to higher bond strength between the grains due to pure grain boundary with no additives. It was also found from the literature that fracture toughness and heat cracking are the most important characteristics for cutting tools for the machining of nickel based superalloys. The superior performance in milling of ceramic tools also indicate that Whisker reinforced and Kyon 2100 ceramic tools are more wear resistance and fracture toughness against thermal and mechanical shock. Figure 5.25 shows the variation of cutting length for Kyon 2100 ceramic tool at the cutting feed of 0.03 mm/tooth.

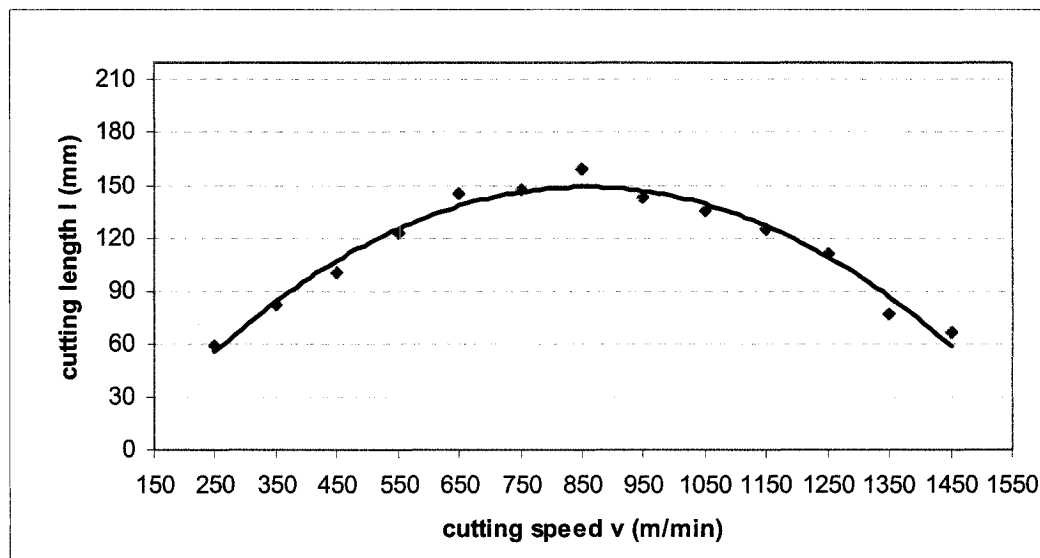


Figure 5.25: Cutting length vs. cutting speed (Kyon 2100 ceramic tool, $f = 0.03$ mm/tooth, dry cutting)

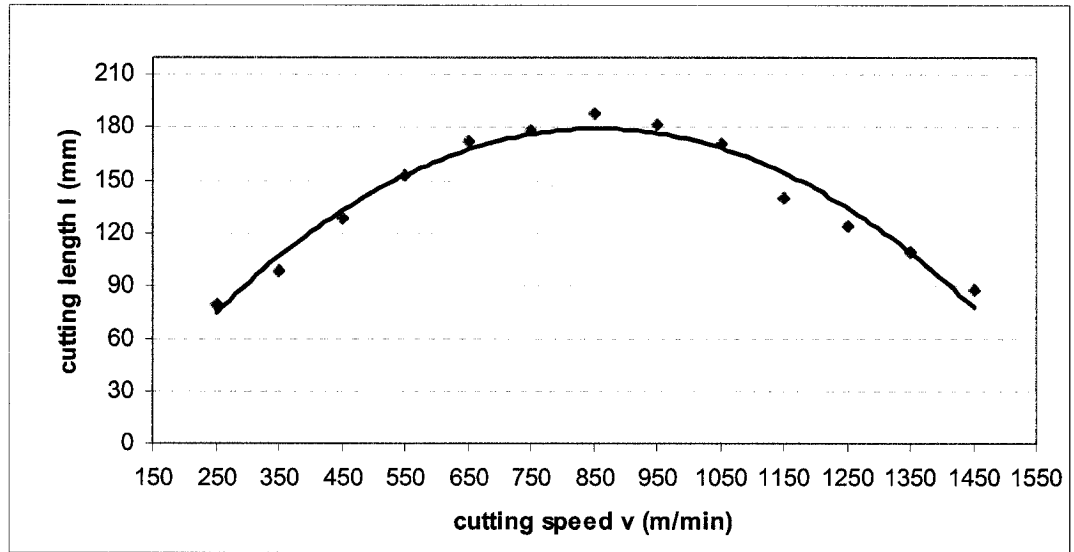


Figure 5.26: Cutting length vs. cutting speed (Kyon 2100 ceramic tool, $f=0.11$ mm/tooth, dry cutting)

Figure 5.26 shows the variation of cutting length for Kyon 2100 ceramic tool at the cutting feed of 0.11 mm/tooth. Since the cutting tip temperature is high in high speed machining of nickel based super alloys, hot hardness is an important parameter of interest. Ceramic tools can be replaced in place of carbide tools in high speed machining operation. The current generation of ceramics can withstand higher temperatures than carbides. The mechanical properties of ceramics are superior than carbide tools. They retain excellent hardness at higher temperatures and do not react chemically with most workpiece materials at higher temperatures. This thesis work has shown that SiC Whisker reinforced and Kyon 2100 ceramic tools can be used to machine nickel based superalloys over a wide range of cutting conditions. From the view point of productivity, it is advantageous to use ceramic tools for milling of nickel based superalloys in high speed machining operation.

5.6 Wear mechanisms examination using microscope (SMM)

The physical mechanism of tool wear is important in metal cutting operation. The dominant form of wear in a given application depends on a number of factors: tool material, workpiece material and cutting conditions. The fundamental nature of the mechanism of wear can be different under various cutting conditions. The work hardening characteristics of nickel based superalloys are the source of many wear mechanisms. On the other hand, microscopic examination is useful technique in the study of wear mechanism and characterization of materials. Investigations of this type are often called “metallographic”. The microscope was set in a reflecting mode during wear mechanism examination. Contrasts in the image produced result from differences in a reflectivity of the various regions of the microstructure. Normally careful surface preparation was necessary to reveal the important details of the wear surface. The following procedures were followed during wear mechanism examination:

- The wear surface of the cutting tool was kept under the microscope. The magnification was adjusted as much as possible to obtain clear image.
- The light was adjusted so that it can directly focus on the wear surface.
- Magnified image was generated and directly exported to the computer, which was connected to the microscope.
- Each wear surface image was saved into the computer for wear mechanism examination under particular cutting condition.

Chapter 5. High speed machining: wear and surface roughness for ceramic tools

5.6.1 Micro analysis of wear mechanisms for ceramic tools

Investigation on tool wear mechanism is needed in order to select appropriate range of cutting conditions. In nickel based superalloys machining operation, wear and fracture of the tool are a major concern. The machining of Inconel 718 resulted in abrasive and adhesive wear mechanism. It was also found that workpiece material adhered with the cutting tool. It was observed from the assessment of the cutting tool (Figure 5.27) that there was a frequent occurrence of abrasive and adhesive wear mechanisms. Generation of abrasion is also probable from the workpiece material which contains different elements especially nickel particle.

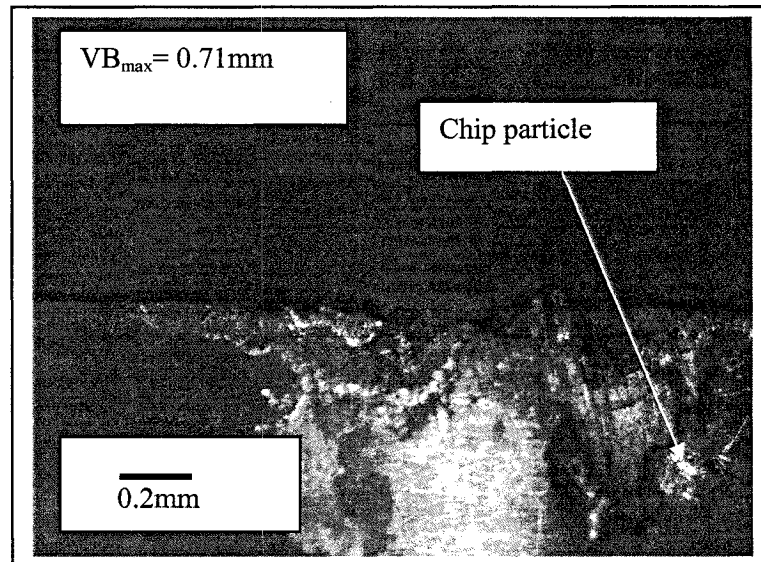


Figure 5.27: SMM micrograph of wear surface (Whisker ceramic tool, cutting speed = 250 m/min, feed= 0.03 mm/tooth)

Figure 5.27 shows flank wear by abrasion and adhesion wear mechanism for Whisker reinforced ceramic tool. Abrasion generally produces flank wear. Maximum flank wear is denoted by VB_{max} . As the cutting operation was continued, abrasion and adhesion wear rates increased. It was reported [Eguzu *et al* 2005] that abrasion and adhesion were found to be dominating tool wear mechanisms when

Chapter 5. High speed machining: wear and surface roughness for ceramic tools

machining nickel based superalloys. Figures 5.28 and 5.29 show the micrograph of wear surface at cutting speeds of 350 m/min and 450 m/min respectively. Flank wear was observed under different cutting conditions.

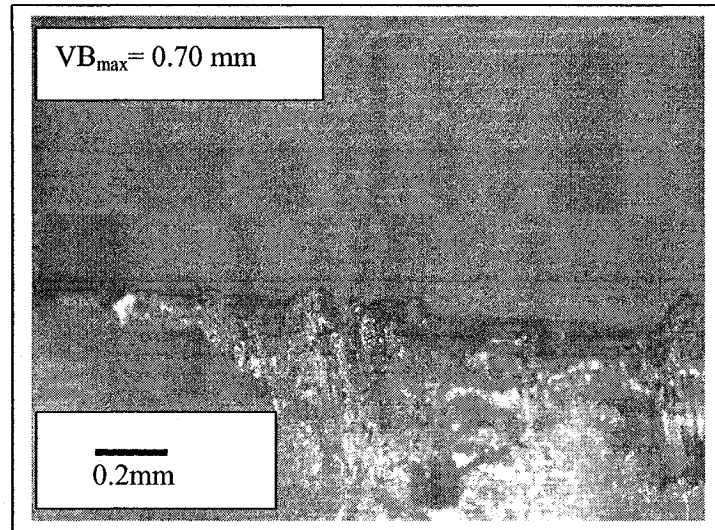


Figure 5.28: SMM micrograph of wear surface (Whisker ceramic tool, cutting speed = 350m/min, feed= 0.03 mm/tooth)

Flank wear pattern however started slowly at the beginning of cut and had a higher rate of growth with increased length of cut. In the majority of cases tool life has been limited by flank wear.

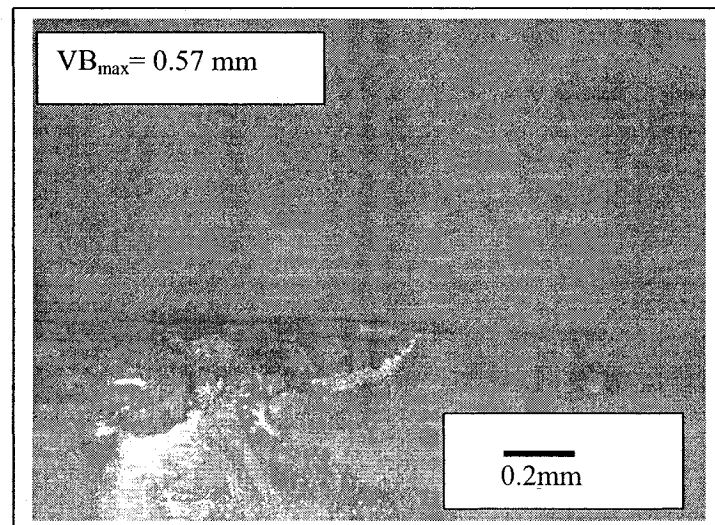


Figure 5.29: SMM micrograph of wear surface (Whisker ceramic tool, cutting speed = 450 m/min, feed= 0.03 mm/tooth)

Chapter 5. High speed machining: wear and surface roughness for ceramic tools

Figures 5.30 and 5.31 show the micrograph of wear surface at cutting speeds of 550 m/min and 650 m/min respectively. During machining operation the tip of the cutting tool was always buried in the workpiece material. Under this condition, the accessibility of the tool nose to air was very limited.

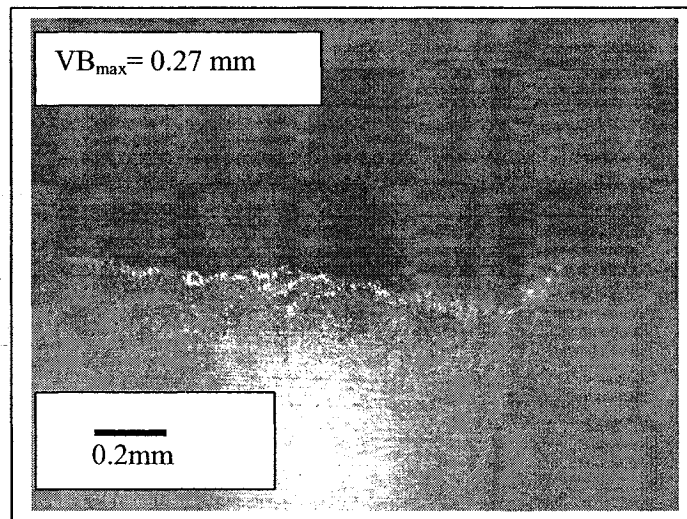


Figure 5.30: SMM micrograph of wear surface (Whisker ceramic tool, cutting speed = 550 m/min, feed= 0.03 mm/tooth)

Therefore the oxidation mechanism was not significant. The high temperature generated during milling of Inconel 718 also promoted the development of stress on the cutting tool. As a result wear rate was faster as the cutting continued.

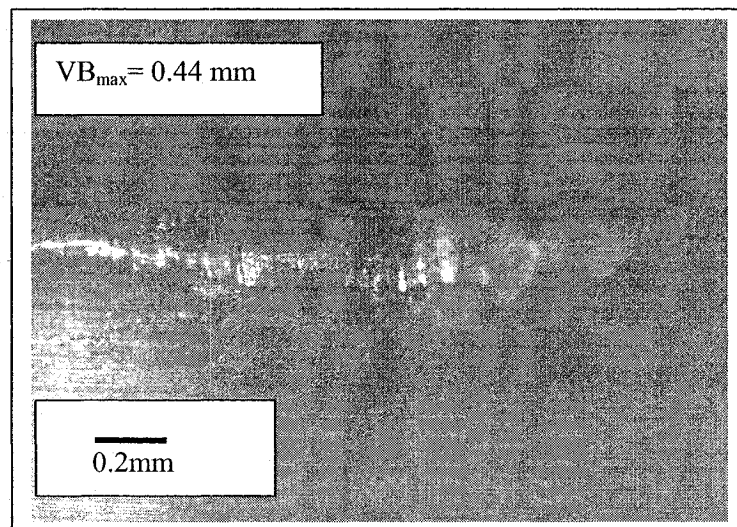


Figure 5.31: SMM micrograph of wear surface (Whisker ceramic tool, cutting speed = 650 m/min, feed= 0.03 mm/tooth)

Chapter 5. High speed machining: wear and surface roughness for ceramic tools

Machining of Inconel 718 with ceramic tools at the cutting speed of 750 m/min and higher resulted in the formation of flank wear but catastrophic failure did not occur. It could be due to high temperature withstand capability of ceramic tools.

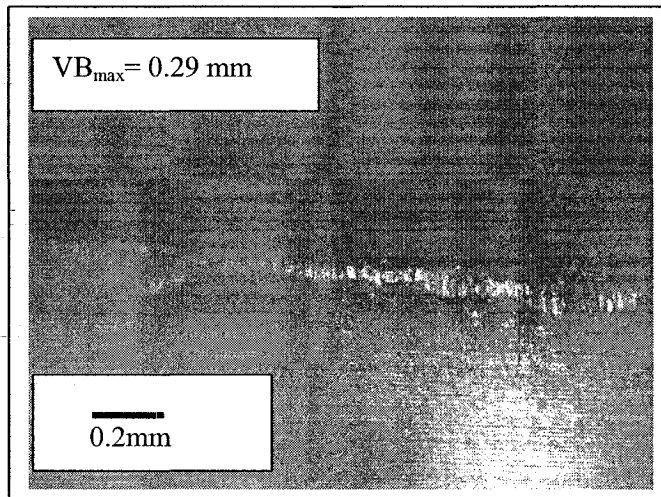


Figure 5.32: SMM micrograph of wear surface (Whisker ceramic tool, cutting speed = 750 m/min, feed= 0.03 mm/tooth)

The whisker reinforced ceramic consists of silicon carbide with alumina. Usually silicon carbide is a less stable compound and the incorporation of silicon carbide into alumina ceramic would be expected to lower the chemical inertness of ceramic tools.

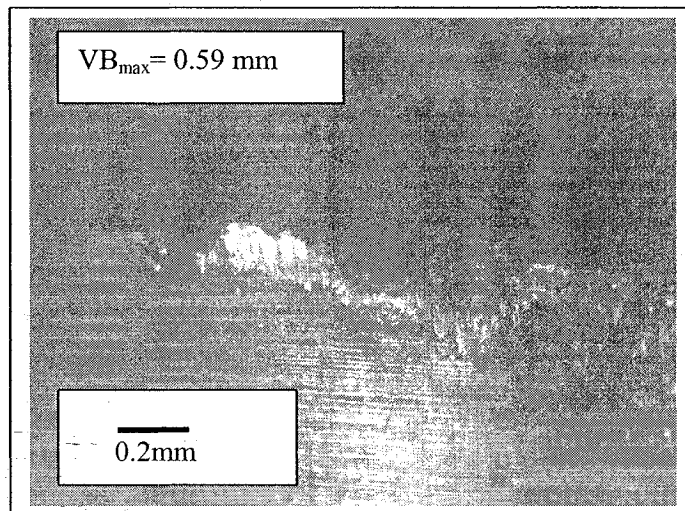


Figure 5.33: SMM micrograph of wear surface (Whisker ceramic tool, cutting speed = 850 m/min, feed= 0.03 mm/tooth)

Chapter 5. High speed machining: wear and surface roughness for ceramic tools

Due to this reason, it is suggested that silicon carbide particles may be involved interactions with the workpiece material. Figures 5.32 and 5.33 show the micrograph of wear surface at cutting speeds of 750 m/min and 850 m/min respectively.

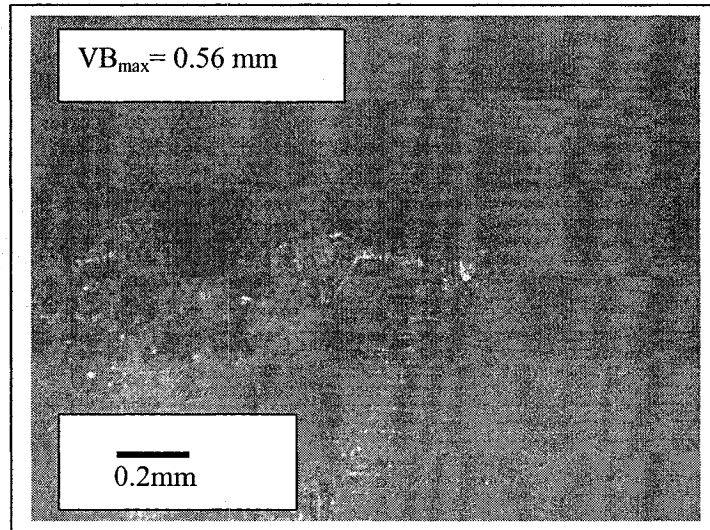


Figure 5.34: SMM micrograph of wear surface (Kyon 2100 ceramic tool, cutting speed = 250 m/min, feed= 0.03 mm/tooth)

Figures 5.34 and 5.35 show the flank wear surface of Kyon 2100 ceramic tool under cutting speeds of 250 m/min and 850 m/min respectively. It was also found that abrasion occurred on Kyon 2100 ceramic tool during machining of Inconel 718.

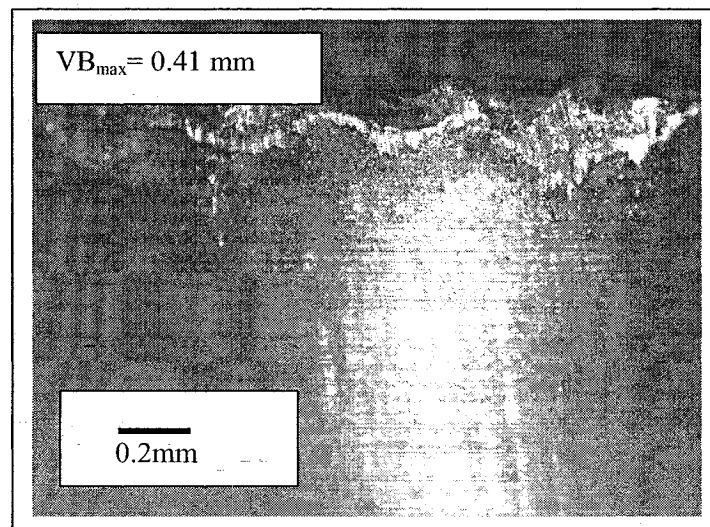


Figure 5.35: SMM micrograph of wear surface (Kyon 2100 ceramic tool, cutting speed = 850 m/min, feed= 0.03 mm/tooth)

Chapter 5. High speed machining: wear and surface roughness for ceramic tools

It was also found that the adhesion was the welding of relatively small chip particles to the sharp sections of the cutting edge (Figures 5.27 and 5.35). Based on the size and shape of the adhered material at the cutting edge, it is most likely that chip particle has been broken away. This type of adhesion can be very detrimental if it stays at the tip of the cutting edge. Therefore, the new cutting edge can adversely affects the chip flow during cutting operation. This kind of adherence was observed during the entire cutting period which increased gradually towards the end of tool life. Figure 5.36 shows the micrograph of wear surface at the cutting speed of 950 m/min.

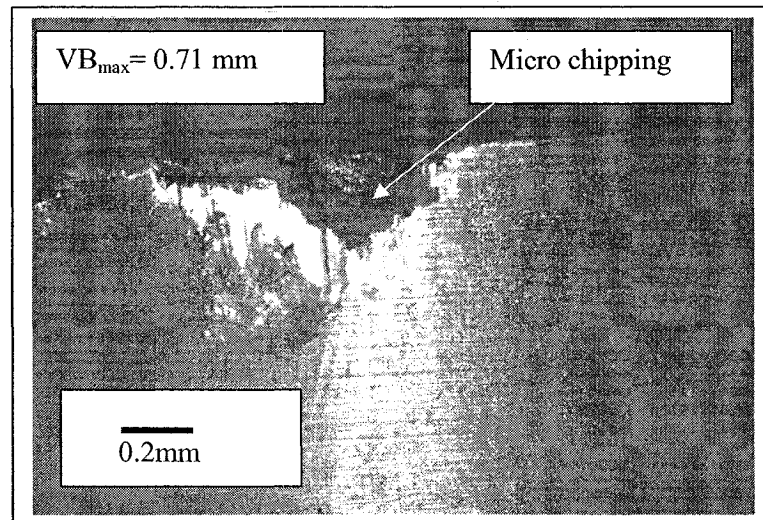


Figure 5.36: SMM micrograph of wear surface (Whisker ceramic tool, cutting speed = 950 m/min, feed = 0.12 mm/tooth)

During machining, the high strength of nickel based superalloys cause high temperatures and stresses in the tool-chip contact area. The tool material in this area is thermally softened and so aid the process of pullout of the tool material. The breaking away of a piece of material from the cutting edge is called micro chipping. It is also found that silicon carbide whisker layers also tear off from the flank surface.

Chapter 5. High speed machining: wear and surface roughness for ceramic tools

It occurs suddenly during the machining process which eventually leads to increase the tool wear. Micro chipping was observed to occur on ceramic tools (Figures 5.36 and 5.37).

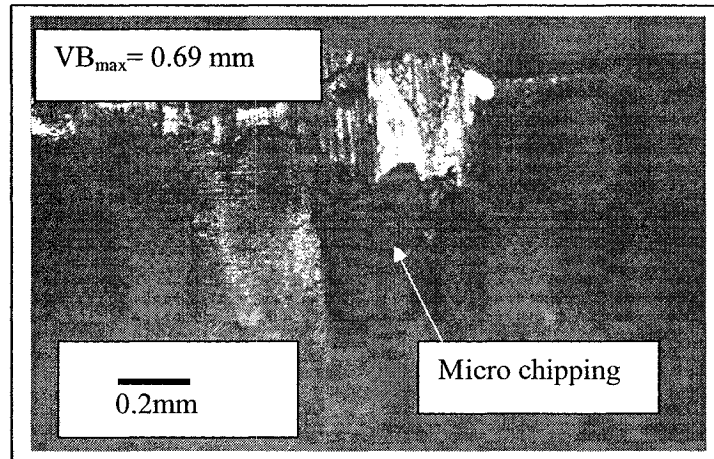


Figure 5.37: SMM micrograph of wear surface (Whisker ceramic tool, cutting speed = 1050 m/min, feed = 0.12 mm/tooth)

However, the occurrence of micro chipping was more frequent on the ceramic tool and it became very severe when the cutting speed and feed were increased (Figure 5.38).

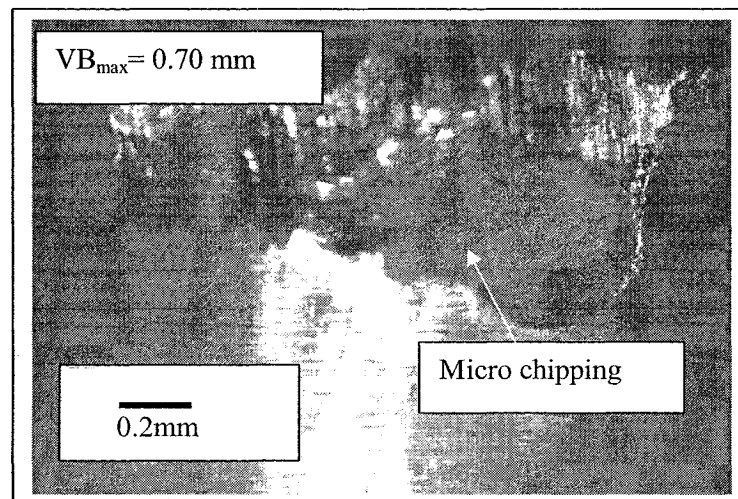


Figure 5.38: SMM micrograph of wear surface (Whisker ceramic tool, cutting speed = 1150 m/min, feed = 0.12 mm/tooth)

Chapter 5. High speed machining: wear and surface roughness for ceramic tools

At higher cutting speeds of 1250 to 1450 m/min, chipping or breaking with associated plastic deformation occurred on the cutting tool thus resulting in premature failure of the tools (Figures 5.39 and 5.40)

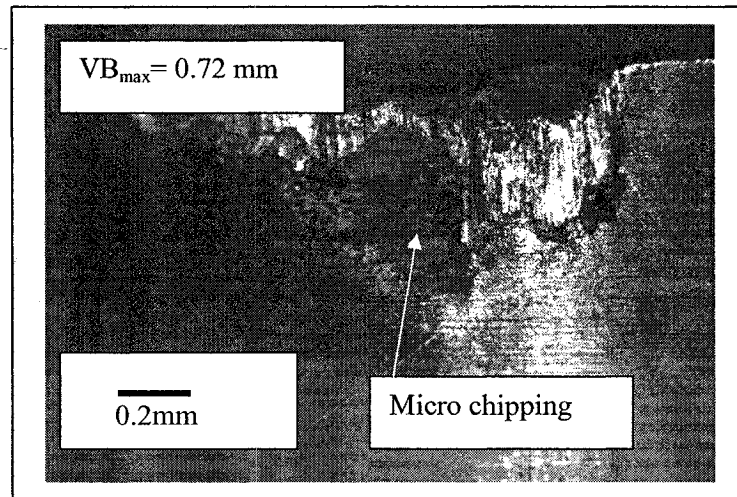


Figure 5.39: SMM micrograph of wear surface (Whisker ceramic tool, cutting speed = 1250 m/min, feed = 0.12 mm/tooth)

This suggest that the strength of the cutting edge was significantly reduced when the cutting at higher speed making it prone to micro chipping and/or plastic deformation.

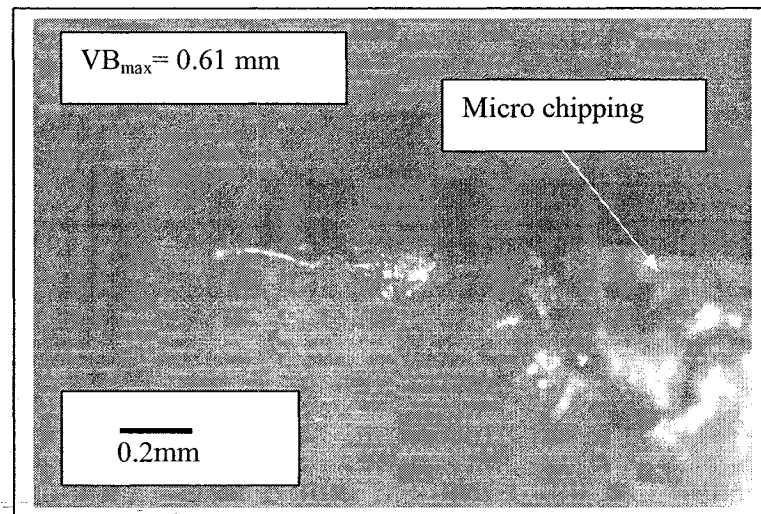


Figure 5.40: SMM micrograph of wear surface (Whisker ceramic tool, cutting speed = 1350 m/min, feed = 0.12 mm/tooth)

Chapter 5. High speed machining: wear and surface roughness for ceramic tools

Once chipping (Figure 5.41) occurred, the shape of the cutting edge was altered subjected to higher stresses on the cutting edge. In addition to this effect, the section of the chipped area also act as stress raisers and lead to a further deformation or breakage of the cutting tool.

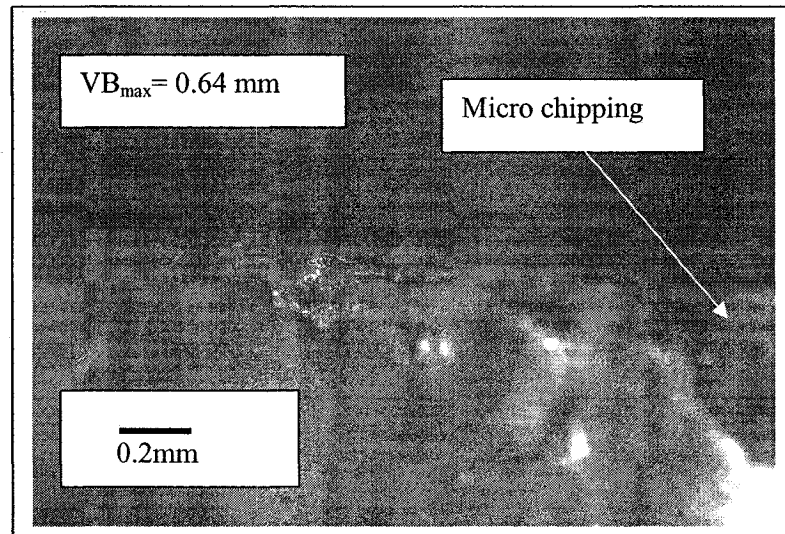


Figure 5.41: SMM micrograph of wear surface (Whisker ceramic tool, cutting speed = 1450 m/min, feed = 0.12 mm/tooth)

Although Whisker reinforced ceramic tool has high temperature withstand capability but it is found that increase in the cutting speed (950 m/min) due will cause higher stresses on the tool. This makes the cutting tool more susceptible to chipping. It is observed that feed rate increases also cause temperature raises which leads to micro chipping. Micro chipping wear shows that the formation of wear has been slow at cutting speed of 950 m/min. Increase in cutting speed (above 950 m/min) accelerated the rate of chipping. Chipping mechanism was found on the ceramic cutting tool at cutting speeds of 950 to 1450 m/min.

Chapter 5. High speed machining: wear and surface roughness for ceramic tools

However, the presence of other types of wear mechanisms such as abrasive and adhesive were also apparent during machining of nickel based super alloys with ceramic tools.

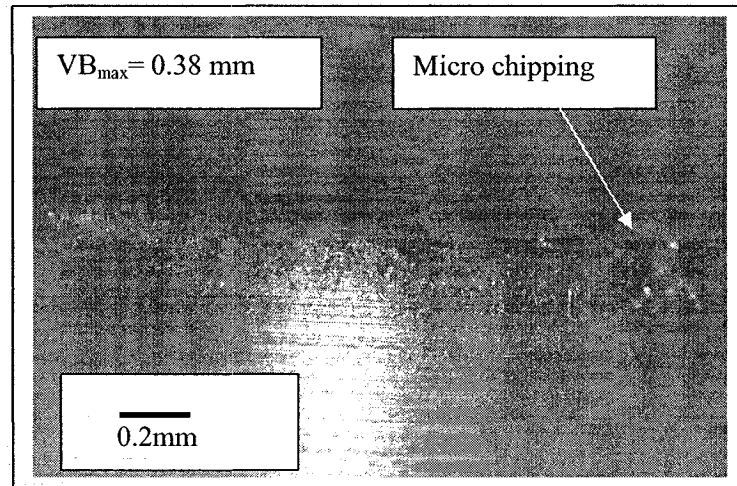


Figure 5.42: SMM micrograph of wear surface (Kyon 2100 ceramic tool, cutting speed = 1050 m/min, feed = 0.12 mm/tooth)

Acceleration of wear rate for Kyon 2100 ceramic tool during machining of nickel based superalloys is probably due to generation of high temperature which has resulted in micro chipping (Figures 5.42 to 5.44).

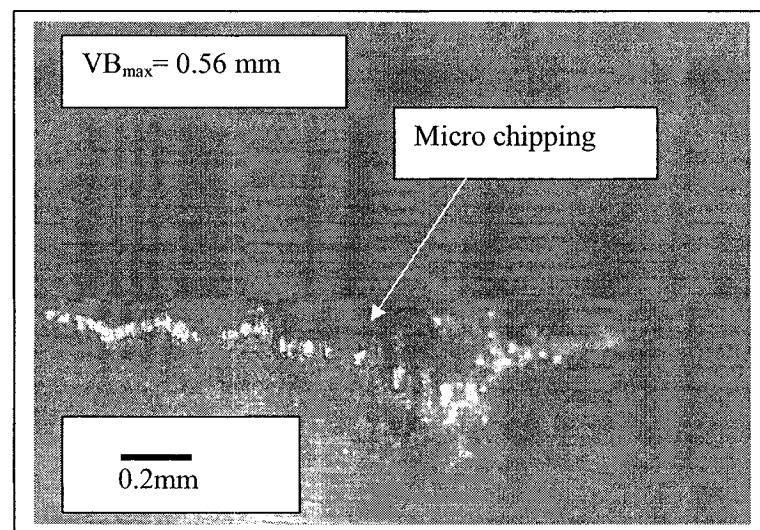


Figure 5.43: SMM micrograph of wear surface (Kyon 2100 ceramic tool, cutting speed = 1150 m/min, feed = 0.12 mm/tooth)

Chapter 5. High speed machining: wear and surface roughness for ceramic tools

A common problem in machining of nickel based superalloys is the development of micro chipping on ceramic tools. Narutaki *et al* [1999] investigated the influence of cutting speed on wear with ceramic tools. They observed that micro chipping was the dominating mechanism during machining of nickel based superalloys.

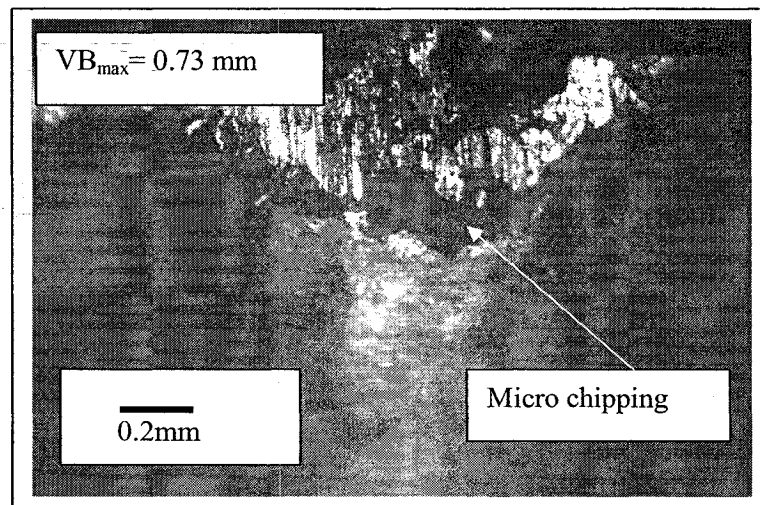


Figure 5.44: SMM micrograph of wear surface (Kyon 2100 ceramic tool, cutting speed = 1250 m/min, feed = 0.12 mm/tooth)

All of the ceramic tools were found to have smaller amount of micro chipping at cutting speed of 250 to 850 m/min. However when the cutting speed exceeded 950 m/min, both ceramic tools showed large amount of micro chipping. It was also found that the resistance towards micro chipping was equal for Whisker reinforced and Kyon 2100 ceramic tools. Flank wear of the Whisker reinforced and Kyon 2100 ceramic tools can be considered as abrasive and adhesive types of wear mechanism.

5.7 X-ray examination for wear surface using EDX spectroscopy

Spectroscopy measures light that is emitted or scattered by material and can be used to study material structure. The purpose of this examination was to investigate the adhesion and diffusion mechanism occurred between workpiece material and cutting tool on the generation of wear. Scanning electron microscope (SEM) fitted with an energy dispersive X-ray (EDX) spectrometer was used for this X-ray examination.

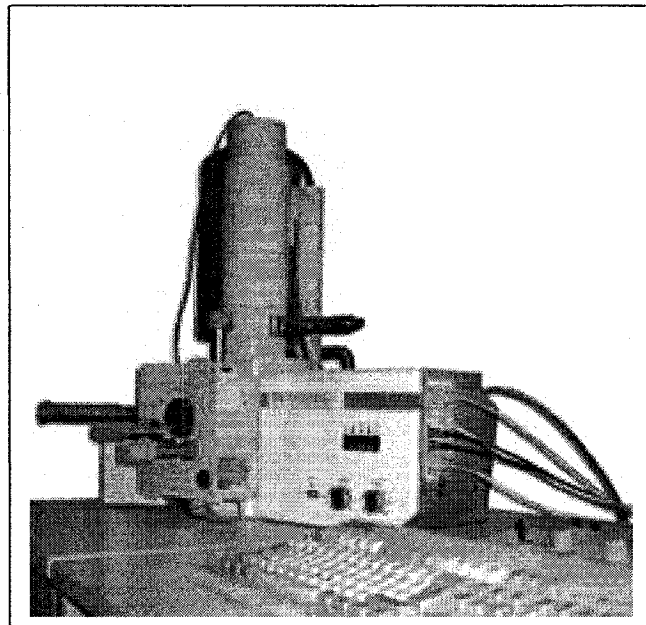


Figure 5.45: X-ray examination instrument (SEM with EDX)

Figure 5.45 shows X-ray examination instrument. Wear surface of the cutting tool was examined using X-ray instrument. The voltage of the X-ray source was set to 15 kV. The energy of the X-ray was analyzed by an electrostatic analyzer.

Chapter 5. - High speed machining: wear and surface roughness for ceramic tools

5.7.1 Microstructure and energy dispersive X-ray (EDX) for ceramic tools

Figures 5.46 to 6.54 show the test specimens having different microstructure of wear surface for ceramic tools. All specimens created considerable amount of tool wear. It was found that flank wear was created by different wear mechanisms. Figure 6.20 shows the microstructure of flank wear surface for Whisker reinforced ceramic tool at cutting speed of 850 m/min. In some regions, while there are some wear marks being observed, on the other hand, in the upper regions there are chips break off in the adhesion and abrasion wear process.

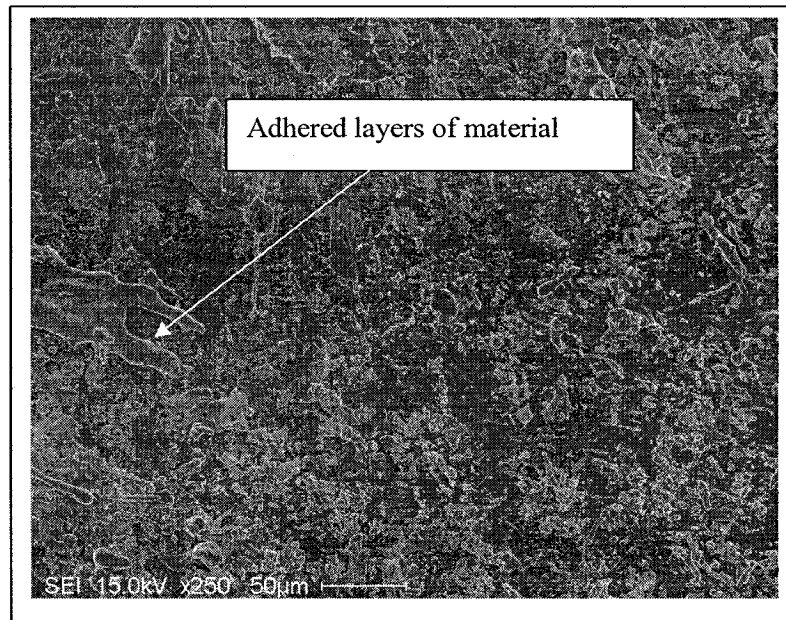


Figure 5.46: Microstructure of wear surface (Whisker ceramic tool, cutting speed = 850 m/min, feed = 0.03 mm/tooth)

In general, there are some diffusive wears observed in the wear surface where the chip leaves during cutting operation. A thin layer of adhered material was observed on flank wear surface. It was found that as the cutting speed was increased to 1250 m/min, the layer thickness was increased but there was no significant difference among the adhered layers of all specimens. It was also found that the flank wear can be attributed to a combination of wear mechanism predominantly adhesive and abrasive. The adhesion and

Chapter 5. High speed machining: wear and surface roughness for ceramic tools

diffusion between workpiece material and ceramic tool were confirmed through energy dispersive X-ray analysis. The X-ray image (Figure 5.47) shows the presence of elements on the wear surface of Whisker reinforced ceramic at cutting speed of 850 m/min. Total energy of X-ray (10 keV) is shown in Figure 5.47.

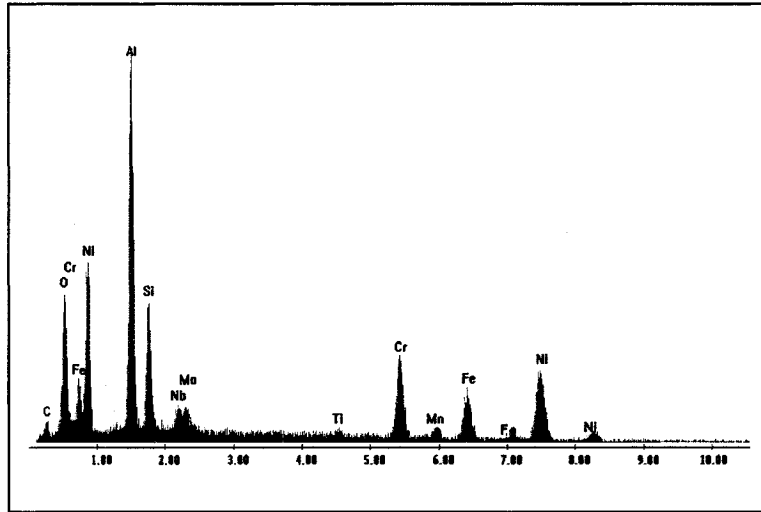


Figure 5.47: Energy dispersive X-ray (EDX) analysis of wear surface (Whisker ceramic tool, cutting speed = 850 m/min, feed = 0.03 mm/tooth)

As for the whisker reinforced ceramic tool, it can be seen that Cr (chromium), Ni (nickel) and other elements from the workpiece were adhered to the cutting tool.

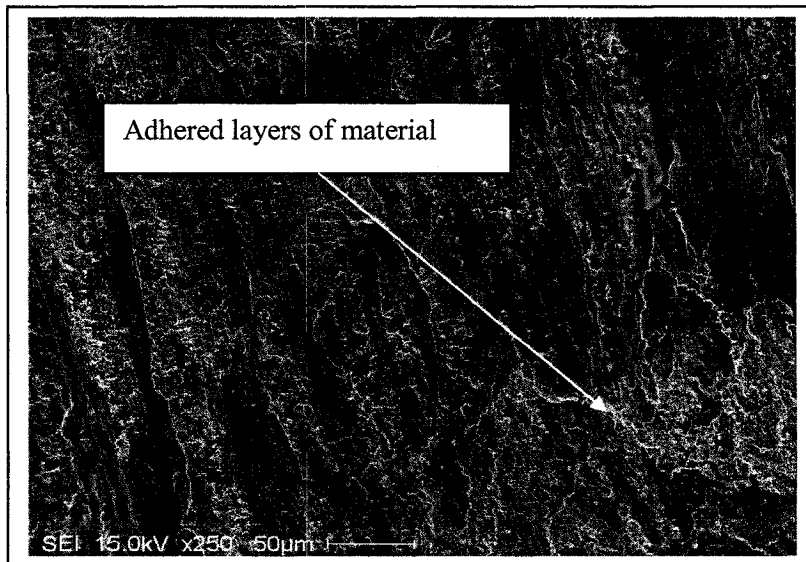


Figure 5.48: Microstructure of wear surface (Whisker ceramic tool, cutting speed = 950 m/min, feed = 0.03 mm/tooth)

Chapter 5. High speed machining: wear and surface roughness for ceramic tools

In addition to this, high concentration of Al (aluminium) was also detected at cutting speed of 850 m/min. Figures 5.48 and 5.49 show the microstructure and X-ray image of Whisker reinforced ceramic wear surface at cutting speed of 950 m/min.

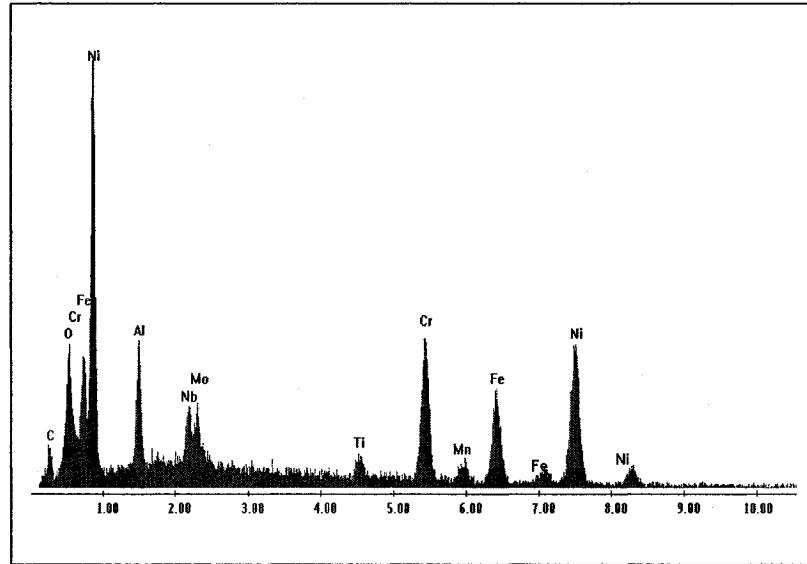


Figure 5.49: Energy dispersive X-ray analysis (EDX) of wear surface (Whisker ceramic tool, cutting speed = 950 m/min, feed = 0.03 mm/tooth)

With an increase of the cutting speed the amount of workpiece material adhered to the cutting tool increased.

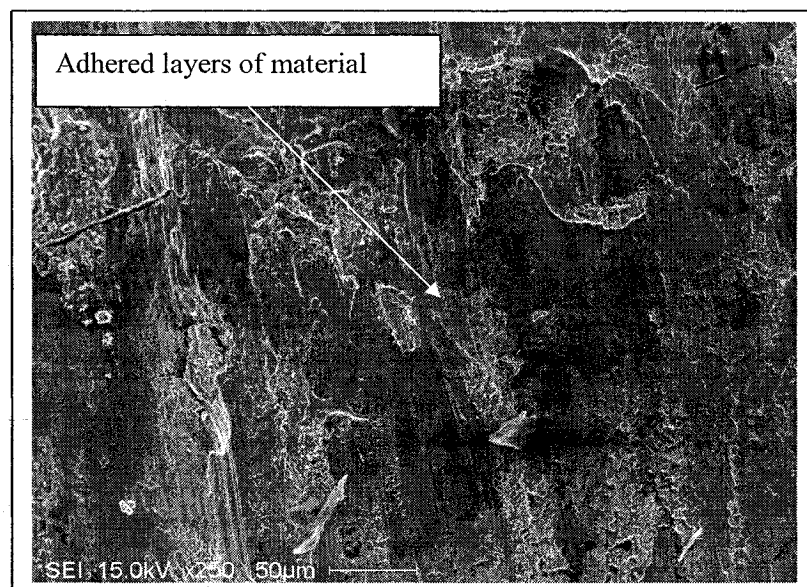


Figure 5.50: Microstructure of wear surface (Whisker ceramic tool, cutting speed = 1250 m/min, feed = 0.12 mm/tooth)

Chapter 5. High speed machining: wear and surface roughness for ceramic tools

It is also found that as the cutting speed increases from 850 m/min to 950 m/min, silicon carbide whiskers tend to dissolve in the workpiece and are replaced by Ni, Cr etc. Figure 5.50 shows the microstructure of whisker reinforced ceramic tool at the cutting speed of 1250 m/min. The interaction between workpiece material and tool material is occurred and the small fragments of tool material are plucked and brought away by the chip. In this case, the action of heat dissolves the tool materials.

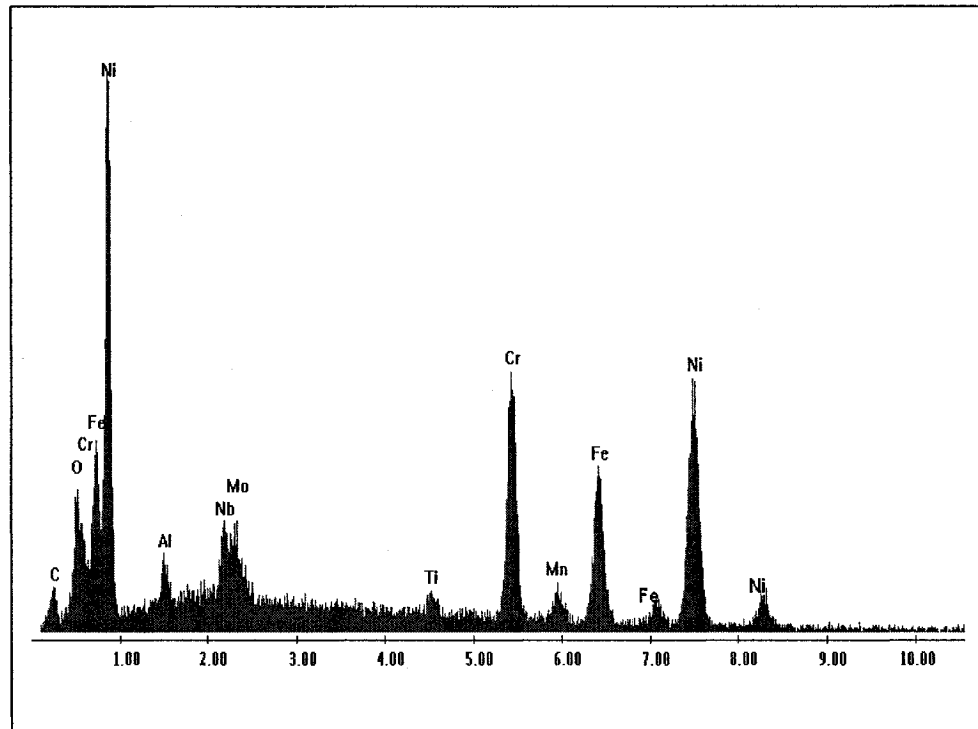


Figure 5.51: Energy dispersive X-ray (EDX) analysis of wear surface
(Whisker ceramic tool, cutting speed = 1250 m/min, feed = 0.12 mm/tooth)

Figure 5.51 shows X-ray analysis for Whisker reinforced ceramic tool at cutting speed of 1250 m/min. Nickel, chromium and other elements are adhered to the tool material and react chemically with SiC (silicon carbide) whiskers. That means that Si (silicon) disappeared from the tool surface at cutting speed of 1250 m/min. This decreases the strength and hardness of the tool material. Furthermore partial SiC whiskers are also

Chapter 5. High speed machining: wear and surface roughness for ceramic tools

oxidized. This oxidation could be aggregated due to increased cutting speed (1250 m/min). For this reason flank wear was found to be higher at 1250 m/min.

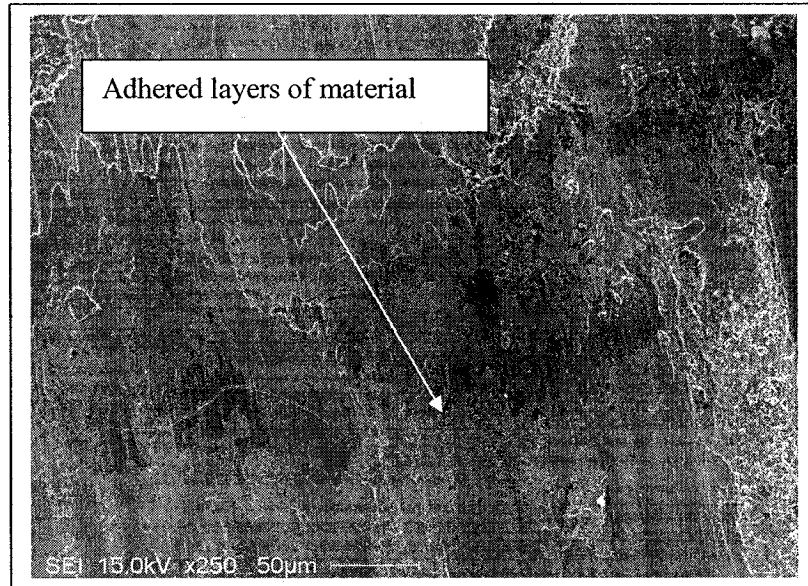


Figure 5.52: Microstructure of wear surface (Kyon 2100 ceramic tool, cutting speed = 850 m/min, feed = 0.03 mm/tooth)

Figure 5.52 shows the microstructure for the Kyon 2100 ceramic tool at cutting speed of 850 m/min. Mutual interaction between the workpiece material and Kyon 2100 ceramic tool can be observed.

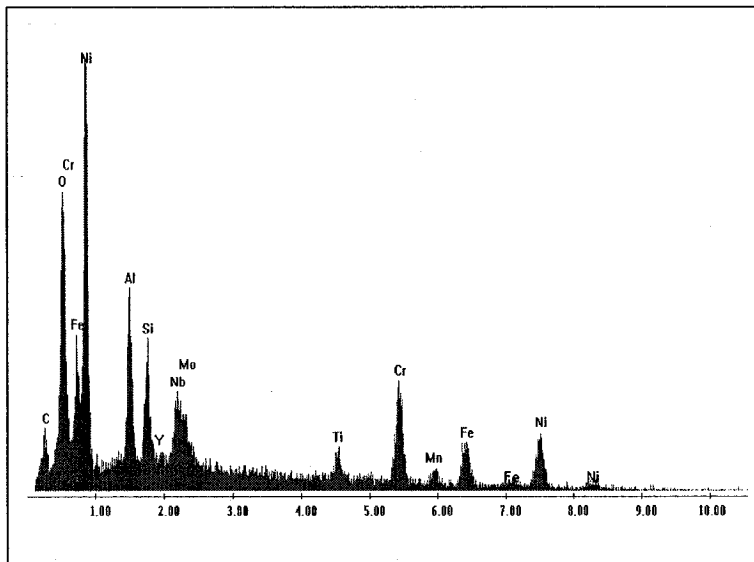


Figure 5.53: Energy dispersive X-ray (EDX) analysis of wear surface (Kyon 2100 ceramic tool, cutting speed = 850 m/min, feed = 0.03 mm/tooth)

Chapter 5. High speed machining: wear and surface roughness for ceramic tools

Figure 5.53 shows the X-ray analysis for Kyon 2100 ceramic tool at cutting speed of 850 m/min. As for the Kyon 2100 ceramic tool, it can be seen that workpiece material adhered to tool material. The adhesion of nickel (Ni), chromium (Cr) and other elements were detected through X-ray analysis. It is also observed that the adhesive wear mechanism takes place on the flank face of the tool as shown in Figure 5.54.

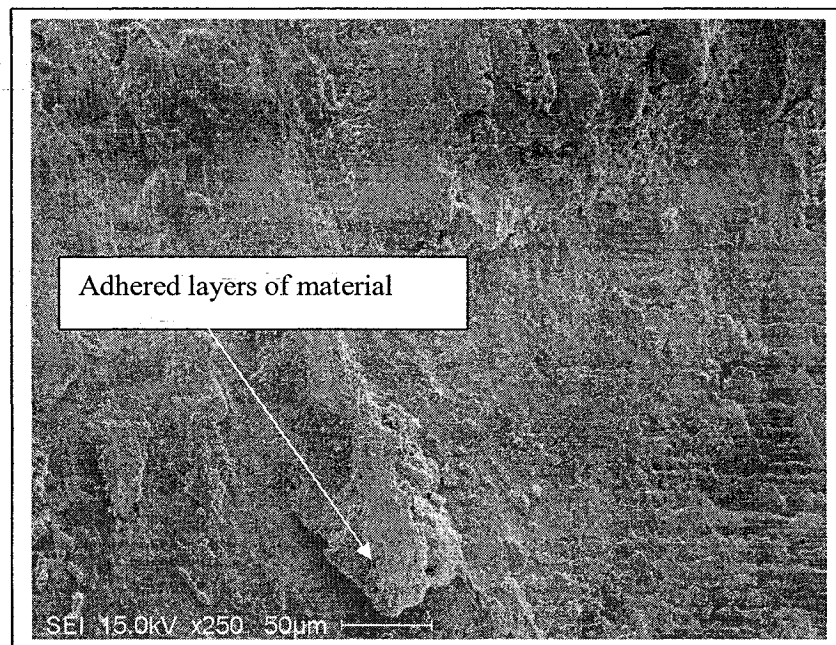


Figure 5.54: Microstructure of wear surface (Kyon 2100 ceramic tool, cutting speed = 1250 m/min, feed = 0.12 mm/tooth)

Figures 5.54 and 5.55 show the microstructure and X-ray analysis for Kyon 2100 ceramic tool at cutting speed of 1250 m/min. The intensity of nickel element on the tool material was found to be higher at cutting speed of 1250 m/min when milling of Inconel 718. It was also observed that adhesion rate of workpiece material to the tool material was higher at cutting speed of 1250 m/min. This promotes the higher value of tool wear since temperatures was higher due to the higher cutting speed. This suggests that it would be essential for further improvement of ceramic tools in order to resist the diffusion and adhesion mechanism at higher cutting speed.

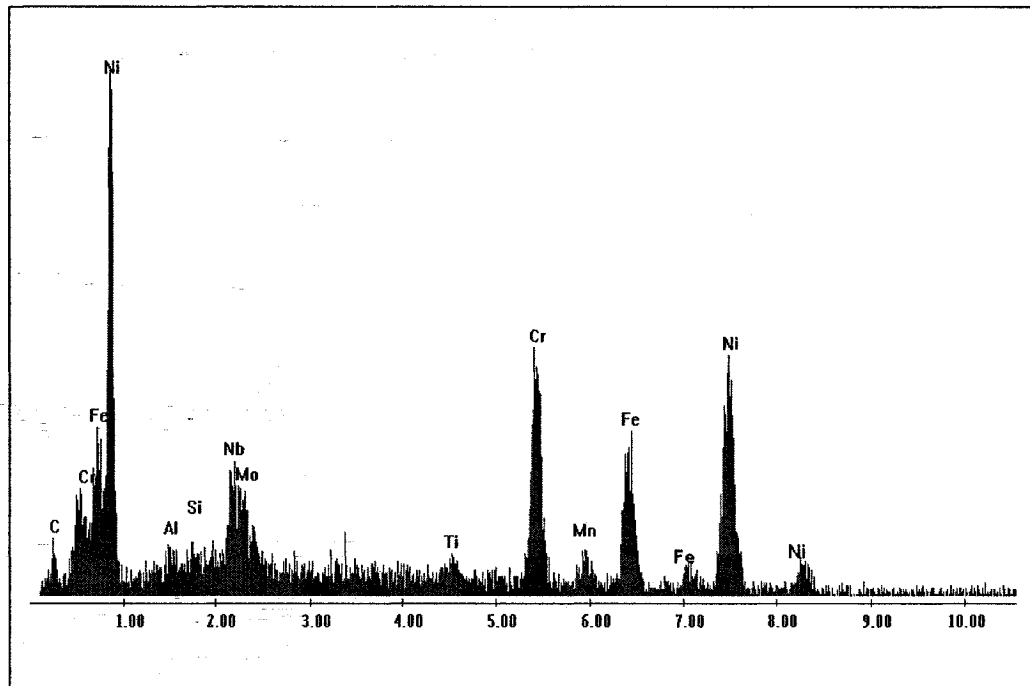


Figure 5.55: Energy dispersive X-ray (EDX) analysis of wear surface (Kyon 2100 ceramic tool, cutting speed = 1250 m/min, feed = 0.12 mm/tooth)

The results of the microanalysis using energy dispersive X-ray indicate that adhesion and abrasion were the major wear mechanisms for both ceramic tools when milling of Inconel 718. The strong bonding between the workpiece and tool material at the high cutting speed is responsible for adhesive wear mechanism. Elbestawi *et al* [1998] also performed EDX analysis for ceramic cutting tool. They mentioned that workpiece material adhered to the tool material as the cutting was continued. Haron *et al* [2005] investigated wear mechanism using EDX method. They also reported that abrasive and adhesive were the dominating mechanism during cutting operation.

5.8 Surface roughness in machining operation

Cutting conditions and hence cutting process will affect the machined surface roughness. The behaviour of roughness profile for workpiece material could be different under various cutting conditions. A small amount of research work was conducted by researchers for the evaluation of surface roughness on nickel based superalloys. Vivancos *et al* [2004] and Chenping [2001] conducted experiments based on surface roughness. However, their study was concentrated on other materials (hardened steel and composite). Kovacevic *et al* [2000] investigated surface profile for stainless steel machined surface in milling operation. They used smaller value of cutting speed and feed for their investigation. Each manufacturing process produces surface finish in a certain range. Therefore, it is necessary to have knowledge about the cutting conditions which will permit us to assure a correct dimensional precision and good surface finish. A comprehensive analysis of surface roughness as well as machined surface examination of Inconel 718 was made under different cutting conditions.

5.8.1 Roughness parameters

The quality of the surface produced was assessed in terms of roughness parameters such as arithmetic mean roughness (R_a) and maximum peak to valley height (R_t). Portable stylus type surface roughness instrument was used to measure machined surface roughness. The surface roughness was measured at four different positions along the length of the machined workpiece. The surface roughness in milling operation depends on cutting conditions. Thus correct cutting conditions can improve machining performance and reduce surface damage during machining operation.

5.8.2 Results of surface roughness under different cutting conditions

Surface roughness was evaluated in milling tests of Inconel 718 using ceramic tools under various cutting conditions. The machined surface finish can be affected by the cutting parameters during machining operation. Normally lower depth of cut results in better surface finish, while higher depth of cut results in higher values of roughness height (R_t). Therefore depth of cut was kept constant at 0.5 mm during milling tests.

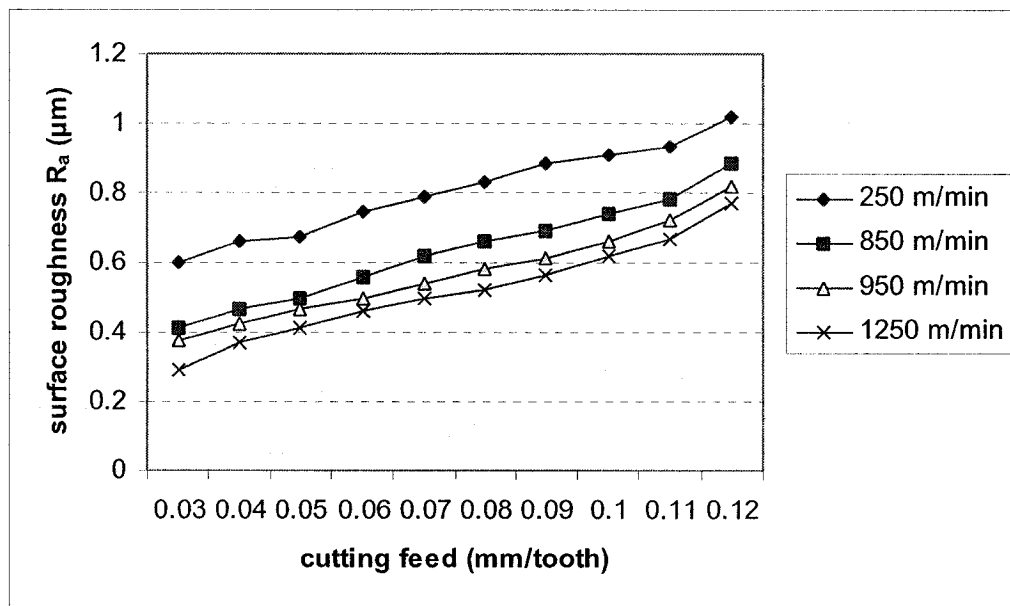


Figure 5.56: Surface roughness (R_a) for Whisker ceramic tool for different cutting speeds

Figure 5.56 shows the variation of surface roughness parameter (R_a) for whisker ceramic tool at cutting speeds of 250 m/min and 1250 m/min respectively. It was found that surface roughness increases as the cutting feed increases. It was also observed that chip breaks away on the machined surface at feed rate of 0.12 mm/tooth, resulting a rough surface during machining operation. On the other hand, the roughness value was low at feed rate of 0.03 mm/tooth and no significant scratches (broken chip) were found on the machined surface.

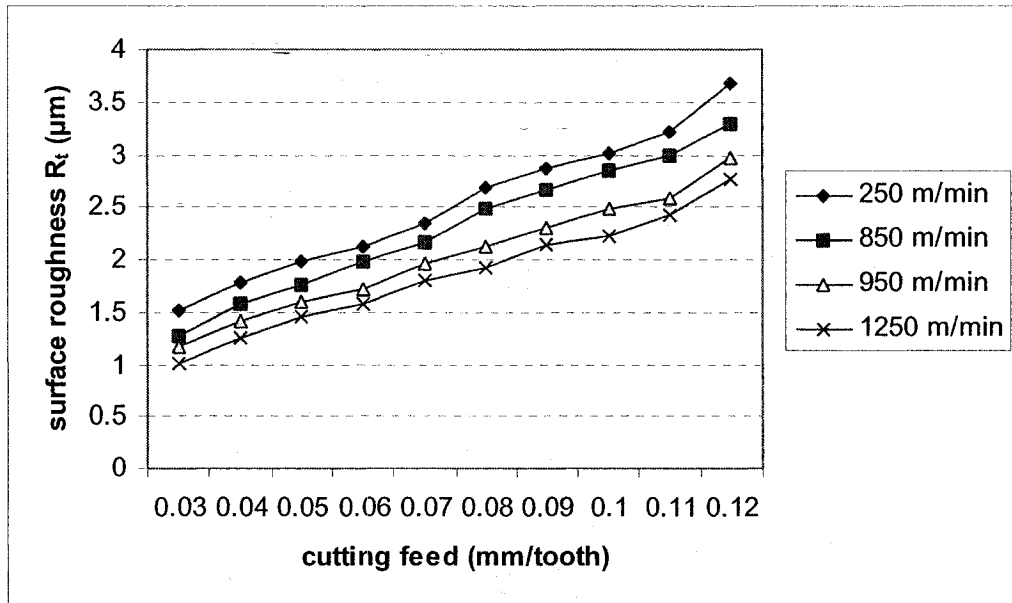


Figure 5.57: Surface roughness (R_t) for Whisker ceramic tool for different cutting speeds

On the other hand, R_t (roughness height) represents the presence of high peaks and deep valleys on the machined surface. It is a good indicator of machined surface roughness. When there were more high peaks and cracks on the machined surface, the value of roughness height (R_t) was found to be high. It was also observed that surface height (R_t) increases as the feed rate increases. Figure 5.57 shows the variation of surface roughness parameter (R_t) for Whisker reinforced ceramic tool at cutting speeds of 250 m/min and 1250 m/min respectively.

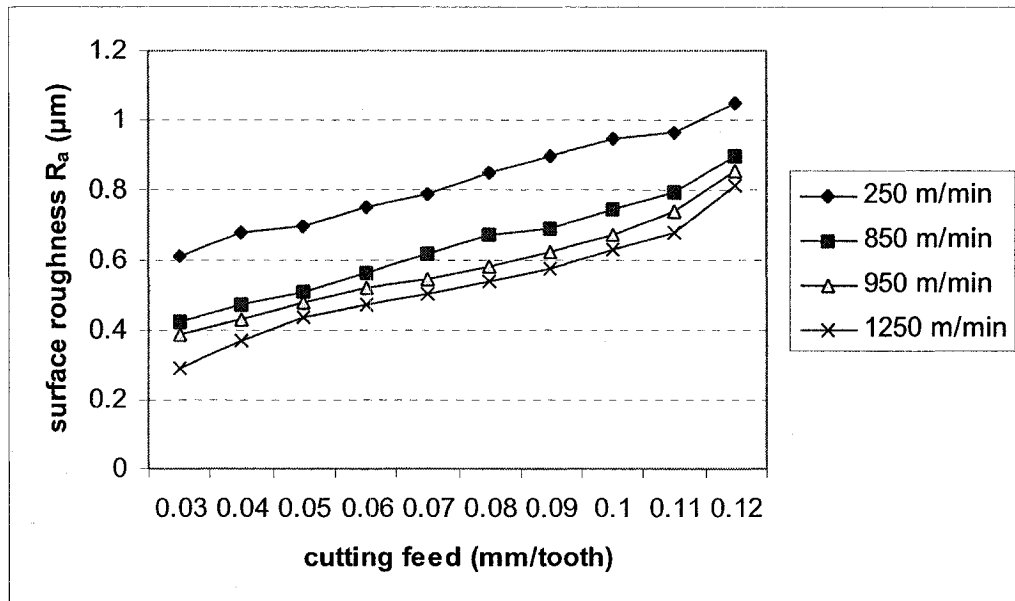


Figure 5.58: Surface roughness (R_a) for Kyon 2100 ceramic tool for different cutting speeds

Figure 5.58 shows the variation of surface roughness parameter (R_a) for Kyon 2100 ceramic tool at cutting speeds of 250 m/min and 1250 m/min respectively. It was found that surface roughness increases as the cutting feed increases. However when cutting speed was increased to 1250 m/min, surface roughness decreased. It was found that Kyon 2100 ceramic tool showed slightly higher roughness value than whisker reinforced ceramic tool. It was also found that as the cutting speed increased the surface roughness decreased. Figure 7.4 shows the variation of surface roughness parameter (R_t) for Kyon 2100 ceramic tool at cutting speeds of 250 m/min and 1250 m/min, respectively.

Chapter 5. High speed machining: wear and surface roughness for ceramic tools

Figure 5.59 shows the variation of surface roughness parameter (R_t) for Kyon 2100 ceramic tool at cutting speeds of 250 m/min and 1250 m/min respectively.

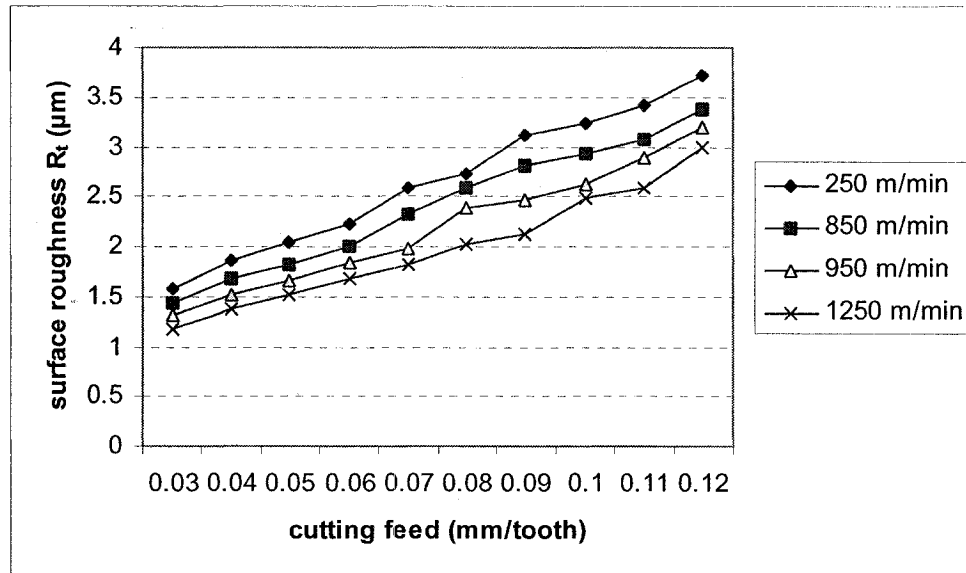


Figure 5.59: Surface roughness (R_t) for Kyon 2100 ceramic tool for different cutting speeds

The roughness height (R_t) increases as the feed increases. However, the roughness height decreases as the cutting speed was increased from 250 to 1250 m/min. It was found that the value of R_t was low at cutting speed of 1250 m/min. This suggests that there are fewer defects on the machined surface. For the range of cutting conditions chosen in this study using ceramic tools, it appears that the overall surface finish of Inconel 718 is better at low feed rate of 0.03 mm/tooth. In the present investigation, for the range of cutting conditions selected, the effect of feed rate seems to be dominant than other cutting parameters. However it was also observed that the surface quality was poor at the low cutting speed (250 m/min). This was due to the presence of short grooves on the machined surface. Hence, higher cutting speeds seem to be the ideal choice for better surface finish. Arunachalam *et al* [2004] reported that the value of surface roughness decreased with increase in the cutting speed.

Chapter 5. High speed machining: wear and surface roughness for ceramic tools

5.8.3 Micro analysis of machined surface

Nickel based superalloys are used in gas turbine applications where good surface stability for fatigue and creep is essential. Therefore, it is important to observe any surface defects (cracks, grooves etc.) during nickel based superalloys machining operation. On the other hand, metallographic examination is valuable for the examination of surface and sub surface characteristics of critical components. In this investigation, machined surface was examined to understand the behaviour of cutting parameters on surface quality in nickel based superalloys machining operation. Metallographic examination of machined surfaces were carried out using optical microscope. For this purpose of metallographic examination, test specimen was machined under different cutting conditions. The machined surface generated by the cutting tool for each cutting condition was investigated.

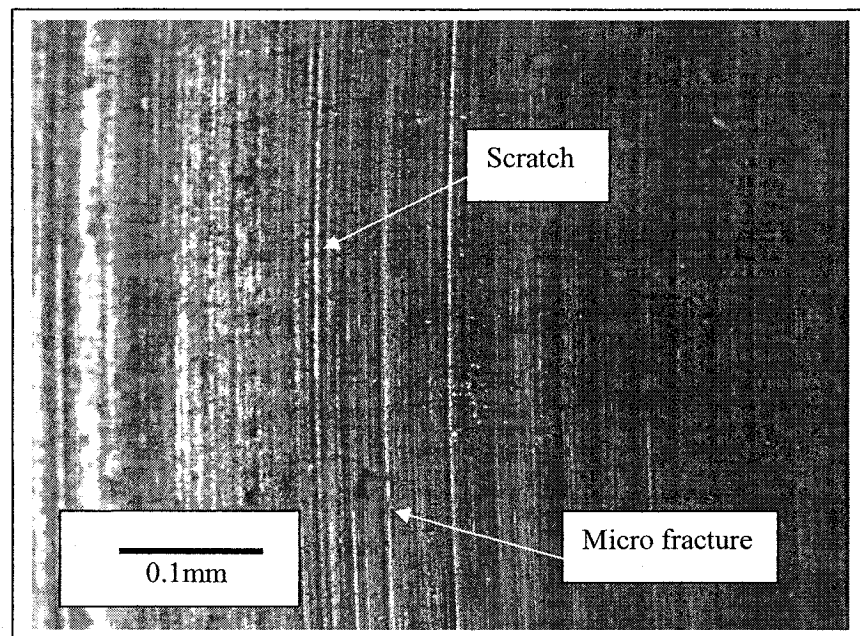


Figure 5.60: Microscopic examination of machined surface (Whisker ceramic tool, $R_a = 0.93 \mu\text{m}$, $R_t = 3.22 \mu\text{m}$, cutting speed = 250 m/min, feed = 0.11 mm/tooth)

Chapter 5. High speed machining: wear and surface roughness for ceramic tools

Figure 5.60 shows the micrograph of machined surface generated by Whisker reinforced ceramic tool at cutting speed 50 m/min and feed of 0.11 mm/tooth. It is found that machined surface produced at low cutting speed (250 m/min) and high feed rate (0.11mm/tooth) was full of short grooves. The short grooves are caused by the cutting edge irregularities during cutting tool penetration into the machined surface. Chips also adhered to the machined surface and scratched the surface at this feed rate condition. Micro cracks were also occurred on all the surfaces produced under higher feed rate conditions. It is believed that these are caused by the brittle fracture of ceramic particles during machining. The roughness parameters (R_a , R_t) for this machined surface were found to be 0.96 μm and 3.22 μm respectively.

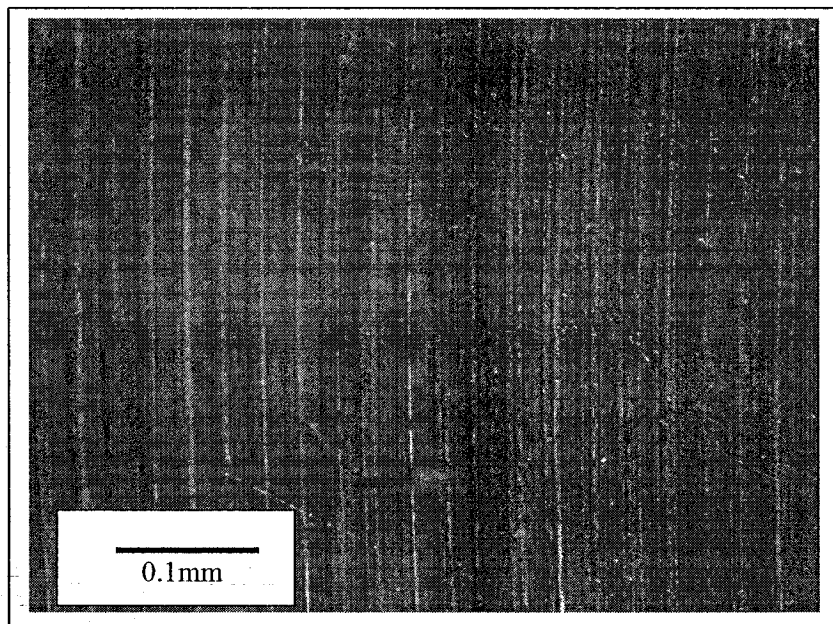


Figure 5.61: Microscopic examination of machined surface (Whisker ceramic tool, $R_a = 0.41 \mu\text{m}$, $R_t = 1.2 \mu\text{m}$, cutting speed = 850m/min, feed = 0.03 mm/tooth)

Chapter 5. High speed machining: wear and surface roughness for ceramic tools

Figure 5.61 shows the micrograph of machined surface generated by Whisker ceramic tool at cutting speed of 850 m/min and feed of 0.03 mm/tooth. It can be observed that no severe scratches were occurred. This could be due to the absence of built-up edge due to higher speed. It can be seen that the defects decrease with the decrease of feed. As a result lower value of surface rough parameters were obtained. The surface produced by higher cutting speed (850 m/min) and low feed rate (0.03 mm/tooth) was found to be better.

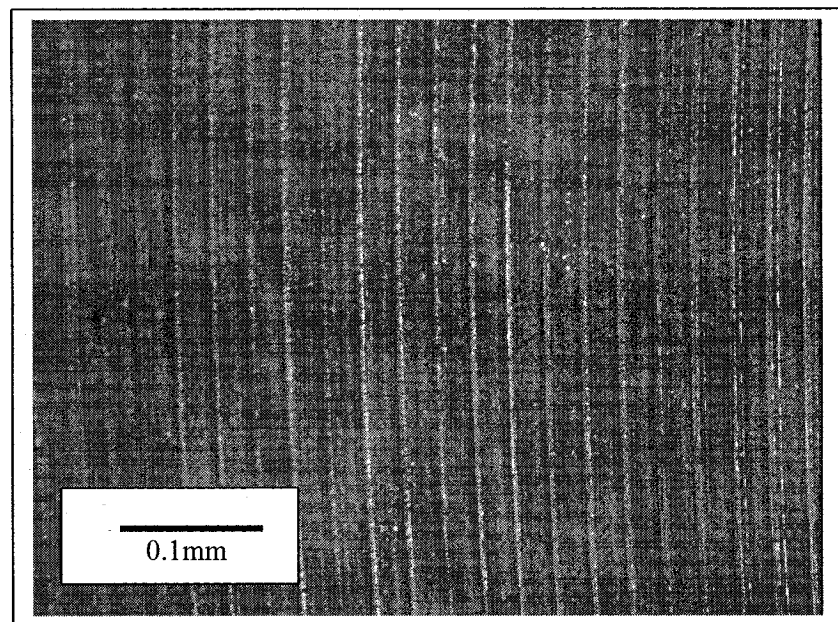


Figure 5.62: Microscopic examination of machined surface (Whisker ceramic tool, $R_a = 0.46 \mu\text{m}$, $R_t = 1.6 \mu\text{m}$, cutting speed = 850m/min, feed = 0.04mm/tooth)

Figure 5.62 shows the micrograph of machined surface generated by Whisker ceramic tool at cutting speed of 850 m/min and feed of 0.04 mm/tooth. It can be seen that surface roughness slightly increased as the feed was increased from 0.03 to 0.04 mm/tooth under the same cutting speed of 850 m/min. The roughness parameters (R_a , R_t) for this machined surface were found to be 0.46 μm and 1.6 μm respectively.

Chapter 5. High speed machining: wear and surface roughness for ceramic tools

Figure 5.63 shows the micrograph of machined surface generated by Whisker ceramic tool at cutting speed of 1250 m/min and feed of 0.08 mm/tooth.

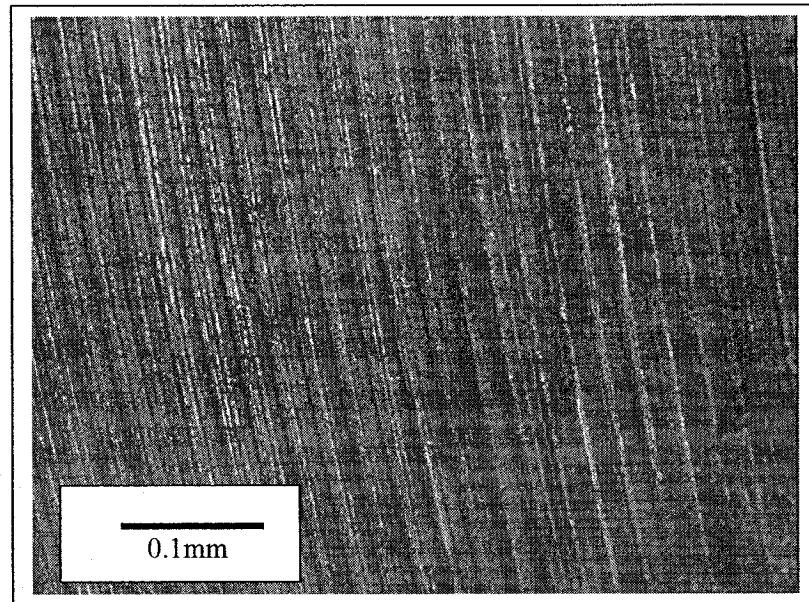


Figure 5.63: Microscopic examination of machined surface (Whisker ceramic tool, $R_a = 0.52 \mu\text{m}$, $R_t = 1.9 \mu\text{m}$, cutting speed = 1250 m/min, feed = 0.08mm/tooth)

From Figure 5.63, it was found that both roughness parameters increased as the feed was increased from 0.04 to 0.08 mm/tooth.

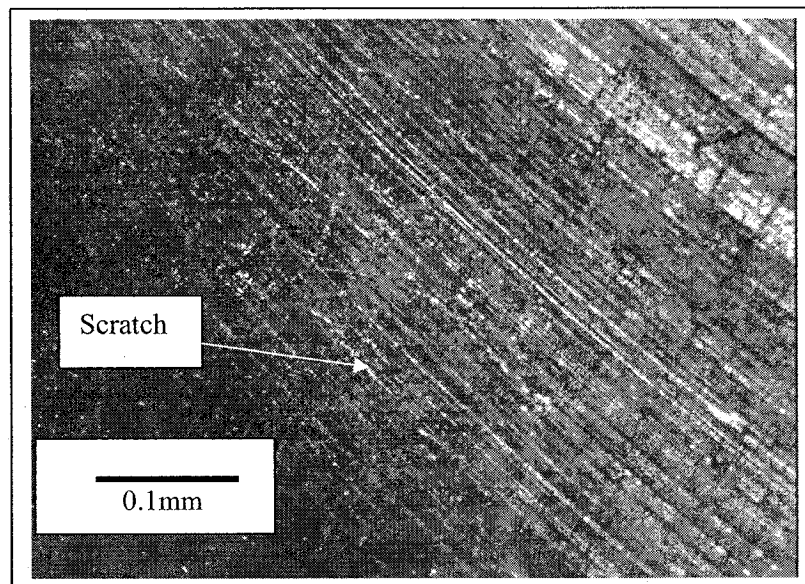


Figure 5.64: Microscopic examination of machined surface (Kyon 2100 ceramic tool, $R_a = 1.05 \mu\text{m}$, $R_t = 3.7 \mu\text{m}$, cutting speed = 250 m/min, feed = 0.12 mm/tooth)

Chapter 5. High speed machining: wear and surface roughness for ceramic tools

Figure 5.64 shows the micrograph of machined surface generated by Kyon 2100 ceramic tool at cutting speed of 250 m/min and feed of 0.12 mm/tooth. It was observed that severe fracture occurred on the machined surface at the higher feed rate (0.12 mm/tooth). It is believed that a high friction at the tool-work interface has led severely scratches on the surface. It was also found that grooves were generated more frequently on the surface so that the machined surface was deteriorated. The roughness parameters (R_a , R_t) for this machined surface were found to be 1.05 μm and 3.7 μm respectively.

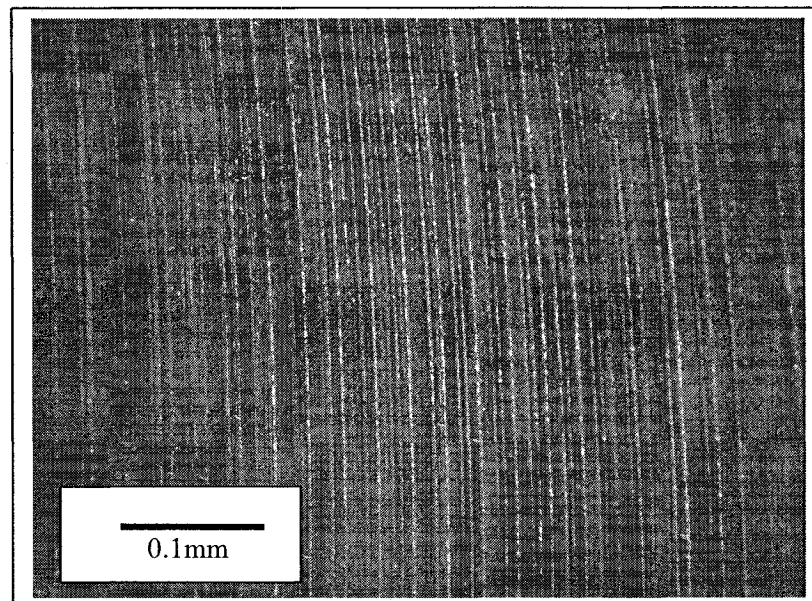


Figure 5.65: Microscopic examination of machined surface (Kyon 2100 ceramic tool, $R_a = 0.5 \mu\text{m}$, $R_t = 1.8 \mu\text{m}$, cutting speed = 850 m/min, feed = 0.05 mm/tooth)

Figure 5.65 shows the micrograph of machined surface generated by Kyon 2100 ceramic tool at the cutting speed of 850 m/min and feed of 0.05 mm/tooth. It can be observed that machined surface obtained at the feed of 0.05 mm/tooth leads to fewer defects on the surface which could cause the lesser value of surface roughness parameters. The roughness parameters (R_a , R_t) for this machined surface were found to be 0.50 μm and 1.8 μm respectively.

Chapter 5. High speed machining: wear and surface roughness for ceramic tools

Figure 5.66 shows the micrograph of machined surface generated by Kyon 2100 ceramic tool at the cutting speed of 850 m/min and feed of 0.07 mm/tooth.

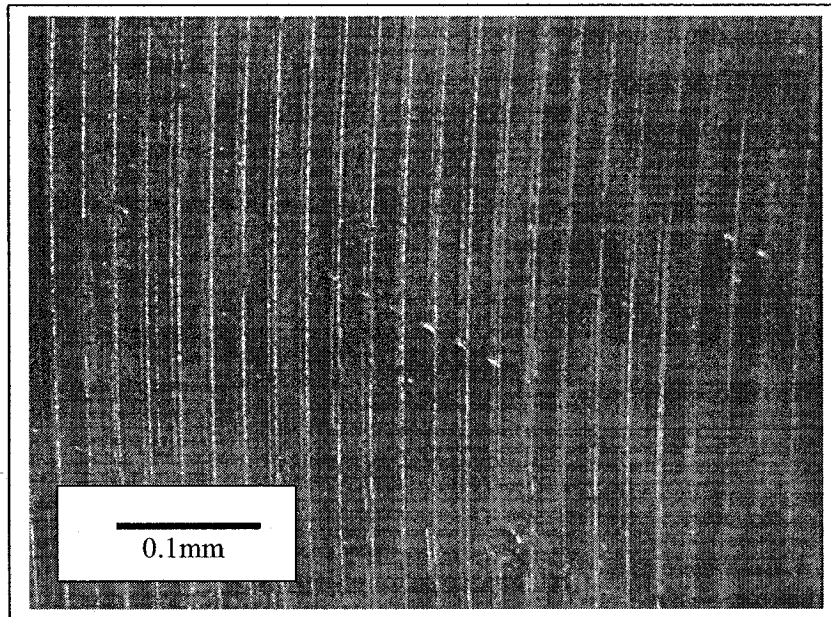


Figure 5.66: Microscopic examination of machined surface (Kyon 2100 ceramic tool, $R_a = 0.62 \mu\text{m}$, $R_t = 2.3 \mu\text{m}$, cutting speed = 850 m/min, feed = 0.07 mm/tooth)

Plastic deformation of the microstructure occurred in the surface zone of the workpiece at high feed rate. The extent of deformation increased as the cutting operation was continued. Moreover as the feed rate was increased, higher values of roughness parameters were obtained. Akasawa *et al* [2003] reported that more defects were observed as the feed was increased.

5.9 Discussion

Significant advantages can be achieved by using high speed milling in manufacturing of the products made of advanced materials. Due to the higher productivity, high speed cutting technologies are commonly used in aerospace industry as well as in die and mold manufacturing for the machining of workpieces with high material removal rate. In high speed machining, the speed and feed to be used in the cutting of nickel based superalloys are related to the type of tool material. The process parameters (cutting speed and feed) which govern the cutting temperature have significant impact on tool wear. On the other hand, nickel based superalloys have a tendency to promote high temperatures during machining. This high temperature can cause the failure of the main toughness mechanisms of the tool material. It is also important to manufacture of parts (nickel based superalloys) at a high level of productivity and quality. To achieve this, any potential improvement of cutting tool materials and machining processes must be considered and evaluated. The choice of cutting tool in high speed machining was critical for cutting nickel based material. Resistance to abrasive wear and thermal deformation in cutting tool is dependent upon the hardness of the cutting tool material. The use of ceramic tools for the machining of nickel based superalloys such as Inconel 718 is important to increase productivity. Ceramics are hard and non reactive that make them attractive as cutting tool materials. The combination of hardness even at extreme temperatures and chemical inertness means that ceramics can run hotter and longer with less wear than other tool materials. Zhao *et al* [1998] reported that ceramic tools have long tool lives and can machine at higher cutting speeds with higher metal removal rates in the right application. These are applications where ceramics based on aluminum oxide (Al_2O_3) and silicon

Chapter 5. High speed machining: wear and surface roughness for ceramic tools

nitride (Si_3N_4) can significantly outperform carbide tools. They mentioned that ceramic cutting tools could take far more heat than carbides. Narutaki et al [1999] reported that ceramic tool material was found to be stronger than other tool materials. The Whisker reinforced ceramic was found to be more wear resistance and fracture resistance against both mechanical and thermal shock. Therefore, we have attempted to study the wear characteristics of ceramic tools in the high speed machining of Inconel 718 for finishing applications. In our study, tool wear under different cutting conditions were analyzed, which will guide the appropriate choosing of the cutting conditions for the optimum performance of ceramic tools. Coolant was not used for this experimental study to avoid thermal shock. The rate of increase of flank wear was high at the beginning of cut but it was found to be reduced with the progress of cutting operation. As for the flank wear, it has generally been considered of mechanical wear such as abrasive wear. From the results of the test, flank wear of ceramic tools when machining of Inconel 718 can be considered a combination of abrasive and adhesive wear mechanisms. The flank wear was found to be more severe at the lowest cutting speed of 250 m/min. However flank wear decreased at the cutting speed increased from 250 to 850 m/min. Flank wear increases as the cutting speed exceeds to 850 m/min. It can be considered that diffusion (reaction) between the tool and Inconel 718 is the cause of large wear. Occurrence of micro chipping of the cutting tools were prominent when machining was carried out at higher cutting speed and higher feed rate. Due to the presence of high stress generated from the cutting action, a layer of burr was observed at the edge of the workpiece during ceramic tests.

Chapter 5. High speed machining: wear and surface roughness for ceramic tools

The presence of burr at the edge of the workpiece is thought to have both thermal and mechanical effects on the cutting tool during nickel based superalloys machining operation. We have seen from micrograph that different wear mechanisms take place on ceramic tools during milling of Inconel 718. Adhesive wear resulted from the action of adhesion between the workpiece and tool material. The rate of wear can be very rapid when an unstable built-up edge is formed on the tool. Once the tool surface is cleaned by chip, there is potential for the creation of continuous adhesive wear. This gives an opportunity for an increase of adhesive wear mechanism rate due to the contact between the chip and tool. An excessive adhered layer and abrasive wear effect seem to be the dominant for the formation of wear. The state of adhesion of workpiece material on the wear surface of a cutting tool was observed by using scanning electron microscope. The high magnification of microstructure shows that chip was adhered to the tool. It was found from microstructure that uniform adhered layer does not exist on the wear surface. On the other hand, abrasive wear occurs when hard particles abrade and remove material from the tool. They may also result from the chip or from the chemical reaction between workpiece and tool. Abrasive mechanism occurred primarily on the flank surface of the tool. It was observed that the thermal effect created by interrupted (milling) cutting is caused the abrasive wear marks on the flank of the tool. Diffusion mechanism was observed for ceramic tools. At higher temperature, the built-up edge that was welded to the tool face served as a source for diffusion. It was found that a small part of the tool material migrates from its original position to the adherent chip. The effectiveness of the diffusion wear on the cutting edge was also observed. It was also found that tool material was diffused to the chip. Therefore, the decreasing hardness and strength of the cutting tool will increase the tool wear. The formation of oxidation was not significant because

Chapter 5. High speed machining: wear and surface roughness for ceramic tools

the constituents of the cutting tool did not react with atmospheric oxygen. At higher cutting speeds, it was found that oxygen cannot penetrate into the chip-tool contact area. The fracture of tool when machining nickel based superalloys was found to be caused by either brittle fracture mechanism or plastic deformation. Micro crack propagation along with pulling up of tool material particles may lead to chipping. The micro crack caused by plastic deformation was found to increase wear at higher cutting feeds (0.12 mm/tooth), which may lead to fracture of the cutting edge. Micro chipping was observed at higher cutting speed, above 950 m/min. It was also found that adhesive and abrasive effect together with micro chipping occurred at the higher cutting speed. Other researchers [Arunachalam *et al* 2004 and Zhao *et al* 1998] also reported that abrasive and adhesive were the main wear mechanism for ceramic tools when machining nickel based superalloys. Examination of the chemical compositions of the wear surface was carried out using energy dispersive X-ray (EDX) method. The presence of nickel (Ni), chromium (Cr) and other elements in the wear surface were detected through EDX (energy dispersive X-ray) analysis. It was found that silicon (Si) has been dissolved into the adherent chip due to higher temperature at the tool-chip interface, thus this condition will accelerate chipping or fracturing. We also studied the effect of cutting parameters such as cutting speed and feed rate on surface roughness in milling operation. The cutting speed and feed rate had significant influence on the value of surface roughness. In the cutting tests performed on Inconel 718, an increase in cutting speed at a constant feed rate caused a noticeable reduction in surface roughness. Machining introduce changes in physical conditions of surface and subsurface of a component which can be characterized as cracks, grooves, fracture etc. The surface of a machined is plastically deformed due to formation of larger shear strains during nickel based superalloys cutting operation. Plastic

Chapter 5. High speed machining: wear and surface roughness for ceramic tools

deformation of the surface zone was associated with the change in grain shape of workpiece material. The built-up edge was broken down on the surface and the broken particles being carried away by the chip. The surface produced at low speed and high feed rate consist of short grooves which are discontinuous in the surface that might have been caused due to the built-up edge formation during cutting operation. Inclusions and other micro fracture occurred at low cutting speed. Microscopic examination of the machined surface revealed no major micro cracks on the machined surface at the higher cutting speed and low feed. This may be explained by the fact that the formation of built-up edge decreased rapidly at high cutting speed. Researcher (Kovacevic *et al*) reported that the machined surface could be improved by increasing cutting speed. The disruption in the cutting action with the cutting tool was absent at higher cutting speed, so that roughness value decreased. Ceramic tools also experienced severe condition at high feed rate in terms of surface roughness. Severely fracture surfaces were occurred at high feed rate condition. The surface defects as well as the depth of cut affected zone increased with increasing feed rate. This could be due to increased friction under dry cutting leading to increased surface shear strains. It will be more advantageous to use high cutting speed and low feed to avoid the formation of groove that was noticed on the machined surface. Since the quality of surface is important for nickel based superalloy machining, cutting parameters should be chosen properly in order to avoid damage of machined surface. We used low depth of cut in order to avoid rubbing of the surface and to reduce the surface defects during nickel based superalloys machining operation.

CHAPTER 6

Wear mechanisms under stable and unstable (chatter) conditions

Chatter vibration is one of the important factors as wear mechanism is very sensitive to chatter. Nickel based superalloys are very hard to machine because of the high thermal and mechanical loading. This material can only be machined at proper cutting conditions and thus we are not free to choose any cutting conditions. For this reason it is necessary to establish stability lobes for selection of proper stable cutting conditions for nickel based superalloys. This chapter will describe wear mechanisms for solid carbide cylindrical end mill tools under stable and unstable (chatter) cutting conditions in milling of nickel based superalloys (Inconel 718).

6.1 Wear mechanisms

Chatter may occur during machining operation, when the cutting speed, feed rate and depth of cut are chosen improperly and it will produce different wear mechanisms. Understanding the wear mechanisms in the machining process will enable us to know the progression of tool wear or failure. Therefore it is important to know the behaviour of wear mechanisms in both cases (stable and unstable) in order to select proper cutting conditions. The fundamental nature of the mechanism of wear can be different under various conditions. There are several wear mechanisms that may occur simultaneously or one of them may dominate. Wear mechanisms can be listed as abrasion, adhesion, diffusion, oxidation, fatigue and chemical mechanism. The dominant wear mechanism in a given application depends on a number of factors: workpiece material, tool material, cutting parameters (speed, feed, depth of cut), stable and unstable (chatter) conditions. One of the key issue during machining of nickel based superalloys is the stability of the cutting process. Unstability has detrimental effect on wear and surface finish of the machined component. A piece of the cutting edge may suddenly fracture during machining due to the presence of chatter. The presence of chatter during machining will increase the rate of wear. Excessive wear will lead to the cutting tool failure and subsequently damage to the machined part as well as machine tool. Although previous researchers reported about wear mechanisms based on cutting conditions but till date no significant research work was carried out about the effect of stable and unstable (chatter) condition on wear mechanisms. It is known that wear is accelerated under unstable conditions even if there is no chipping or breakage of the tool. Due to the detrimental

Chapter 6. Wear mechanisms under stable and unstable (chatter) conditions

effect of chatter (unstable) on wear, more research works should be done in order to understand the process of wear mechanisms. Ceramic tool is very sensitive to chatter vibration. If chatter appears during milling with ceramic tool, then excessive notch wear will be occurred and ultimately tool will be failed. So it is very difficult to compare wear mechanisms with ceramic tool under stable and unstable (chatter) conditions. Thus, we selected solid carbide cylindrical end mill tool instead of ceramic tool in order to compare wear mechanisms under stable and unstable (chatter) conditions. The aim of this research work is to investigate wear mechanisms for solid carbide cylindrical end mill tools under stable and unstable (chatter) conditions in milling of nickel based superalloys (Inconel 718). Tool point vibration response was obtained using impact hammer and the resulting vibration was measured using an accelerometer mounted at the tool point. The frequency domain vibration and force signals or Frequency Response Function (FRF) were used to generate the corresponding stability lobe diagram. Wear mechanisms were determined using scanning metallographic microscope for better understanding of microscopic effects in various stable and unstable cutting conditions.

6.2 Determination of cutting force coefficients from cutting forces

Mechanistic approach [Altintas 2000] was used in order to determine cutting force coefficients from cutting forces. In this approach, the average milling forces per tooth period can be expressed by equation (6.1)

$$\overline{F}_q = \frac{1}{\phi_p} \int_{\phi_{st}}^{\phi_{ex}} F_q(\phi) d\phi \quad (6.1)$$

Chapter 6. Wear mechanisms under stable and unstable (chatter) conditions

The following equations (6.2) to (6.4) can be obtained by integrating cutting forces.

$$\begin{aligned} \overline{F}_x = & \left\{ \begin{aligned} & \frac{Nac}{8\pi} (K_{tc} \cos 2\phi - 2K_{rc}\phi + K_{rc} \sin 2\phi) \\ & + \frac{Na}{2\pi} (-K_{te} \sin \phi + K_{re} \cos \phi) \end{aligned} \right\}_{\phi_{st}}^{\phi_{ex}} \end{aligned} \quad (6.2)$$

$$\begin{aligned} \overline{F}_y = & \left\{ \begin{aligned} & \frac{Nac}{8\pi} (K_{tc} 2\phi - K_{tc} \sin 2\phi + K_{rc} \cos 2\phi) \\ & - \frac{Na}{2\pi} (K_{te} \cos \phi + K_{re} \sin \phi) \end{aligned} \right\}_{\phi_{st}}^{\phi_{ex}} \end{aligned} \quad (6.3)$$

$$\overline{F}_z = \left\{ \frac{Na}{2\pi} (-K_{ac} c \cos \phi + K_{ae} \phi) \right\}_{\phi_{st}}^{\phi_{ex}} \quad (6.4)$$

The average cutting forces ($\overline{F}_x, \overline{F}_y, \overline{F}_z$) in milling can be defined as a function of cutting conditions (a = depth of cut, c = chip load) and cutting coefficients ($K_{rc}, K_{re}, K_{tc}, K_{te}, K_{ac}$ and K_{ae}). The entry and exit angles are $\phi_{st} = 0$ and $\phi_{ex} = \pi$ respectively for full immersion milling operation. When full immersion conditions are applied to equations (6.2) to (6.4), the average forces per tooth period can be expressed by equation (6.5).

$$\begin{aligned} \overline{F}_x = & -\frac{Na}{4} K_{rc} c - \frac{Na}{\pi} K_{re} \\ \overline{F}_y = & +\frac{Na}{4} K_{tc} c + \frac{Na}{\pi} K_{te} \\ \overline{F}_z = & +\frac{Na}{\pi} K_{ac} c + \frac{Na}{2} K_{ae} \end{aligned} \quad (6.5)$$

Chapter 6. Wear mechanisms under stable and unstable (chatter) conditions

where, N is the number of tooth in the cutter, the subscripts r , t , and a corresponds to the radial, tangential and axial force coefficients respectively.

The average cutting force can be expressed by a linear function of feed rate (c) and an offset contributed by the edge forces:

$$\bar{F}_q = \bar{F}_{qc}c + \bar{F}_{qe} \quad (6.6)$$

The equation (6.7) can be evaluated from equations (6.5) and (6.6):

$$\left. \begin{aligned} K_{tc} &= \frac{+4\bar{F}_{yc}}{Na} \\ K_{te} &= \frac{+\pi\bar{F}_{ye}}{Na} \\ K_{rc} &= \frac{-4\bar{F}_{xc}}{Na} \\ K_{re} &= \frac{-\pi\bar{F}_{xe}}{Na} \\ K_{ac} &= \frac{+\pi\bar{F}_{zc}}{Na} \\ K_{ae} &= \frac{+2\bar{F}_{ze}}{Na} \end{aligned} \right\} \quad (6.7)$$

6.2.1 Experimental procedures for cutting force test

Cutting force coefficients were determined from cutting forces for nickel based superalloys. The cutting force coefficients are necessary in order to establish stability lobes for nickel based superalloys. We performed tests on a CNC milling machine (MITSUI SEIKI-HU 40T) at Ecole Polytechnique Manufacturing Laboratory. Figure 6.1 shows the CNC milling machine. The workpiece (Inconel 718) was mounted on the dynamometer. The dynamometer was mounted on the machine table to measure cutting forces. The dynamometer was connected to the charge amplifier and finally the charge amplifier was connected to the computer-data acquisition system. The three component cutting forces were measured using dynamometer as shown in the measurement setup in Figures 6.2 and 6.3. In order to determine cutting forces, we measured the cutting forces during full immersion cuts with eight (8) different feed rates (0.015 mm/flute to 0.05 mm/flute) at cutting speed of 70 m/min (1170 rpm). The depth of cut (0.5 mm) was kept constant for all tests. The cutting tool was four flute TiAlN coated solid carbide cylindrical end mill (C430-NIAGARA). The diameter and helix angle of cutting tool are 19.05 mm and 30° respectively. Water based coolant was used during machining operation. We repeated test in order to ensure the reliability of measurements.



Figure 6.1: CNC milling machine

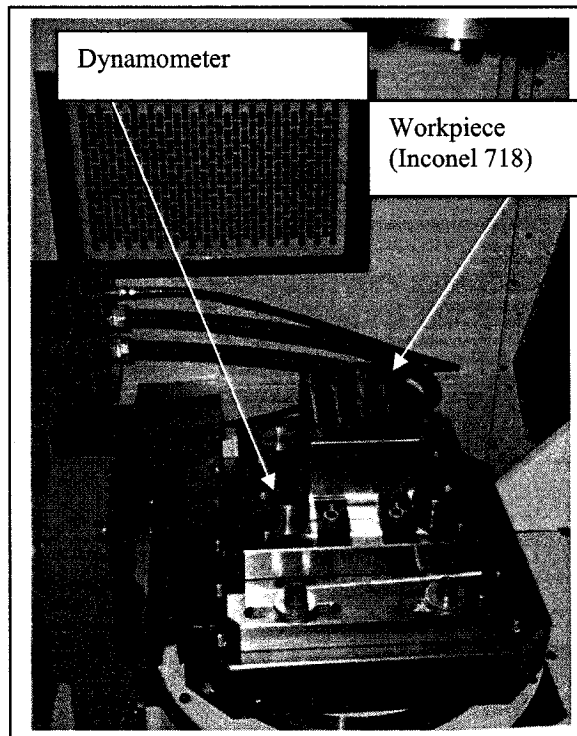


Figure 6.2: Dynamometer and Workpiece

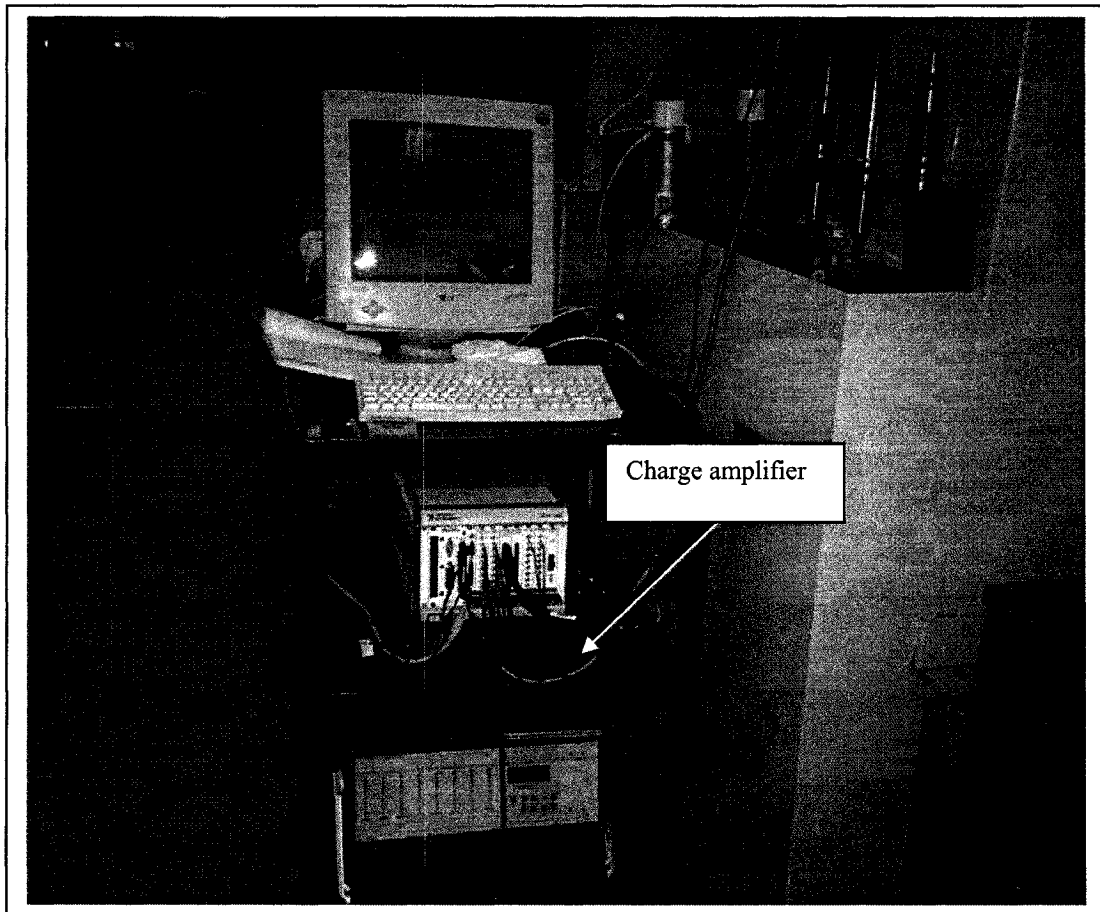


Figure 6.3: Charge amplifier and Computer-data acquisition system for cutting force measurement

Microphone can be used to check the stability of cutting process. In this system microphone was attached with a PC-based acoustic chatter detection system (MALDAQ) that was capable to detect chatter. The RPM of the cutter and number of teeth is responsible for creating the tooth passing frequency. Based on the cutting conditions, the relative magnitude of sound was monitored and thus cutting stability was maintained. For this purpose a microphone was placed near the cutting during cutting operation. It was found that the tooth passing frequency (calculated from spindle speed and number of

Chapter 6. Wear mechanisms under stable and unstable (chatter) conditions

tooth) was closed to the dominant frequency (frequency obtained from sound spectrum). Thus we made sure that chatter did not appear during cutting force tests. Figure 6.4 shows the microphone and data acquisition system.

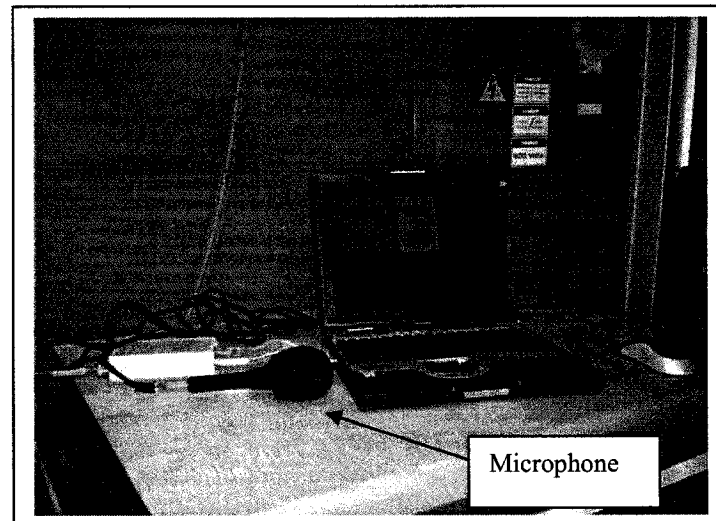


Figure 6 4: Microphone with data acquisition system

A measurement data-acquisition software (House-Labview) was installed into the computer in order to capture the cutting forces (which were exerted by dynamometer). During cutting tests cutting forces for each cutting condition (feed rate) were saved in to the computer.

6.2.2 Cutting force coefficients

Three components (F_x, F_y, F_z) of cutting forces were analyzed using data-acquisition software and determined average cutting forces for each feed rate condition. Average cutting forces were plotted for different feed rates (Figure 6.5). Correlation between the average cutting forces and feed rate was obtained by performing the linear regression between the average measured forces and feed rate.

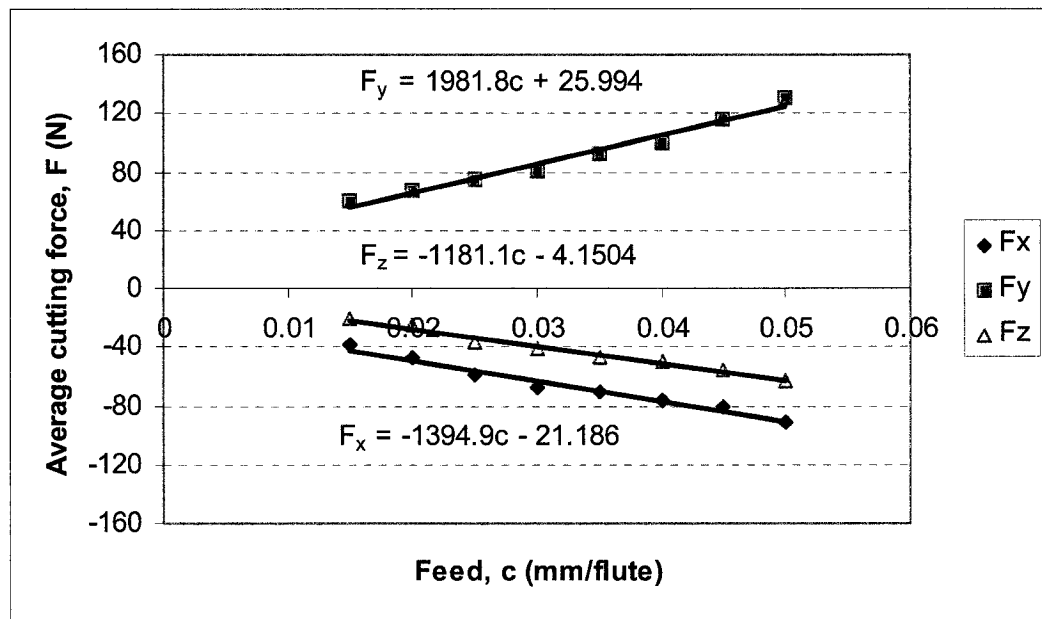


Figure 6.5: Average cutting force vs. Feed (cutting speed =70 m/min (1170 rpm), depth of cut=0.5 mm, full immersion)

The corresponding equations of the linear curves can be expressed by

$$\bar{F}_x = -1394.9c - 21.186 \quad (6.8)$$

$$\bar{F}_y = 1981.8c + 25.994 \quad (6.9)$$

$$\bar{F}_z = -1181.1c - 4.1504 \quad (6.10)$$

Chapter 6. Wear mechanisms under stable and unstable (chatter) conditions

The first terms of above equations (6.8 to 6.10) on the right hand side correspond to actual cutting force components and second terms are edge force components.

We determined cutting force coefficients for solid carbide cylindrical end mill at 0.5mm depth of cut using Equation (6.7). The average cutting force coefficients are $K_{tc} = 3963.6$ N/mm², $K_{rc} = 2789.8$ N/mm², $K_{ac} = -1854.33$ N/mm², $K_{te} = 40.811$ N/mm, $K_{re} = 33.26$ N/mm and $K_{ae} = -4.1504$ N/mm respectively. The tangential (K_{tc}) and radial (K_{rc}) cutting force coefficients are important parameters in order to establish stability lobes. The edge cutting forces (K_{te} , K_{re} , K_{ae}) are caused by friction on the cutting edge.

6.3 Determination of machine tool dynamics (vibration)

The dynamics of a machine tool structure need to be measured in order to establish stability lobes. The machine tool dynamics were determined by tap test (hammer test). In the tap test, the machine tool is excited by hitting it with a hammer with force sensor. This impact will excite the structure over a certain frequency range. In milling, the machine tool structure is flexible in X and Y directions. So we usually need to consider the flexibility in the X-Y plane (two directions), because the flexibility in Z-direction is much smaller (the stiffness in Z-direction is much higher). In our tests, we neglected the dynamic behaviour in Z-direction; therefore we measured transfer functions in two directions (X and Y) for the prediction of dynamic behaviour. We selected a hammer with force sensor (Model No: 086C04) for hitting the cutting tool. An accelerometer (Model No: PCB 352C22) was used to measure vibratory signal. This accelerometer was attached on the solid carbide cylindrical end mill tool using special wax (Figure 6.6). The original overhanging length of cutting tool was 60 mm.

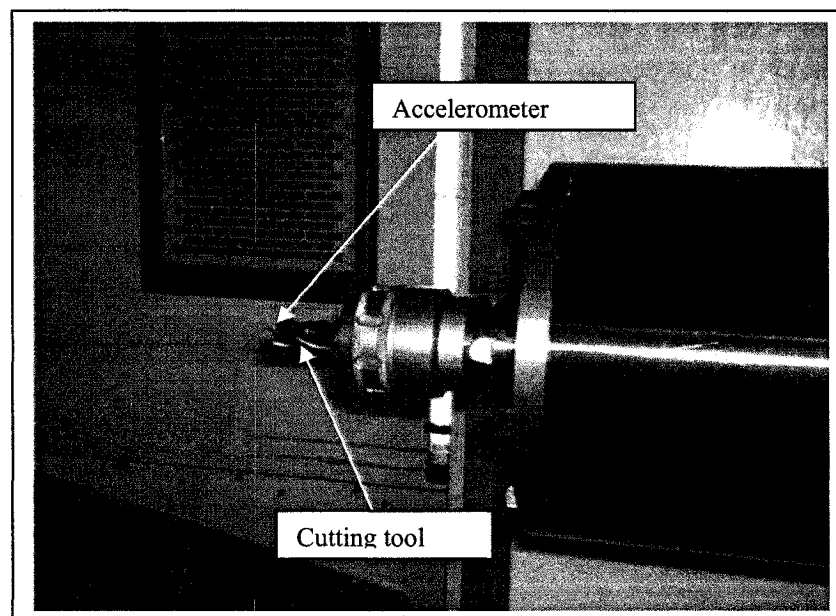


Figure 6.6: Attachment of accelerometer on the cutting tool

Chapter 6. Wear mechanisms under stable and unstable (chatter) conditions

The amplified force signal line (hammer connection) was connected to the input channel and the accelerometer signal line was connected to the other channel of the data acquisition system (Figure 6.7).



Figure 6.7: Hammer with Data acquisition system

The tool was hit using hammer with as perfect an alignment as possible with the axis measured. In order to minimize errors during vibration testing, we always took several measurements and averaged them. Firstly, the tool was hit by hammer in X-direction (attaching accelerometer in the X direction) and measured signals using data acquisition system. After each hit, the signals were examined to identify whether it was a good hit. A hit was considered bad if a multiple hit (hammer bounces or loses contact) occurred. When enough good hits were collected, they were averaged and signals of hammer and

Chapter 6. Wear mechanisms under stable and unstable (chatter) conditions

accelerometer were stored into the computer through data acquisition system. Secondly, the accelerometer was attached on the cutting tool in Y-direction and hit the tool in the line of alignment of Y-direction. We followed same procedure for Y-direction as we have done for X-direction. Tests were repeated in order to obtain more reliable results. The dynamic characteristics were determined by the spectrum of impact force signal and accelerometer signal. A modal analysis software (CutPro) was installed into a Laptop and was used for identification of transfer function parameters. The power spectrum of signal indicates amplitude vs. frequency curve. The power spectrum was used in order to verify the transfer function measurement signals. Figures 6.8 and 6.9 show the magnitude of transfer function in X and Y directions.

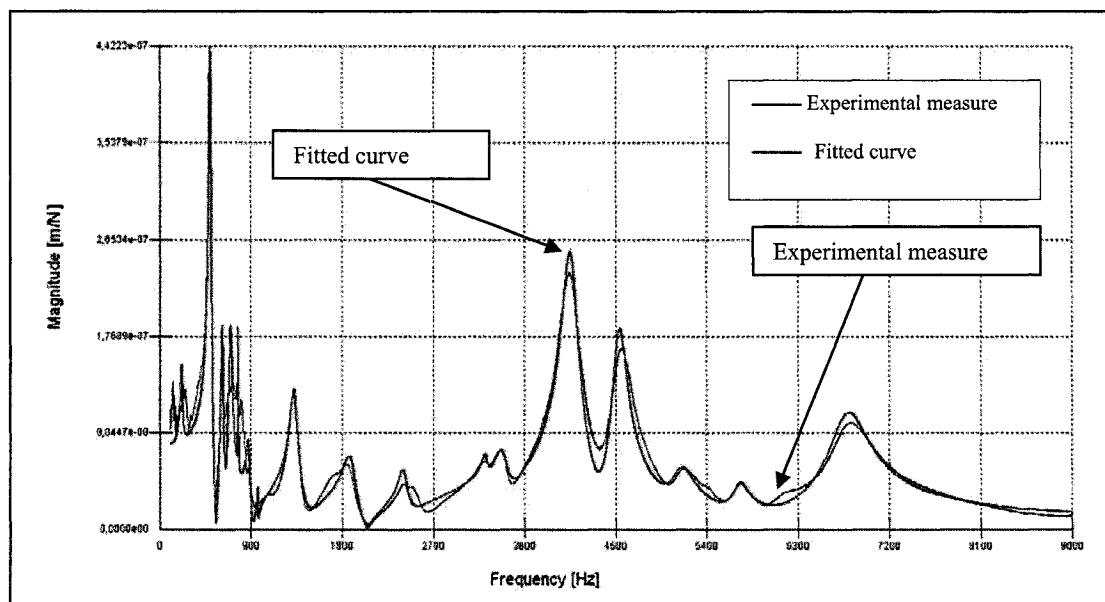


Figure 6.8: Magnitude of transfer function in X direction

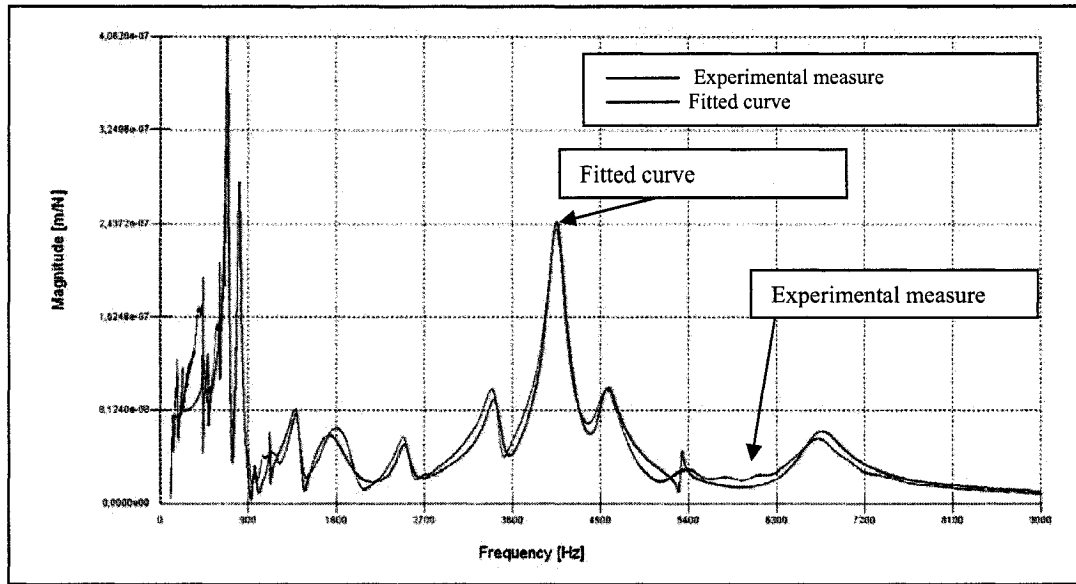


Figure 6.9: Magnitude of transfer function in Y direction

Modal parameters (transfer function parameters) were analyzed using CutPro software by selecting the option of modal/residue. Tables 6.1 and 6.2 show modal parameters.

Table 6.1: Identified modal parameters in X direction

Mode	Frequency ω_n [Hz]	Damping ratio ζ	Mode of residue (m/N) $\sigma \pm j\nu$
1	325.58	0.1004	$1.9768 E - 06 - j 7.2622 E - 06$
2	497.93	0.0253	$-6.6374 E - 06 - j 3.4161 E - 05$
3	618.42	0.0074	$1.007 E - 06 - j 1.4013 E - 06$
4	715.27	0.0383	$3.7519 E - 06 - j 4.0844 E - 06$
5	770.85	0.0012	$-3.3632 E - 07 - j 3.4019 E - 07$
6	869.64	0.0171	$5.3488 E - 07 - j 9.9161 E - 07$
7	1331.71	0.0317	$-1.5227 E - 06 - j 3.3363 E - 05$
8	1893.24	0.0354	$-2.115 E - 05 - j 8.6622 E - 06$
9	2404.10	0.0169	$1.5746 E - 06 - j 2.1736 E - 06$
10	3211.60	0.0163	$3.4044 E - 07 - j 4.0137 E - 06$
11	3391.51	0.0238	$-2.0780 E - 06 - j 2.1766 E - 05$
12	4047.24	0.0274	$-1.9473 E - 06 - j 1.4435 E - 04$
13	4535.32	0.0244	$-6.4548 E - 06 - j 9.7686 E - 05$
14	5142.51	0.0264	$-2.6473 E - 06 - j 2.1773 E - 05$
15	5727.30	0.0153	$-6.7679 E - 06 - j 1.2038 E - 05$
16	6802.74	0.0314	$-1.0064 E - 04 - j 8.1560 E - 05$

Chapter 6. Wear mechanisms under stable and unstable (chatter) conditions

Table 6.2: Identified modal parameters in Ydirection

Mode	Frequency ω_n [Hz]	Damping ratio ζ	Mode of residue (m/N) $\sigma \pm j\nu$
1	398.36	0.0024	$-3.7878 E - 08 - j 1.9472 E - 06$
2	496.43	0.0109	$2.8854 E - 07 - j 4.8557 E - 07$
3	613.22	0.0092	$-1.157 E - 07 - j 1.0164 E - 07$
4	691.78	0.0171	$-4.6912 E - 06 - j 2.6601 E - 05$
5	811.61	0.0211	$-5.1964 E - 06 - j 2.7080 E - 05$
6	971.86	0.0098	$-2.8791 E - 07 - j 8.7020 E - 07$
7	1171.60	0.0338	$-1.1566 E - 06 - j 2.5420 E - 06$
8	1399.50	0.0346	$-2.2025 E - 06 - j 1.9188 E - 05$
9	1847.52	0.1077	$1.7640 E - 05 - j 9.9120 E - 05$
10	2506.48	0.0256	$2.6092 E - 06 - j 1.6896 E - 05$
11	3429.62	0.0221	$-8.0960 E - 06 - j 3.7085 E - 05$
12	4052.70	0.0236	$3.4240 E - 06 - j 1.2214 E - 04$
13	4558.34	0.0262	$-1.3526 E - 05 - j 4.1829 E - 05$
14	5369.20	0.0138	$-5.0982 E - 07 - j 2.6060 E - 06$
15	6729.38	0.0309	$-2.5410 E - 05 - j 4.2910 E - 05$

6.3.1 Establishment of stability lobes

In milling, the cutter always cuts into a surface created in the previous pass, such as the preceding tooth of a milling cutter. If the system vibrates, the tooth produces waves on the surface which are regenerated in the following pass. That is the self-excitation mechanism or chatter vibration. Altintas [2000] presented chatter vibration on machine tools by explaining the fundamental mechanism of chip thickness. He developed the analytical stability lobes formulation by considering the dynamic displacement of the milling cutter and workpiece. Altintas [2000] established the following equations for chatter stability analysis.

The expression for chatter-free depth of cut (a_{lim}) can be found as

$$a_{lim} = \frac{-2\pi \wedge_R}{NK_t} (1 + \kappa^2) \quad (6.1)$$

where

K_t = cutting force coefficient

$$\kappa = \frac{\wedge_I}{\wedge_R} = \frac{\sin \omega_c T}{1 - \cos \omega_c T}$$

$\varepsilon = \pi - 2\psi$ is the phase shift between the inner and outer modulations. Thus, if k is the number of full vibration waves (i.e., lobes), then

$$\omega_c T = \varepsilon + 2k\pi \quad (6.2)$$

The spindle speed (n) can be calculated by finding tooth passing frequency period (T).

$$n = \frac{60}{NT} \quad (6.3)$$

Chapter 6. Wear mechanisms under stable and unstable (chatter) conditions

Stability lobes were established for nickel based superalloys in milling operation. After determination of cutting force coefficient and dynamics (transfer function), these data were used in the CutPro software to establish the stability lobes. In order to simulate stability lobes, we specified cutting force coefficients (K_{rc} , K_{re} , K_{tc} , K_{te} , K_{ac} and K_{ae}), tool geometry and used measured transfer function file (Measured.t.f.file) directly. Figure 6.8 shows the stability lobes for nickel based superalloys.

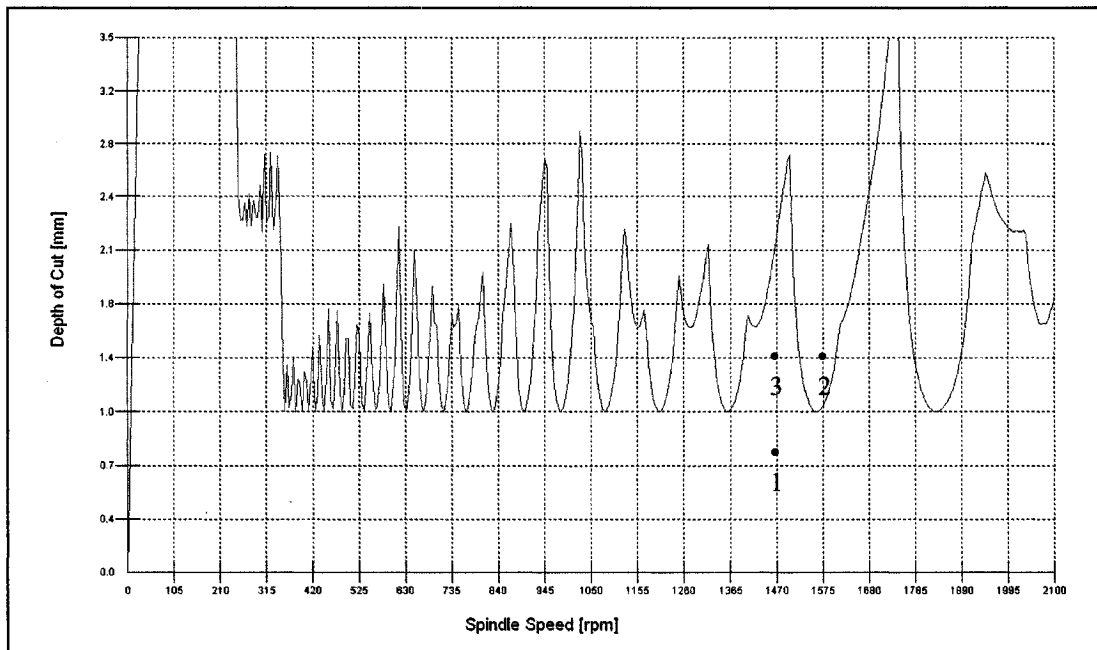


Figure 6.10: Stability lobes for half immersion down milling

In order to achieve stable cutting process, it is important to avoid chatter between the tool and workpiece when cutting with an end mill. Certain parameters determine whether stable cut or unstable cut (chatter) occur and there exists a depth of cut limit at which the cutting process becomes stable under all cutting speeds. A stability lobe diagram is a plot that separates unstable cutting combinations of depth of cut and spindle speed from stable

Chapter 6. Wear mechanisms under stable and unstable (chatter) conditions

combinations. The points (which indicate depth of cut and spindle speed), below the dividing line will represent stable cutting condition and the points above the dividing line will represent unstable (chatter) condition. In Figure 6.10, cutting conditions 1 and 3 are stable but 2 is unstable. It can be seen that point 1 is absolutely stable since changes in speed do not affect stability and point 3 is conditionally stable. It is also noted in the stability lobe of Figure 6.10 that if we draw a straight line through the depth of cut for points 3 and 2, the cutting process becomes unstable for the change of cutting speed. It is seen that cutting speed plays an important role in its effect on the limits of depth of cut. The stable speed ranges become narrower as the cutting speed becomes slower. There is hardly any stability pocket at low cutting speed, which is due to the many tightly packed vibration waves at each tooth period. The overlapping of the low speed range starts at 500 rpm. These stability lobes are obtained by an analytical solution in which process damping has not been considered. In reality the stability limit is higher at lower speeds because of the process damping. Jumping in the stability lobes at the low speed in Figure 6.10 occurs because of two different modes, which have phase shift in the analytical solution cut at certain lobe number. In the reality stability lobes limit will be around 1 mm if we continue simulation for higher or infinite number of waves ($k \rightarrow \infty$) on the surface for one tooth period. The highest stability, permitting the highest value of depth of cut is obtained with the cutting speed at which the tooth passing frequency closes to dominant frequency of the system. The minimum stable depth of cut seems to be about 1 mm for all cutting conditions in half immersion down milling for our case. While in some instances stable depth of cut may be increased up to two or three times by choosing high

Chapter 6. Wear mechanisms under stable and unstable (chatter) conditions

cutting speed. The stability diagram is especially convenient for determining the stability status for machining conditions. We know that stability depends on dynamic behaviour of the system, cutting coefficients and cutting conditions. For this reason, we analyzed stability lobes by two approaches. One approach is to change cutting condition (changing depth of cut and spindle speed). The other approach is to change the dynamic behaviour of the system (modification of length of cutting tool). The effect of dynamic behaviour of the system on the stability was addressed in the following section.

6.3.2 Determination of the effect of dynamic behaviour of the system on stability

The effect of dynamic behaviour on stability was determined by changing the overhanged length of cutting tool. The tool length was kept longer in order to increase the flexibility. The cutting tool was overhanged to the tool holder-spindle (overhung tool length = 80 mm) in order to keep the cutting tool more flexible (Figure 6.11).

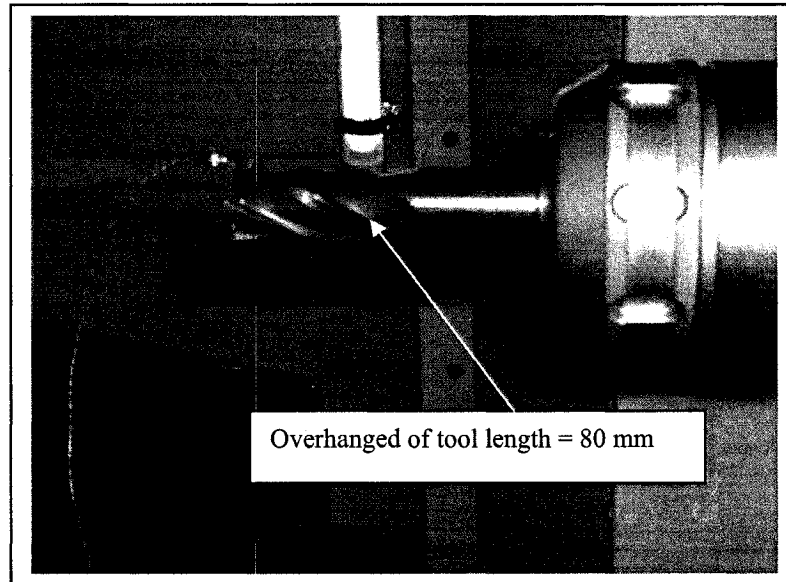


Figure 6.11: Vibration test for greater overhanged tool length

Cutting dynamics (transfer function) were determined for this system. After finishing tests, we analyzed modal parameters (transfer function) using modal analysis CutPro software. Stability lobes were established using cutting coefficients (K_{rc} , K_{re} , K_{tc} , K_{te} , K_{ac} and K_{ae}), tool geometry and measured transfer function parameters.

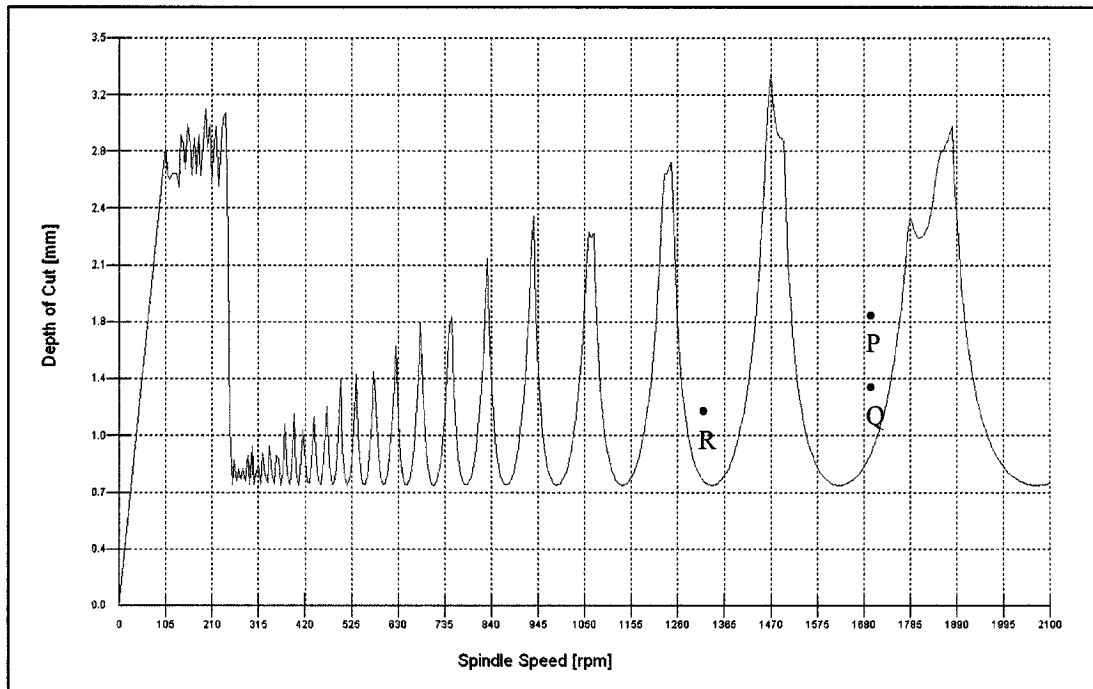


Figure 6.12: Stability lobes for the change of dynamic behaviour, half immersion down milling

Figure 6.12 shows the stability lobes for the change of dynamic system. In this system the tool length was longer to increase the flexibility. It was found that minimum stable depth of cut seems to be about 0.74 mm for this dynamic system but minimum stable depth of cut was found to be 1 mm for previous dynamic system (Figure 6.10). It was observed that stable points may become unstable due to the influence of dynamic behaviour on the stability. For example cutting conditions of P, Q and R (Figure 6.12) were found to be unstable but those cutting conditions were stable in Figure 6.10. Therefore, change of dynamic behaviour of the system (change of cutting tool length) has an effect on stability lobes.

6.4 Microphone sound spectrum and wear mechanisms

The microphone was placed near the cutting zone to record sound spectrum during cutting operation. The microphone was connected to the MALDAQ data acquisition system in order to monitor the sound spectrum. From the sound spectrum we determined the stable and unstable (chatter) cutting conditions. We determined wear mechanisms for nickel based superalloys under stable and unstable (chatter) conditions.

6.4.1 Analysis of microphone sound spectrum

The sound spectrum of microphone was recorded in order to detect stable or unstable (chatter) conditions. From the sound spectrum the presence of chatter vibration was determined. Different cutting conditions were selected from stability lobes (Figure 6.10). Sound spectrum results in the form of FFT were analyzed using MALDAQ data acquisition system. The following sound spectrum results are presented in order to better understanding of tooth passing frequency, dominant frequency and chatter frequency during the milling process.

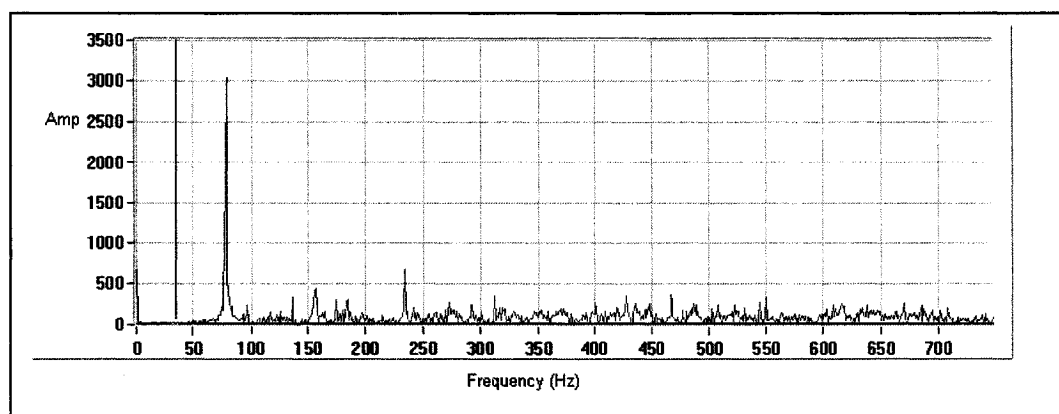


Figure 6.13: Microphone sound spectrum (Cutting speed =1170 rpm, depth of cut = 1.2 mm)

Chapter 6. Wear mechanisms under stable and unstable (chatter) conditions

Figure 6.13 shows the sound spectrum for the cutting speed of 1170 rpm (70 m/min) and depth of cut of 1.2 mm. The tooth passing frequency (calculated from the spindle speed and number of tooth) is 78 Hz. It was found that the tooth passing frequency closed to dominant frequency (frequency obtained from sound spectrum), then there was no chatter in the machining process. This condition is stable cut. From stability lobes (Figure 6.10), we also found that the depth of cut 1.2 mm was stable cut at the cutting speed of 1170 rpm. Further we increased the cutting speed of 1505 rpm (90 m/min) and depth of cut of 1.4 mm. Figure 6.14 shows the sound spectrum for the cutting speed of 1505 rpm.

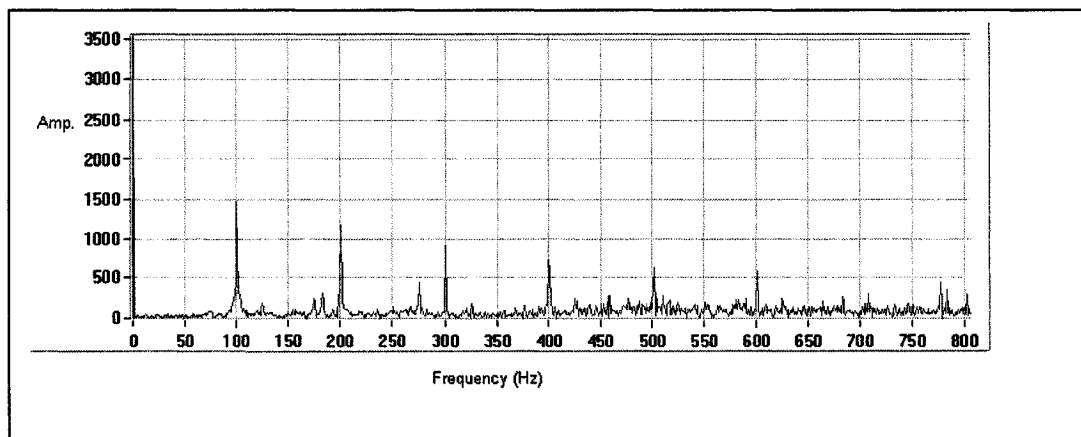


Figure 6.14: Microphone sound spectrum (Cutting speed =1505 rpm, depth of cut = 1.4 mm)

The tooth passing frequency (calculated from the spindle speed and number of tooth) is 100.33 Hz. In the sound spectrum, we can clearly see that the tooth passing frequency is 100 Hz and harmonics (200, 300Hz etc.). That means the tooth passing frequency closes to dominant frequency (frequency obtained from sound spectrum). There was no chatter in this cutting condition. This is stable cut. We also found from stability lobes (Figure

Chapter 6. Wear mechanisms under stable and unstable (chatter) conditions

6.10) that the depth of 1.4 mm was stable under the cutting speed of 1505 rpm. A further increase in depth of cut of 3.3 mm results the presence chatter in the machining process. Figure 6.15 shows the sound spectrum for the cutting speed of 1505 rpm and depth of cut 3.3 mm.

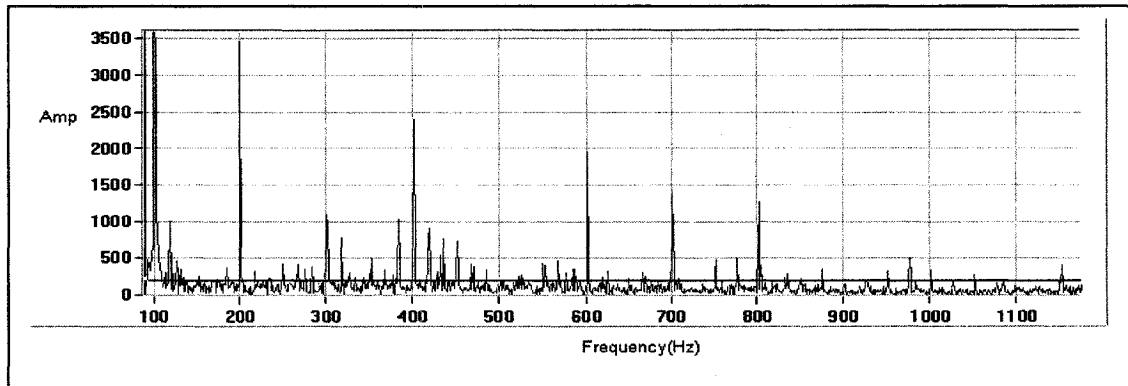


Figure 6.15: Microphone sound spectrum (Cutting speed =1505 rpm, depth of cut = 3.3 mm, unstable cut)

In the spectrum, we can see that the dominant frequency is 100 Hz and harmonics (200, 300, 400 Hz). This test also showed chatter frequencies, which were probably came from the mode in X and Y directions. Therefore this test cut is unstable (chatter) that means chatter appeared during the machining process. We found from the stability lobes (Figure 6.10) that the depth of cut 3.3 mm was unstable at the cutting speed of 1505 rpm. Wear mechanisms for stable and unstable (chatter) conditions are presented in the following section.

6.4.2 Determination of wear mechanisms

Cutting conditions (cutting speed and depth of cut) were selected from stability lobes (Figure 6.10) for wear tests. Cutting tests were carried out at cutting speeds from 50 m/min (836 rpm) to 90 m/min (1505 rpm) for half immersion down milling operation. Different depth of cuts were chosen for different cutting speeds under stable and unstable conditions. Water based coolant was used for all cutting tests. Cutting test was repeated for each cutting speed.

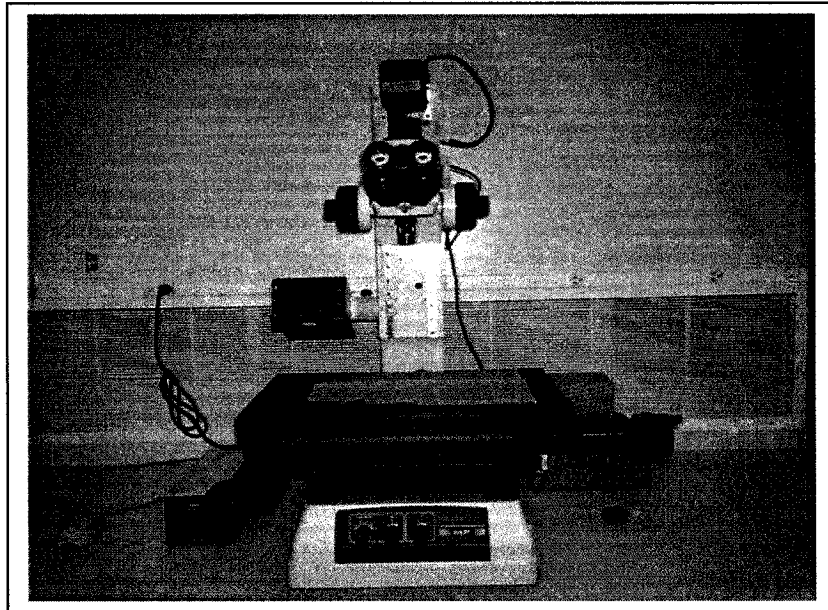


Figure 6.16: Tool wear measuring microscope

Cutting tests were stopped, when the maximum flank wear reached at 0.70 mm [ISO]. Tool wear was measured using wear measuring microscope (Figure 6.16). After measuring tool wear, wear mechanisms were determined using scanning metallographic microscope (Figure 6.17).



Figure 6.17: SMM microscope for wear mechanisms

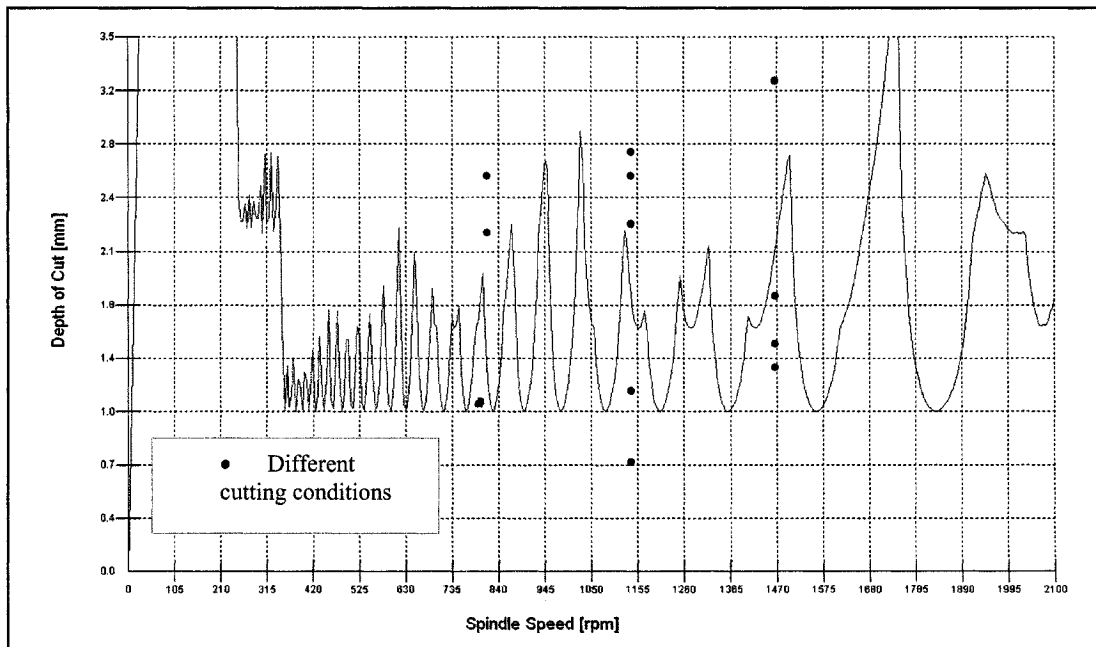


Figure 6.18: Stability lobes for half immersion down milling

Chapter 6. Wear mechanisms under stable and unstable (chatter) conditions

Firstly cutting speed of 50 m/min (836 rpm) and different depth of cuts were selected (stable and unstable conditions) from stability lobes (Figure 6.18). Then cutting tests were performed at the cutting speed of 50 m/min (836 rpm) and different depth of cuts. It was observed (Figures 6.19 and 6.20) that rate of flank wear was slow at depth of cut of 1 mm. This was related to the stable cutting in the absence of chatter vibration. On the other hand, intense flank wear occurred (Figure 6.21), when the depth of cut was increased. It was observed that the cutting edge (Figures 6.22 and 6.23) was broken after three passes of cutting operation. This may be associated with chatter vibration. Micrograph (6.22) showed that main wear mechanisms were abrasion and strong adhesion between tool and workpiece. Strong built edge up was also observed at low cutting speed under unstable condition. Figure 6.19 shows the variation of flank wear at the cutting speed of 50 m/min under stable cut.

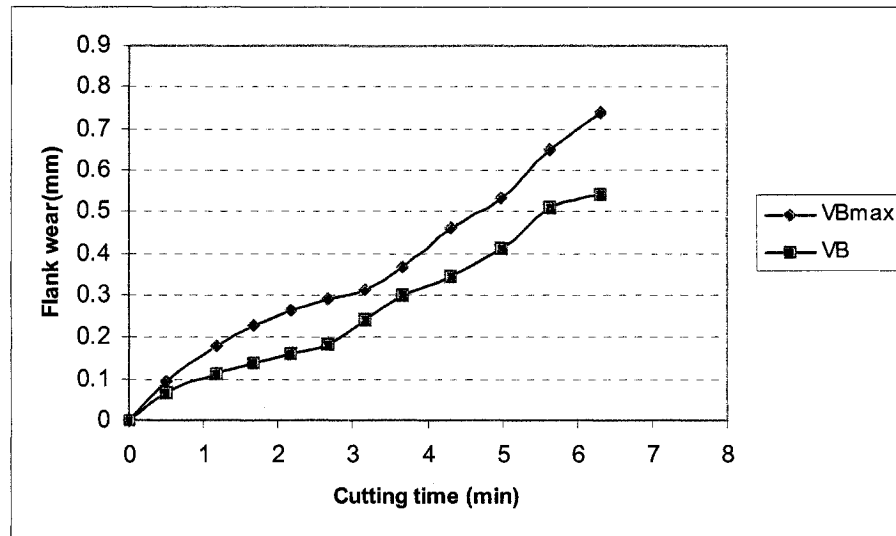


Figure 6.19: Flank wear vs. Cutting time, cutting speed = 50 m/min (836rpm,) depth of cut = 1 mm, feed= 0.025 mm/tooth, stable cut

Figure 6.20 shows wear surface (end of tool life) for the cutting speed of 50 m/min and depth of cut of 1mm.

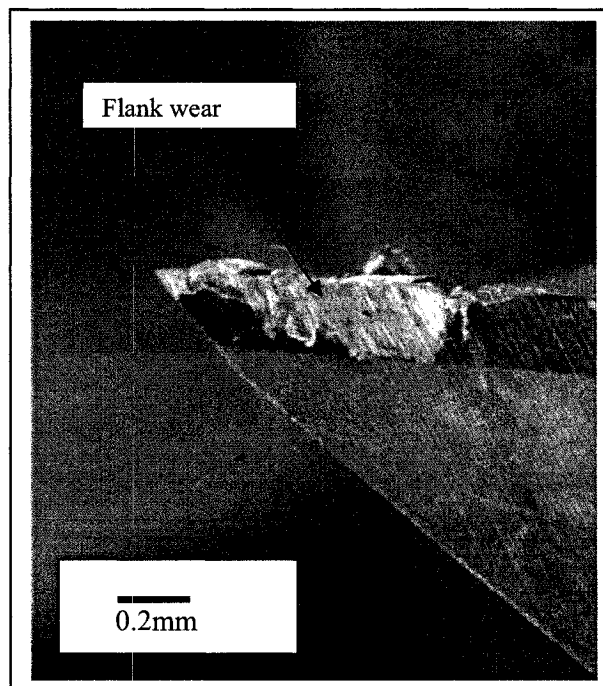


Figure 6.20: Wear surface, Cutting speed= 50 m/min (836 rpm), depth of cut = 1 mm , feed = 0.025 mm/tooth, stable cut

Chapter 6. Wear mechanisms under stable and unstable (chatter) conditions

Figure 6.21 shows the variation of flank wear at the cutting speed of 50 m/min under stable and unstable cut.

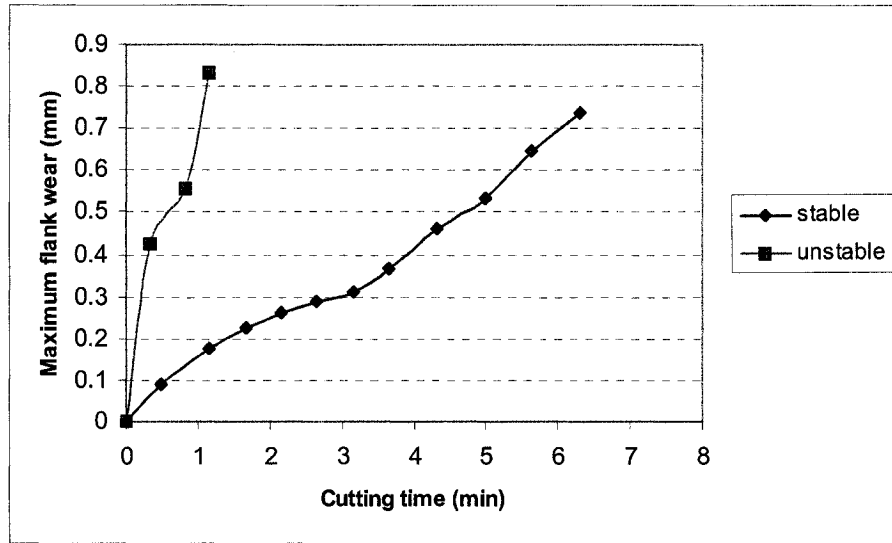


Figure 6.21: Maximum flank wear vs. Cutting time, cutting speed = 50 m/min (836rpm,) stable depth of cut = 1 mm, unstable depth of cut =2.2 mm feed= 0.025 mm/tooth

Figure 6.22 shows wear surface (end of tool life) for the cutting speed of 50 m/min and depth of cut of 2.2 mm under unstable cut.

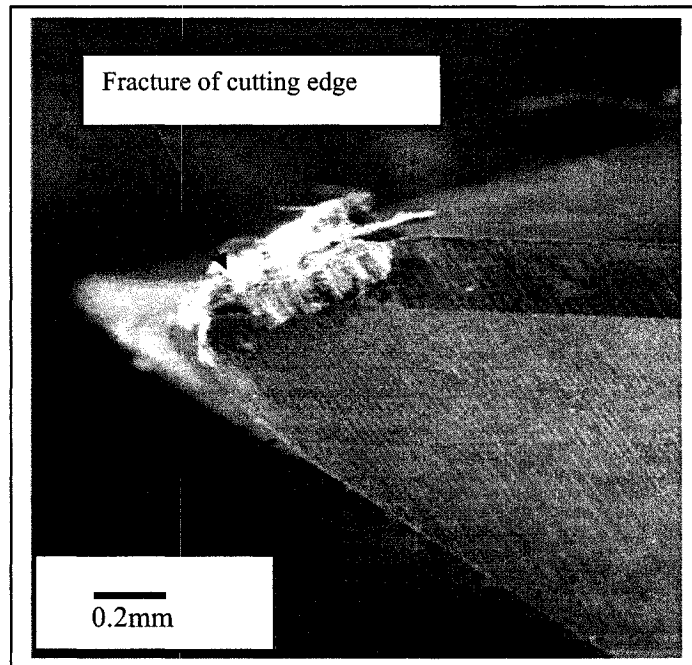


Figure 6.22: Wear surface, cutting speed= 50 m/min (836 rpm), depth of cut = 2.2 mm, feed = 0.025 mm/tooth, unstable(chatter)

Chapter 6. Wear mechanisms under stable and unstable (chatter) conditions

Figure 6.23 shows micrograph for the cutting speed of 50 m/min and depth of cut of 2.2 mm under unstable cut.

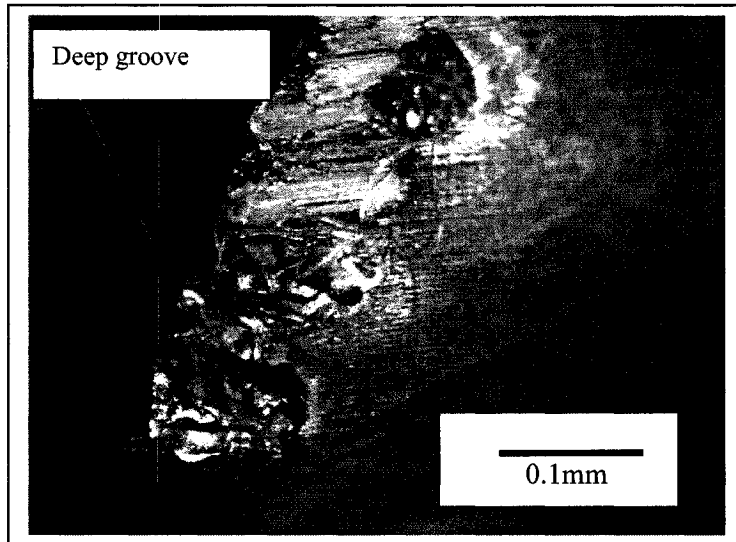


Figure 6.23: SMM micrograph of wear surface, cutting speed= 50 m/min (836 rpm), depth of cut = 2.2 mm, feed = 0.025 mm/tooth, unstable(chatter)

Figure 6.24 shows wear surface (end of tool life) for the cutting speed of 50 m/min and depth of cut of 2.5 mm under unstable cut.

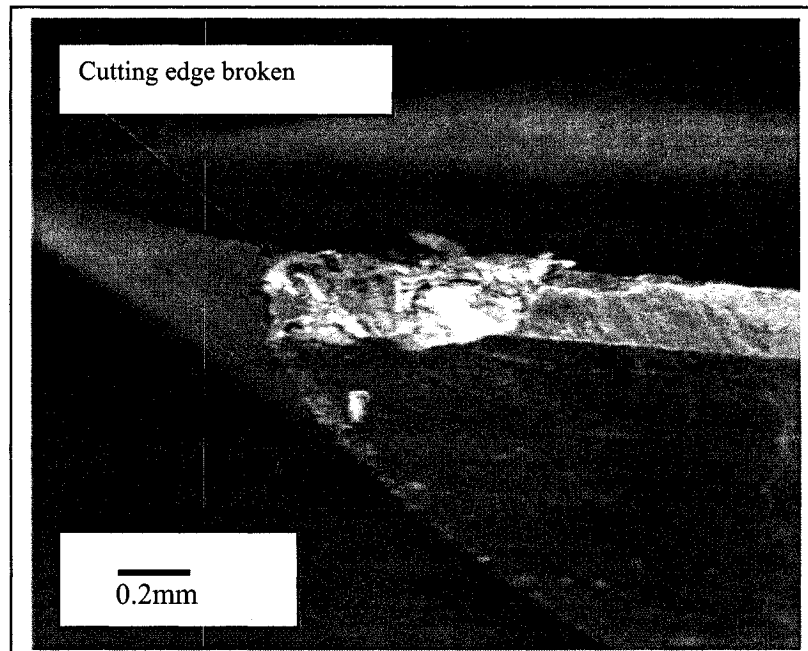


Figure 6.24: Wear surface, cutting speed= 50 m/min (836 rpm), depth of cut = 2.5 mm, feed = 0.025 mm/tooth, unstable(chatter)

Chapter 6. Wear mechanisms under stable and unstable (chatter) conditions

Figure 6.25 shows micrograph for the cutting speed of 50 m/min and depth of cut of 2.5 mm under unstable cut.

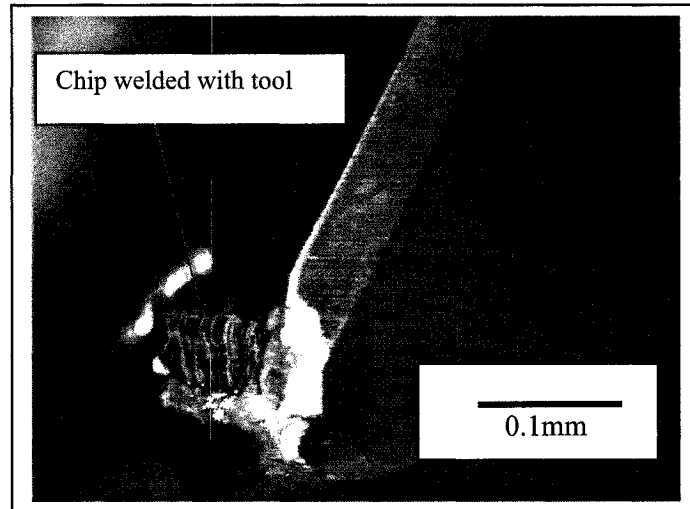


Figure 6.25: SMM micrograph of wear surface, cutting speed= 50 m/min (836 rpm), depth of cut = 2.5 mm, feed = 0.025 mm/tooth, unstable(chatter)

Further cutting speed at the level of 70 m/min (1170 rpm) and depth of cut from 0.7 mm to 1.2 mm were selected under stable conditions. Examination of the cutting edges (Figures 6.26 and 6.27) showed that carbide tools had steady wear progression at all depth of cuts under stable condition. From sound spectrum of microphone, it was observed that chatter did not occur during cutting process. Tool wear was found to be rapid (Figures 6.28 and 6.29) at depth of cut of 2.2mm under unstable cutting condition. This was mainly attributed to removal of coated layer from the carbide tools. So the wear resistance of the tool was significantly decreased leading to failure of the cutting tool by the presence of chatter.

Chapter 6. Wear mechanisms under stable and unstable (chatter) conditions

Figure 6.26 shows the variation of flank wear at the cutting speed of 70 m/min under stable cut.

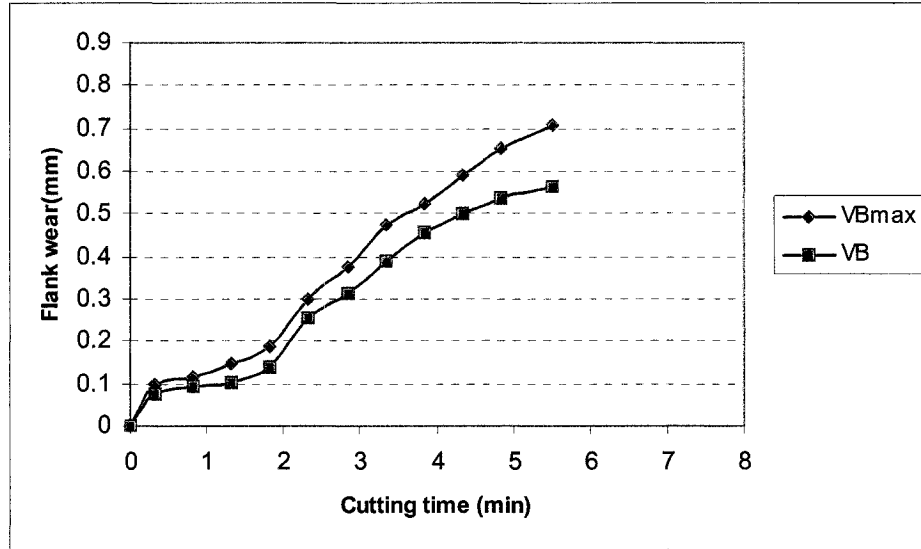


Figure 6.26: Flank wear vs. Cutting time, cutting speed = 70 m/min (1170 rpm,) depth of cut = 0.7 mm, feed= 0.025 mm/tooth, stable cut

Figure 6.27 shows wear surface (end of tool life) for the cutting speed of 70 m/min and depth of cut of 0.7 mm under stable cut.

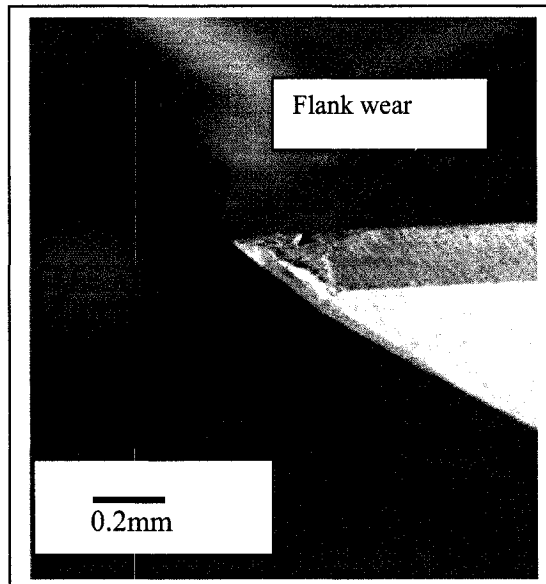


Figure 6.27: Wear surface, cutting speed= 70 m/min (1170 rpm), depth of cut = 0.7 mm , feed = 0.025 mm/tooth, stable cut

Chapter 6. Wear mechanisms under stable and unstable (chatter) conditions

Figure 6.28 shows the variation of flank wear at the cutting speed of 70 m/min under stable and unstable cut.

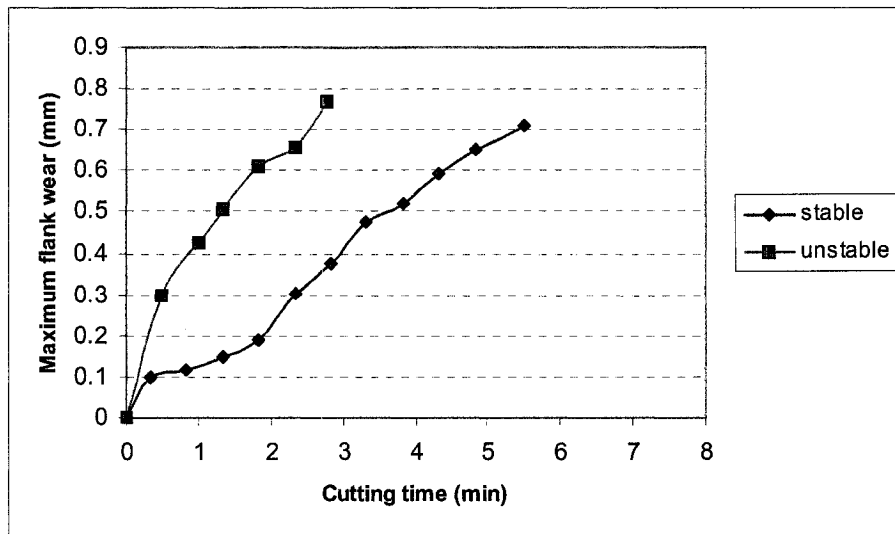


Figure 6.28: Maximum flank wear vs. Cutting time, cutting speed = 70 m/min (1170 rpm,) stable depth of cut = 0.7 mm, unstable depth of cut = 2.2 mm feed = 0.025 mm/tooth

Figure 6.29 shows wear surface (end of tool life) for the cutting speed of 70 m/min and depth of cut of 2.2 mm under unstable cut.

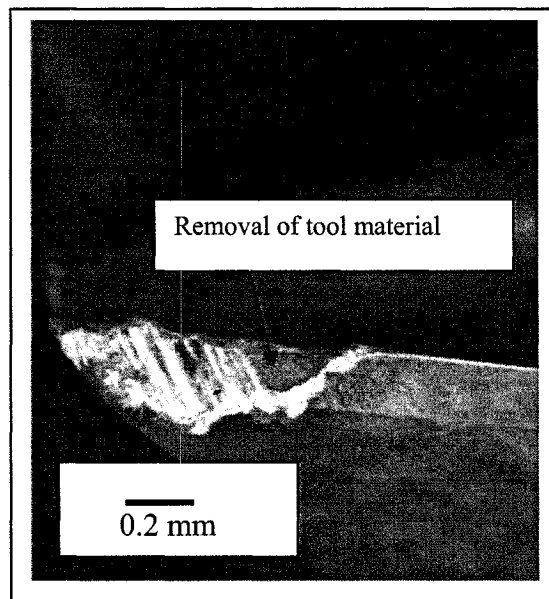


Figure 6.29: Wear surface, cutting speed = 70 m/min (1170 rpm), depth of cut = 2.2 mm, feed = 0.025 mm/tooth, unstable (chatter)

Chapter 6. Wear mechanisms under stable and unstable (chatter) conditions

Figure 6.30 shows the variation of flank wear at the cutting speed of 70 m/min under stable cut.

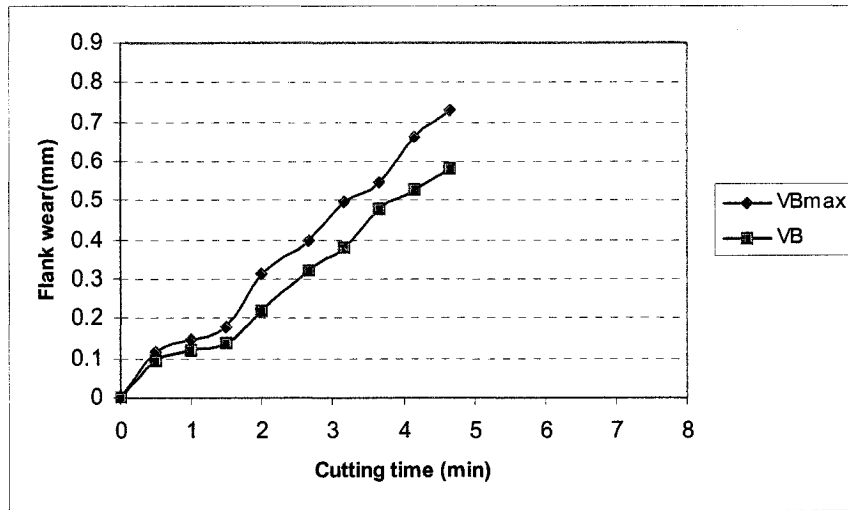


Figure 6.30: Flank wear vs. Cutting time, cutting speed = 70 m/min (1170 rpm,) depth of cut = 1.2 mm, feed= 0.025 mm/tooth, stable cut

Figure 6.31 shows wear surface (end of tool life) for the cutting speed of 70 m/min and depth of cut of 1.2 mm under stable cut.

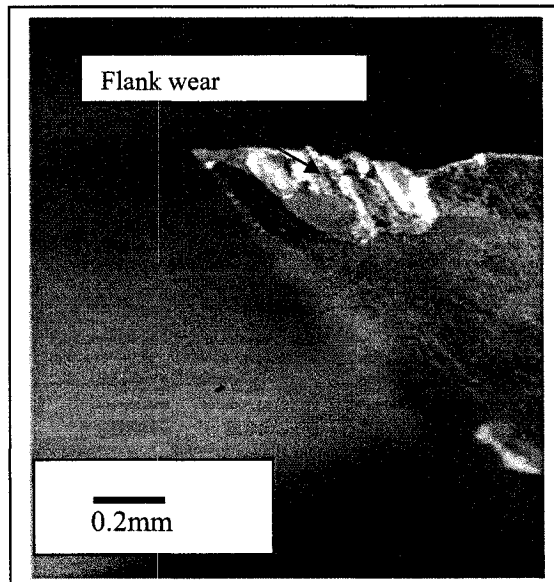


Figure 6.31: Wear surface, cutting speed= 70 m/min (1170 rpm), depth of cut = 1.2 mm , feed = 0.025 mm/tooth, stable cut

Chapter 6. Wear mechanisms under stable and unstable (chatter) conditions

Figure 6.32 shows the variation of flank wear at the cutting speed of 70 m/min under stable and unstable cut.

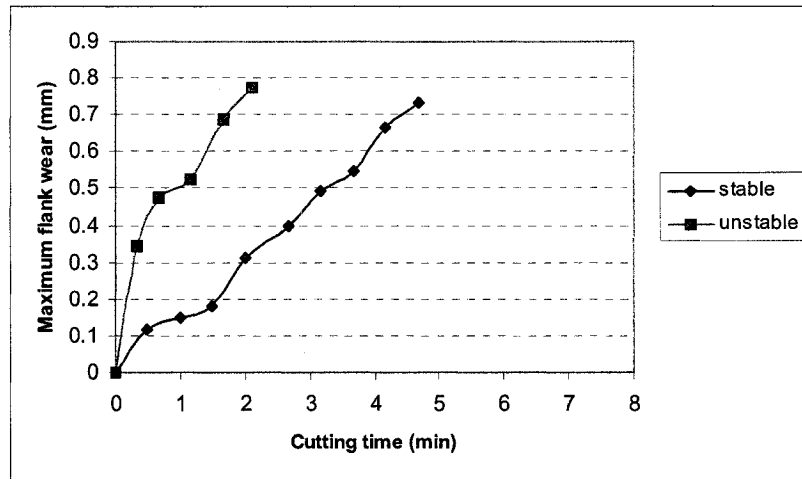


Figure 6.32: Maximum flank wear vs. Cutting time, cutting speed = 70 m/min (1170 rpm,) stable depth of cut = 1.2 mm, unstable depth of cut = 2.5 mm feed = 0.025 mm/tooth

Figure 6.33 shows wear surface (end of tool life) for the cutting speed of 70 m/min and depth of cut of 2.5 mm under unstable cut.

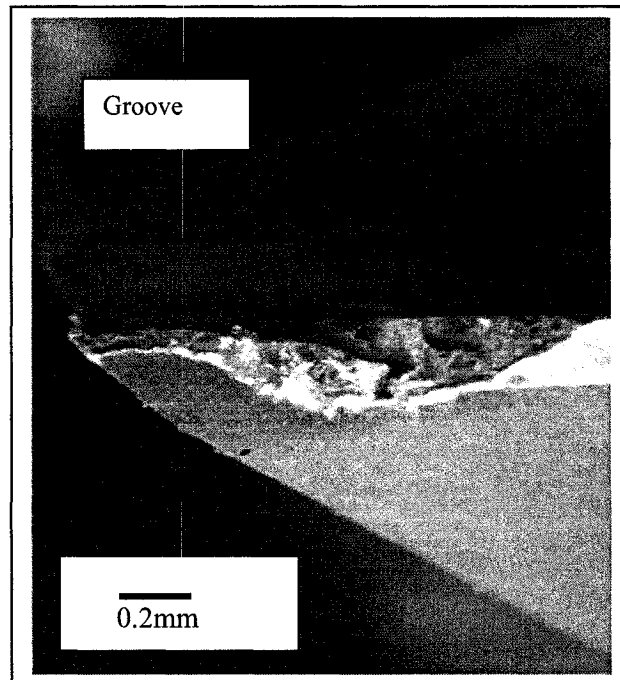


Figure 6.33: Wear surface, cutting speed = 70 m/min (1170 rpm), depth of cut = 2.5 mm, feed = 0.025 mm/tooth, unstable (chatter)

Chapter 6. Wear mechanisms under stable and unstable (chatter) conditions

Figure 6.34 shows micrograph for the cutting speed of 70 m/min and depth of cut of 2.5 mm under unstable cut.

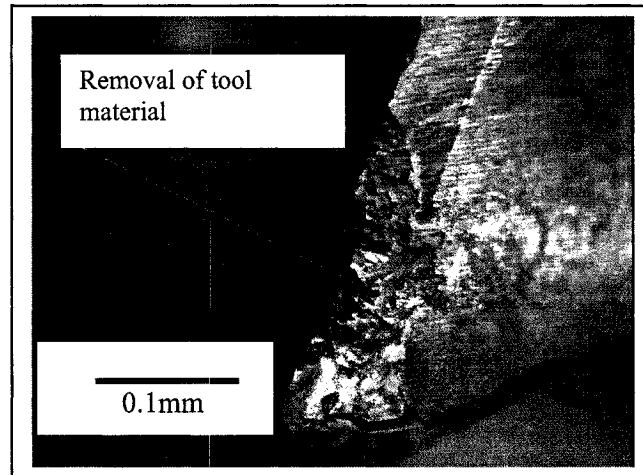


Figure 6.34: SMM micrograph of wear surface, cutting speed= 70 m/min (1170 rpm), depth of cut = 2.5 mm, feed = 0.025 mm/tooth, unstable(chatter)

Figure 6.35 shows wear surface (end of tool life) for the cutting speed of 70 m/min and depth of cut of 2.8 mm under unstable cut.

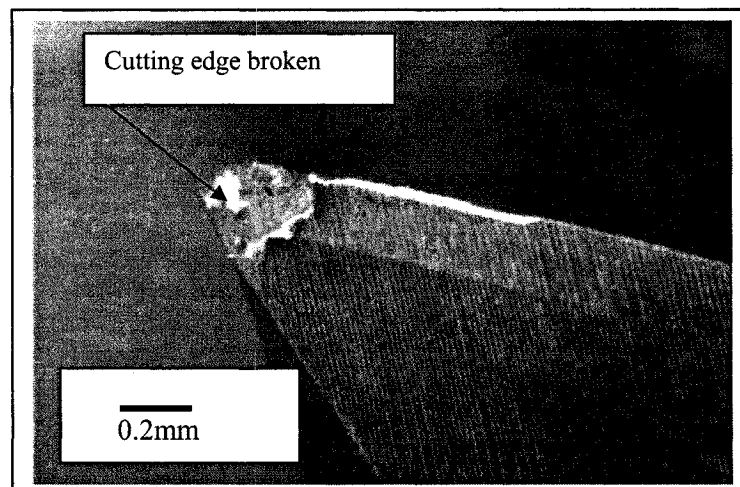


Figure 6.35: Wear surface, cutting speed= 70 m/min (1170 rpm), depth of cut = 2.8 mm, feed = 0.05 mm/tooth, unstable(chatter)

Chapter 6. Wear mechanisms under stable and unstable (chatter) conditions

Figure 6.36 shows micrograph for the cutting speed of 70 m/min and depth of cut of 2.8 mm under unstable cut.

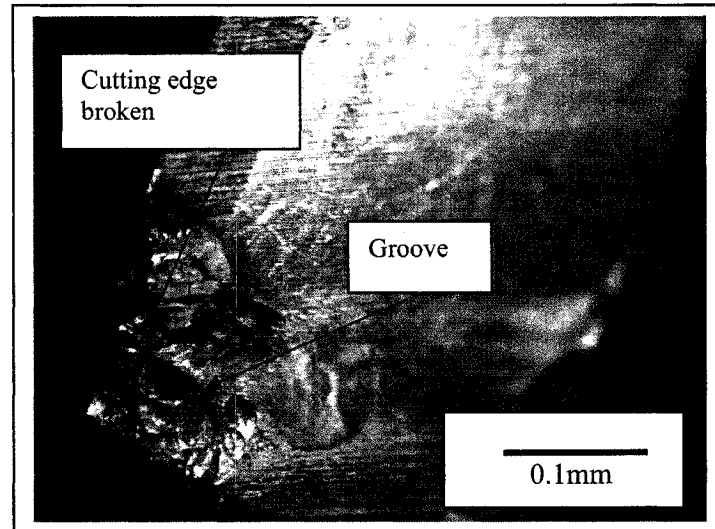


Figure 6.36: SMM micrograph of wear surface, cutting speed= 70 m/min (1170 rpm), depth of cut = 2.8 mm, feed = 0.05 mm/tooth, unstable(chatter)

Again cutting tests were performed at cutting speed of 90 m/min (1505 rpm) under stable and unstable conditions. Figures 6.37 and 6.38 showed that no cutting edge fracture was observed under stable condition. On the other hand, excessive flank wear (Figures 6.39 and 6.40) was the dominant failure mode at depth of cut of 3.3 mm (unstable condition). It could be due to a combination of high temperature, thermal and mechanical shock/stress, as well as the adhesion of the work material on the tool face. Figure 6.41 shows micrograph for the cutting speed 90 m/min and depth of cut 3.3 mm under unstable cut. The micrograph shows the presence of deep grooves on the wear surface for unstable cutting condition, suggesting that mainly abrasive, adhesion and some diffusion mechanisms were operative during machining operation. The deeper grooves also indicated that abrasive mechanism was the highest among others.

Chapter 6. Wear mechanisms under stable and unstable (chatter) conditions

Figure 6.37 shows the variation of flank wear at the cutting speed of 90 m/min under stable cut.

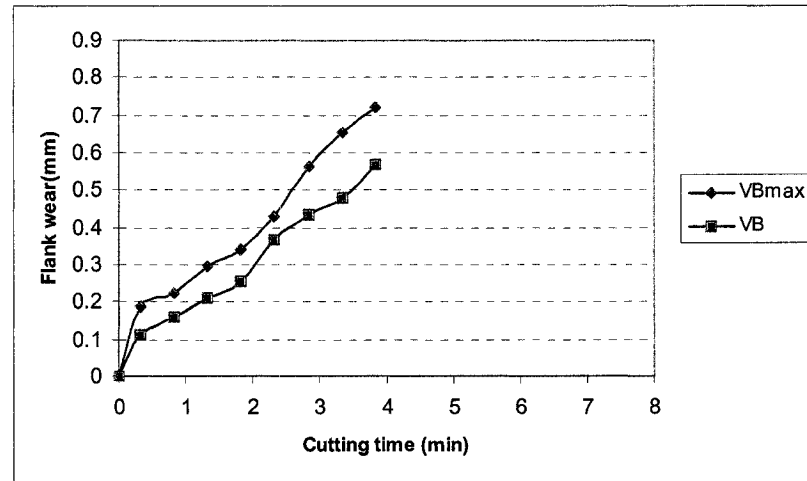


Figure 6.37: Flank wear vs. Cutting time, cutting speed = 90 m/min (1505 rpm,) depth of cut = 1.4 mm, feed= 0.025 mm/tooth, stable cut

Figure 6.38 shows wear surface (end of tool life) for the cutting speed of 90 m/min and depth of cut of 1.4 mm under stable cut

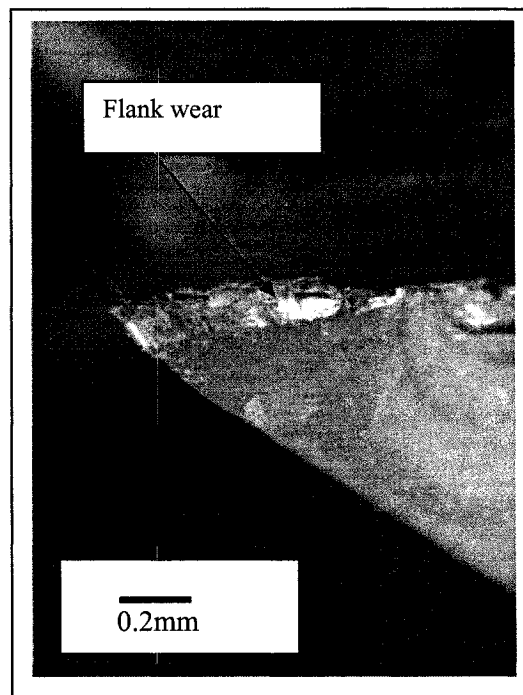


Figure 6.38: Wear surface, cutting speed= 90 m/min (1505 rpm), depth of cut = 1.4 mm, feed = 0.025 mm/tooth, stable cut

Chapter 6. Wear mechanisms under stable and unstable (chatter) conditions

Figure 6.39 shows the variation of flank wear at the cutting speed of 90 m/min under stable and unstable cut.

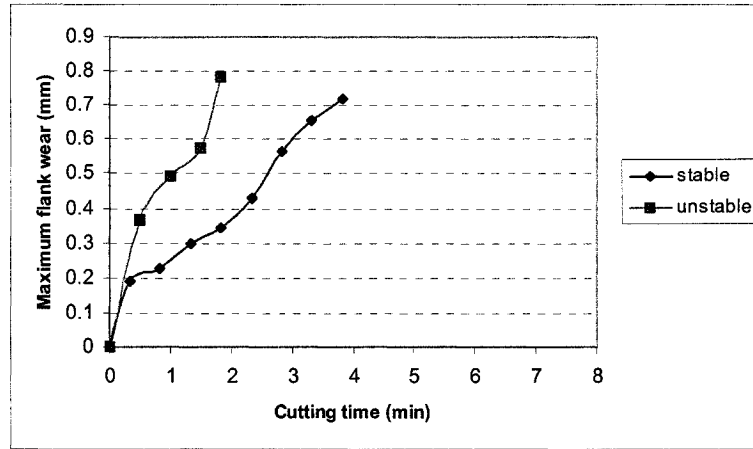


Figure 6.39: Maximum flank wear vs. Cutting time, cutting speed = 90 m/min (1505 rpm,) stable depth of cut = 1.4 mm, unstable depth of cut = 3.3 mm feed = 0.025 mm/tooth

Figure 6.40 shows wear surface (end of tool life) for the cutting speed of 90 m/min and depth of cut of 3.3 mm under unstable cut.

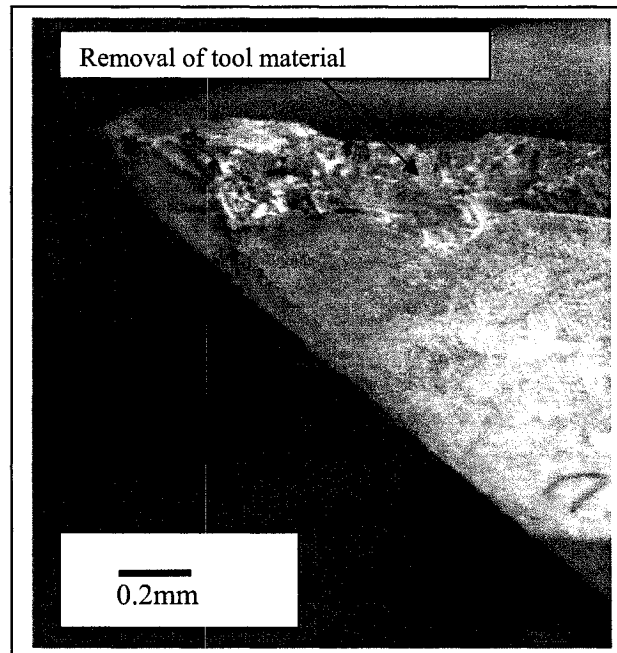


Figure 6.40: Wear surface, cutting speed = 90 m/min (1505 rpm), depth of cut = 3.3 mm, feed = 0.025 mm/tooth, unstable (chatter)

Chapter 6. Wear mechanisms under stable and unstable (chatter) conditions

Figure 6.41 shows micrograph for the cutting speed of 90 m/min and depth of cut of 3.3 mm under unstable cut.

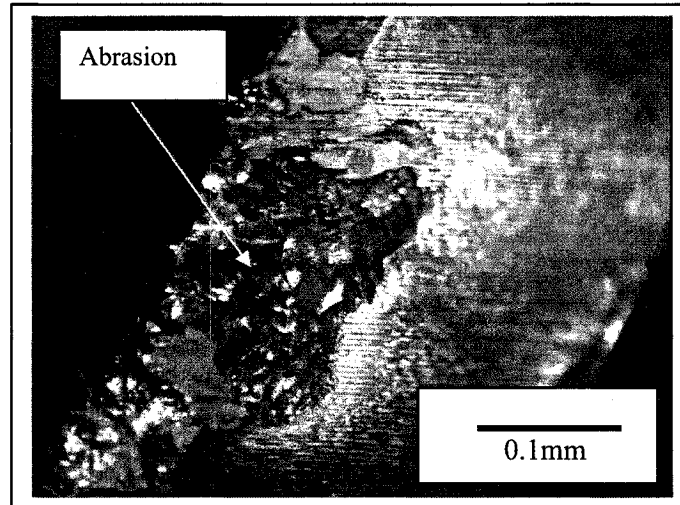


Figure 6.41: SMM micrograph of wear surface, cutting speed= 90 m/min (1505 rpm), depth of cut = 3.3 mm, feed = 0.025 mm/tooth, unstable(chatter)

Figure 6.42 shows the variation of flank wear at the cutting speed of 90 m/min under stable cut.

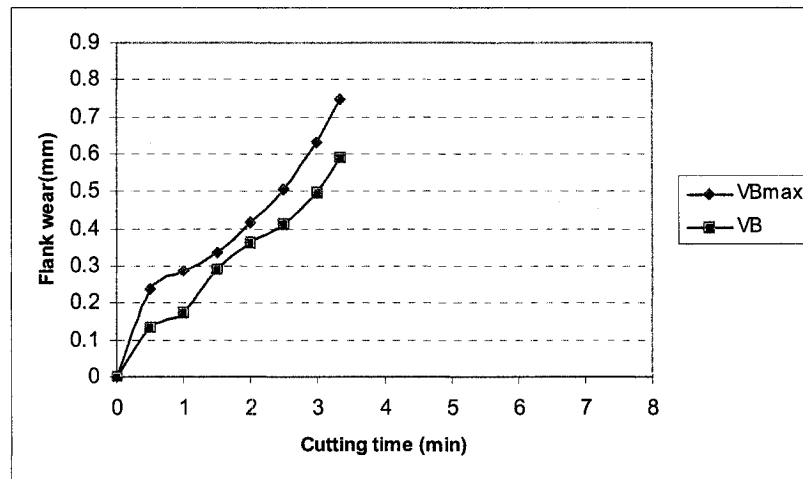


Figure 6.42: Flank wear vs. Cutting time, cutting speed = 90 m/min (1505 rpm,) depth of cut = 1.6 mm, feed= 0.025 mm/tooth, stable cut

Chapter 6. Wear mechanisms under stable and unstable (chatter) conditions

Figure 6.43 shows wear surface (end of tool life) for the cutting speed of 90 m/min and depth of cut of 1.6mm under stable cut.

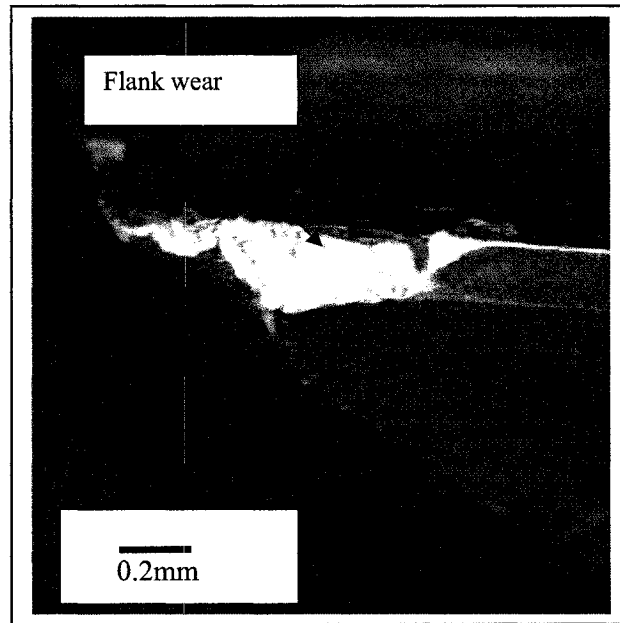


Figure 6.43: Wear surface, cutting speed= 90 m/min (1505 rpm), depth of cut = 1.6 mm , feed = 0.025 mm/tooth, stable cut

Figure 6.44 shows the variation of flank wear at the cutting speed of 90 m/min under stable cut.

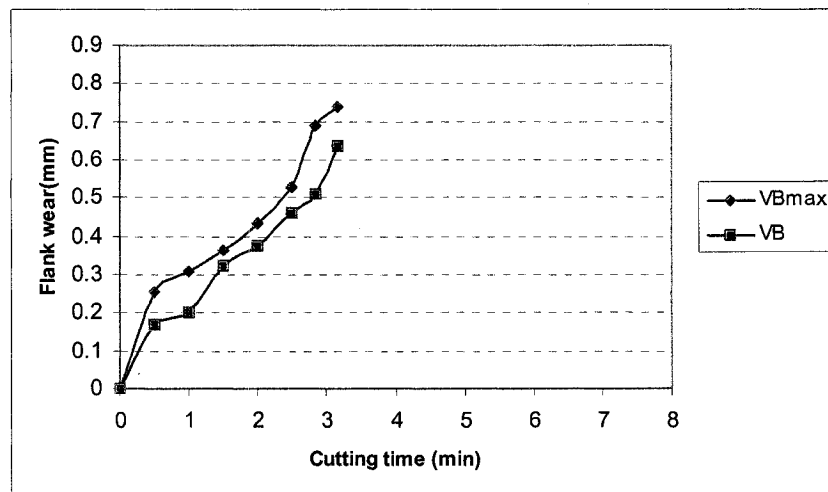


Figure 6.44: Flank wear vs. Cutting time, cutting speed = 90 m/min (1505 rpm,) depth of cut = 1.8 mm, feed= 0.025 mm/tooth, stable cut

Chapter 6. Wear mechanisms under stable and unstable (chatter) conditions

Figure 6.45 shows wear surface (end of tool life) for the cutting speed of 90 m/min and depth of cut of 1.8 mm under stable cut.

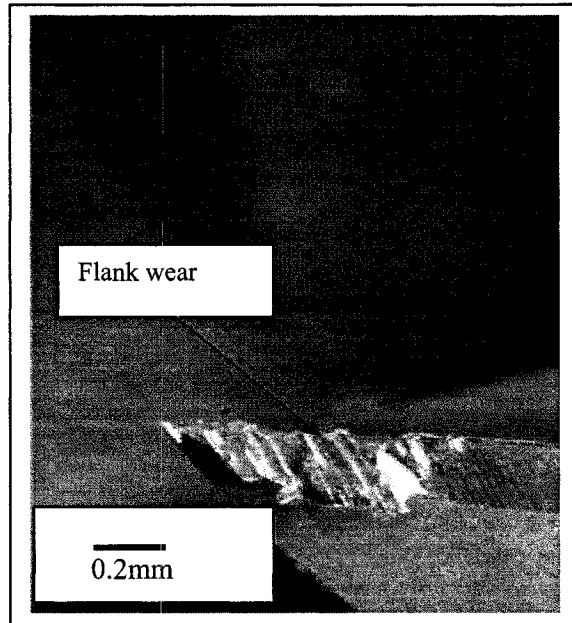


Figure 6.45: Wear, cutting speed= 90 m/min (1505 rpm), depth of cut = 1.8 mm, feed = 0.05 mm/tooth, stable cut

6.5 Discussion

Chatter vibration occurs during machining operation due to improper selection of cutting conditions (cutting speed, feed and depth of cut). Chatter vibration accelerates tool wear and causes more frequent tool breakage and premature wear of the spindle, locators and machine bearings. Due to the detrimental effects of chatter to both product and the manufacturing process, it is necessary to establish stability lobes in order to select proper cutting conditions. This chapter presents stability lobes and wear mechanisms under stable and unstable cutting conditions. Stability lobes were established for nickel based superalloys. It was found that the minimum stable depth of cut was 1 mm. So

Chapter 6. Wear mechanisms under stable and unstable (chatter) conditions

chatter will not occur under this depth of cut at any spindle speed. In order to verify the stability lobes, different depths of cuts and cutting speeds were selected. Cutting tests were conducted by monitoring sound spectra of a microphone. It was observed that all cutting conditions selected from stability lobes conformed with experimental results. From the stability lobes, proper cutting conditions can be selected for chatter-free machining operation. On the other hand, chatter vibration is believed to be one of the factors that accelerate different wear mechanisms. Wear mechanisms were analyzed using a scanning metallographic microscope. The progression of tool wear was found to be slow at all cutting speeds (50 m/min, 70 m/min and 90 m/min) under stable condition. This may be related to the absence of chatter vibration during the machining operation. It was observed from the micrograph images that with the increase in depth of cut (unstable condition) wear occurred towards the cutting edge and resulted in breakage of the cutting edge at the cutting speed of 50 m/min. The main reason for this kind of wear behaviour appears to be the localized tensile stresses imposed on the tool by interrupted chip flow during unstable cutting. The stresses were imposed by the chip detachment during the tool exit and by the sudden ejection of the adhered chip on the entry of cutting tool. Flank wear and a broken cutting edge were the causes of failure at the cutting speed of 50 m/min under an unstable condition. It was observed that wear formation results from a combination of many factors and not necessarily from a single wear mechanism under unstable condition. The major wear mechanisms were abrasion and adhesion. Built up edge was a major problem at low cutting speed (50 m/min) under an unstable condition. On the other hand, built up edge was not observed at cutting speeds of 70 m/min and 90

Chapter 6. Wear mechanisms under stable and unstable (chatter) conditions

m/min under unstable condition. The wear pattern of TiAlN coated end mills at cutting speeds of 70 m/min and 90 m/min were completely different from the cutting speed of 50 m/min. It was interesting to note that the flank wear value was highest at a low cutting speed (50 m/min) and was lowest at high cutting speeds (70 m/min and 90 m/min) under an unstable condition. From the point of view of acceleration of wear, a cutting speed of 50 m/min should be avoided in case of unstable cutting operation. Wear developed more on the flank face than on the rake face particularly at cutting speeds of 70 m/min to 90 m/min for all depths of cut (0.7 mm to 3.3 mm). Excessive flank wear occurred at a high cutting speed (90 m/min) under an unstable condition. This could be due to the removal of the TiAlN layer from the cutting edge under such an unstable condition. Non uniform flank wear was found at the end of each test under unstable cutting condition. It was observed that the diffusion mechanism tends to limit tool performance at a cutting speed of 90 m/min under an unstable condition. Tool failure caused by flank wear may partly be attributed to the diffusion wear mechanism that occurred by a process of chemical dissolution of the tool material and the presence of nickel particles in Inconel 718. The abrasion wear mechanism was also observed when machining nickel based superalloys with carbide tools. The coated layer from the tool substrate, and hard abrasive particles contained in the nickel based superalloys were mainly responsible for the abrasion mechanism which accelerates flank wear under an unstable condition. This research work will help manufacturing industries to determine wear mechanisms and selection of proper cutting conditions for nickel based superalloys machining operation.

CHAPTER 7

Milling process

Tool wear and surface roughness are the most commonly used criteria for assessing machinability of material. However, other components of machining criteria such as cutting conditions and chip thickness are also used for assessing machinability of material. Insperger *et al* [2003] discussed the importance of cutting parameters in milling operation. They did not mention the effect of feed rates in milling operation. In early studies, some analytical expressions [Astakhov and Shuvet, 1997] for machining process were developed. Their models can not provide chip thickness in milling operation. For this reason, we discussed the effect of chip thickness in milling operation.

7.1 Effect of cutting parameters on milling process

We presented a mathematical model in order to compare between up milling and down milling process. In milling, surfaces can be generated by two distinctly different methods. Up milling is the traditional way to mill called conventional milling; the cutter rotates against the direction of feed of the workpiece. In down milling the rotation is in the same direction as the feed. The method of chip formation is completely different in the two cases. In up milling the chip is very thin at the beginning where the tooth first contacts the workpiece and increases in thickness becoming a maximum, where the tooth leaves the workpiece. In down milling maximum chip thickness occurs close to the point at which the tooth contacts the workpiece. Alauddin *et al* [1998] stated that when milling of Inconel 718, tool wear decreased in down milling. Ng *et al* [2000] reported that down milling generated the longest tool life. In up milling as shown in Figure 8.1 the cutter rotates with velocity " n " and the minimum chip thickness is at a point "A" where the tooth comes in contact with the workpiece and the maximum at point "N" where the tooth leaves the workpiece.

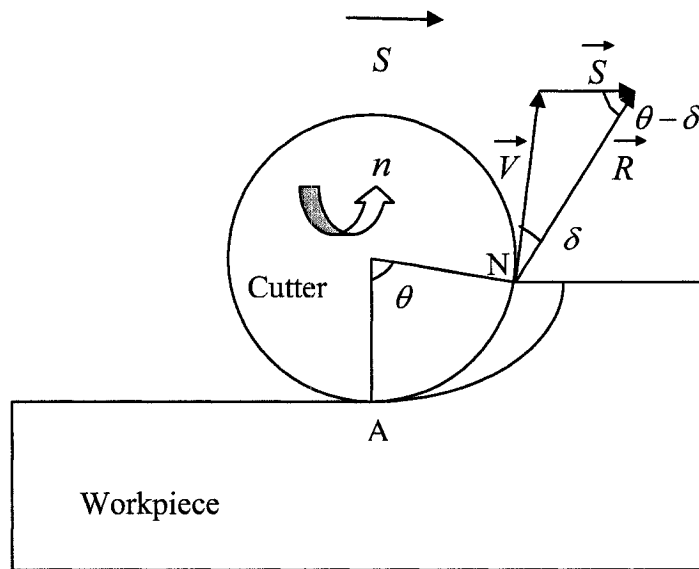


Figure 7.1: Up milling

The following relation can be written from the cutting speed diagram (Figure 7.1), where change of angle " δ " is unknown.

$$\frac{V}{\sin(\theta - \delta)} = \frac{S}{\sin \delta} \quad (7.1)$$

The change of angle " δ " can be expressed by equation (7.2), where " θ " is contact angle.

$$\delta = \tan^{-1} \left(\frac{\sin \theta}{\frac{V}{S} + \cos \theta} \right) \quad (7.2)$$

The relationship between resultant cutting speed " R " and cutting speed " V " can be expressed as follows:

$$\frac{R}{\sin(180 - \theta)} = \frac{V}{\sin(\theta - \delta)} \quad (7.3)$$

The resultant cutting speed " R " can be expressed as follows:

$$R = \frac{V \sin(180 - \theta)}{\sin(\theta - \delta)} \quad (7.4)$$

In down milling as shown in Figure 7.2 the cutter rotates with velocity " n " and the maximum thickness is at a point "B" where the tooth comes in contact with the workpiece and the minimum thickness at the point "M" where the tooth leaves the workpiece.

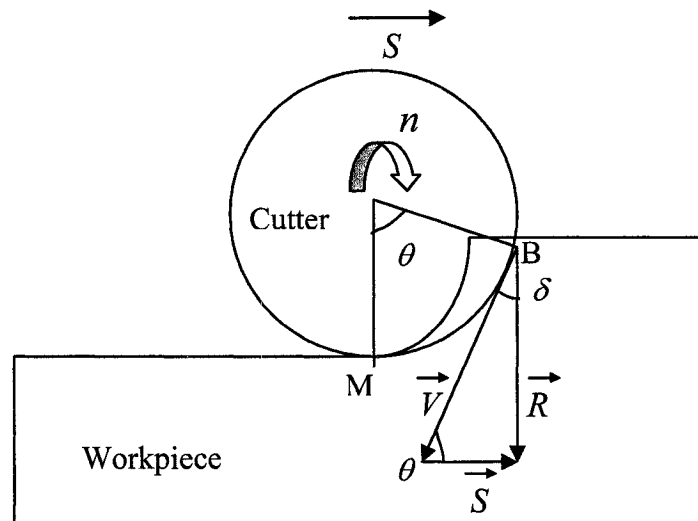


Figure 7.2: Down milling

The relationship between cutting speed " V " and feed " S " can be expressed as follows:

$$\frac{V}{\sin(180 - \theta - \delta)} = \frac{S}{\sin \delta} \quad (7.5)$$

The change of angle " δ " can be expressed by equation (7.6), where " θ " is contact angle.

$$\delta = \tan^{-1} \left(\frac{\sin \theta}{\frac{V}{S} - \cos \theta} \right) \quad (7.6)$$

The relationship between resultant cutting speed " R " and cutting speed " V " can be expressed as follows:

$$\frac{R}{\sin \theta} = \frac{V}{\sin(180 - \theta - \delta)} \quad (7.7)$$

The resultant cutting speed " R " can be expressed as follows:

$$R = \frac{V \sin \theta}{\sin(180 - \theta - \delta)} \quad (7.8)$$

These established mathematical equations for resultant cutting speed " R " are shown in equation (7.4) for up milling and equation (7.8) for down milling process. We calculated resultant cutting speed " R " at cutting speed of 1500 m/min and feed of 2 mm/tooth for half immersion milling operation. The variation is shown from 5° contact angle because cutter does not cut the workpiece at 0° contact angle.

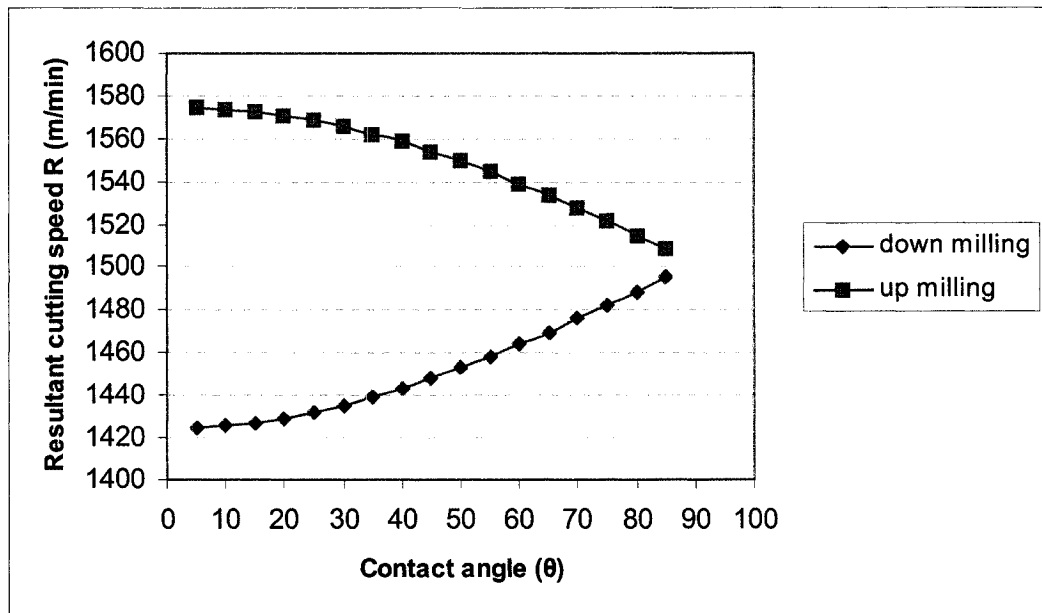


Figure 7.3: Resultant cutting speed (R) vs. Contact angle (θ) (cutting speed = 1500 m/min, feed = 2 mm/tooth)

Figure 7.3 shows that resultant cutting speed " R " is higher in up milling than down milling at feed of 2 mm/tooth and cutting speed of 1500 m/min. The method of milling here described as down milling is compared with up milling on the basis of cutting parameters such as resultant cutting speed " R " and feed " S ". It was observed that resultant cutting speed " R " was higher in up milling than down milling. Therefore the cutting condition is more favorable in down milling than in up milling process. Insperger *et al* [2003] investigated the effect of stability condition primarily between up and down milling orientations. Their experimental results showed that different stability behaviour occurred for up milling and down milling at the same cutting conditions.

7.2 Analytical prediction of uncut chip thickness

The chip thickness influences the machining accuracy and tool life. Therefore it is important to understand the formation of uncut chip thickness during machining operation. We established an analytical model to predict uncut chip thickness in milling operation. The early research in machining mechanics dealt with the chip formation mechanism in turning operation. Astakhov and Shuvet [1997] showed that chip thickness was constant in turning operation. Due to the nature of relative contact between the workpiece and the tool, the chip thickness is not constant in milling operation but starts with a zero thickness and increases in up milling and starts with finite thickness and decreases to zero in down milling. Friction between the tool and the chip in metal cutting influences built-up edge (BUE) formation and tool wear. The formation of a built-up edge on the tool leads to adhesion between the chip and tool.

Chips are generally hot when they emerge from the cutting zone. If they collect on the machine tool or within the machined part, they can produce thermal distortions which will lead to dimensional errors in the machined part. This mechanism can be a source of significant error in precision machining processes. The uncut chip thickness (t_c) is a fundamental variable of the cutting process, which can be altered by a number of practical variables such as radius of cutter (R), width of cutter (w) and feed per tooth (f_t). The chip thickness can be found from Figure 7.4, where " f_t " is the feed per tooth, " R " is the radius of cutter and " w " is the width of cut.

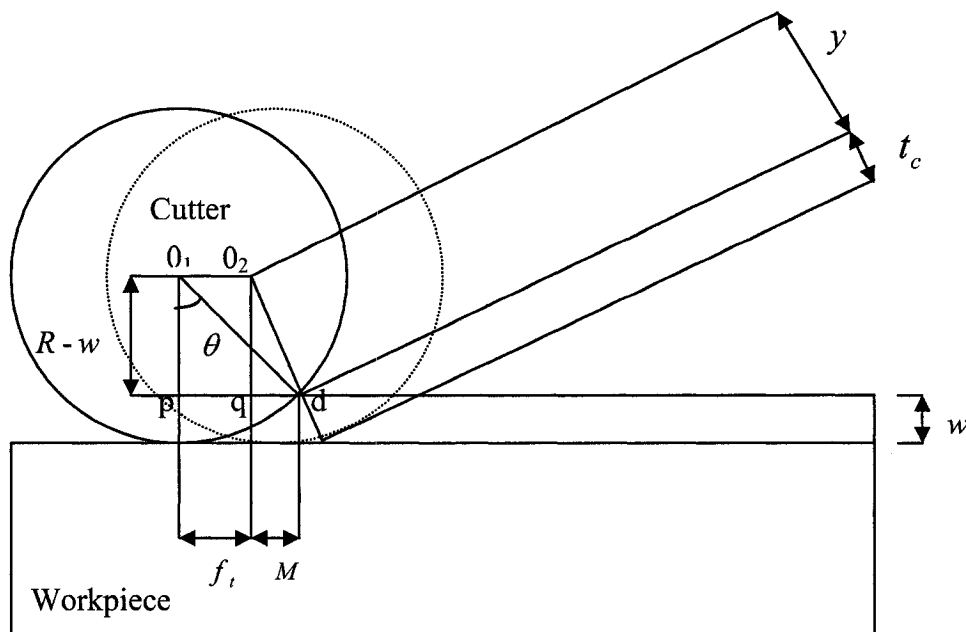


Figure 7.4: Chip thickness in milling operation

The following relations can be written from triangles ΔO_2qd and ΔO_1pd (Figure 7.4),

$$y = \sqrt{(R - w)^2 + M^2} \quad (7.9)$$

Where "M" is

$$M = \sqrt{R^2 - (R - w)^2} - f_t \quad (7.10)$$

Putting the value of "M" in equation (7.9), the followings can be found,

$$y = \sqrt{(R - w)^2 + \left\{ \sqrt{R^2 - (R - w)^2} - f_t \right\}^2} \quad (7.11)$$

Equation (7.11) can be reorganized as follows:

$$y = \sqrt{R^2 - 2f_t \sqrt{2Rw - w^2} + f_t^2} \quad (7.12)$$

Finally, the uncut chip thickness (t_c) can be expressed as follows:

$$t_c = R - \sqrt{R^2 - 2f_t \sqrt{2Rw - w^2} + f_t^2} \quad (7.13)$$

Where "R" is the radius of the cutter, " f_t " is the feed per tooth and "w" is the width of cut. Figure 7.4 shows that the thickness variation of the cut for a circular tooth path. We assumed circular tooth path, which means that the workpiece is stationary during a tooth engagement and then moves suddenly by feed per tooth (f_t) before the next tooth starts a cut. The uncut chip thickness is defined by " t_c " can be determined by equation (7.13). Therefore the purpose of the chip thickness determination is to provide a physical picture of chip formation during milling operation.

7.3 Discussion

A mathematical model for change of resultant cutting speed with the change of contact angle of the cutting tooth with the workpiece was established. It was found that the resultant cutting speed was higher in up milling than in down milling. Considering the effect of cutting parameters (resultant cutting speed and chip load), the cutting condition is more favorable in down milling than that for up milling process. Insperger *et al* [2003] investigated the stability condition between up milling and down milling process and came to similar conclusions. In turning operation, the primary deformation zone is a narrow zone in which large strains are imparted to the chip. It indicates that the curvature of the chip results directly from the primary deformation zone. On the other hand, milling operation is a metal removal process using a cutting tool with one or more teeth rotating about a fixed axis. Milling is therefore an intermittent cutting process, each tooth producing a chip of variable thickness. An analytical model for uncut chip thickness was established. It can be found that the uncut chip thickness is dependent on the feed per tooth, cutter radius and width of cut.

CHAPTER 8

Summary, conclusions and suggested future work

This thesis has explored the potential for milling nickel based superalloys using carbide and ceramic tools. In this chapter, the summary, conclusions and future work are presented.

8.1 Summary

Nickel based superalloys have been widely used in the aerospace and nuclear industries due to their exceptional thermal resistance and its ability to retain mechanical properties at high temperatures. However, tool wear is a key issue in nickel based superalloys machining operations because of the detrimental effect that a worn tool has on the surface finish of the machined component. Therefore, it was necessary to predict tool life with sufficient accuracy on the basis of controllable process parameters since it is an essential part of any machining system to change a worn or damaged cutting tool at the right time.

There are several factors that cause tool deterioration of which two are wear mechanisms and cutting conditions. Just as a properly selected cutting tool produces good quality machined parts and lasts longer, so an improperly selected cutting tool wears faster and produces parts of deteriorating surface quality. Therefore tool wear and surface roughness are important parameters during a nickel based superalloys machining operation. Cutting fluid or coolant has a considerable influence on tool wear and surface finish because it reduces friction during machining with corresponding reduction in generated heat. Interest in ceramics as a high speed cutting tool material was based primarily on its favorable material properties including hardness. Ceramics generally remain unaffected at a high temperature, which means that the cutting tool tip is relatively unaffected at high cutting speeds. Analysis of wear and surface roughness for ceramic tools were undertaken in this thesis in order to have a clear understanding of mechanisms that affect the performance of ceramic cutting tools. It is also clear that the temperature developed during machining plays an important role in controlling tool life and wear mechanisms. The presence of high temperatures during machining increases the rate of chemical interaction between the workpiece and tool. Therefore, energy dispersive X-ray (EDX) analysis was conducted in order to investigate the intensity of the interactions between elements of the work piece and the ceramic cutting tool. Chatter vibration occurs because of the dynamic interaction between the workpiece and the cutting tool and causes unstable cutting, poor surface quality and high tool wear. For this reason, stability lobes were established in order to identify a stable cutting condition for nickel based superalloys. Wear mechanisms were also determined under stable and unstable (chatter) conditions. Therefore, this study helps to explain the wear behavior in metal (Inconel 718) cutting and serves as a starting point for a better understanding and prediction of the

effects of flank wear, surface roughness, coolant, chatter vibration and wear mechanisms under different cutting conditions.

8.2 Conclusions

Based on the detailed discussion of results presented in the previous chapters, the following conclusions are made:

- Coolant had a significant influence on tool wear and surface finish during machining of nickel based super-alloys with carbide tools. Tool life was longer in wet (coolant) cutting operation and the surface finish produced was better than that in dry cutting. Also, the severity of damage on the machined surface, in terms of cracks and total area affected, was less when coolant was applied. For this reason, coolant should always be used when machining nickel based superalloys with carbide tools.
- TiAlN coated carbide tools performed better than uncoated tools and should be used when machining Inconel 718. Indeed, when using uncoated tools, catastrophic and instantaneous failures actually occurred, especially when the cutting speed was increased.
- Different types of carbide tools were examined using a scanning metallographic microscope from which it was seen that adhesion and abrasion wear mechanisms occurred.
- Whisker reinforced and Kyon 2100 ceramic tools can be used in milling nickel based superalloys at high cutting speeds during which both showed not only superior wear resistance but also superior fracture resistance.

- This thesis has demonstrated that increasing the cutting speed actually reduces the rate and amount of tool wear when machining Inconel 718 with ceramic tools.
- The results of the microanalysis using the scanning metallographic microscope indicate that different wear mechanisms occurred for ceramic tools under various cutting conditions. The adhesion between workpiece material and ceramic layers were confirmed through energy dispersive X-ray (EDX) analysis. Micro chipping also occurred at high feed rates when machining nickel based superalloys with ceramic tools. Selection of proper cutting conditions may be effective in reducing many types of wear mechanisms.
- For ceramic tools, cutting parameters produced different effects on surface roughness values. The machined surface produced at low speed and high feed rate was full of short grooves whereas the quality of the machined surface was better at high cutting speeds. Therefore, cutting parameters (speed and feed rate) should be chosen properly in order to obtain a good surface finish.
- Stability lobes were established for nickel based superalloys and can be used to determine stable cutting condition when machining nickel based super-alloys. Chatter, however, is one of the major limitations in machining nickel based superalloys, resulting in tool breakage and poor surface quality. Therefore wear mechanisms were determined in order to identify the progression of tool wear or failure under both stable and unstable (chatter) conditions.
- A mathematical model for the milling process was established. When considering the effect of resultant cutting speed, the cutting condition is more favorable in

down-milling than in up-milling. An analytical model for chip thickness will also provide a better understanding of chip formation mechanisms during the milling process.

8.3 Suggested future work

We would like to make the following recommendations for future work:

- We conducted experiments during dry and wet cutting operations using carbide tools. Few research works have been conducted in order to determine the effect of the MQL (Minimal quantity lubrication) system which has a great influence on tool wear, surface roughness and chip formation during the machining operation. Therefore, an attempt can be made for further study to compare MQL, dry cutting and wet cutting (coolant) based on surface finish, tool wear and chip formation under different cutting conditions.
- Experiments were conducted for nickel based super-alloys with ceramic tools during high speed machining operation. PCBN (Polycrystalline cubic boron nitride) tools can be used for nickel based super-alloys in high speed milling operations. Therefore, a detailed study of wear and surface roughness should be performed using PCBN cutting tools.
- We investigated the wear mechanism for carbide and ceramic tools for nickel based material machining. Therefore, wear mechanisms for PCBN cutting tools should be investigated in order to determine the effect of mechanisms under different cutting conditions.

REFERENCES

- [1] I. T. Alzaharnah, "Suppressing vibrations of machining processes in both feed and radial directions using an optimal control strategy in the case of interrupted cutting", *Journal of Materials Processing Technology*, Vol. 172, pp. 305-310, 2006.
- [2] A. C. Araujo, J. L. Silveira, M. B. Jun, S. G. Kapoor and R. Devor, "A model for thread milling cutting forces", *International Journal of Machine Tools and Manufacture*, Vol. 46, pp. 2057-2065, 2006.
- [3] A. Albrecht, S. S. Park, Y. Altintas and G. Pritschow, "High frequency bandwidth cutting force measurement in milling using capacitance displacement sensors", *International Journal of Machine Tools and Manufacture*, Vol. 45, pp. 993-1008, 2005.
- [4] T. Akasawa, H. Sakurai, M. Nakamura, T. Tanaka and K. Takano, "Effects of free-cutting additives on the machinability of austenite stainless steel", *Journal of Materials Processing Technology*, Vol. 143, pp. 66-71, 2003.
- [5] S. Agrawal, A.K. Charabarti and A. B. Chattopadhyay, "A study of the machining of cast austenitic stainless steels with carbide tools", *Journal of Materials Processing Technology*, Vol. 52, pp. 610-620, 1995.
- [6] R. M. Arunachalam, M. A. Mannan and A. C. Spowage, "Residual stress and surface roughness when facing age hardened Inconel 718 with CBN and ceramic cutting tools", *International Journal of Machine Tools and Manufacture*, Vol. 44, pp. 879-887, 2004.
- [7] M. Alauddin, M. A. EI-Baradie and M. S. J. Hashmi, "Tool life testing in the end milling of Inconel 718", *Journal of Materials Processing Technology*, Vol. 55, pp. 321-330, 1998.
- [8] A. Abrao and D. Aspinwall, "The surface integrity of hardened steel", *Wear*, Vol. 196, pp. 279-284, 1996.

- [9] T. Aoyama, "Development of a mixture supply system for machining with minimal quantity lubrication", *Annals of the CIRP*, Vol. 51, pp. 34-46, 2003.
- [10] Y. Altintas, "Manufacturing automation", Cambridge University press, 2000
- [11] J. L. Andreasen and L. D. Chiffre, "Automatic chip breakage detection in turning by frequency analysis of cutting force", *Annals of the CIRP*. Vol. 42, pp. 44-53, 1993.
- [12] P. Astakhov and V. P. Shuvets, "Chip Structure of classification based on mechanism of its formation", *Journal of Materials Processing Technology*, Vol. 67, pp. 24-32, 1997.
- [13] E. J. A. Armarego, "A mechanics of cutting approach for force prediction in machining operation", *Journal of Engineering and Production*, Vol. 11, pp. 1-18, 1997.
- [14] D. Arsecularatne, R. F. Fowle and P. Mathew, "Prediction of chip flow direction, cutting forces and surface roughness in turning", *Journal of Manufacturing Science and Engineering*, Vol. 120, pp. 1-12, 1998.
- [15] P. K. Baro, S. S. Joshi and S. G. Kapoor, "Modeling of cutting forces in a face milling operation with self-propelled round insert milling cutter", *International Journal of Machine Tools and Manufacture*, Vol. 45, pp. 831-839, 2005.
- [16] E. Budak, "Analytical models for high performance milling, Part I: cutting forces, structural deformations and tolerance integrity", *International Journal of Machine Tools and Manufacture*, Vol. 46, pp. 1478-1488, 2006.
- [17] E. Budak, "Analytical models for high performance milling, Part II: process dynamics and stability", *International Journal of Machine Tools and Manufacture*, Vol. 46, pp. 1489-1499, 2006.

- [18] U. Bravo, O. Altuzarra, L. N. Lopez, J. A. Sanchez and F. J. Campa, "Stability limits of milling considering the flexibility of the workpiece and the machine", *International Journal of Machine Tools and Manufacture*, Vol. 45, pp. 1669-168
- [19] J. Barry and G. Byrne, "Cutting tool wear in the machining of hardened steel", *Wear*, Vol. 247, pp. 139-151, 2001.
- [20] G. Brandt, "Wear mechanism of alumina based cutting tools when machining steel", *Wear*, Vol. 196, pp. 39-56, 1996.
- [21] D. Burta, R. Sowerby and I. Yellowley. "Stress distribution in orthogonal cutting operation", *International Journal of Machine Tools and Manufacture*, Vol. 34, pp. 721-729, 1994.
- [22] C. K. Chen and Y. M. Tsao, "A stability analysis of turning a tailstock supported flexible workpiece", *International Journal of Machine Tools and Manufacture*, Vol. 46, pp. 1518-1525, 2006.
- [23] L. R. Castro, P. Vieville and P. Lipinski, "Correction of dynamic effects on force measurements made with piezoelectric dynamometers", *International Journal of Machine Tools and Manufacture*, Vol. 46, pp. 1707-1715, 2006.
- [24] Y. Cao and Y. Altintas, "Modeling of spindle bearing and machine tool systems for virtual simulation of milling operations", *International Journal of Machine Tools and Manufacture*, Vol. 46, pp. 1638-1645, 2006.
- [25] J. F. A. Caroline, H. Y. Feng and W. M. Lau, "Machining of an aluminium composite using diamond inserts", *Journal of Materials Processing Technology*, Vol. 102, pp. 25-29, 2000.

- [26] S. Chowdhuri, S. S. Joshi, P. K. Rao and N. B. Ballal, "Machining aspects of a high carbon Fe₃Al alloy", *Journal of Materials Processing Technology*, Vol. 147, pp. 131-138, 2004.
- [27] K. L. Chelule, T. J. Coole and D. G. Cheshire, "An investigation into machinability of hydroxyapatite for bone restoration implants", *Journal of Materials Processing Technology*, Vol. 135, pp. 242-246, 2003.
- [28] K. Chenping, "High performance machining of SiC whisker reinforced aluminium composite by self propelled rotary tools", *Annals of the CIRP*, Vol. 50, pp. 59-62, 2001.
- [29] R. T. Coelho, L. R. Silva, "A. Braghini and A.A. Bezerra, Some effects of cutting edge preparation and geometric modifications when turning Inconel 718 at high cutting speeds", *Journal of Materials Processing Technology*, Vol. 148, pp. 147-153, 2004.
- [30] L. A. Dobrzanski and K. Golombek, "Structure and properties of the cutting tools made from cemented carbides and cermets with the TiN-mono, gradient-multi (Ti,Al,Si) N+TiN nanocrystalline coatings", *Journal of Materials Processing Technology*, Vol. 164, pp. 805-815, 2005.
- [31] U. A. Dabade, S. S. Joshi and N. Ramakrishnan, "Analysis of surface roughness and chip cross-sectional area while machining with self-propelled round inserts milling cutter", *Journal of Materials Processing Technology*, Vol. 132, pp. 305-312, 2003.
- [32] J. Du, E. B. Lee and D. H. Hyun, "A study on the modeling of tool motion and high-accuracy surface generation by the use of cutting-force signals", *Journal of Materials Processing Technology*, Vol. 47, pp. 101-117, 1994.
- [33] K. Danai and A. G. Ulsoy, "A dynamic state model for on-line tool wear estimation in turning", *Transaction of ASME, Journal of Engg. for Industry*, Vol. 109, pp. 396-399, 1987.

- [34] A. Erturk, H. N. Ozguven and E. Budak, “ Effect analysis of bearing and interface dynamics on tool point for chatter stability in machine tools by using a new analytical model for spindle-tool assemblies”, *International Journal of Machine Tools and Manufacture*, Vol. 46, pp. 1523-1532, 2006.
- [35] A. Erturk, E. Budak and H. N. Ozguven, “Selection of design and operational parameters in spindle-holder-tool assemblies for maximum chatter stability by using a new analytical model”, *International Journal of Machine Tools and Manufacture*, Vol. 46, pp. 16561-1668, 2006.
- [36] E. O. Ezugwu, J. Bonney, D. A. Fadre and W. F. Sales, “Machining of nickel base Inconel 718 alloy with ceramic tools under finishing conditions with various coolant supply pressures”, *Journal of Materials Processing Technology*, Vol. 162, pp. 609-614, 2005.
- [37] M. EI-Gallab and M. Sklad, “Machining of Al/SiC particulate metal-matrix composites part I: Tool performance”, *Journal of Materials Processing Technology*, Vol. 83, pp. 151-158, 1998.
- [38] M. EI-Gallab and M. Sklad, “Machining of Al/SiC particulate metal-matrix composites part II: Workpiece surface integrity”, *Journal of Materials Processing Technology*, Vol. 83, pp. 271-285, 1998.
- [39] M. A. El-Bestawi, “T.I.Ei-Wardany, D.Yan and M.Tan, Performance of whisker – reinforced ceramic tools in milling nickel based super alloy”, *Annals of the CIRP*, Vol. 43, pp. 18-23, 1998.
- [40] S. Ekinovic, S. Dolinsek and E. Begovic, “Machinability of 90MnCrV8 steel during high speed machining”, *Journal of Materials Processing Technology*, Vol. 162, pp. 603-608, 2005.

- [41] M. Fontaine, A. Devillez, A. Moufki and D. dudzinski, “ Predictive force model for ball end milling and experimental validation with a wavelike form machining test”, *International Journal of Machine Tools and Manufacture*, Vol. 46, pp. 367-380, 2006.
- [42] J. R. Ferreira, N. L. Coppini and G. W. Miranda, “Machining optimization in carbon fiber reinforced composite materials”, *Journal of Materials Processing Technology*, Vol. 92-93, pp. 135-140, 1999.
- [43] J. Gradisek, M. Kalveram, T. Insperger, K. Weinnert, G. Stepan, E. Govekar and I. Grabec, “On stability prediction for milling”, *International Journal of Machine Tools and Manufacture*, Vol. 45, pp. 769-781, 2005.
- [44] A. Gatto and L. Iuliano, “Advanced coated ceramic tools for machining super alloys”, *International Journal of Machine Tools and Manufacture*, Vol. 37, pp. 591-605, 1997.
- [45] F. Giusti, M. Santochi and G. Tantussi, “On line sensing of flank and crater wear of cutting tools”, *Annals of the CIRP*, Vol. 36, pp. 44 -56, 1987.
- [46] R. F. Hamade, C. Y. Seif and F. Ismail, “ Extracting cutting force coefficients from drilling experiments”, *International Journal of Machine Tools and Manufacture*, Vol. 46, pp. 387-396, 2006.
- [47] S. N. Huang, K. K. Tan, Y. S. Yong, C. W. Silva, H. L. Goh and W. W. Tan, “ Tool wear detection and fault diagnosis based on cutting force monitoring”, *International Journal of Machine Tools and Manufacture*, Vol. 46, pp. 493-508, 2006.
- [48] F. Y. Huang, H. M. Chow, S. L. Chen and K. A. Yan, “The machinability of KOVAR material”, *Journal of Materials Processing Technology*, Vol. 87, pp. 112-118, 1999.

- [49] C. H. Haron, A. Ginting and H. Arshad, "Performance of alloyed uncoated and CVD coated carbide tools in dry milling of titanium alloy Ti-6242S", *Journal of Materials Processing Technology*, Vol. 166, pp. 1-6, 2005.
- [50] K. A. Hossein and Z. Yahya, "High speed end milling of AISI 304 stainless steel using new geometrically developed carbide inserts", *Journal of Materials Processing Technology*, Vol. 162, pp. 596-602, 2005.
- [51] F. Hasler, "New dimensions in high speed machining", *Journal of Industrial and Production Engineering*, Vol. 12, pp. 43-48, 1998.
- [52] J. C. Haman, F.L. Maitre and D. Guillet, "Selective transfer built-up layer displacement in high speed machining-consequences on tool wear and cutting forces", *Annals of the CIRP*, Vol. 40, pp. 17-23, 1994.
- [53] T. Insperger, B. P. Mann, G. Stepan and P. V. Bayly, "Stability of up milling and down Milling: analytical methods", *International Journal of Machine Tools and Manufacture*, Vol. 43, pp. 25-34, 2003.
- [54] A. Jawaid, S. Koksai and S. Sharif, "Cutting performance and wear characteristics of PVD coated and uncoated carbide tools in face milling Inconel 718 aerospace alloy", *Journal of Materials Processing Technology*, Vol. 116, pp. 2-9, 2001.
- [55] I. S. Jawahir, P. X. Li, R. Gosh and E. L. Exner, "A new parametric approach for the assessment of comprehensive tool wear in coated grooved tools", *Annals of the CIRP*, Vol. 43, pp. 52-58, 1998.
- [56] A. S. Jhita and V. K. Jain, "On the tool wear during face turning", *Proceedings of the International Machine Tool Design and Research Conference*, Macmillan, UK, pp. 247-253, 1992.

- [57] S. J. Kim, H. U. Lee and D. W. Cho, "Feed rate scheduling for indexable end milling process based on an improved cutting force model", *International Journal of Machine Tools and Manufacture*, Vol. 46, pp. 1589-1597, 2006.
- [58] K. Kudou, T. Ono and S. Okada, "Crater wear characteristics of a Fe-diffused carbide tool", *Journal of Materials Processing Technology*, Vol. 132, pp. 255-261, 2003.
- [59] S. Katayama and M. Toda, "Machinability of medium carbon graphitic steel", *Journal of Materials Processing Technology*, Vol. 62, pp. 358-362, 1996.
- [60] F. M. Kustas, L. L. Fehrebnacher and R. Komanduri, "Nano coatings on cutting tools for dry machining", *Annals of the CIRP*, Vol. 40, pp. 11-23, 1997.
- [61] R. Kovacevic, C. Charukuthota and R. Mohan, "Improving milling performance with high pressure water jet assisted cooling/lubrication", *Trans. of ASME Journal of Manufacturing Science and Engineering*, Vol. 117, pp. 331-339, 1995.
- [62] W. Konig and E. Essel, "New tool materials-wear mechanisms and applications", *Annals of the CIRP*, Vol. 45, pp. 34-43, 1996.
- [63] H. Z. Liming, H. Zeng and X. Q. Chen, "An experimental study of tool wear and cutting force variation in the end milling of Inconel 718 with coated carbide inserts", *Journal of Materials Processing Technology*, Vol. 180, pp. 296-304, 2006.
- [64] L. Li and H. A. Kishawy, "A model for cutting forces generated during machining with self-propelled rotary tools", *International Journal of Machine Tools and Manufacture*, Vol. 46, pp. 1388-1394, 2006.
- [65] A. Lamikiz, L. N. Lacalle, J. A. Sanchez and M. A. Salgado, "Cutting force estimation in sculptured surface milling", *International Journal of Machine Tools and Manufacture*, Vol. 44, pp. 1511-1526, 2004.

- [66] X. Liu and K. Cheng, "Modeling the machining dynamics of peripheral milling", *International Journal of Machine Tools and Manufacture*, Vol. 45, pp. 1301-1320, 2005.
- [67] A. Locasto, S. Valvo, E. Luchini and S. Micari, "Wear performance of cutting tools materials when cutting steel", *Journal of Materials Processing Technology*, Vol. 28, pp. 25-36, 1991.
- [68] Y. S. Liao and R. H. Shiue, "Carbide tool wear mechanism in turning of Inconel 718 super alloy", *Wear*, Vol. 193, pp. 16-24, 1996.
- [69] L. N. Lacalle, C. Angulo, A. Lamikiz and J. A. Sanchez, "Experimental and numerical investigation of the effect of spray cutting fluids in high speed milling", *Journal of Materials Processing Technology*, Vol. 172, pp. 11-15, 2005.
- [70] P. M. Lister and G. Barrow, "Tool condition monitoring systems", *Proceedings of the International Machine Tool Design and Research Conference*, Macmillan, UK, pp. 271-288, 1996.
- [71] G. H. Lim, "Tool wear monitoring in machine turning", *Journal of Materials Processing Technology*, Vol. 51, pp. 25-27, 1995.
- [72] Z. C. Lin and D. Y. Chen, "A study of cutting with a CBN tool", *Journal of Materials Processing Technology*, Vol. 49, pp. 149-164, 1995.
- [73] L. A. Looney, J. M. Monaghan, P. O. Reily and D. M. Tasplin, "The turning of an Al /SiC metal-matrix composite", *Journal of Materials Processing Technology*, Vol. 33, pp. 453-468, 1992.
- [74] K. L. Ming and S. Y. Liang, "Modeling of cutting forces in dry machining under tool wear effect", *International Journal of Machine Tools and Manufacture*, Vol. 46, pp. 1789-1797, 2006.

- [75] A. Moufki, A. Devillez, M. Segreti and D. Dudzinski, "An analytical model of non linear vibrations in orthogonal cutting and experimental validation", *International Journal of Machine Tools and Manufacture*, Vol. 46, pp. 436-449, 2006.
- [76] M. R. Movahhedy and J. M. Gerami, "Prediction of spindle dynamics in milling by sub-structure coupling", *International Journal of Machine Tools and Manufacture*, Vol. 46, pp. 243-251, 2006.
- [77] M. R. Movahhedy and P. Mosaddegh, "Prediction of chatter in high speed milling including gyroscopic effects", *International Journal of Machine Tools and Manufacture*, Vol. 46, pp. 996-1001, 2006.
- [78] R. Mahdavinejad, "Finite element analysis of machine and workpiece instability in turning", *International Journal of Machine Tools and Manufacture*, Vol. 45, pp. 753-760, 2005.
- [79] M. Masuda, Y. Kuroshima and Y. Chujo, "Failure of tungsten carbide-cobalt alloy tools in machining of carbon materials", *Wear*, Vol. 169, pp. 135-140, 1993.
- [80] R. Mackinnon, G. E. Wilson and A. J. Wilkinson, "Tool condition monitoring using multi component force measurements", *Proceedings of the International Machine Tool design and Research Conference*, Macmillan, UK, pp. 317-324, 1996.
- [81] R. Milovic and M. L. Wise, "Tool wear in the machining of leaded free-cutting steel", *Proceedings of the International Machine Tool Design and Research Conference*, Macmillan, UK pp. 287- 299, 1995.
- [82] S. Nelson, J. K. Schueller and J. Tlusty, "Tool wear in milling hardened die steel", *Trans. of ASME, Journal of Manufacturing Science and Engineering*, Vol. 120, pp. 669-673, 1998.

- [83] N. Narutaki, Y. Yamane, S. Tashima and H. Kuroki, "A new advanced ceramic for dry machining", *Annals of the CIRP*, Vol. 40, pp. 19-23, 1997.
- [84] N. Narutaki, Y. Yamane, K. Hayashi and T. Kitagawa, "High-speed machining of Inconel 718 with ceramic tools", *Annals of the CIRP*, Vol. 44, pp. 10-23, 1999.
- [85] E. G. Ng, D. W. Lee, A. R. C. Sharman, R. C. Dewes and D. Aspinwall, "High speed ball nose end milling of Inconel 718", *Annals of the CIRP*, Vol. 49, pp. 41-46, 2000.
- [86] R. Nair, K. Danai and S. Malkin, "Turning process identification through force transients", *Transaction of ASME, Journal of Engg. for Industry*, Vol. 114, pp. 1-7, 1992.
- [87] B. Ozturk, I. Lazoglu and H. Erdim, "Machining of free surface for cutting force measurement", *International Journal of Machine Tools and Manufacture*, Vol. 46, pp. 736-746, 2006.
- [88] O. E. K. Omar, T. E. Wardnay, E. Ng and M. A. Elbestawi, "An improved cutting force and surface topography prediction model in end milling", *International Journal of Machine Tools and Manufacture*, Vol. 46, pp. 1411-1422, 2006.
- [89] Y. Ozcatalbas and F. Ercan, "The effects of heat treatment on the machinability of mild steels", *Journal of Materials Processing Technology*, Vol. 136, pp. 227-238, 2003.
- [90] A. Pramanick, L. C. Zang and J. A. Arsecularatne, "Prediction of cutting forces in machining of metal matrix composites", *International Journal of Machine Tools and Manufacture*, Vol. 46, pp. 1795-1803, 2006.
- [91] W. Polini and S. Turchetta, "Force and specific energy in stone cutting by diamond tool", *International Journal of Machine Tools and Manufacture*, Vol. 44, pp. 1189-1196, 2004.

- [92] G. Peigne, H. Paris, D. Brissaud and A. Gousskov, "Impact of the cutting dynamics of small radial immersion milling operations on machined surface roughness", *International Journal of Machine Tools and Manufacture*, Vol. 44, pp. 1133-1142, 2004.
- [93] J. Paro, H. Hanninen and V. Kauppinen, "Tool wear and machinability of X5CrMnN 1818 stainless steels", *Journal of Materials Processing Technology*, Vol. 119, pp. 14-20, 2001.
- [94] G. Poulachon, A. Moisan and I. S. Jawahir, "Tool wear mechanisms in hard turning with polycrystalline cubic boron nitride tools", *Wear*, Vol. 250, pp. 576-586, 2001.
- [95] E. Posti and I. Nieminen, "Coating thickness effects on the life of titanium nitride PVD coated tools", *Journal of Materials and Manufacturing processes*, Vol. 4, pp. 239-252, 1989.
- [96] A. Rashid and C. M. Nicolescu, "Active vibration control in palletized work holding system for milling", *International Journal of Machine Tools and Manufacture*, Vol. 46, pp. 1626-1636, 2006.
- [97] N. S. K. Reddy and P. V. Rao, "Experimental investigation to study the effect of solid lubricants on cutting forces and surface quality in end milling", *International Journal of Machine Tools and Manufacture*, Vol. 46, pp. 189-198, 2006.
- [98] M. Rahamn, S. Ramakrisna, J. R. S. Prakash and D. C. G. Tan, "Machinability study of fiber reinforced composite", *Journal of Materials Processing Technology*, Vol. 89-90, pp. 292-297, 1999.
- [99] C. A. Rocha, W. F. Sales, C. Sperb and A. Mendes, "Evaluation of the wear mechanisms and surface parameters when machining internal combustion engine valve

- seats using PCBN tools”, *Journal of Materials Processing Technology*, Vol. 145, pp. 397-406, 2004.
- [100] M. Rahman, W. K. H. Seah and T. T. Teo, “The machinability of Inconel 718”, *Journal of Materials Processing Technology*, Vol. 63, pp. 199-204, 1997.
- [101] M. Rahman, A. S. Kumar and M. R. Choudury, “Identification of effective zones for high pressure coolant in milling”, *Annals of the CIRP*, Vol. 49, pp. 18-23, 2000.
- [102] A. C. Rapier, “A theoretical investigation of the temperature distribution in the metal cutting process”, *Journal of materials processing technology*, Vol. 46 pp. 18-28, 1993.
- [103] C. Rubenstein, “The mechanics of continuous chip formation in oblique cutting”, *International Journal of Machine Tools and Manufacture*, Vol. 23, pp. 11-20, 1993.
- [104] T. L. Schmitz, J. Couey, E. Marsh, N. Mauntler and D. Hughes, “Run out effects in milling: surface finish, surface location error and stability”, *International Journal of Machine Tools and Manufacture*, Vol. 46, pp. 1216-1228, 2006.
- [105] S. M. Son, H. Lim and J. H. Ahn, “The effects of vibration cutting on minimum cutting thickness”, *International Journal of Machine Tools and Manufacture*, Vol. 46, pp. 2066-2072, 2006.
- [106] E. Solis, C. R. Peres, J. E. Jimenez, J. R. Alique and J. C. Monje, “A new analytical-experimental method for the identification of stability lobes in high speed milling”, *International Journal of Machine Tools and Manufacture*, Vol. 44, pp. 1591-1597, 2004.

- [107] Y. L. Su, S. H. Yao, C. S. Wei, W. H. Kao and C. T. Wu, "Design and performance analysis of TiCN-coated cemented carbide milling cutters", *Journal of Materials Processing Technology*, Vol. 87, pp. 82-89, 1999.
- [108] P. S. Sreejith and B. K.A. Ngoi, "Dry machining of the future", *Journal of Materials Processing Technology*, Vol. 101, pp. 287-291, 2000.
- [109] Y. L. Su, T. H. Liu, C. T. Su, S. H. Yao, W. H. Kao and K. W. Cheng, "Wear of CrC-coated carbide tools in dry machining", *Journal of Materials Processing Technology*, Vol. 171, pp. 108-117, 2005.
- [110] R. B. Schroeter, R. Kratochvil and J. O. Gomes, "High speed finishing milling of industrial graphic electrodes" *Journal of Materials Processing Technology*, Vol. 162, pp. 296-302, 2005.
- [111] S. Smith, W. R. Winfough and J. Halley, "The effect of tool length on metal removal rate in machining operation", *Annals of the CIRP*, Vol. 47, pp. 32-40, 1998.
- [112] N. Tomac and K. Tonnessen, "Machinability of particulate aluminium matrix composites", *Annals of the CIRP*, Vol. 38, pp. 10-23, 1992.
- [113] J. Vivancos, C. J. Luis, L. Costa and J. A. Ortiz, "Optimal machining parameters selection in high speed milling hardened steels for injection moulds", *Journal of Materials Processing Technology*, Vol. 155, pp. 1505-1512, 2004..
- [114] M. Wan, W. H. Zhang, G. H. Qin and G. Tan, "Efficient calibration of instantaneous cutting force coefficients and cutting parameters for general end mills", *International Journal of Machine Tools and Manufacture*, Vol. 46, pp. 688-696, 2006.

References

- [115] W. L. Weingaertner, R. B. Schroeter, M. L. Polli and J. O. Gomes, "Evaluation of high speed end milling dynamics stability through audio signal measurement", *Journal of Materials Processing Technology*, Vol. 179, pp. 133-138, 2006.
- [116] T. Wakabayashi, I. Inasaki, S. Suda and H. Yokota, "Tribological characteristics and cutting performance of lubricant esters for semi-dry machining", *Annals of the CIRP*, Vol. 52, pp. 45-53, 2003.
- [117] R. Werthein, A. Satran and A. Ber, "Modifications of the cutting tool geometry in milling", *Annals of the CIRP*, *Annals of the CIRP*, Vol. 43, pp. 24-30, 1994.
- [118] D. M. William and S. H. Crandall "Random vibration in mechanical systems", Academic press, London, 1963.
- [119] Q. Yanming and Z. Zehua, "Tool wear and its mechanism for cutting SiC particle-reinforced aluminium matrix composites", *Journal of Materials Processing Technology*, Vol. 100, pp. 194-199, 2000.
- [120] D. Zhou., Z. Jianhua and A. Xing, "Failure mechanisms of a ceramic tool when machining nickel-based alloys", *Wear*, Vol. 208, pp. 220-225, 1998.
- [121] J. M. Zhou, M. Andersson and J. E. Stahl, "A system for monitoring cutting tool spontaneous failure based on stress estimation", *Journal of Materials Processing Technology*, Vol. 48, pp. 231-237. 1995.